JAERI - M
90-035

EVALUATION REPORT ON SCTF CORE-III TESTS S3-7 AND S3-8

(INVESTIGATION OF TIE PLATE WATER TEMPERATURE DISTRIBUTION EFFECTS ON WATER BREAK-THROUGH AND CORE COOLING DURING REFLOODING IN PWRS WITH COMBINED-INJECTION-TYPE ECCS)

March 1990

Tsutomu OKUBO, Tadashi IGUCHI, Takamichi IWAMURA, Hajime AKIMOTO
Akira OHNUKI, Yutaka ABE, Akihiko MINATO*, Isao SAKAKI**
Hiromichi ADACHI and Yoshio MURAO

日 本 原 子 力 研 究 所
Japan Atomic Energy Research Institute

JAERI-Mレポートは，日本原子力研究所が不定期に公刊している研究報告書です。
入手の問合わせは，日本原子力研究所技術情報部情報資料課（〒319-11茨城県那珂郡東海村）あて，お申しこしください。なお，このほかに財団法人原子力弘済会資料センター（〒319-11 茨城県那珂郡東海村日本原子力研究所内）で複写による実費頒布をおこなっております。

JAERI-M reports are issued irregularly.
Inquiries about availability of the reports should be addressed to Information Division, Department of Technical Information, Japan Atomic Energy Research Institute, Tokai-mura, Naka-gun, Ibaraki-ken 319-11, Japan.

編集兼発行　日本原子力研究所
印　　刷　㈱原子力資料サービス

JAERI-M 90-035

Evaluation Report on SCTF Core-III Tests S3-7 and S3-8

(Investigation of Tie Plate Water Temperature Distribution Effects on Water Break-through and Core Cooling during Reflooding in PWRs with Combined-injection-type ECCS)

Tsutomu OKUBO, Tadashi IGUCHI, Takamichi IWAMURA, Hajime AKIMOTO
Akira OHNUKI, Yutaka ABE, Akihiko MINATO*, Isao SAKAKI**
Hiromichi ADACHI and Yoshio MURAO

Department of Reactor Engineering
Tokai Research Establishment
Japan Atomic Energy Research Institute
Tokai-mura, Naka-gun, Ibaraki-ken

(Received February 2, 1990)

It has been said that the Emergency Core Cooling (ECC) water injected into the hot legs flows into the upper plenum and then falls back to the core (*i.e.* break-through) during reflood phase in a German type Pressurized Water Reactor (GPWR) with the combined-injection-type ECCS, and that the break-through occurs where the water temperature at the tie plate area is lower and subcooled. Based on this information two tests were conducted with the Slab Core Test Facility (SCTF) Core-III in order to investigate the effects of the water temperature distribution at the tie plate area on the break-through and the core cooling.

In these tests, the subcooled ECC water was injected just above the Upper Core Support Plate (UCSP) in order to establish the desired water temperature distribution at the tie plate area. In one test (Test S3-7) the ECC water injection above the UCSP was performed above Bundles 3 and 4, and in the other test (Test S3-8) above Bundles 7 and 8 during initial 60 s and then was changed to above Bundles 3 and 4. The test data were compared

---

* Hitachi, Ltd.
** Toshiba, Ltd.

with those of Test S3-SH1, in which the injection was performed above Bundles 7 and 8 and the other test conditions were the same as in Tests S3-7 and S3-8.

Analyzing these test data, the following has been found : The break-through occurs where the water temperature at the tie plate area is sub-cooled and the core cooling is enhanced significantly in the break-through region. The break-through location changes, with some time lag, following the change of the water temperature distribution at the tie plate area. Furthermore, the core cooling in the non-break-through regions is almost the same regardless of the location of the break-through.

Keywords: Reactor Safety, PWR, LOCA, Combined-injection-type ECCS, Reflood Experiments, Break-through, Core Cooling, Heat Transfer, Two-phase Flow

SCTF第3次炉心試験S3－7・S3－8評価報告書

（複合注水型ECCS付PWRの再冠水過程に於けるブレークスルーおよび炉心冷却に及ぼすタイプレート水温分布の影響の検討）

日本原子力研究所東海研究所原子炉工学部

大久保　努・井口　　正・岩村　公道・秋本　　肇

大貫　　晃・阿部　　豊・湊　　明彦*・榊　　勲**

安達　公道・村尾　良夫

（1990年2月2日受理）

複合注水型ECCSを備えた西ドイツ型PWR（GPWR）の再冠水過程では，高温側配管に注入された緊急炉心冷却（ECC）水が上部プレナムに流入し，更に炉心へ落下（ブレークスルー）すると言われており，また，ブレークスルーはタイプレート付近の水温が低くサブクールになっている所で生ずると言われている。これらの情報に基づいて，タイプレート付近の水温分布がブレークスルーおよび炉心冷却に与える影響を検討するため，平板炉心試験装置（SCTF）の第3次炉心を用いて2回の試験を実施した。

これらの試験では，サブクールECC水を上部炉心板（UCSP）直上に注入して所望のタイプレート付近での水温分布を達成した。2つのうち一方の試験（試験S3－7）では，UCSP直上へのECC注水をバンドル3，4の上方で行ない，もう一方の試験（試験S3－8）では，最初の60秒はバンドル7，8の上方でその後バンドル3，4の上方へ切換えて注水を行なった。これらの試験のデータは，別の試験S3－SH1のデータと比較検討された。この試験では，バンドル7，8の上方に注入が行なわれ，他の試験条件は，試験S3－7やS3－8と同一であった。

これらの試験データを解析して，以下の事柄が明らかとなった。ブレークスルーは，タイプレート付近での水温がサブクールの所で生じ，ブレークスルー域では，炉心冷却が著しく増大する。また，ブレークスルーの位置は，多少の時間遅れを伴ってタイプレート付近での水温分布の変化に追随して変化する。更に，ブレークスルーの生じていない領域での炉心冷却は，ブレークスルーの位置に関係無く同程度である。

東海研究所：〒319－11　茨城県那珂郡東海村白方字白根2－4

＊　（株）日立製作所

＊＊　（株）東　芝

Contents

目　　次

List of Tables

List of Figures

1. Introduction

The Slab Core Test Facility (SCTF) test program is a part of the large scale reflood test program[1] together with the Cylindrical Core Test Facility (CCTF) test program[2], which are performed by Japan Atomic Energy Research Institute (JAERI) under a contract with Atomic Energy Bureau of Science and Technology Agency of Japan. The SCTF test program is also one of the research activities based on the trilateral agreement among JAERI, the United States Nuclear Regulatory Commission (USNRC) and the Federal Minister for Research and Technology (BMFT) of the Federal Republic of Germany (FRG).

There are three test series (Core-I, -II and -III) in the SCTF test program. The SCTF Core-I[3] and Core-II[4] test series have been already performed mainly to investigate the two-dimensional thermo-hydrodynamic behavior in the core during the reflood phase of a loss-of-coolant accident (LOCA) of a Westinghouse type (US/J-type) pressurized water reactor (PWR) with the cold-leg-injection-type emergency core cooling system (ECCS). On the other hand, one of the major objectives of the SCTF Core-III[5] test series is to investigate the effectiveness of the combined-injection-type ECCS in a German type PWR (GPWR). In addition, simulation tests for a US/J-type PWR were also conducted with the SCTF Core-III for further investigation of the two-dimensional thermo-hydrodynamic behavior.

The reflood phenomena for PWRs with the combined-injection-type ECCS have been investigated mainly in FRG, since PWRs of such type are manufactured only there. One of the main characteristics of them is the heterogeneous core thermo-hydrodynamic behavior. However, the test facilities used for the investigation are rather small for the investigation of it. Then it is necessary to investigate it further with a facility having a full radius core. Therefore, tests to study the reflood phenomena for PWRs with the combined-injection-type ECCS have been performed with the SCTF, because it has a full radius core.

According to the previous investigation on reflooding of GPWRs, it is said that the ECC water injected into the hot legs flows into the upper plenum and then falls back to the core, which is usually called break-through, and cools down the core. And the break-through is said to occur where the water temperature at the tie plate area is lower and subcooled. Therefore, two tests were performed in order to investigate the effects of

water temperature distribution at the tie plate area on break-through and core cooling behaviors during the reflood phase of a GPWR under evaluation model (EM) conditions. These tests are named Test S3-7 (Run 711) and Test S3-8 (Run 712). This report describes the major results of these tests and discussion on them.

A brief description of the SCTF Core-III is presented in Appendix A. Some selected data obtained in Tests S3-7 and S3-8 are presented in Appendices B and C, respectively, for better understanding of the test results.

A brief information on these tests are presented in the following:

(1) Test names

GPWR simulation core cooling EM tests

where, GPWR: German PWR with the combined-injection-type ECCS
EM : Evaluation model

(2) Test numbers

S3-7 (Run 711) and S3-8 (Run 712)

where, S : SCTF
3 : Core-III
7 or 8: Sequential number of the main test

(3) Objective of tests

To investigate the effects of water temperature distribution at tie plate area on the break-through and the core cooling phenomena during the reflood phase in a GPWR.

(4) Type of tests

Refill and reflood separate effect tests simulating a GPWR under the EM conditions.

2. Test Description

2.1 Test Facility[5]

The SCTF was originally designed to study two-dimensional effects on thermal hydraulics during the reflood phase in a PWR core with full length radius.[3],[4]

Flow diagram of the SCTF is shown in Fig. 2.1. The SCTF is simulating a 200% cold-leg-large-break with a simplified primary system and can be operated at the system pressure less than 0.6 MPa. It consists of a pressure vessel, an intact loop, a broken loop at the pressure vessel side, and a broken loop at the steam-water separator side.

Figure 2.2 shows a vertical cross section of the pressure vessel. The pressure vessel includes a simulated core, an upper plenum with its internals, a lower plenum, a core baffle region and a downcomer. The configurations of the upper plenum structure and the end box simulate those of a 1,300 MWe class GPWR as practically as possible.

The core is full-height, full-radius and one-bundle width one. The core flow area scaling ratio is 1/24 to a typical 1,300 MWe class GPWR. 1,888 electrical heater rods are installed in the core. Dimensions of a heater rod is 10.7 mm in diameter and 3,613 mm in heated length simulating those of PWRs. The maximum available power supplied to the core is 10 MW.

The heater rods are assembled in a 16 x 16 square array bundle positioned with grid spacers. Eight bundles are installed in a row in the core, as shown in Fig. 2.2. In the SCTF, the leftmost bundle in the figure is named Bundle 1 and orderly to the right direction the bundles are named Bundle 2, 3, ..., 8. Since the downcomer and the hot leg are connected to Bundle 8 side, Bundle 1 and 8 sides are corresponding to the central and the peripheral sides of PWRs, respectively.

The ECC water can be injected into the lower plenum, the cold leg and the upper plenum in the SCTF. Since the SCTF has no injection port in the hot leg, the hot leg injection of ECC water in PWRs with the combined-injection-type ECCS was substituted by the upper plenum injection. The ECC water can be injected into the upper plenum from both top and side wall.

The core and the upper plenum are enveloped by honeycomb thermal insulators with wall plates to minimize the wall thermal effects.

Description of the SCTF Core-III is presented more in detail in Appendix A.

2.2 Test Conditions and Sequence

2.2.1 Conditions and Sequence of Test S3-7

Conditions for Test S3-7 were selected to simulate the refill and reflood phenomena under the EM conditions for a GPWR 200% cold-leg-large-break LOCA. The bases for the test conditions are summarized later in Sec. 2.3. Table 2.1 shows the planned and the measured test conditions.

Figure 2.3 shows the conceptual set-up of the facility for Test S3-7. The ECC water was injected from an injection port located just above the UCSP (side injection port UCSP3) and four injection ports located at the top of upper plenum (top injection ports UP1, UP2, UP3 and UP4). The port UP1 is located above Bundles 7 and 8 of the core. The port UP2, the ports UCSP3 and UP3, and the port UP4 are located above Bundles 5 and 6, Bundles 3 and 4, and Bundles 1 and 2, respectively.

Orifice diameters for the steam-water separator side broken cold leg, the intact cold leg and the pump simulator are 86.4, 179.9 and 173.7 mm, respectively. No orifice is inserted into the pressure vessel side broken cold leg. Water in the steam-water separator was drained to the containment tank II to keep the maximum water level in the steam-water separator at 1.1 m.

Figure 2.4 shows the sequence of Test S3-7. In this figure, the time when the maximum clad temperature reached 670 ^{o}C is defined as 0 s. The pressure in the containment tank II was kept constant at 0.3 MPa by controlling discharge rate of the steam through the blow valve to the atmosphere after 0 s. The ECC water was injected both into the side and the top of the upper plenum after 0 s. The ECC water injection rate from the side was 30 kg/s by UCSP3. The water temperature for this was set at 70 ^{o}C. The injection rates from the top were 2.5 kg/s each by UP1 through UP4. The temperature of the water was 35 ^{o}C. The core power was initially set at 7.5 MW and was decreased to simulate a decay as shown in Fig. 2.4.

2.2.2 Conditions and Sequence of Test S3-8

Conditions for Test S3-8 were also selected to simulate the reflood phenomena under the EM condition for a GPWR 200% cold-leg-large-break LOCA. The bases for the test conditions are the same as for Test S3-7 and summarized in Sec. 2.3. Table 2.2 shows the planned and the measured test conditions.

The conceptual set-up of the facility for Test S3-8 is the same as for Test S3-7 (See Fig. 2.3). The ECC water was injected from the injection ports located just above the UCSP (side injection port UCSP1 or UCSP3) and four injection ports located at the top of upper plenum (top injection ports UP1, UP2, UP3 and UP4). In the present test, the side injection was initiated using UCSP1 above Bundles 7 and 8, and then 60 s after the initiation, the injection port was switched to UCSP3 (above Bundles 3 and 4). Except for the ECC water injection location during the initial 60 s, test conditions are the same as for Test S3-7 described in the previous section.

Figure 2.5 shows the sequence of Test S3-8. In this figure, the time when the maximum clad temperature reached 670 ^{o}C is defined as 0 s. Except for the ECC water injection location during the initial 60 s, the test sequence is the same as for Test S3-7 described in the previous section.

2.3 Bases for Test Conditions

Bases for test conditions are summarized in Table 2.3. They are the same for both tests. A brief explanation is as follows:

(1) Pressure

According to a TRAC calculation, pressure in the pressure vessel is about 0.3 MPa during the reflood period. Pressure in the containment tank II was initially set at 0.3 MPa and was intended to be kept constant during the reflood phase. However, the initial pressure in the primary system was set at 0.6 MPa and decreased to 0.3 MPa after 0 s by opening the blowdown valves (*i.e.* V1 and V2 in Fig. 2.3) in order to simulate the end of the blowdown and the refill phases.

(2) Core power

Core power for the present tests were determined by the following equation:

$$P_{SCTF} = P_{o\ GPWR} \times S_F \times (\text{Old ANS} \times 1.03 + \text{Act.})$$
$$(t \text{ s after scram})$$

where, $P_{o\ GPWR} = 3{,}765$ MW

$$S_F = \text{Scaling ratio} = \frac{\text{SCTF core volume}}{\text{GPWR core volume}} = \frac{0.8931}{21.5} = \frac{1}{24.07}$$

$t = 25$ s

As a result,

$$P_{SCTF} = 7.5 \text{ MW}$$

(3) Power profile

Radial power ratio in the present tests at a given radius F(r) were determined to simulate that in a GPWR. Namely,

$$F(r)_{SCTF} = k \cdot F(r)_{GPWR}$$

where, $F(r)_{SCTF}$ is based on the slab geometry, while $F(r)_{GPWR}$ is based on the sector or circular geometry. The constant k was determined to achieve

$$(F(r)_{SCTF})_{Average} = 1.0$$

(4) Initial clad temperature

Initial clad temperature was determined to simulate the stored energy in rods at the pressure of 0.6 MPa. The referred data base is the test result of PKL-IIB-2 performed in FRG.

(5) Mode of ECC injection

Since the present tests are separate effect tests to investigate the effects of the ECC water temperature distribution at the tie plate area on the water break-through and the core cooling behaviors, the ECC water was injected on the UCSP and the top of the upper plenum instead of the hot leg. The injection location on the UCSP was corresponding location above Bundle 3 and 4 in Test S3-7, and above Bundles 7 and 8 in the initial 60 s and thereafter Bundles 3 and 4 in Test S3-8, while only above Bundles 7 and 8 in Test S3-SH1[6], which is the base case test for what is call the core cooling separate effect test.

Selection base for ECC injection mode is summarized in Table 2.3. This is one of the EM conditions and based on the following situation proposed by FRG:

(i) ECC water injected into the broken cold leg is not effective
(ii) One HPCI pump and one LPCI pump are not working
(iii) One Acc in the hot leg is under repair
(iv) One valve in the hot leg injection line is closed as an assumption of the single failure.

(6) ECC injection rate and temperature

According to the mode of the ECC injection presented above, the injection rates are determined as:

3 Acc + 2.6 LPCI (cold leg)
2 Acc + 1.0 LPCI (upper plenum)

The total ECC water injection rate was determined based on the TRAC calculational results. Out of the total ECC water injected into the upper plenum, 30 kg/s of the water was injected from the side on the UCSP and the rest (10 kg/s) was injected radially uniformly at the top of the upper plenum with the lower temperature than the side injection. The water temperature for the side injection was 70 ^{o}C to simulate the fluid temperature just on the UCSP in the CCTF combined injection test (Test C2-19)[7], while the temperature for the top injection was 35 ^{o}C to give enough subcooling to condense all the steam flowed into the upper plenum. This is also based on the results of the CCTF test, which showed the complete condensation of the steam in the upper plenum.

2.4 Measured Boundary conditions

2.4.1 Measured Boundary Conditions of Test S3-7

The major measured test conditions are listed in Table 2.1. Table 2.4 shows the chronology of events occurred during the test. Figures 2.6 to 2.11 show the measured boundary conditions of the test.

There observed no significant differences between the planned and the measured except for the pressure in the containment tank II. The pressure was controlled at 0.3 MPa by venting the excessive steam. However, the steam was not enough to keep the pressure at 0.3 MPa because of significant condensation due to the subcooled ECC water, so that the pressure decreased gradually and was 0.24 MPa at 440 s, as shown in Fig. 2.6.

2.4.2 Measured Boundary Conditions of Test S3-8

The major measured test conditions are listed in Table 2.2. Table 2.5 shows the chronology of events occurred during the test. Figures 2.12 to 2.17 show the measured boundary conditions of the test.

There observed no significant differences between the planned and the measured except for the pressure in the containment tank II. The pressure was controlled at 0.3 MPa by venting the excessive steam. However, the steam was not enough to keep the pressure at 0.3 MPa because of significant condition due to the subcooled ECC water, so that the pressure decreased gradually and was 0.25 MPa at 420 s, as shown in Fig. 2.12.

Table 2.1 Test conditions for Test S3-7

Item	Planned	Measured
Pressure (MPa)		
Containment tank	0.3	0.24 ∿ 0.32
Pressure vessel	0.3	0.24 ∿ 0.32
Power		
Initial power (MW)	7.5	7.5
Decay curve	ANS × 1.03 + Act.	ANS × 1.03 + Act.
Time after scram (s)	25	25
Radial profile	Flat	Flat
Peak clad temperature at ECC water injection initiation (K)	943	964.5
ECC water injection location	UCSP3, UP1 ∿ 4	UCSP3, UP1 ∿ 4
UCSP3 injection		
Injection rate (kg/s)	30	30
Water temperature (K)	343	335 ∿ 378
UP injection		
Injection rate (kg/s)	4 × 2.5	4 × 2.5
Water temperature (K)	308	308 ∿ 327

Table 2.2 Test conditions for Test S3-8

Item	Planned	Measured
Pressure (MPa)		
Containment tank	0.3	0.25 ∿ 0.31
Pressure vessel	0.3	0.25 ∿ 0.32
Power		
Initial power (MW)	7.5	7.5
Decay curve	ANS x 1.03 + Act.	ANS x 1.03 + Act.
Time after scram (s)	25	25
Radial profile	Flat	Flat
Peak clad temperature at ECC water injection initiation (K)	943	970
ECC water injection location	UCSP1 or UCSP3 UP1 ∿ 4	UCSP1 or UCSP3 UP1 ∿ 4
UCSP injection		
Injection rate (kg/s)	30	30
Water temperature (K)	343	337 ∿ 386
UP injection		
Injection rate (kg/s)	4 x 2.5	4 x 2.5
Water temperature (K)	308	310 ∿ 323

Table 2.3 Summary of bases of test conditions

Pressures		
in PV	0.6 MPa → 0.3 MPa	Blowdown from 0.6 MPa
in CT II	0.3 MPa	TRAC calculation
Power		
Initial power	7.5 MW	Scaled value (Following Eq.)
Decay curve	P_0 × (Old ANS × 1.03 + Act.)	Similar to GPWR-EM
Timing at 0.6 MPa	25 s after scram	
$P_{SCTF} = P_{O\ GPWR} \times S_F \times$ (Old ANS × 1.03 + Act.) after t sec		
$P_{O\ GPWR}$	= 3765 MW	
S_F	= 0.8931/21.5 = 1/24.07	
t	= 25	
Power profile	1.04:1.08:1.08:1.04 :1.04:1.04:0.97:0.71	Reserved GPWR power profile against radius
Clad temperature		
Initial PCT (0.6 MPa, GPWR profile)	700°C	・Preserved GPWR initial stored energy ・Referred PKL-IIB-2 result
ECC mode		
CL	3 Acc + 2.6 LPCI	・ECC into broken loop is not considered ・One HL valve is under single failure ・One (LPCI + HPCI) is not working ・One Acc is under repair
HL	2 Acc + 1 LPCI	

Table 2.4 Chronology of events for Test S3-7

Item	Time (s)
Core power "ON"	0
Core power decay initiation	111.6
UCSP3 injection initiation	112.0
UP injection initiation	113.7
BOCREC	157.0
Whole core quench	307.5

Table 2.5 Chronology of events for Test S3-8

Item	Time (s)
Core power "ON"	0
Core power decay initiation	112.8
UCSP injection initiation	113.0
UP injection initiation	115.8
BOCREC	159.5
Switch from UCSP1 to UCSP3	172.5
whole core quench	317.5

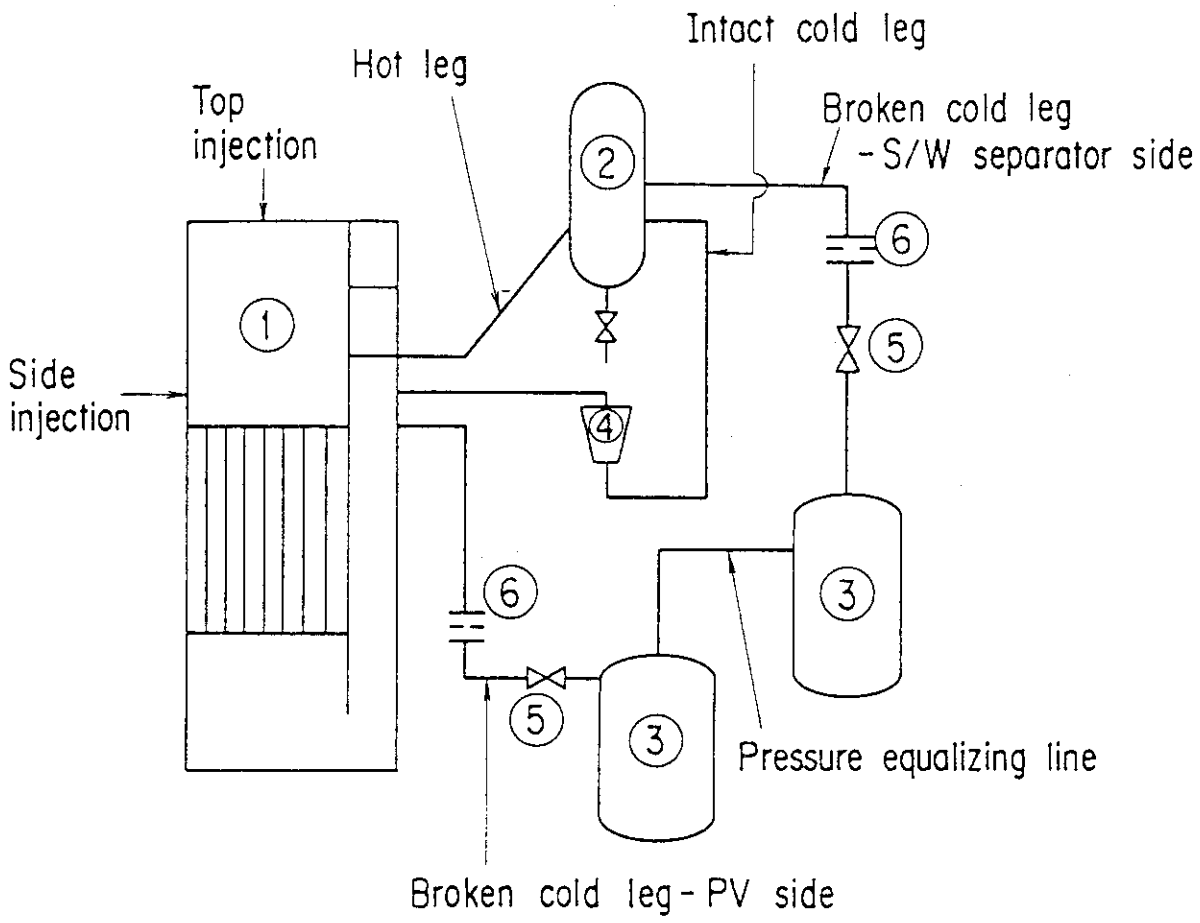

① Pressure vesel
② Steam / water separator
③ Containment tanks
④ Pump simulator
⑤ Break valves
⑥ Flow resistance simulators

Fig. 2.1 Flow diagram of SCTF

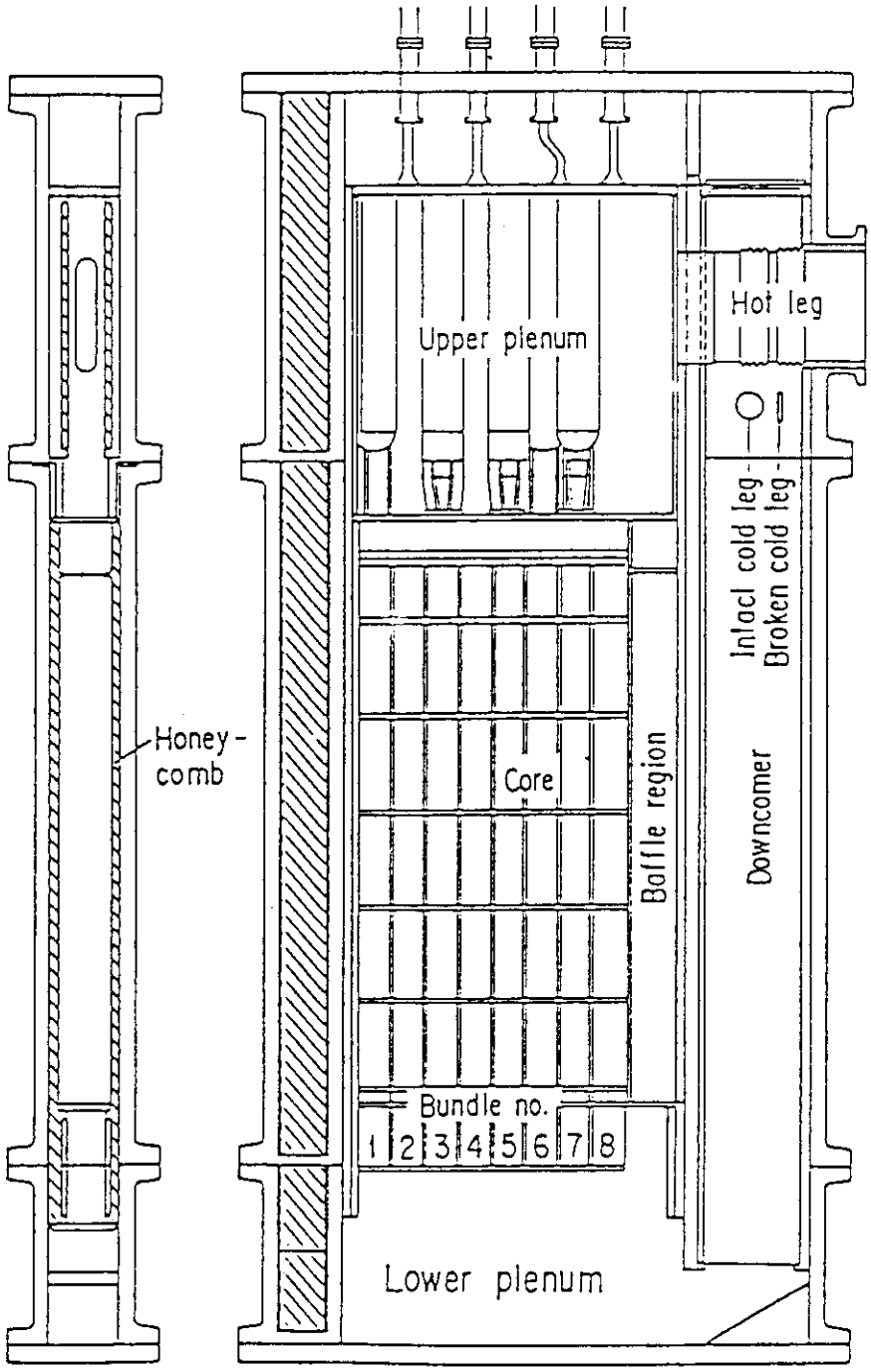

Fig. 2.2 Vertical cross section of pressure vessel

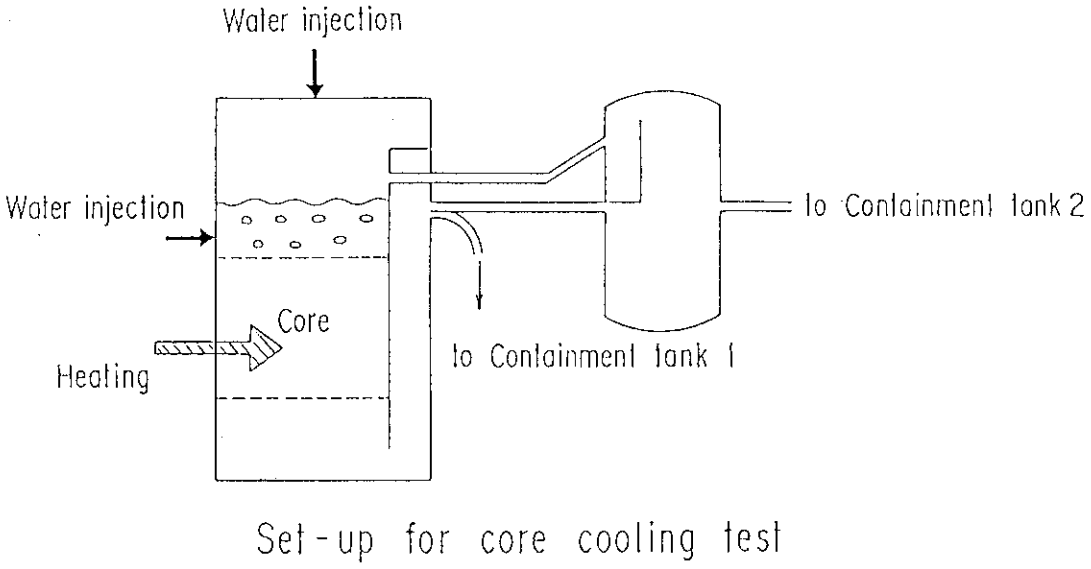

Fig. 2.3 Conceptual set-up of tests

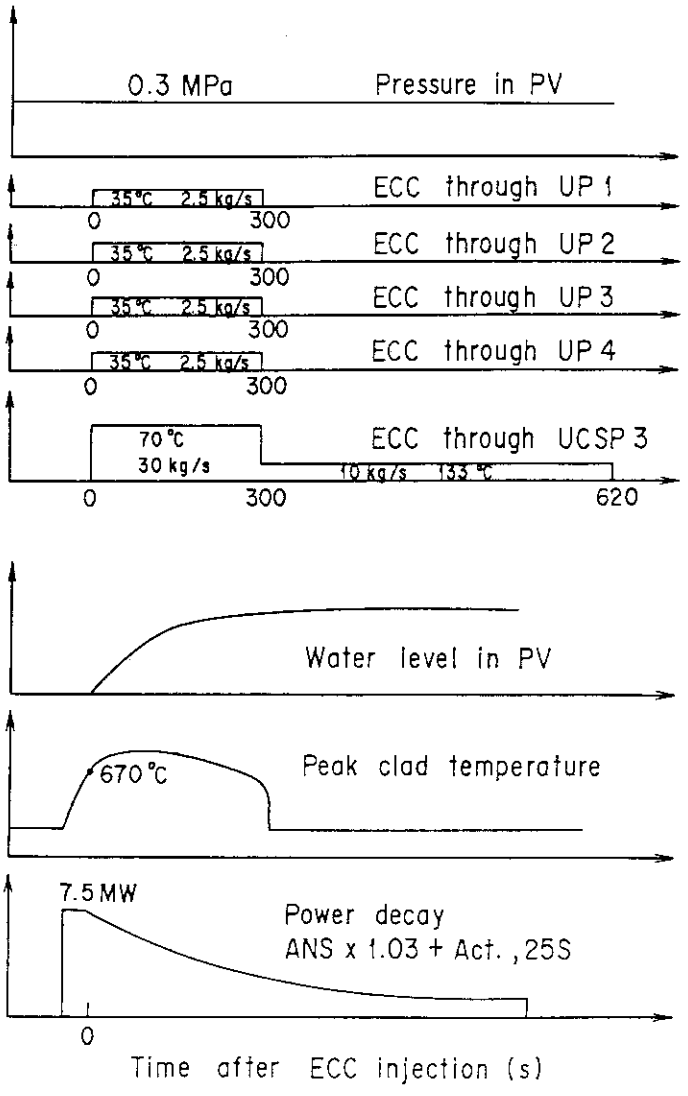

Fig. 2.4 Sequence of Test S3-7

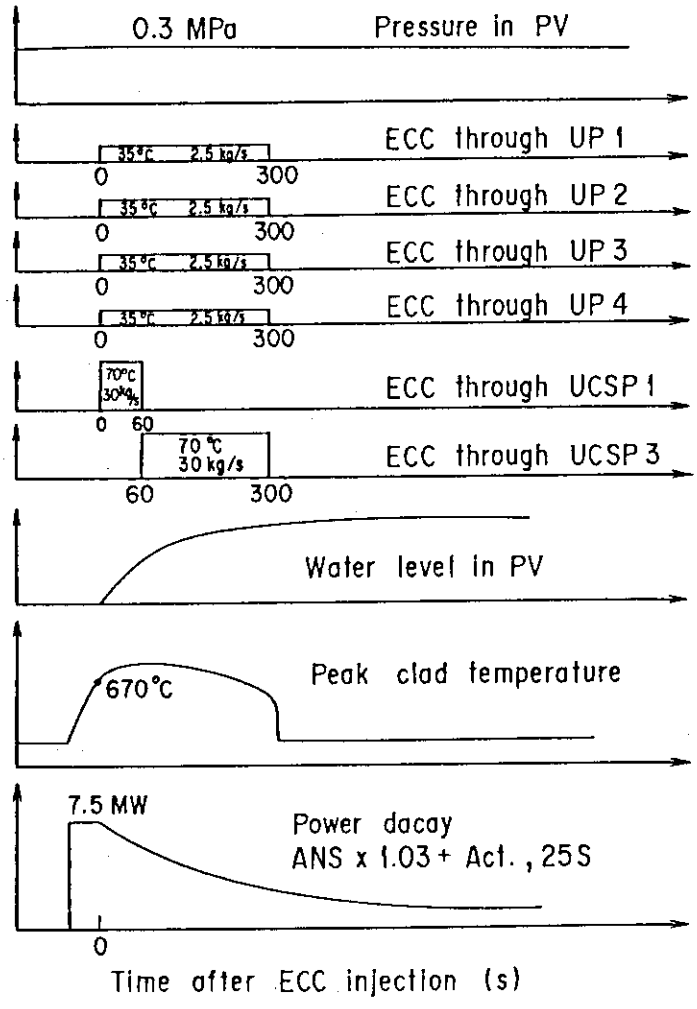

Fig. 2.5 Sequence of Test S3-8

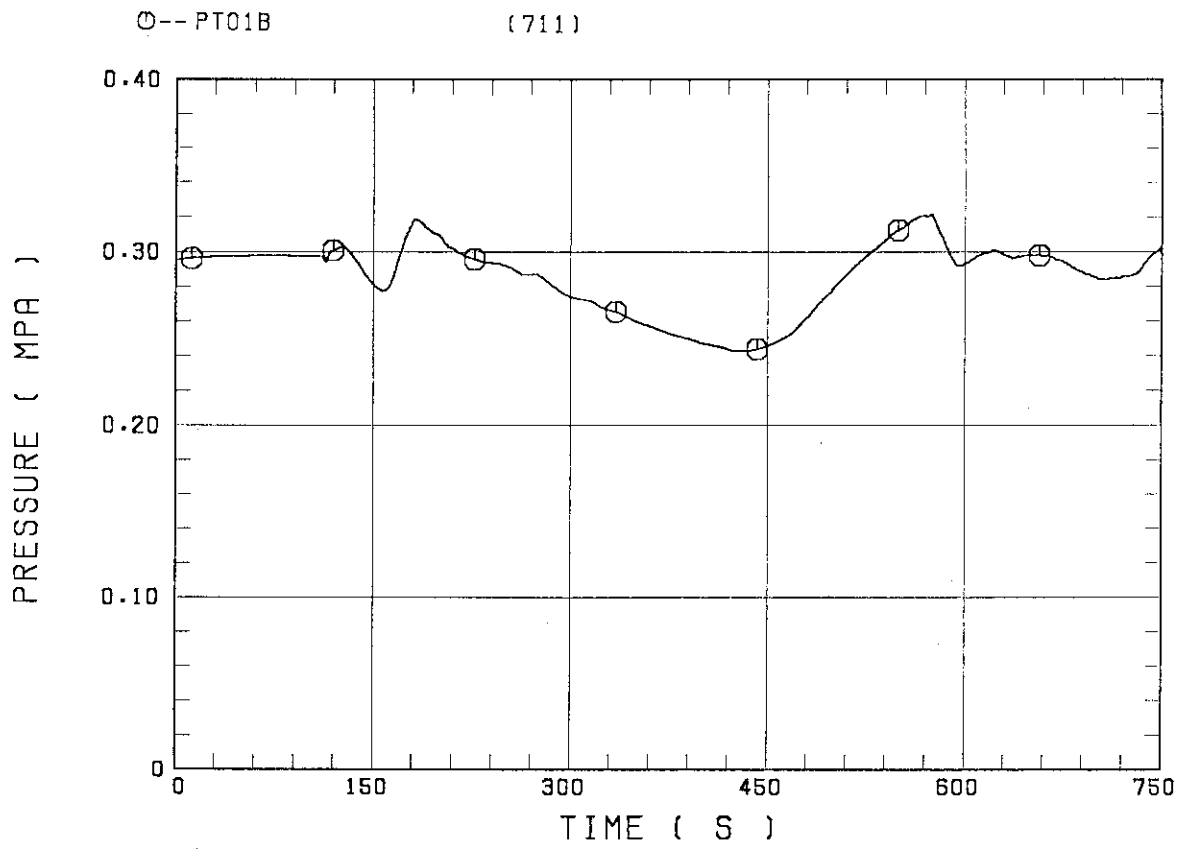

Fig. 2.6 Containment tank II pressure

⏀-- UCSP1 (711) △-- UCSP2 (711)
+-- UCSP3 (711) ×-- UCSP4 (711)

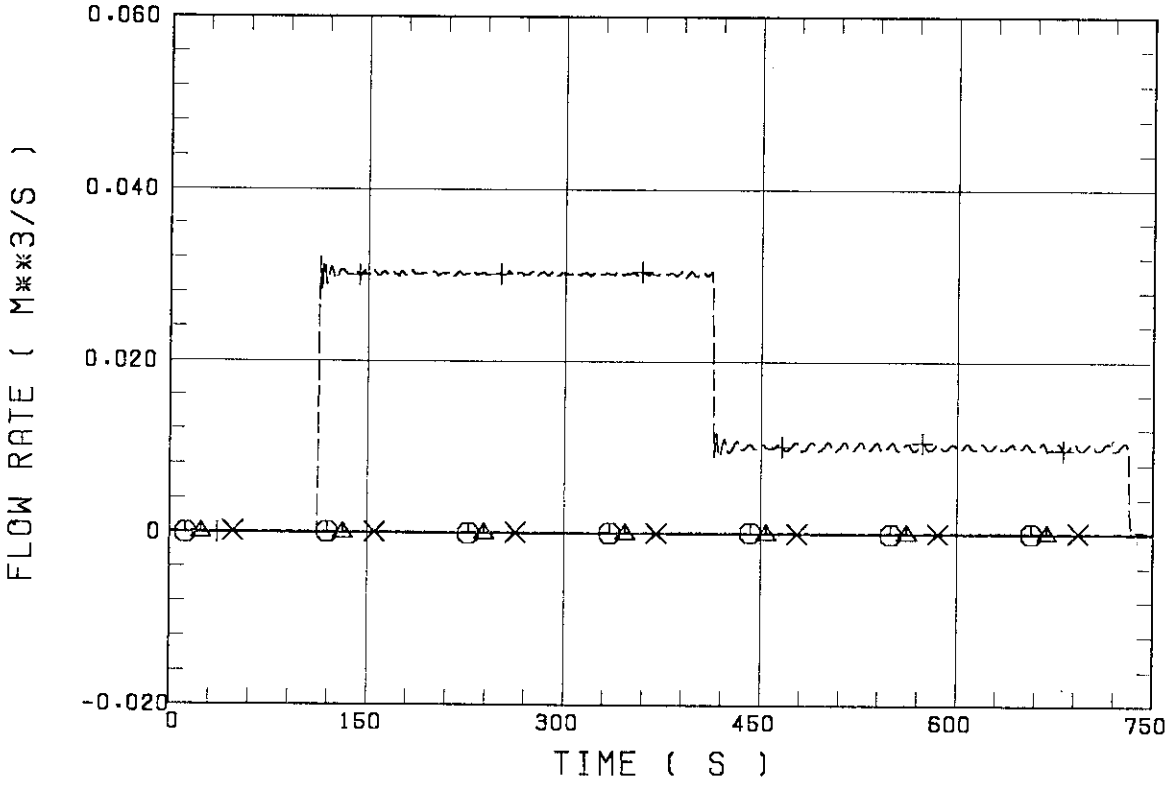

Fig. 2.7 ECC water injection rates for side injection on UCSP

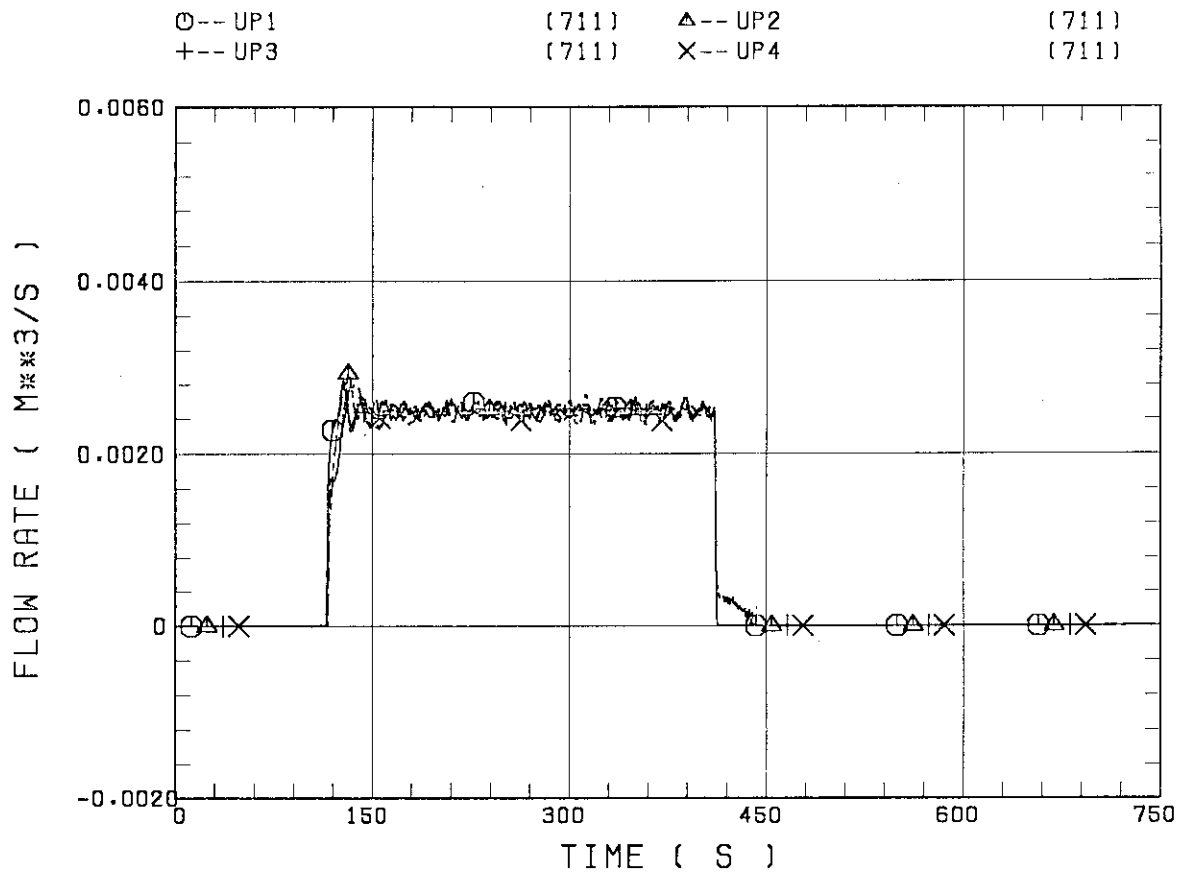

Fig. 2.8 ECC water injection rates for top injection at upper plenum

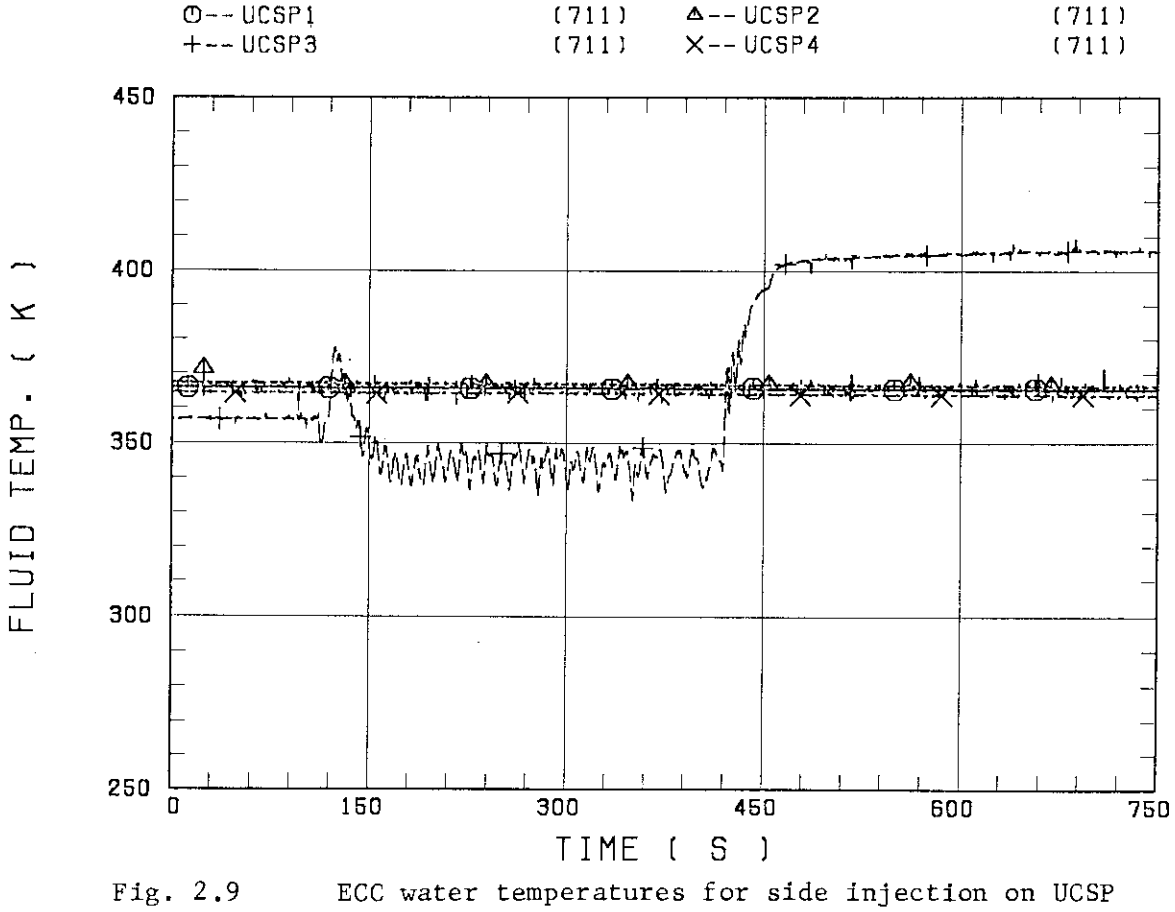

Fig. 2.9 ECC water temperatures for side injection on UCSP

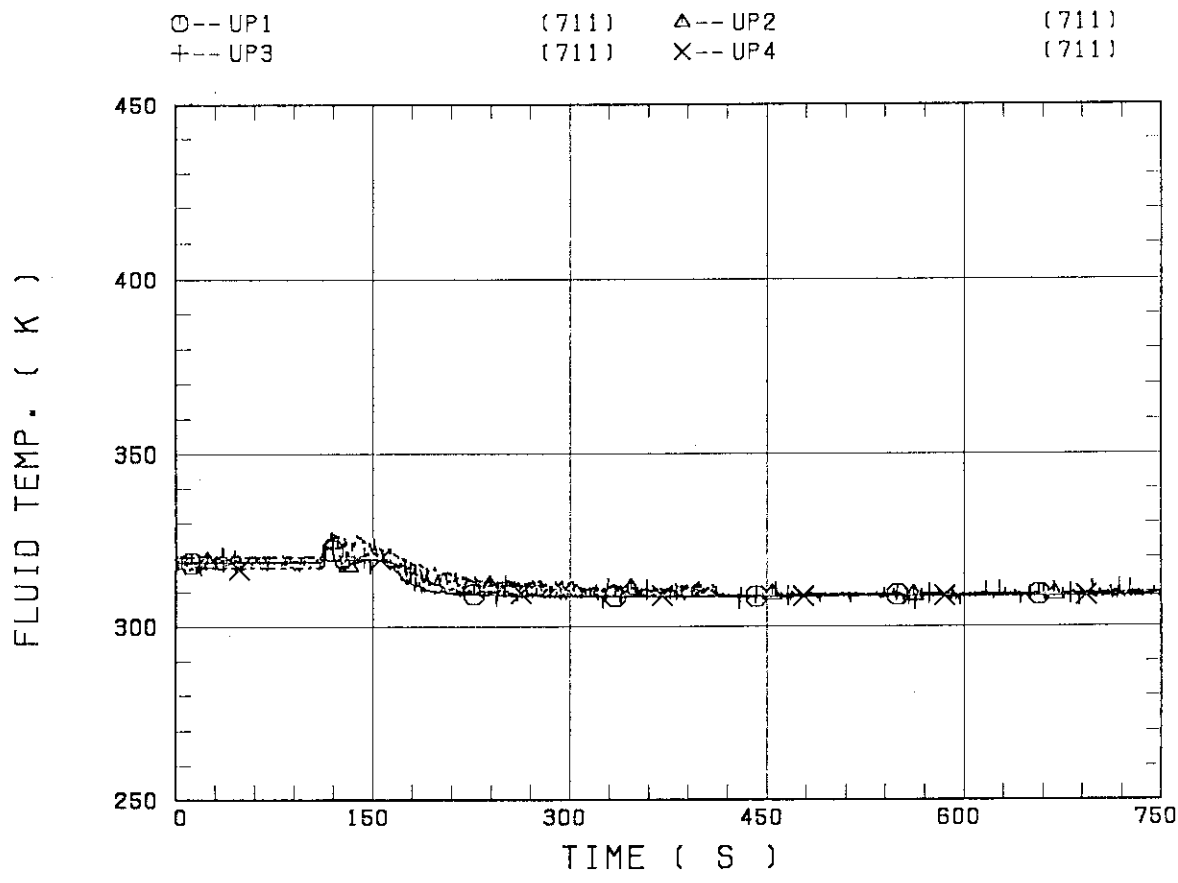

Fig. 2.10 ECC water temperatures for top injection at upper plenum

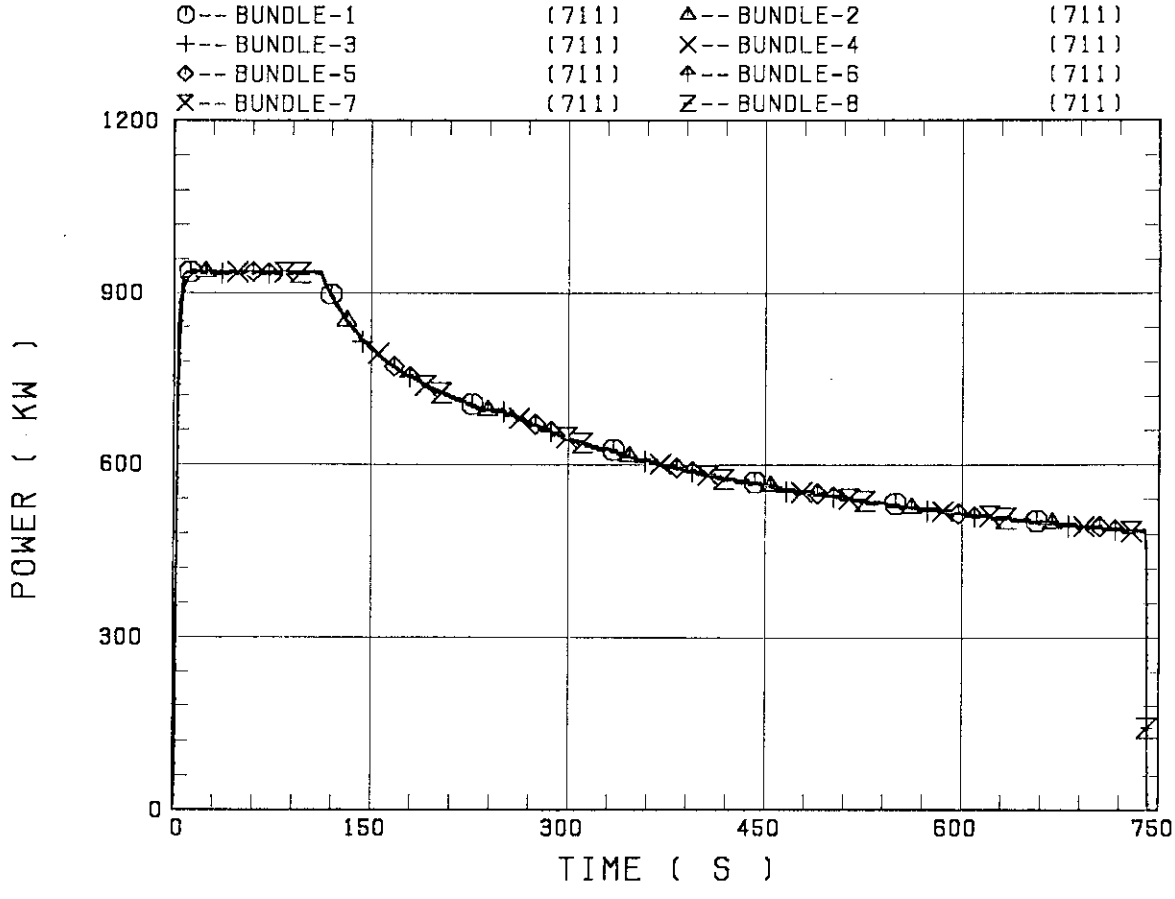

Fig. 2.11 Supplied core powers for each bundle

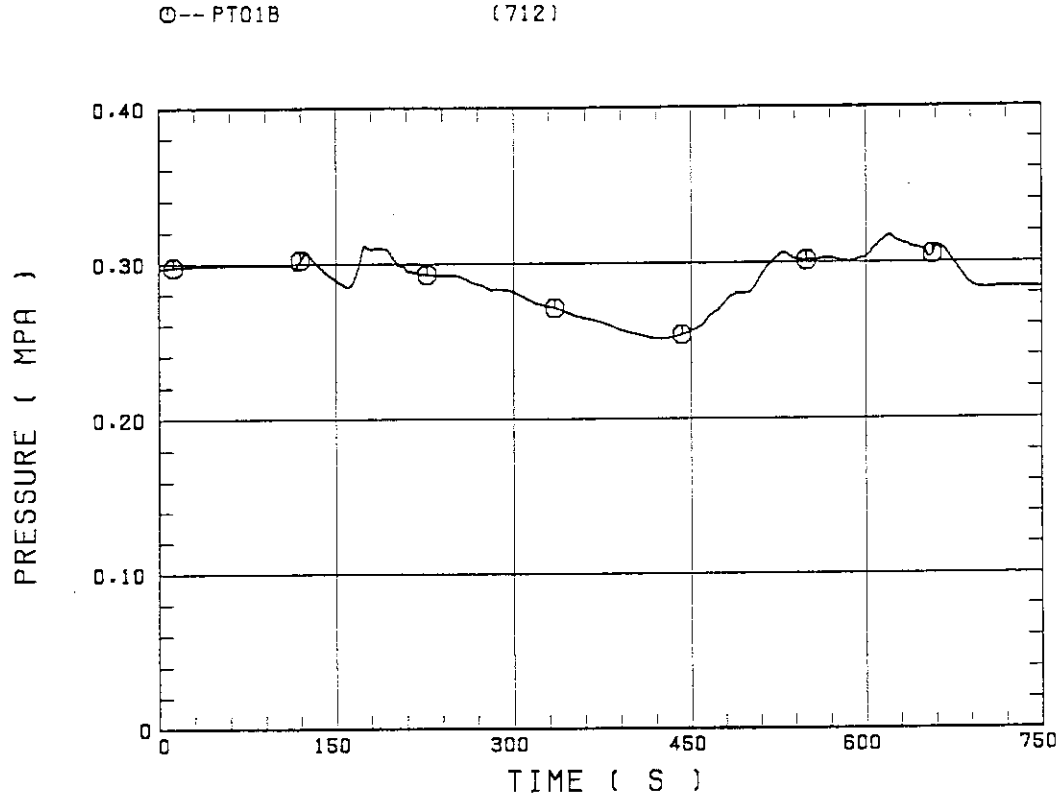

Fig. 2.12 Containment tank II pressure

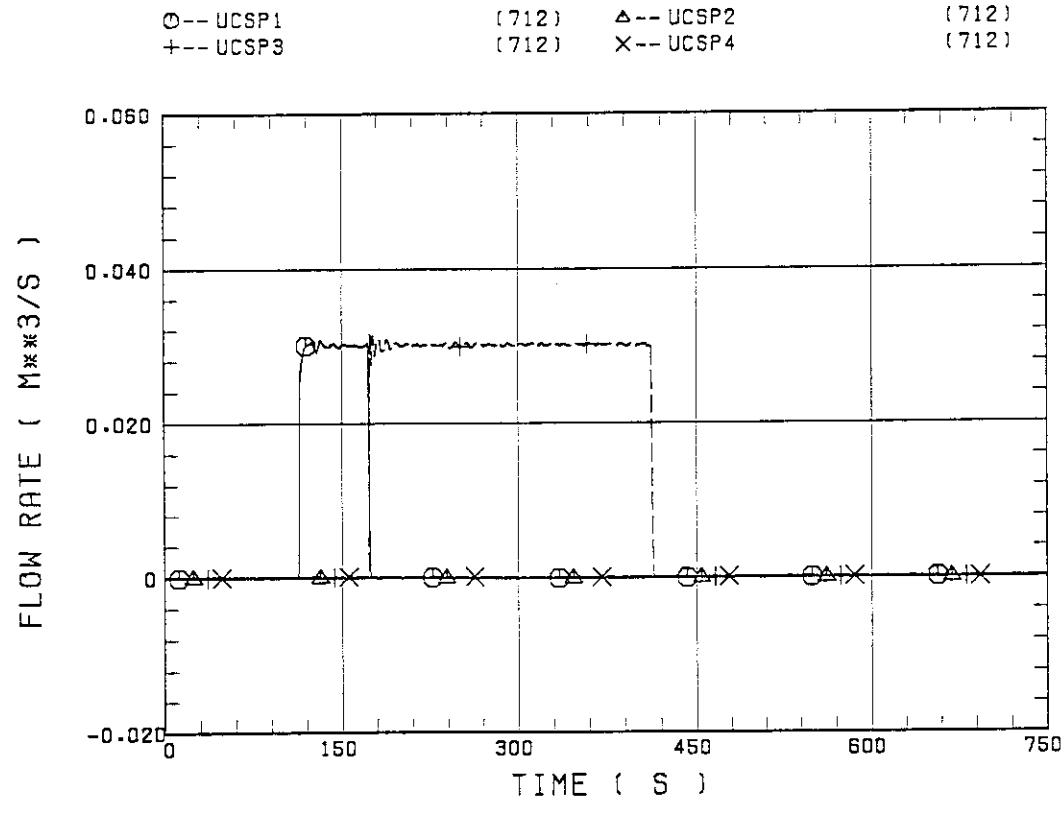

Fig. 2.13 ECC water injection rates for side injection on UCSP

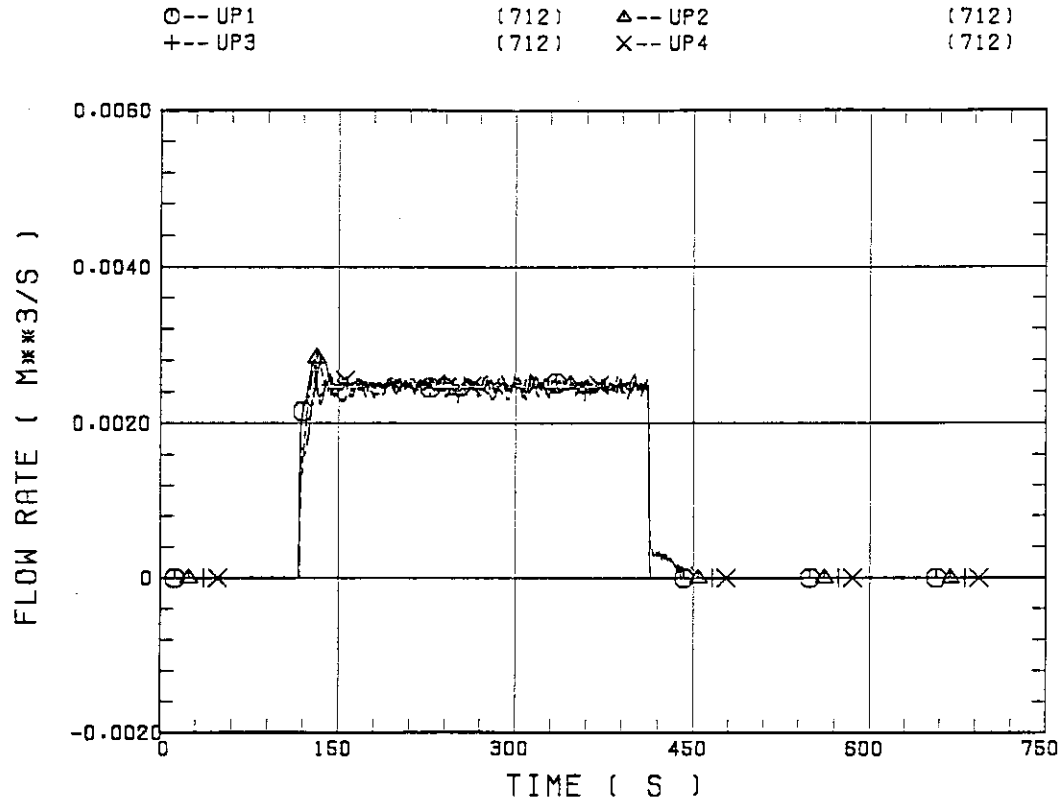

Fig. 2.14 ECC water injection rates for top injection at upper plenum

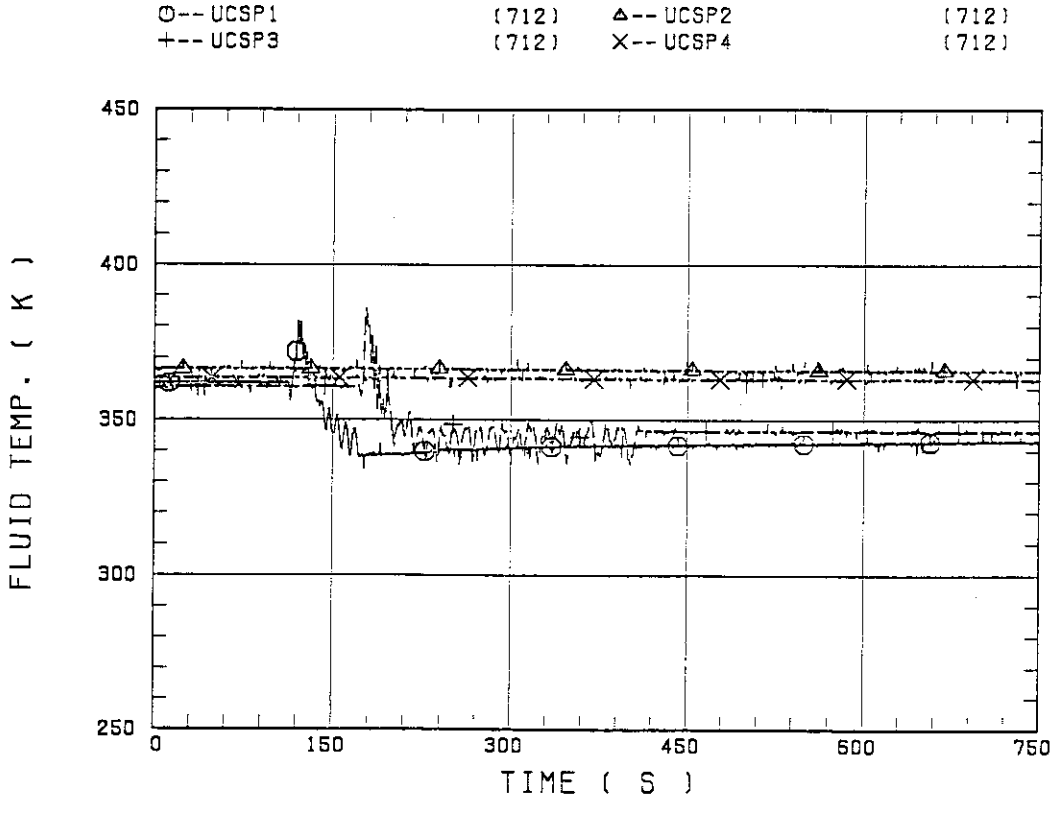

Fig. 2.15 ECC water temperatures for side injection on UCSP

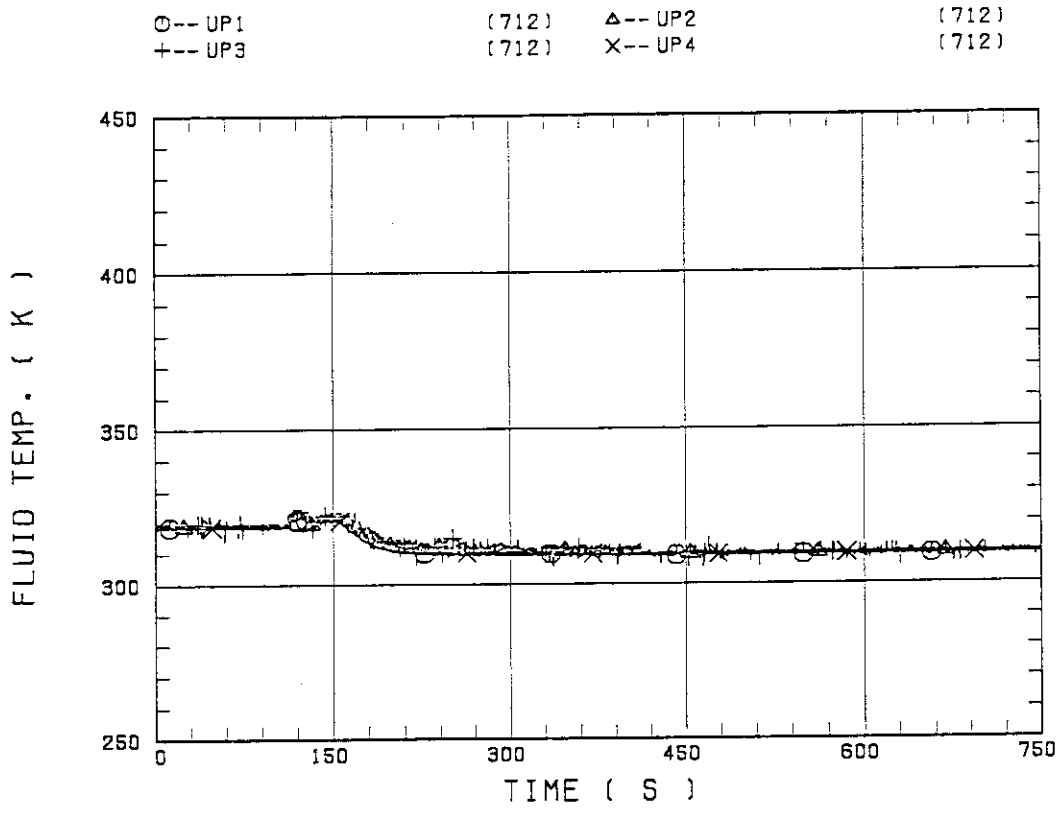

Fig. 2.16 ECC water temperatures for top injection at upper plenum

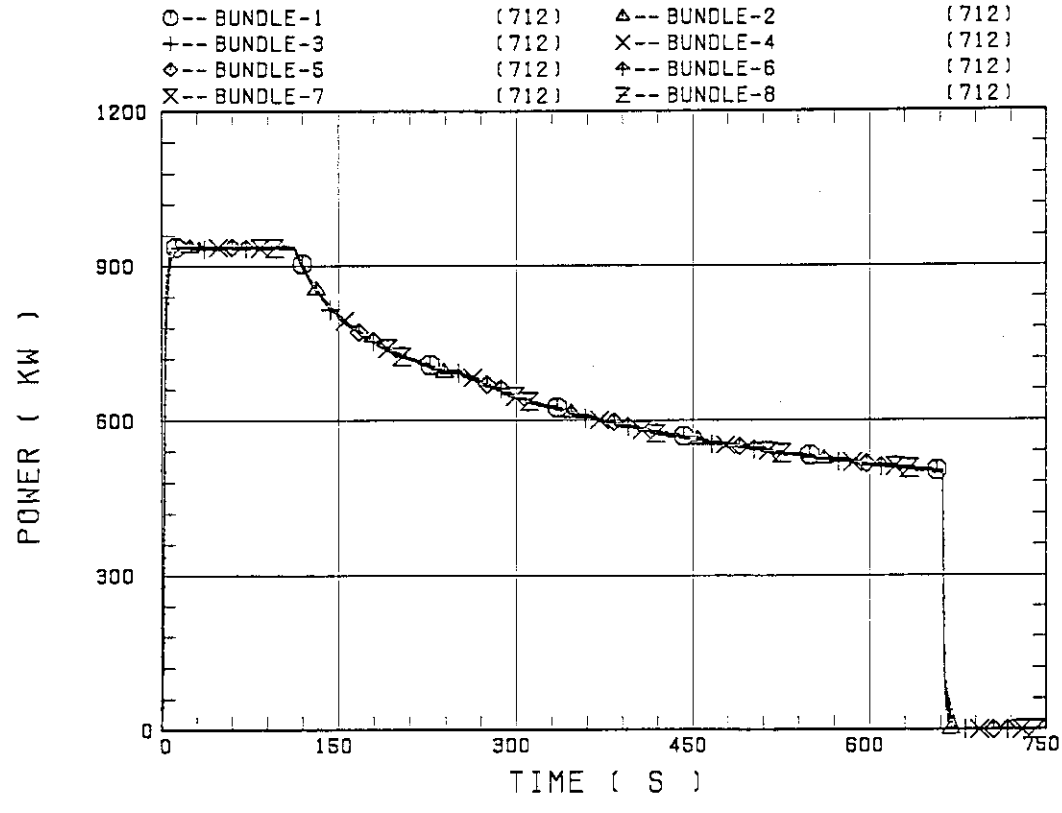

Fig. 2.17 Supplied core powers for each bundle

3. Test Results and Discussion

In this report test data of SCTF Test S3-SH1[6] are also utilized, because the test is the base case test to Tests S3-7 and S3-8. The test conditions for Test S3-SH1 were the same as those for Tests S3-7 and S3-8 except for the water injection location just above the UCSP. In test S3-SH1, the injection location was above Bundles 7 and 8. Major test conditions and chronologies of events are compared among those three tests in Tables 3.1 and 3.2, respectively.

3.1 Break-through Behavior

Occurrence of the break-through is judged based on the data from the fluid temperature, the differential pressure, the break-through detector and the mass flow measurements around the tie plate. The mass flow measurements at the tie plate are performed with an advanced instrumentation (named "flow module") supplied by the USNRC. This consists of drag body, turbine meter, differential pressure cell, thermocouples and pressure gauge. The final outputs from this are the steam and water individual mass flow rates with their directions.

3.1.1 Break-through Behavior observed in Test S3-7

Figures 3.1(a) through (d) show the data for the differential pressures, the fluid temperatures, the break-through detector forces and the water mass flow rates around the tie plate, respectively. For Test S3-7 the differential pressures across tie plate above Bundles 3 and 4 are negative after the ECC water injection initiation. This suggests the occurrence of the break-through above Bundles 3 and 4. On the other hand, the data above the other bundles are positive especially remarkably after the reflood initiation. The positive differential pressure suggests two-phase up-flow and no break-through. Fluid temperatures just below the tie plate hole above Bundles 3 and 4 are lower and subcooled after the ECC water injection initiation, whereas those above the other bundles are identical to the saturation temperature after the reflood initiation. This also suggests the occurrence of the break-through above Bundles 3 and 4. Forces of break-through detectors above Bundles 3 and 7 are shown in Fig. 3.1(c). There are only two break-through detectors in the SCTF. The data above

Bundle 3 shows down-flow, whereas those above Bundle 7 shows up-flow. Tie plate water mass flow rates are shown in Fig. 3.1(d) for Bundles 4, 5 and 8. The flow modules are installed only above Bundles 1, 4, 5 and 8, and it did not work well above Bundle 1. The data only above Bundle 4 show negative value, whereas the others show positive value. These information also suggest the occurrence of the break-through above Bundles 3 and 4.

Figures 3.2(a) through (d) show the same kind of data as Figs. 3.1(a) through (d) for Test S3-SH1. In this test, the ECC water (70 ^{o}C) injection just above the UCSP was performed above Bundles 7 and 8 in order to make the fluid temperature above Bundles 7 and 8 lower and subcooled. From these data the break-through is considered to occur above Bundles 7 and 8 in Test S3-SH1.

3.1.2 Break-through Behavior observed in Test S3-8

Figures 3.3(a) through (d) also show the same kind of data for Test S3-8. In this test, the ECC water injection just above the UCSP was performed above Bundles 7 and 8 during the initial 60 s and then changed to above Bundles 3 and 4 thereafter.

Figure 3.3(a) shows that the tie plate differential pressures above Bundles 7 and 8 are negative during about 60 s after the ECC water injection initiation, whereas they become positive after that time. On the other hand, the data above Bundle 4 are positive during about 60 s after the ECC water injection initiation and becomes negative thereafter. However, the data above Bundle 3 are positive and instead of this the data above Bundle 5 are negative between 60 and 120 s. As shown in Fig. 3.3(b), fluid temperatures above Bundles 7 and 8 are subcooled during about 60 s after the ECC water injection initiation, whereas becomes identical to the saturation temperature thereafter. The data above Bundles 3 and 4, on the other hand, show the saturation or higher temperature during about 60 s after the ECC water injection initiation, while start to show subcooling thereafter. It should be noted here that the fluid temperatures above bundles 3 and 4 are oscillating between the saturation temperature and the subcooled between 15 and 85 s. The similar oscillatory transients are also observed in the tie plate differential pressures above Bundles 3 and 4 (see, Fig. 3.3(a)).

Above data suggest the break-through occurred above Bundles 7 and 8

during the initial 60 s after the ECC water injection and then moved its location to above around Bundles 3 and 4 thereafter, although it took about 70 s to establish the stable break-through above around Bundles 3 and 4. This change of the break-through location corresponds to the change of the ECC water injection location in the test. The data for the break-through detector forces (Fig. 3.3(c)) and water mass flow rates (Fig. 3.3(d)) at the tie plate also support the break-through behavior suggested above.

In Test S3-8 the break-through is considered to occur strongly above Bundle 4 after the change of the ECC water injection location just above the UCSP, whereas above Bundle 3 the break-through is considered to be weak and instead of this there also observed the weak break-through above Bundle 5.

The reason for this little shifting of the break-through location toward Bundle 5 is considered to be the initial ECC water injection above Bundle 7 and 8 in this test. As observed in Fig. 3.3(b), the fluid temperatures around the tie plate were low and subcooled above Bundle 5 and 6 during the initial period, which is considered to be resulted from the subcooled ECC water injection above Bundles 7 and 8. This suggests the fluid temperature above Bundle 5 was already lower than those above Bundles 3 and 4 when the ECC water injection location was changed, resulting in the weak break-through above Bundle 5 due to the partial supply of the subcooled ECC water injected above Bundles 3 and 4.

Another characteristic behavior observed in Test S3-8 is the oscillatory break-through between 15 and 85 s. As already described there observed no break-through above Bundle 3 and 4 before 15 s. This means that the saturated two-phase up-flow is established in that area before the initiation of the ECC water injection there and this suppresses the occurrence of the stable break-through for about 70 s repeating the occurrence and the halt one after the other. The duration of this type of oscillatory break-through is considered to be varied depending on the magnitudes of the subcooling and the injection rate of the ECC water.

3.1.3 Summary

Figure 3.4(a) through (c) show the fluid temperature distribution in the core two-dimensionally at several selected times for Tests S3-SH1, S3-7 and S3-8, respectively. They also give the information on the break-

through and are consistent with the results and discussion above.

Summarizing test results and discussion presented above,

(1) The break-through occurs at the location where the water temperature is subcooled at the tie plate area.

(2) The break-through location changes following the change of the water temperature distribution at the tie plate area. In this case, it was observed to take a certain time (70 s in Test S3-8) to establish the new stable break-through.

3.2 Core Cooling Behavior

3.2.1 Core Cooling Behavior observed in Test S3-7

Figures 3.5(a) and (b) show the clad surface temperatures for Test S3-7 at 1.905 m and 2.76 m elevations, respectively. Figures 3.6(a) and (b) show the corresponding heat transfer coefficients. The temperatures in Bundles 3 and 4 start to decrease immediately after the ECC water injection and quench very early. Also in Bundles 2 and 5, which are neighbor bundles to Bundles 3 and 4, good core cooling is observed before reflood initiation. However, their core cooling become worse around reflood initiation and the heat transfer coefficients become very close to those of the other non-break-through bundles after the reflood initiation. At the top region of the core, the effect of the break-through on core cooling in the non-break-through region is not negligible, making the quench times earlier, as shown in Fig. 3.7.

Therefore, it is recognized that the core cooling is significantly different between the break-through region and the non-break-through region, and the core cooling in the break-through region is significantly good. Also, the core cooling in the non-break-through region is almost identical after the reflood initiation regardless of the distance from the break-through region in the central region of the vertical direction. These are the same characteristics as observed in Test S3-SH1[6]. Figure 3.8 shows the comparison of the rod surface temperatures between Test S3-7 and S3-SH1 at 1.905 m elevation. The transients in Bundle 1, non-break-through region, are close to each other in both tests. The transients in the break-through region, Bundles 3 and 4 in Test S3-7 and Bundles 7 and 8 in Test S3-SH1, are also close to one another in both tests. Therefore, although the break-through location was different between Tests S3-7 and

S3-SH1, core cooling behaviors in the break-through region and in the non-break-through region were observed to be close to each other in the two tests, respectively.

3.2.2 Core Cooling Behavior observed in Test S3-8

Figure 3.9(a) and (b) show the clad surface temperatures for Tests S3-8 at 1.905 m and 2.76 m elevations, respectively. Figures 3.10(a) and (b) show the corresponding heat transfer coefficients. The temperatures in Bundles 7 and 8 start to decrease immediately after the ECC water injection. After the reflood initiation, the rod in Bundle 7 quenches soon, however, the temperature of the rod in Bundle 8 goes up after the change of the ECC water injection location from above Bundles 7 and 8 to above Bundles 3 and 4. After the change of the injection location, the temperatures in Bundles 4 and 5 starts to decrease, however, the decrease is not monotonous but stepwise. This stepwise core cooling is considered to result from the oscillatory break-through behavior mentioned in Sec. 3.1.2.

Figure 3.11(a) and (b) show the comparison of rod surface temperatures between Tests S3-8 and S3-SH1 for the non-break-through region and the break-through region, respectively. The comparison in the non-break-through region, *i.e.* Bundle 1, shows the different transients after the change of the injection location. As previously described, the break-through was not stable but oscillatory after the change of the injection location in Test S3-8. This is considered to result in the worse core cooling in this test comparing to that in Test S3-SH1. Figure 3.11(b) shows the drastic effect of the injection location change. In Bundle 8, the temperature transients in both tests are almost identical before the change of the injection location. However, after the change, the temperature in Test S3-8 starts to increase and quenches much later, whereas that in Test S3-SH1 continues to decrease and quenches soon. On the other hand, in Bundle 4, the core cooling in Test S3-8 is not much better comparing to that in Test S3-SH1. This is considered to result from the oscillatory break-through behavior in Test S3-8 as already mentioned.

Therefore, it can be said that when the break-through location is changed during reflooding and when it takes some time to establish the stable break-through, the core cooling after the change of the break-through location becomes worse in both the break-through and the non-break-

through regions.

3.2.3 Summary

Summarizing the test results and discussion above,

(1) When the stable break-through occurs, the core cooling behavior is distinguished clearly between the break-through region and the non-break-through region, and the core cooling in the break-through region is significantly good.

(2) Even when the break-through locations are different, the core cooling in each non-break-through region is almost the same being regardless of the difference in the break-through location, and so is in the break-through region.

(3) When the break-through location is changed during reflooding and when it takes a certain time to establish a new stable break-through, the core cooling in the non-break-through region becomes worse.

3.3 Other Thermo-hydrodynamic Behaviors

3.3.1 Core and Upper Plenum Differential Pressures

Figure 3.12(a) and (b) show apparent core void fractions converted from differential pressure data for Test S3-7 and S3-8, respectively. Except for the top section, values are in good agreement among bundles at each elevation in both tests. Figures 3.13(a) and (b) show upper plenum water levels converted from the upper plenum differential pressures above the UCSP for Tests S3-7 and S3-8, respectively. These figures show the upper plenum differential pressure or water level is also radially uniform. On the other hand, those two data for Test S3-SH1 are not radially uniform[6]. Figures 3.14(a) and (b) show the examples. The reason for the difference among those data is considered to be the break-through location. The break-through locations in Tests S3-7 and S3-8 are around Bundles 3 and 4, which is horizontally middle of the SCTF, and the break-through water is considered to be easily distributed horizontally equally comparing to the peripheral break-through case (*i.e.* Test S3-SH1).

Figures 3.15(a) and (b) show the comparison of core and upper plenum differential pressures between Tests S3-7 and S3-SH1, respectively. Core differential pressures in the lower half section are close to each other,

whereas those in the upper half section are different a lot and Test S3-7 gives the lower value. On the other hand, the upper plenum differential pressure of Test S3-7 is higher than in Test S3-SH1 and the difference is close to the difference in the core differential pressure.

Figure 3.16 shows the core horizontal differential pressures for Test S3-7. Data shown in the figure indicate the pressure at Bundle 4 is lower than those at Bundles 1, 2 and 8 before the arrival of water accumulation front, whereas the pressure becomes higher after that. This suggests that the steam flows to the break-through region from the non-break-through region above water accumulation front, whereas the water flows from the break-through region to the non-break-through region below that. This phenomena is also observed in Test S3-SH1[6], but is not clear in Test S3-8.

3.3.2 Steam Generation and Condensation in Vessel

The estimated maximum steam generation rates of all bundles are shown in Figs. 3.17(a) and (b) for Test S3-7 and S3-8, respectively. They are calculated by the heat releases from the rods. As shown in the figures, the heat release occurs immediately after the ECC water injection in the break-through region, whereas it occurs after the reflood initiation in the non-break-through region. Figures 3.18(a) and (b) show the steam mass flow rates condensed in the core (in the non-break-through region) and the upper plenum for Test S3-7 and S3-8, respectively. In Test S3-7 the average steam generation rate in the non-break-through region is about 4 kg/s and its condensation rate is about 2 kg/s. This means about 50% of the generated steam is condensed in the core, probably due to the cross flow to the break-through region and the subcooling of the reflooding water. On the other hand, in the upper plenum, the condensation rate is very high and over 80%. The tendency is the same as in Test S3-8.

Table 3.1 Comparison of major test conditions

Test No.	S3-SH1	S3-7	S3-8
Pressure (MPa)	0.3	*	*
Init. core power (MW)	7.3	*	*
Power decay	ANS×1.03+Act.	*	*
Radial power distribution	Flat	*	*
Max. init. clad temp. (K)	943	*	*
UCSP inj. rate (kg/s)	30	*	*
UCSP inj. temp. (K)	343	*	*
UCSP inj. location	Above B. 7 & 8	Above B. 3 & 4	Above B. 7 & 8 (0 - 60 s) Above B. 3 & 4 (60 - 300 s)
UP inj. rate (kg/s)	4×2.5	*	*
UP inj. temp. (K)	308	*	*
UP inj. location	All	*	*
LP init. water level (m)	0	*	*

* : The same as for Test S3-SH1 (base case).

Table 3.2 Comparison of chronologies of events

Test No.	S3-SH1	S3-7	S3-8
Core power "ON"	0 s	0 s	0 s
UCSP injection initiation	111.0	112.0	113.0
Core power decay initiation	111.5	111.6	112.8
UP injection initiation	113.5	113.7	115.8
Reflood initiation	157.0	157.0	159.5
Whole core quench	289.5	307.5	317.5

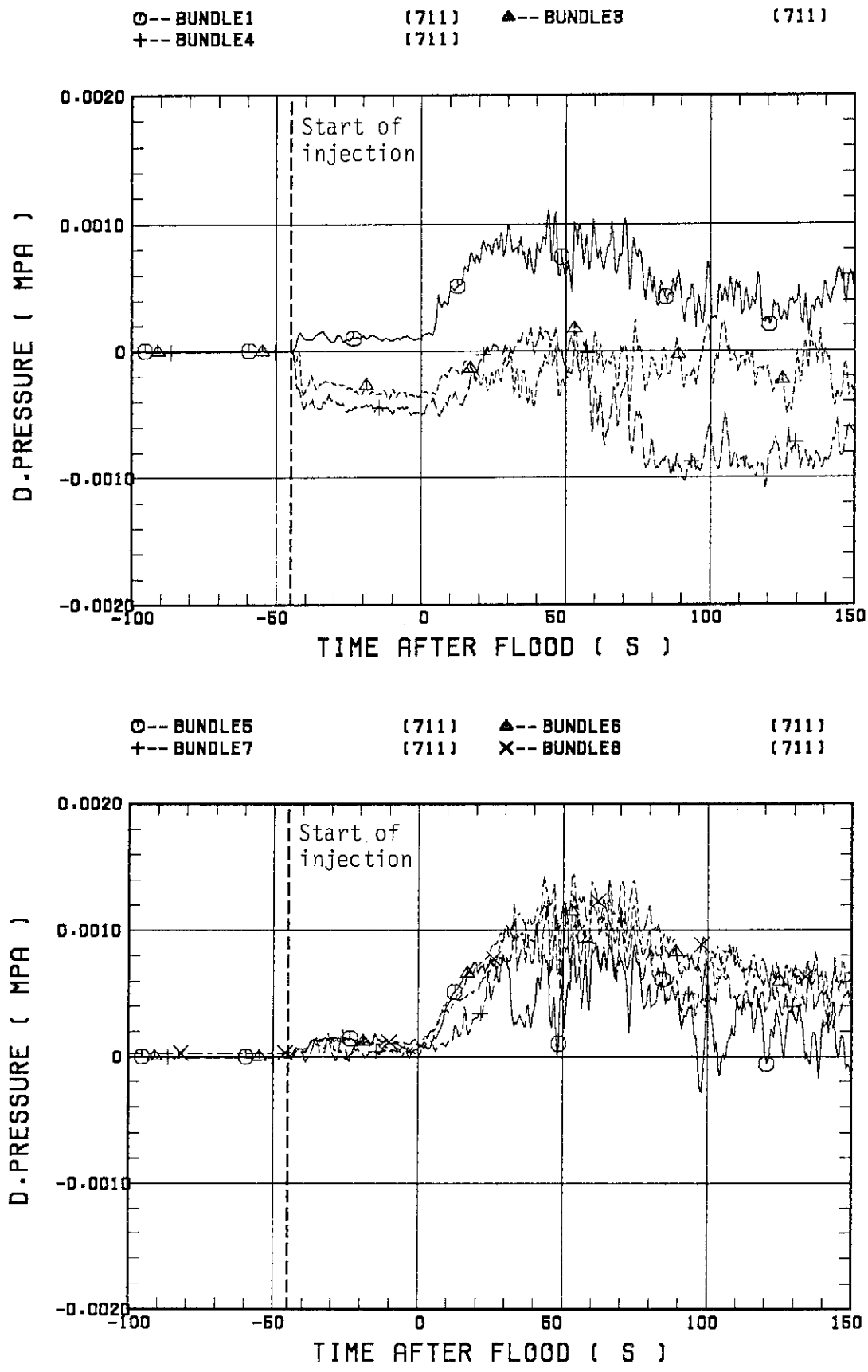

Fig. 3.1(a) Differential pressures across tie plate for Test S3-7

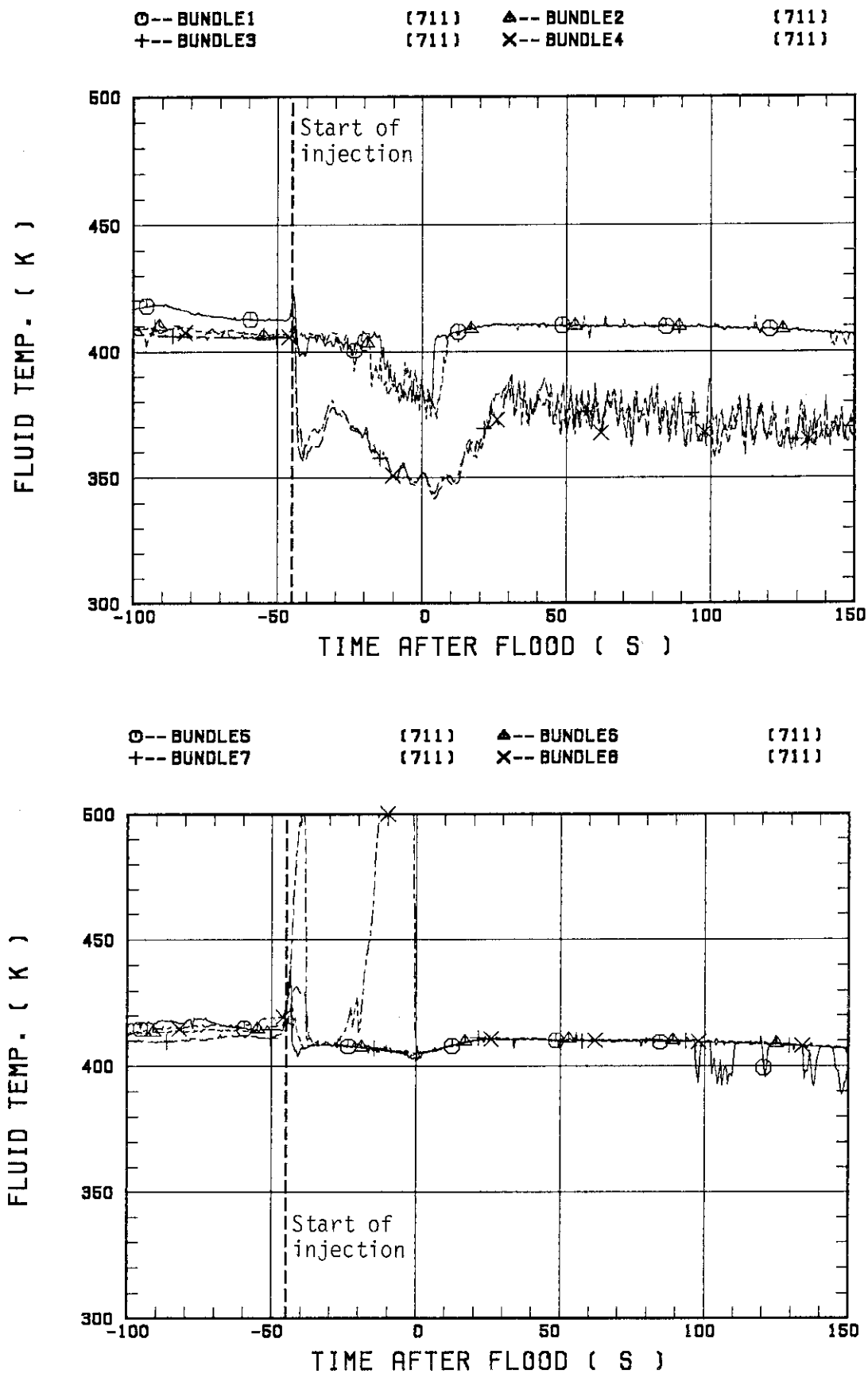

Fig. 3.1(b) Fluid temperatures just below tie plate hole for Test S3-7

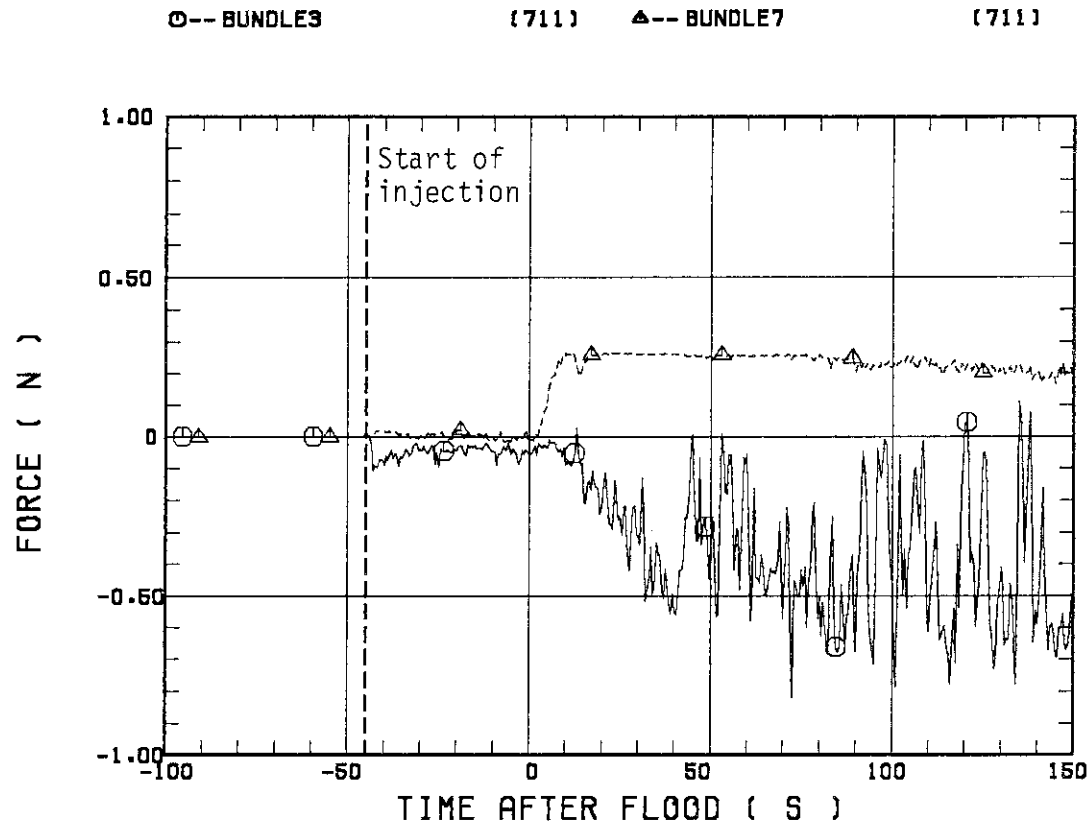

Fig. 3.1(c) Break-through detector forces for Test S3-7

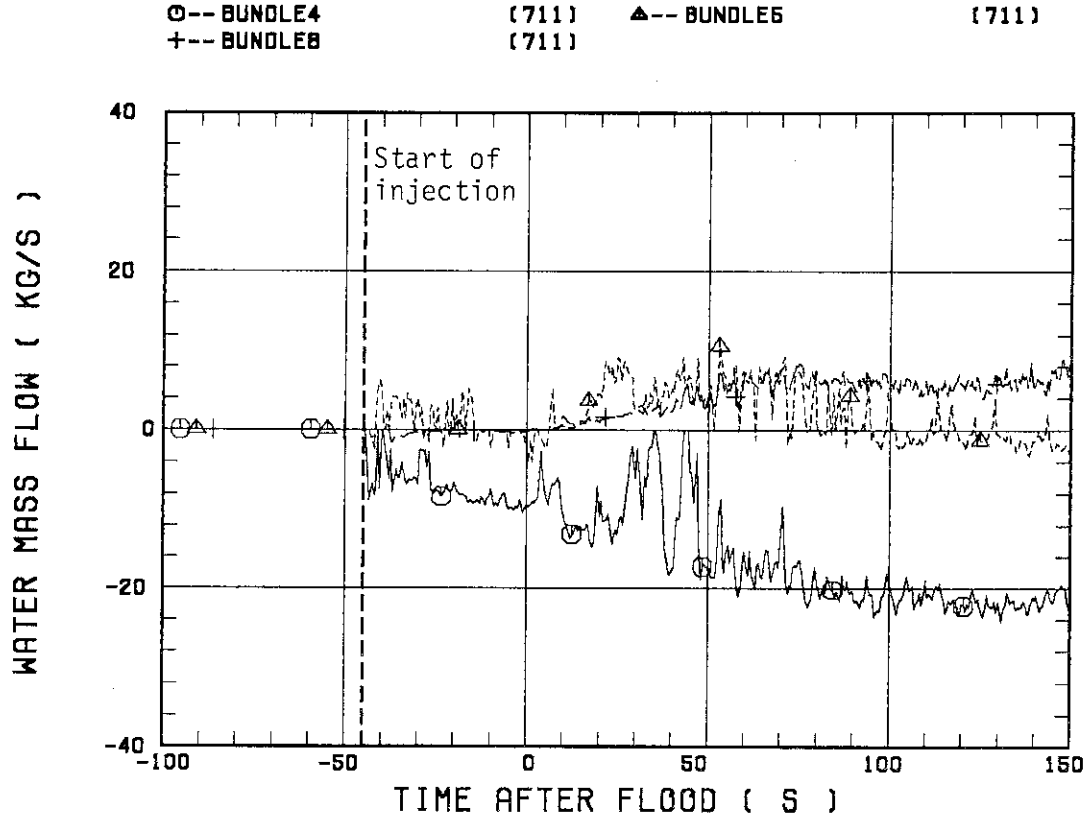

Fig. 3.1(d) Water mass flow rates at tie plate for Test S3-7

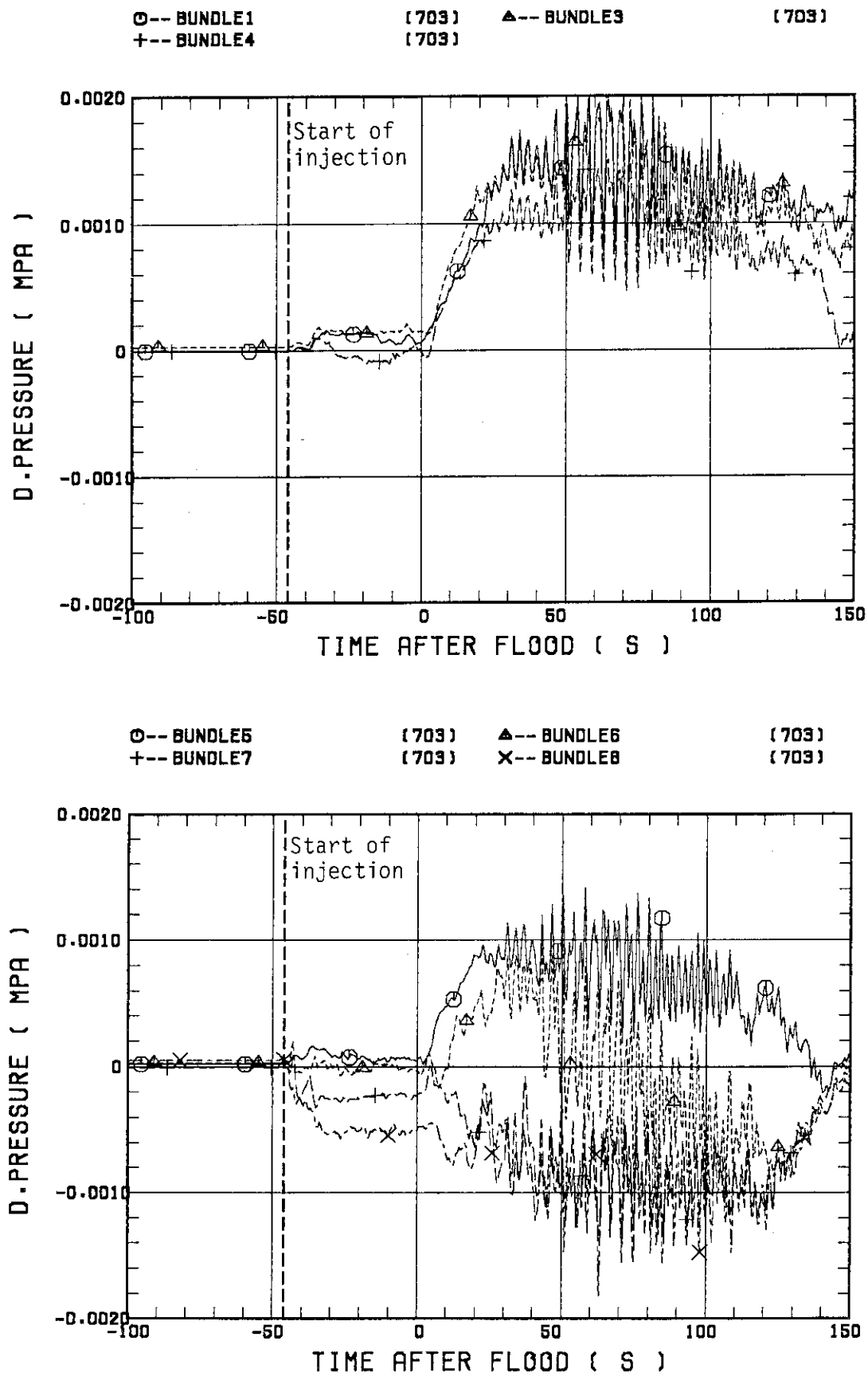

Fig. 3.2(a) Differential pressures across tie plate for Test S3-SH1

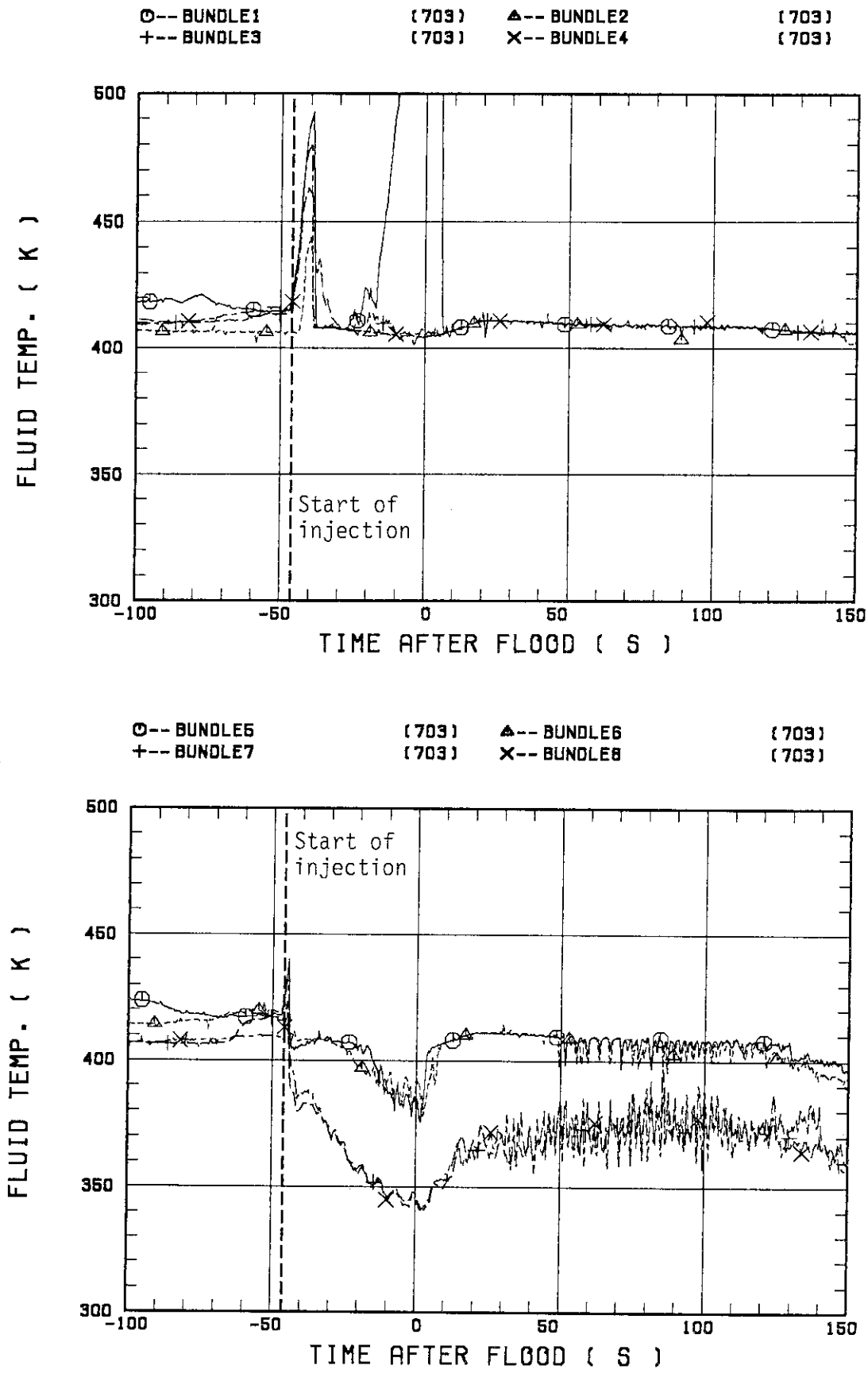

Fig. 3.2(b) Fluid temperatures just below tie plate hole for Test S3-SH1

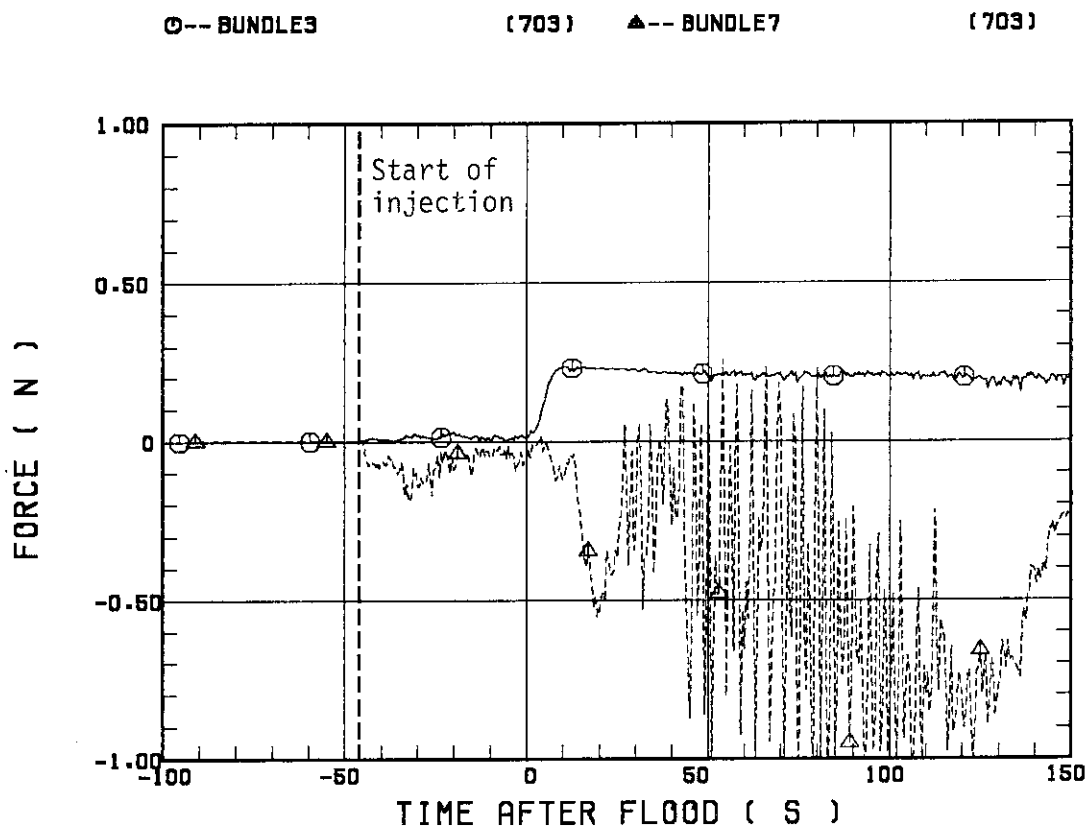

Fig. 3.2(c) Break-through detector forces for Test S3-SH1

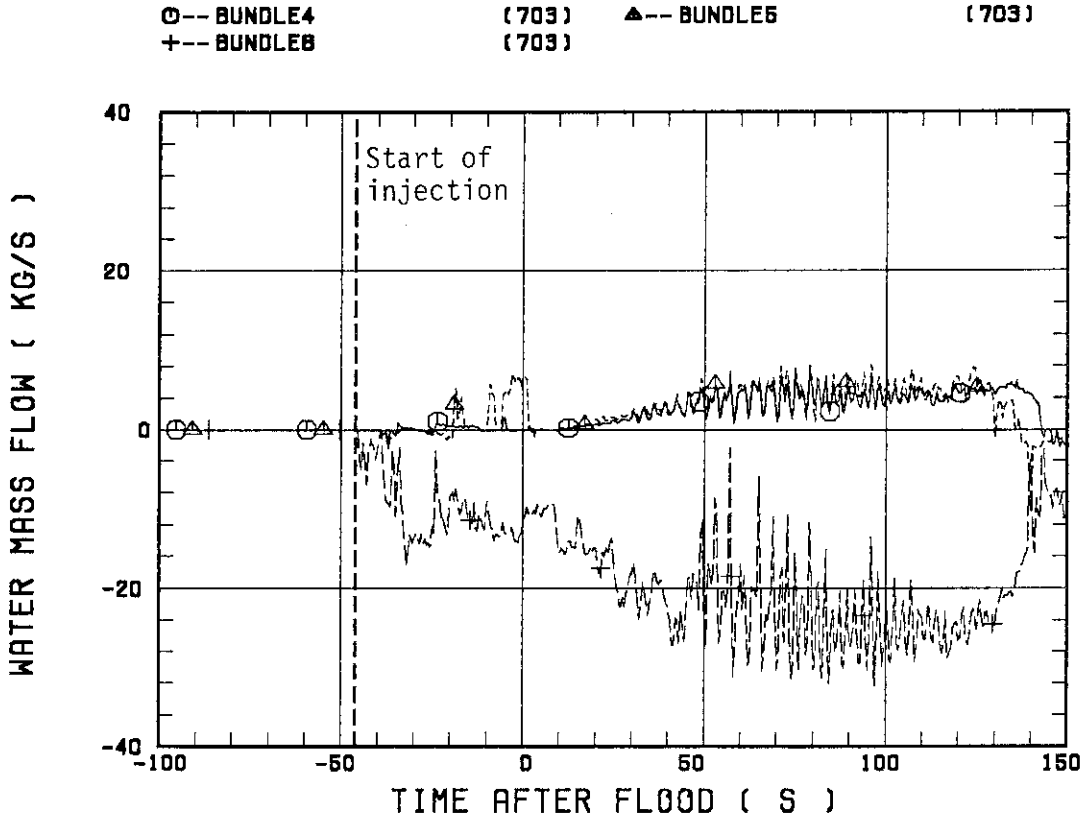

Fig. 3.2(d) Water mass flow rates at tie plate for Test S3-SH1

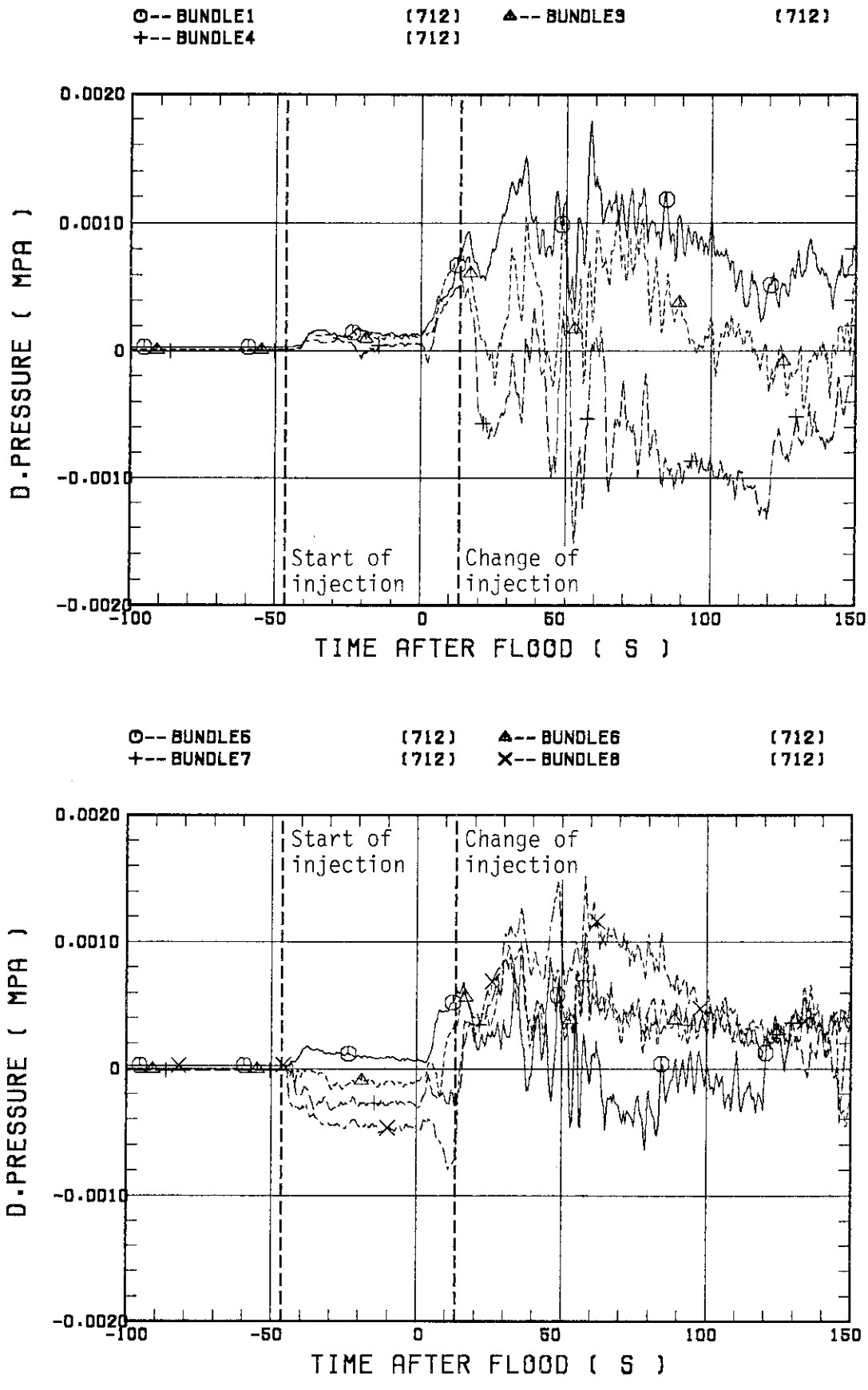

Fig. 3.3(a) Differential pressures across tie plate for Test S3-8

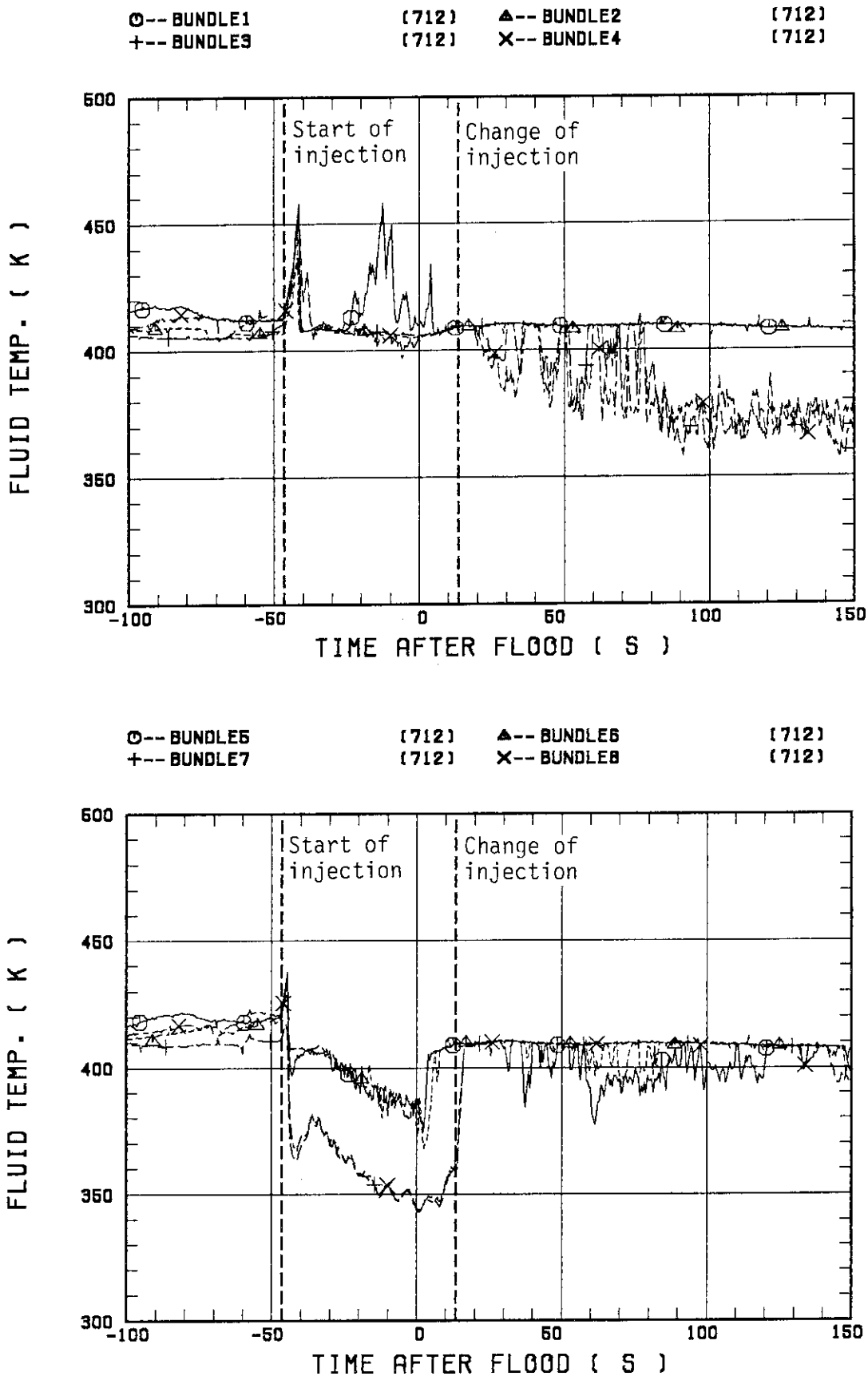

Fig. 3.3(b) Fluid temperatures just below tie plate hole for Test S3-8

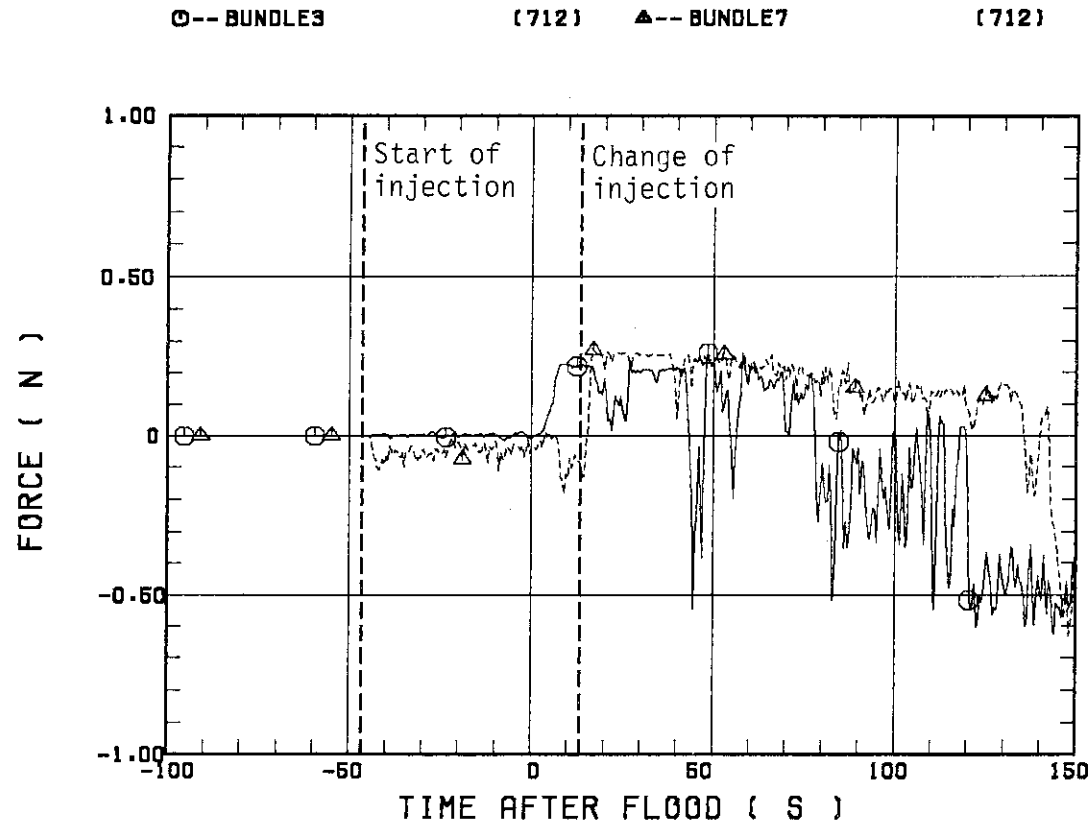

Fig. 3.3(c) Break-through detector forces for Test S3-8

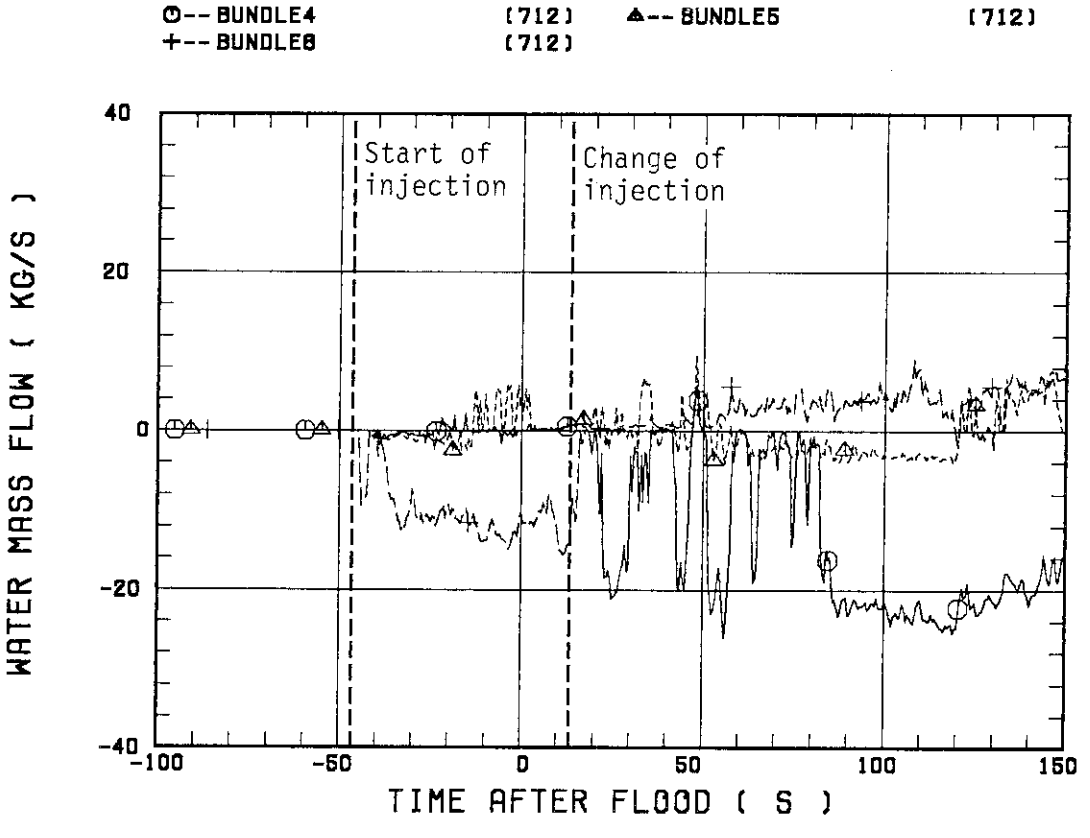

Fig. 3.3(d) Water mass flow rates at tie plate for Test S3-8

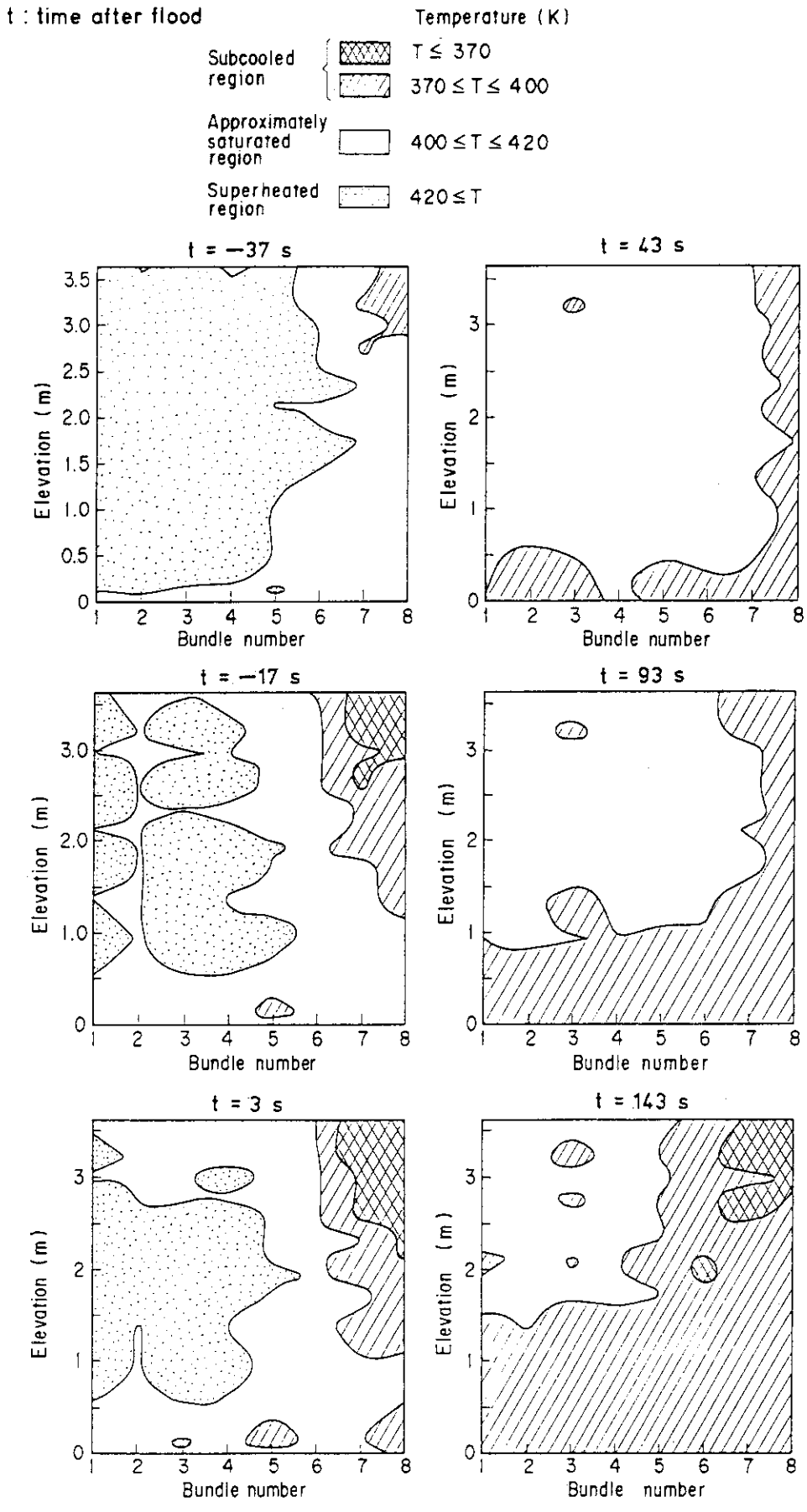

Fig. 3.4(a) Core fluid temperature distribution for Test S3-SH1

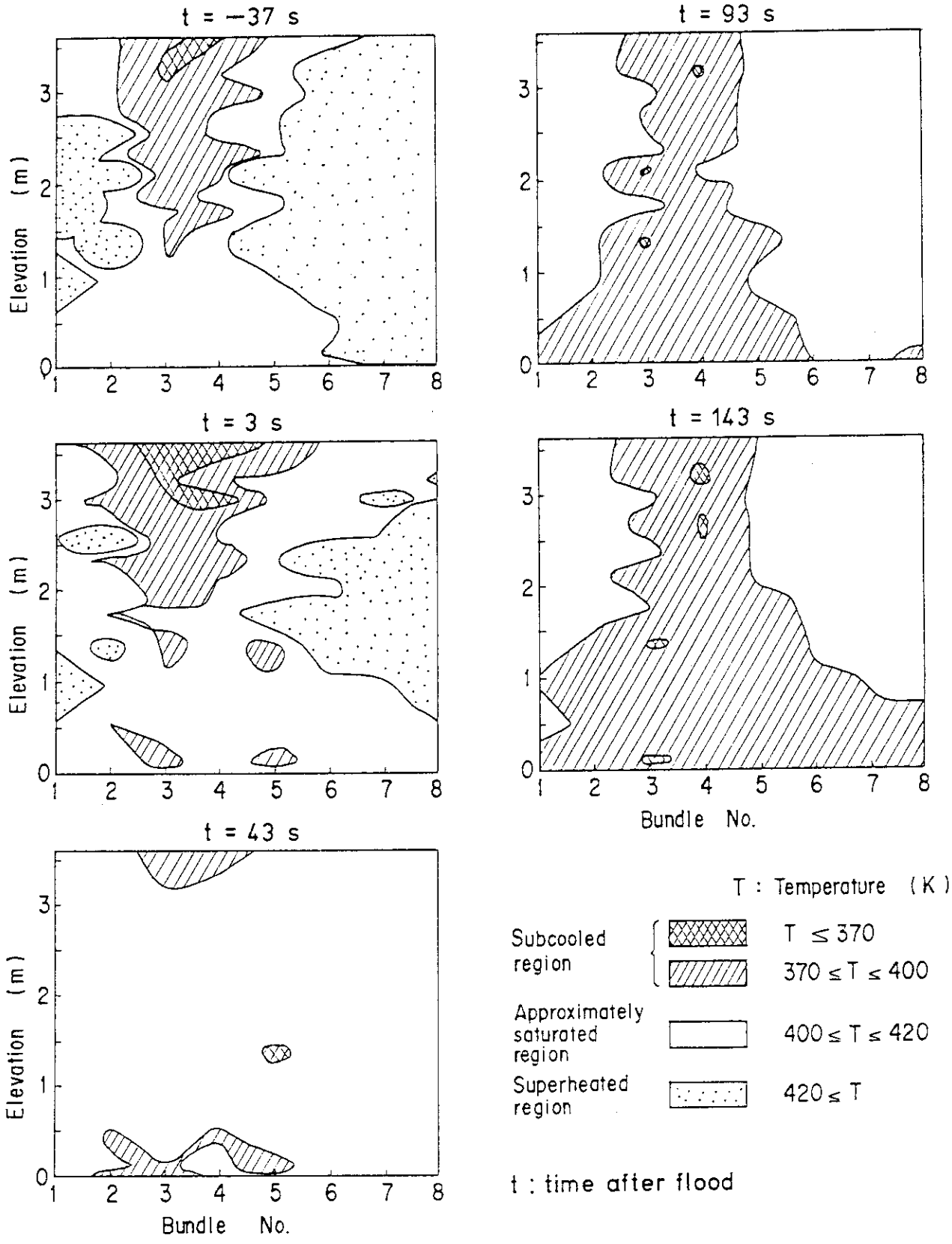

Fig. 3.4(b) Core fluid temperature distribution for Test S3-7

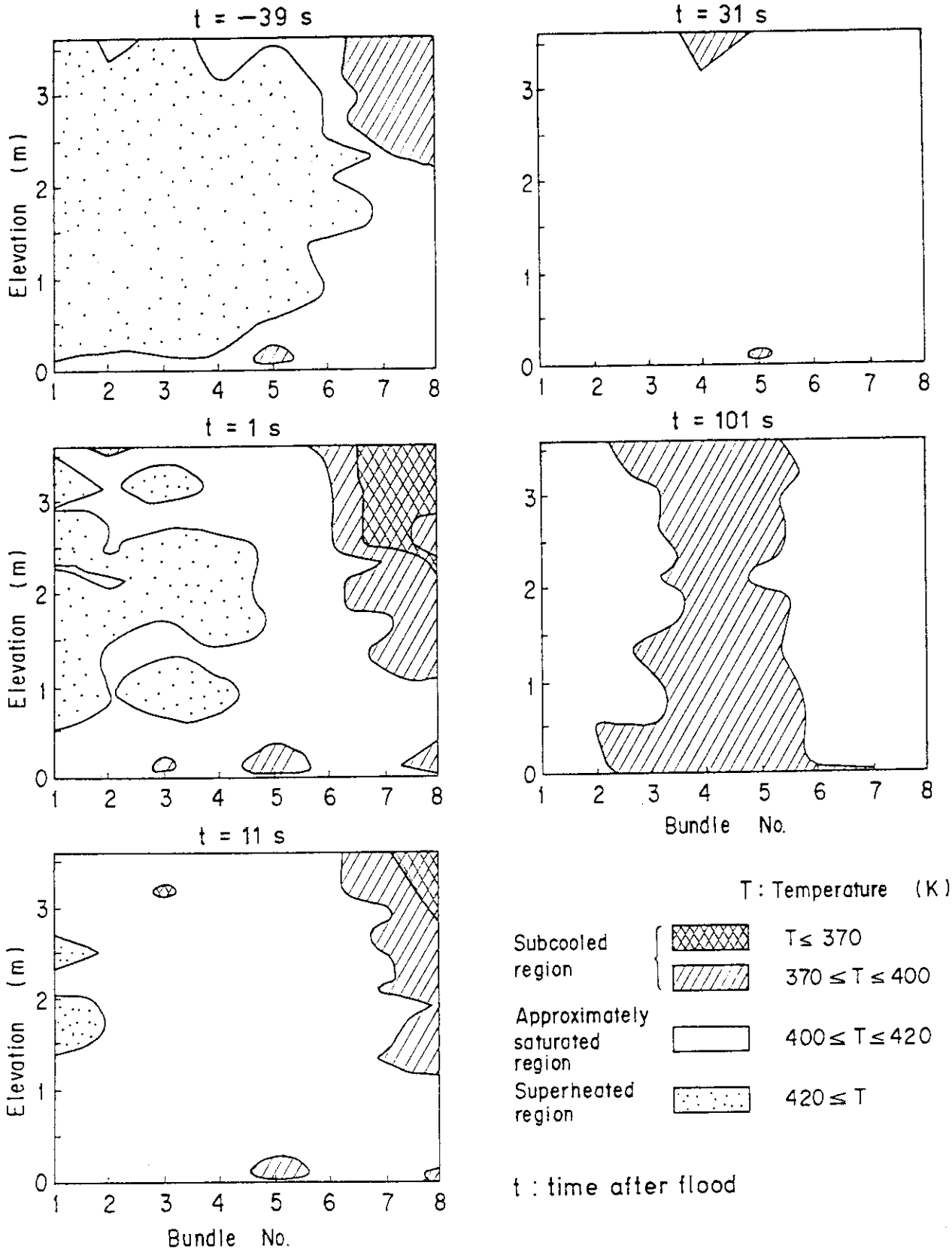

Fig. 3.4(c) Core fluid temperature distribution for Test S3-8

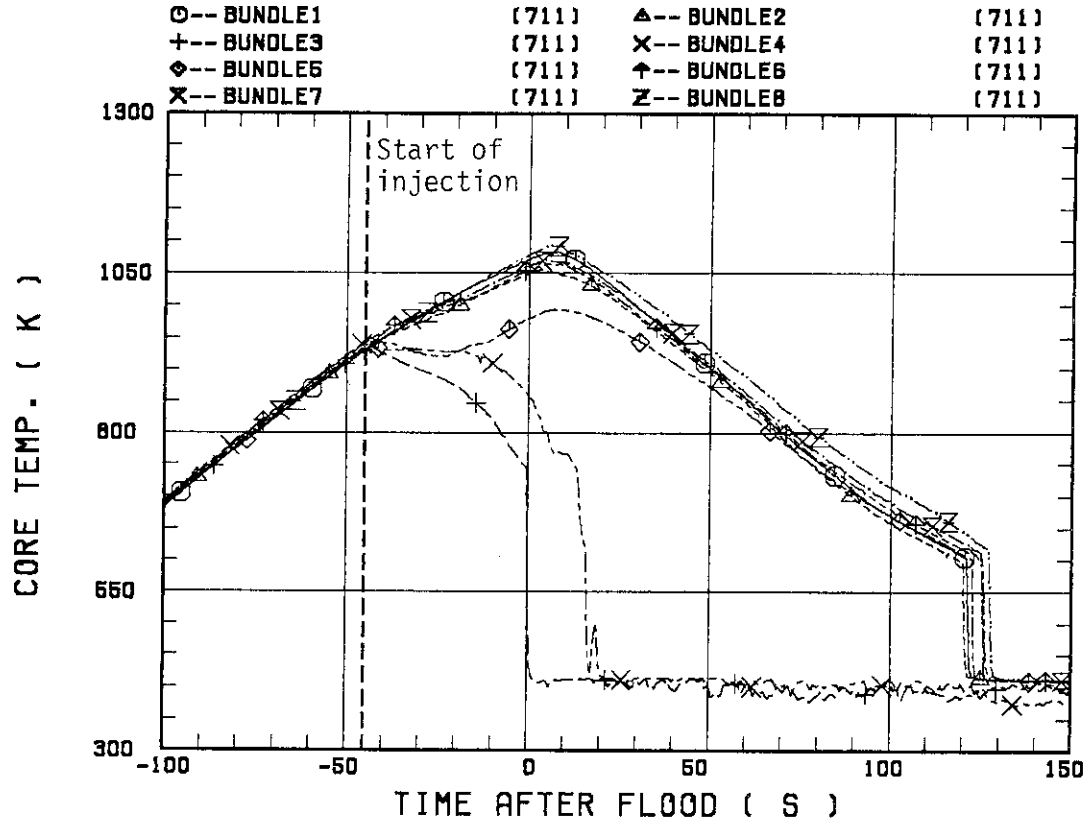

Fig. 3.5(a) Clad surface temperatures at 1.905 m elevation for Test S3-7

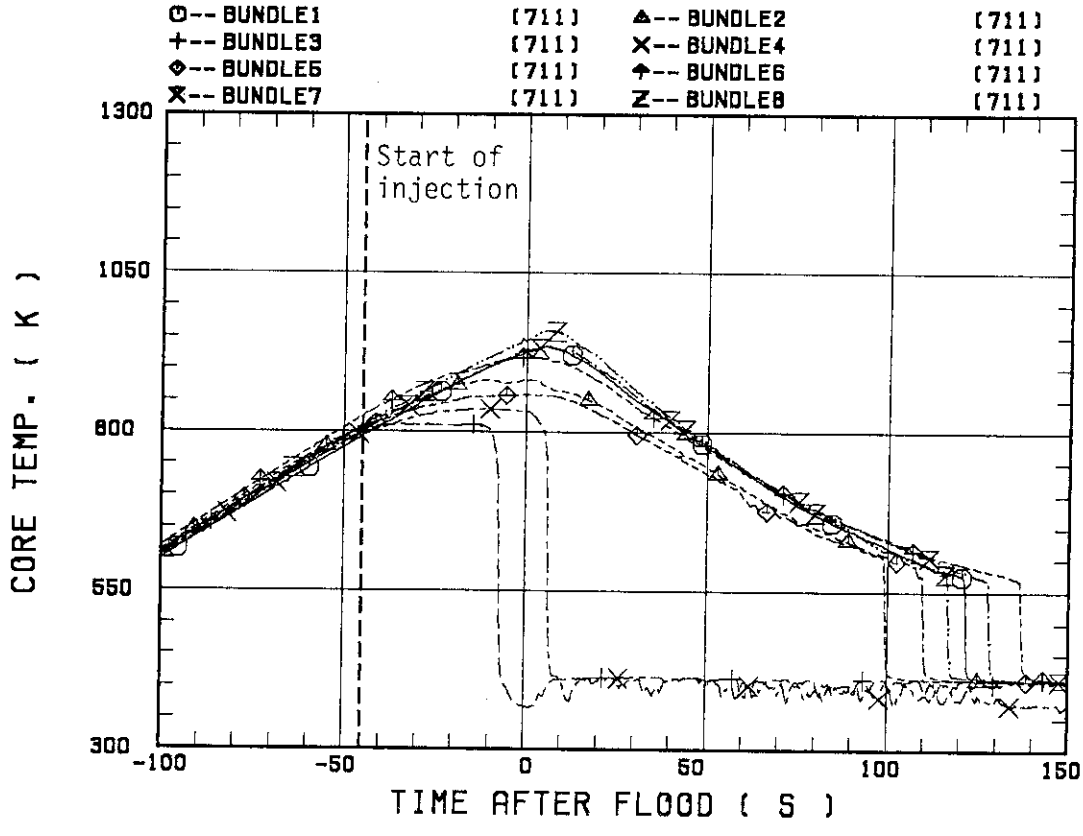

Fig. 3.5(b) Clad surface temperatures at 2.76 m elevation for Test S3-7

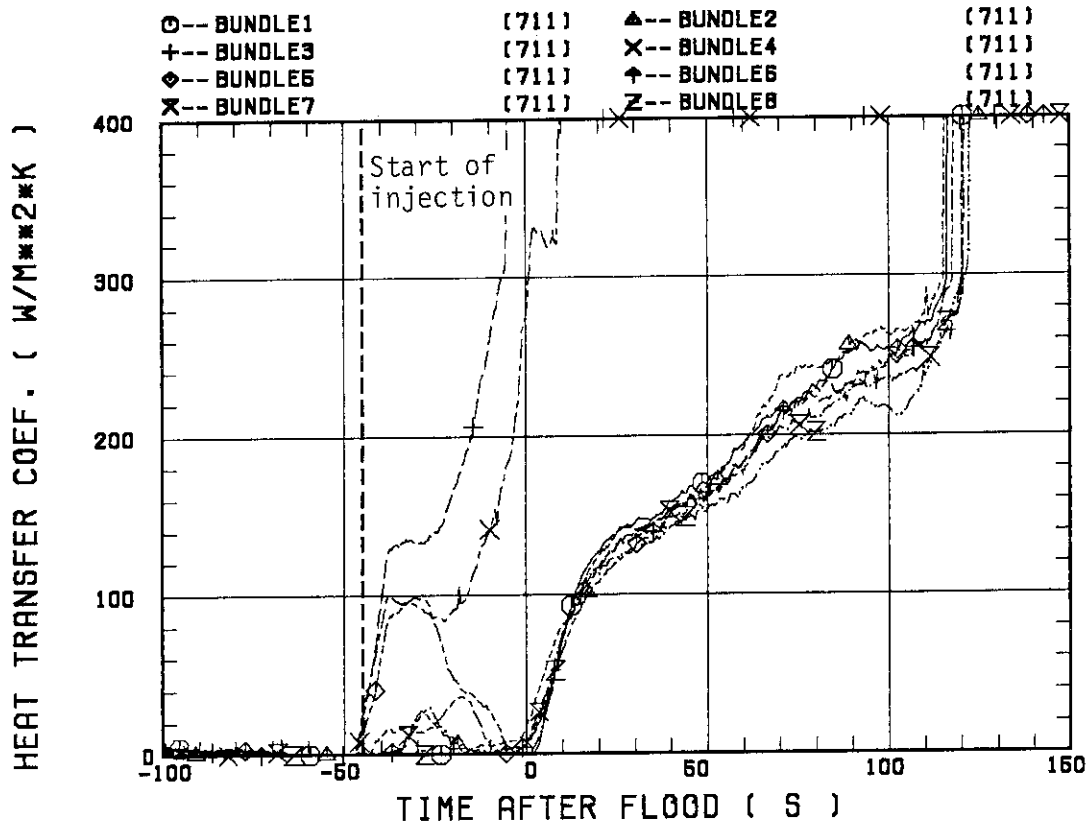

Fig. 3.6(a) Heat transfer coefficients at 1.905 m elevation for Test S3-7

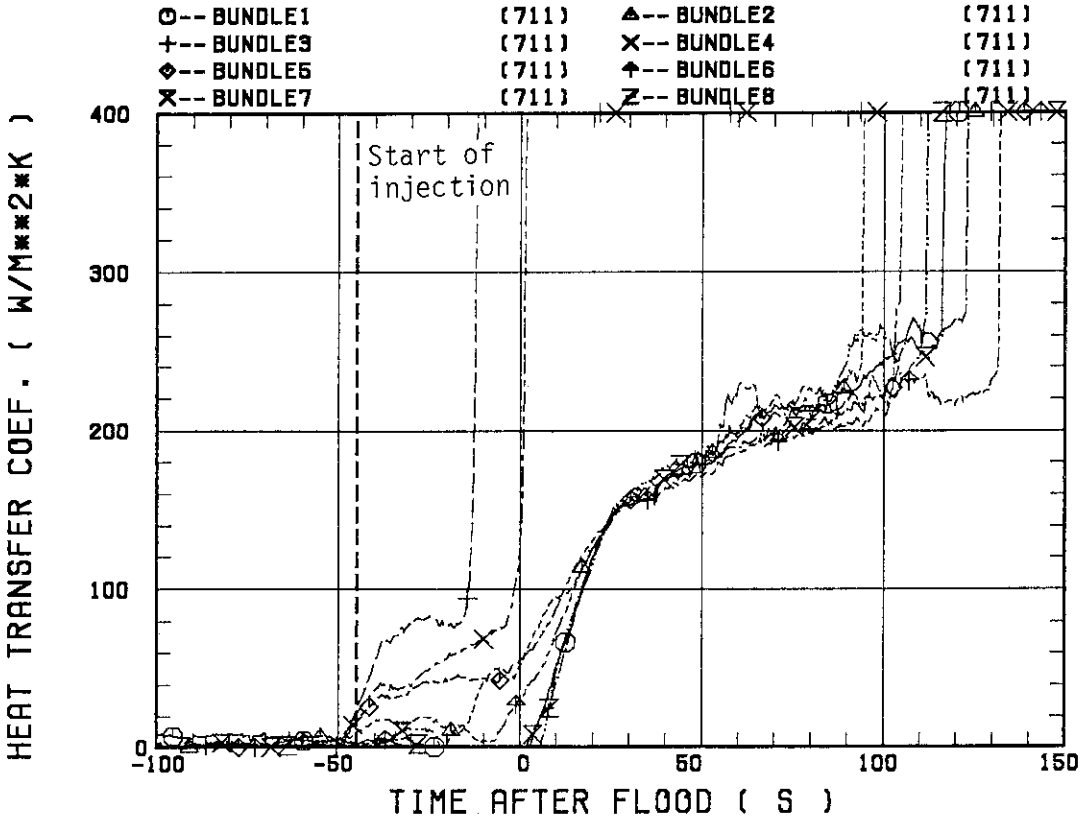

Fig. 3.6(b) Heat transfer coefficients at 2.76 m elevation for Test S3-7

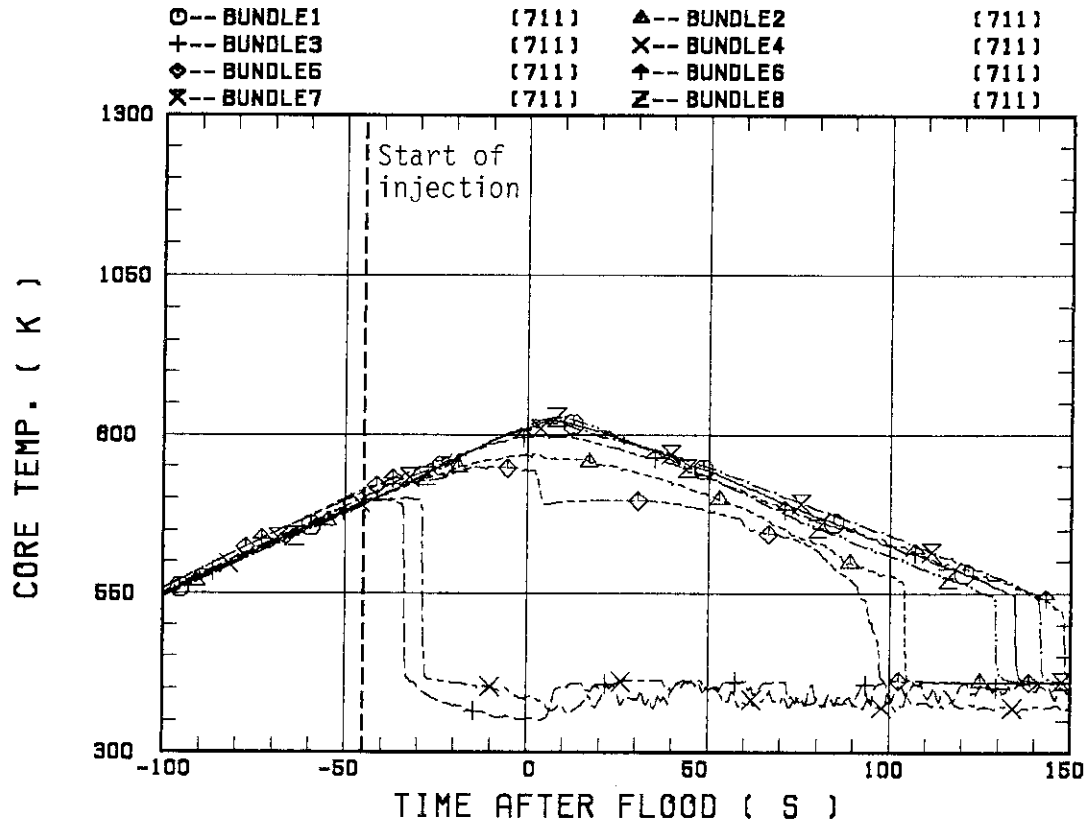

Fig. 3.7 Clad surface temperatures at 3.19 m elevation for Test S3-7

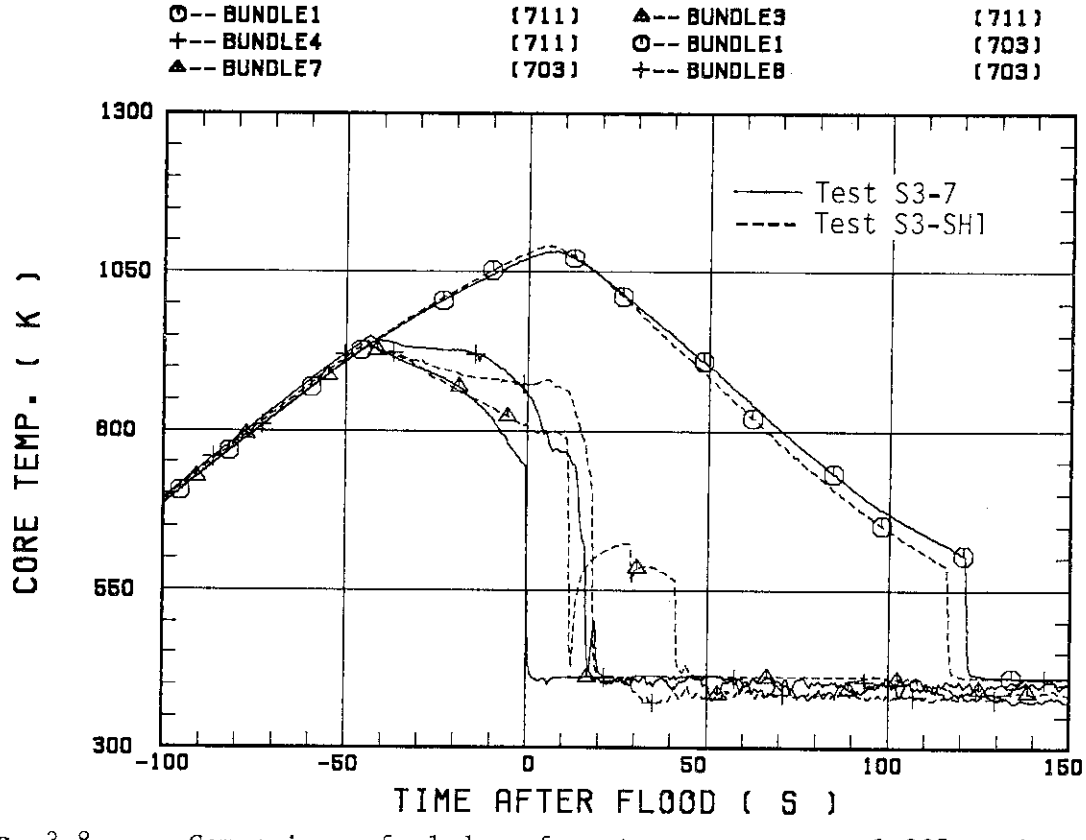

Fig. 3.8 Comparison of clad surface temperatures at 1.905 m elevation between Test S3-7 and S3-SH1

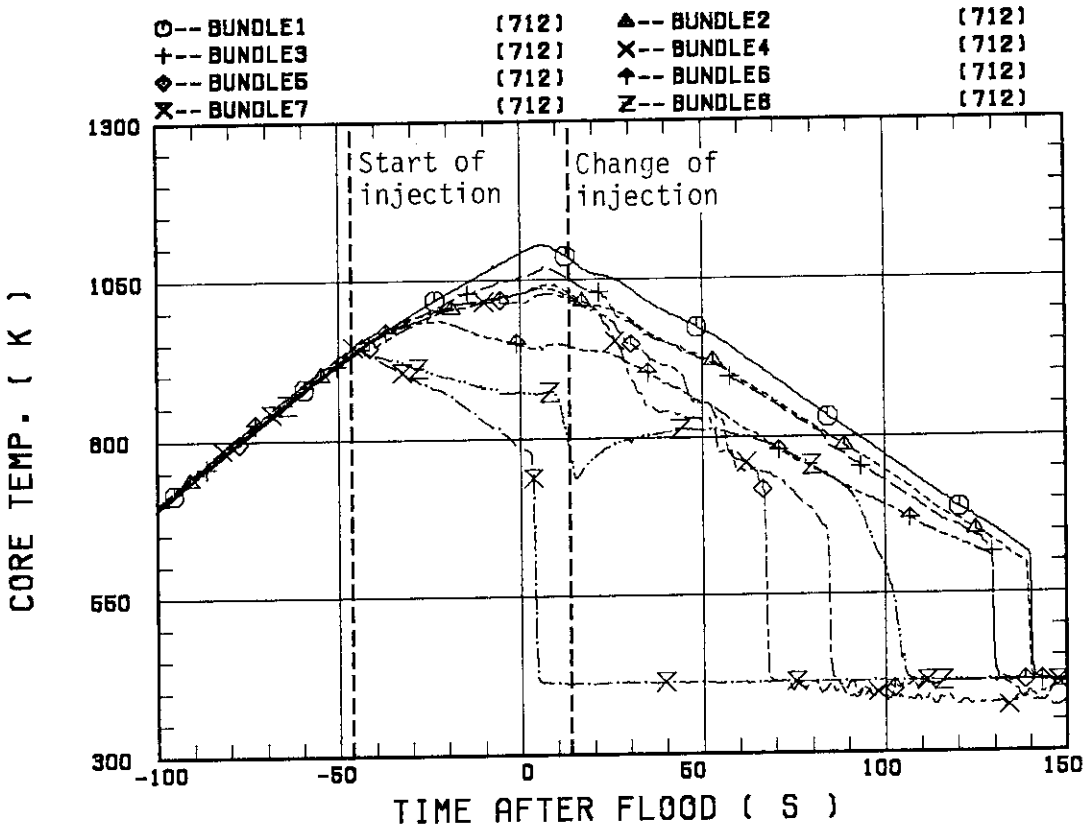

Fig. 3.9(a) Clad surface temperatures at 1.905 m elevation for Test S3-8

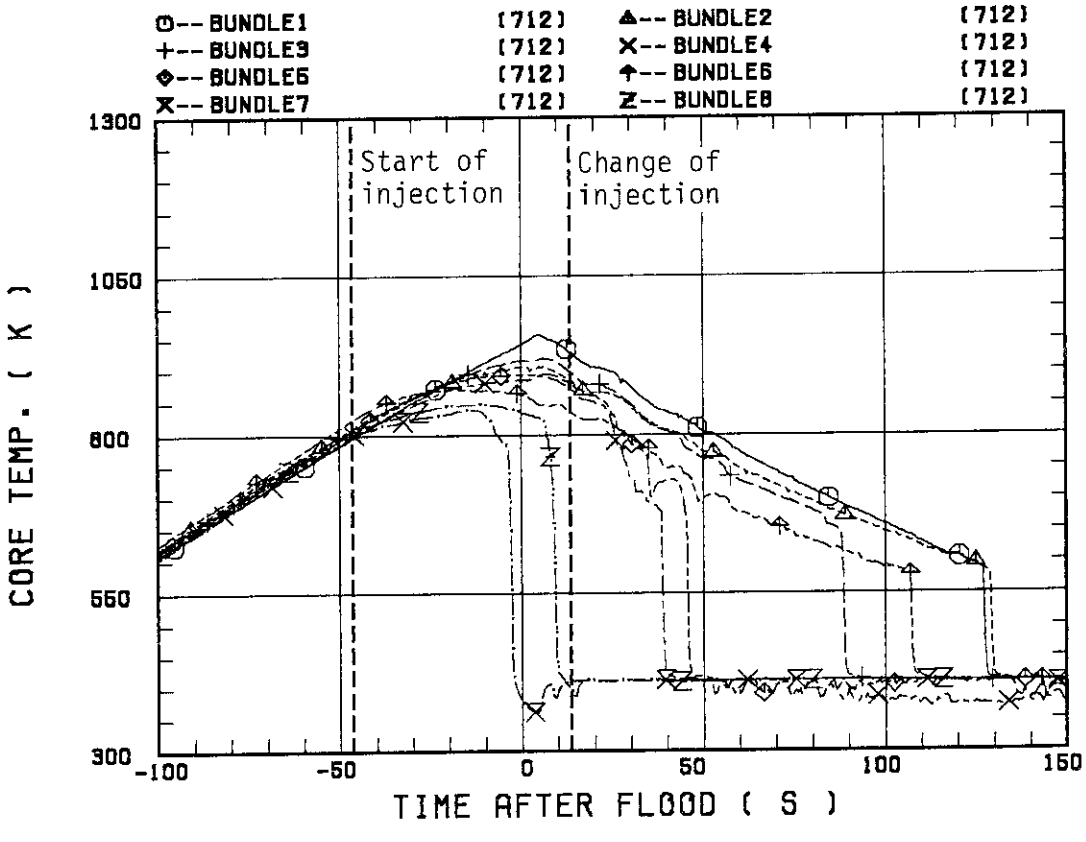

Fig. 3.9(b) Clad surface temperatures at 2.76 m elevation for Test S3-8

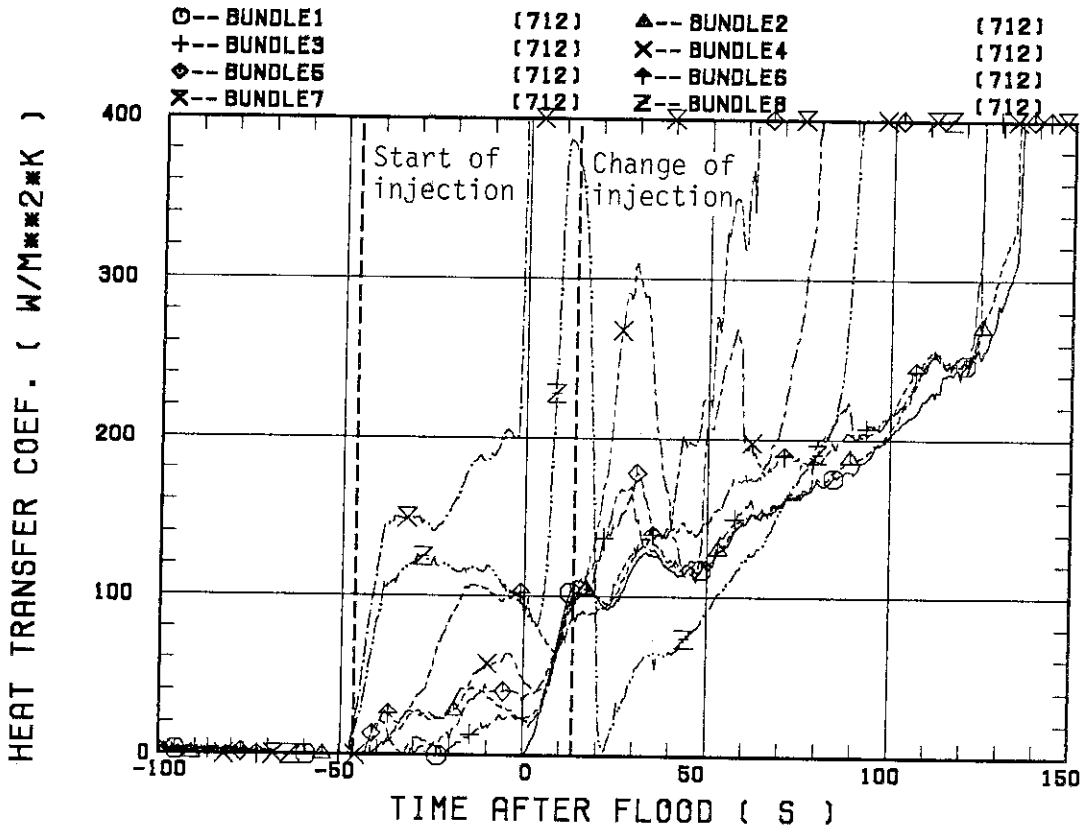

Fig. 3.10(a) Heat transfer coefficients at 1.905 m elevation for Test S3-8

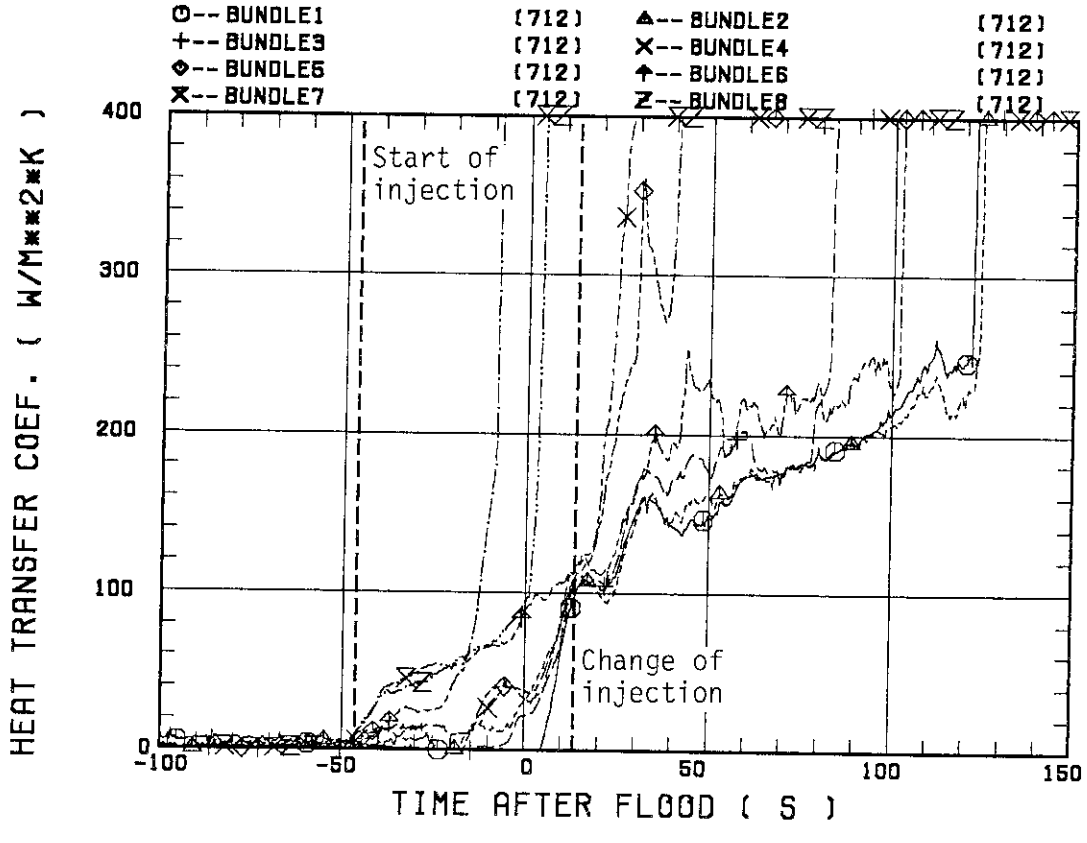

Fig. 3.10(b) Heat transfer coefficients at 2.76 m elevation for Test S3-8

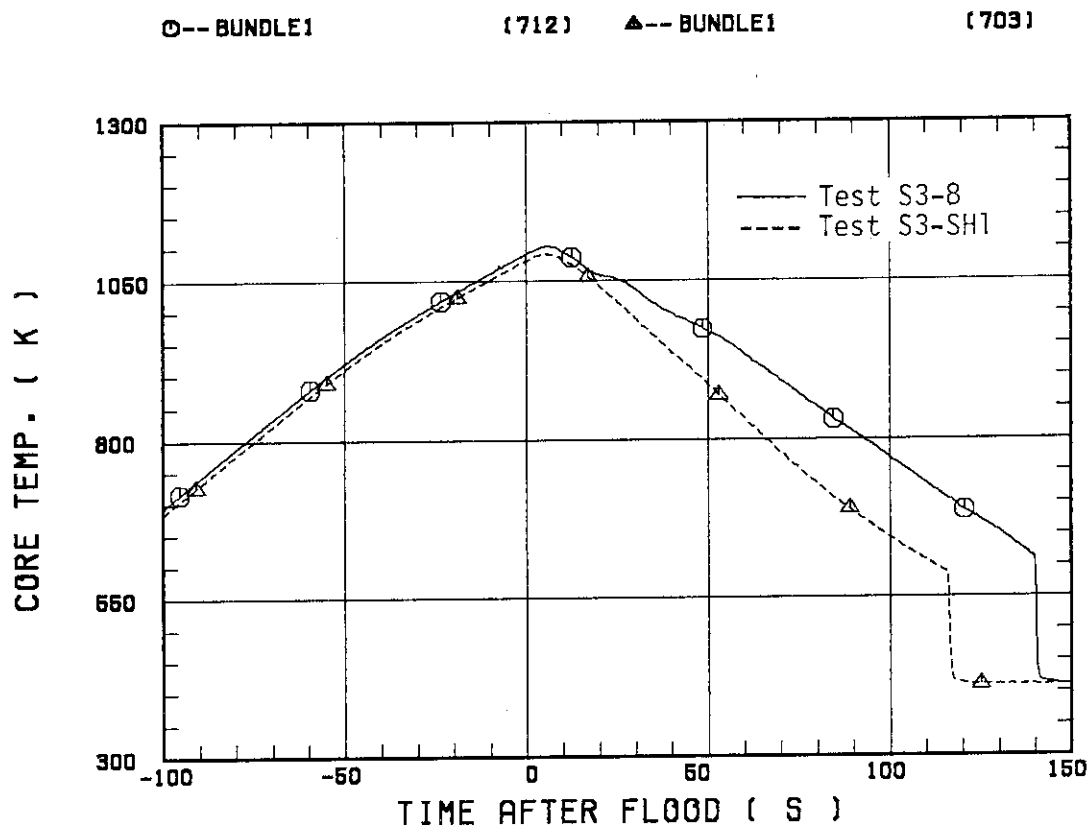

Fig. 3.11(a) Comparison of rod surface temperatures between Tests S3-8 and S3-SH1 in non-break-through region

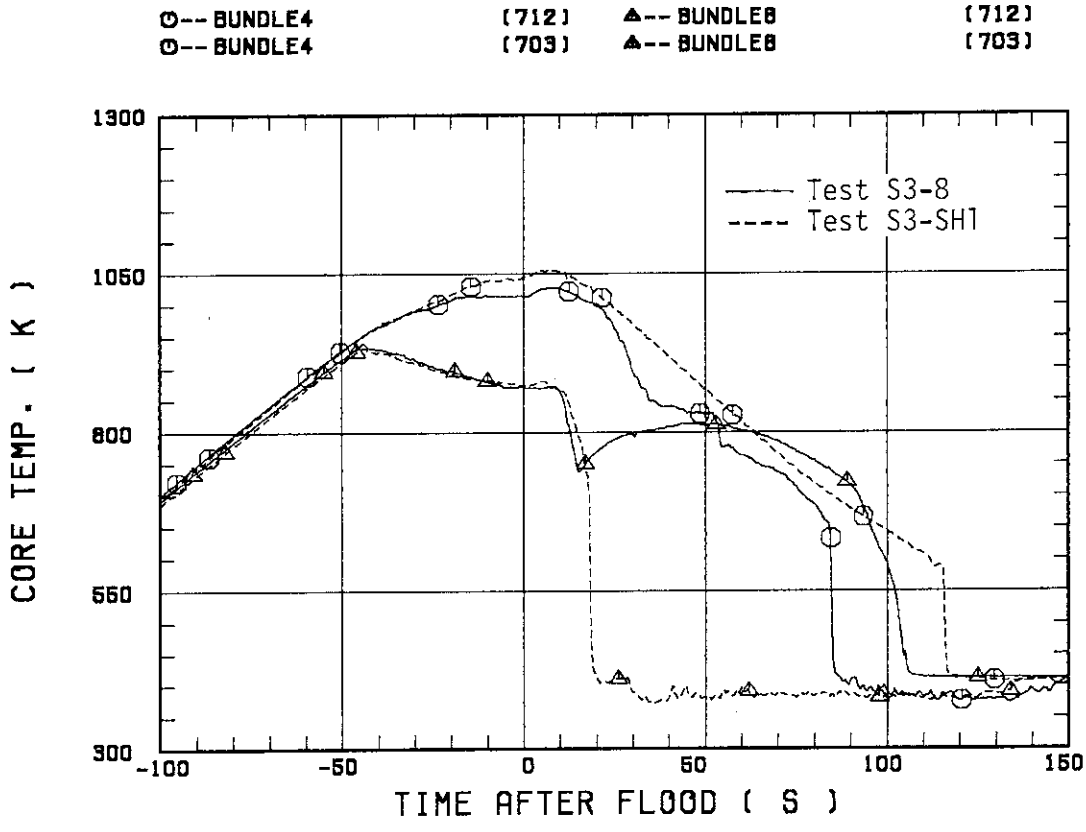

Fig. 3.11(b) Comparison of rod surface temperatures between Tests S3-8 and S3-SH1 in break-through region

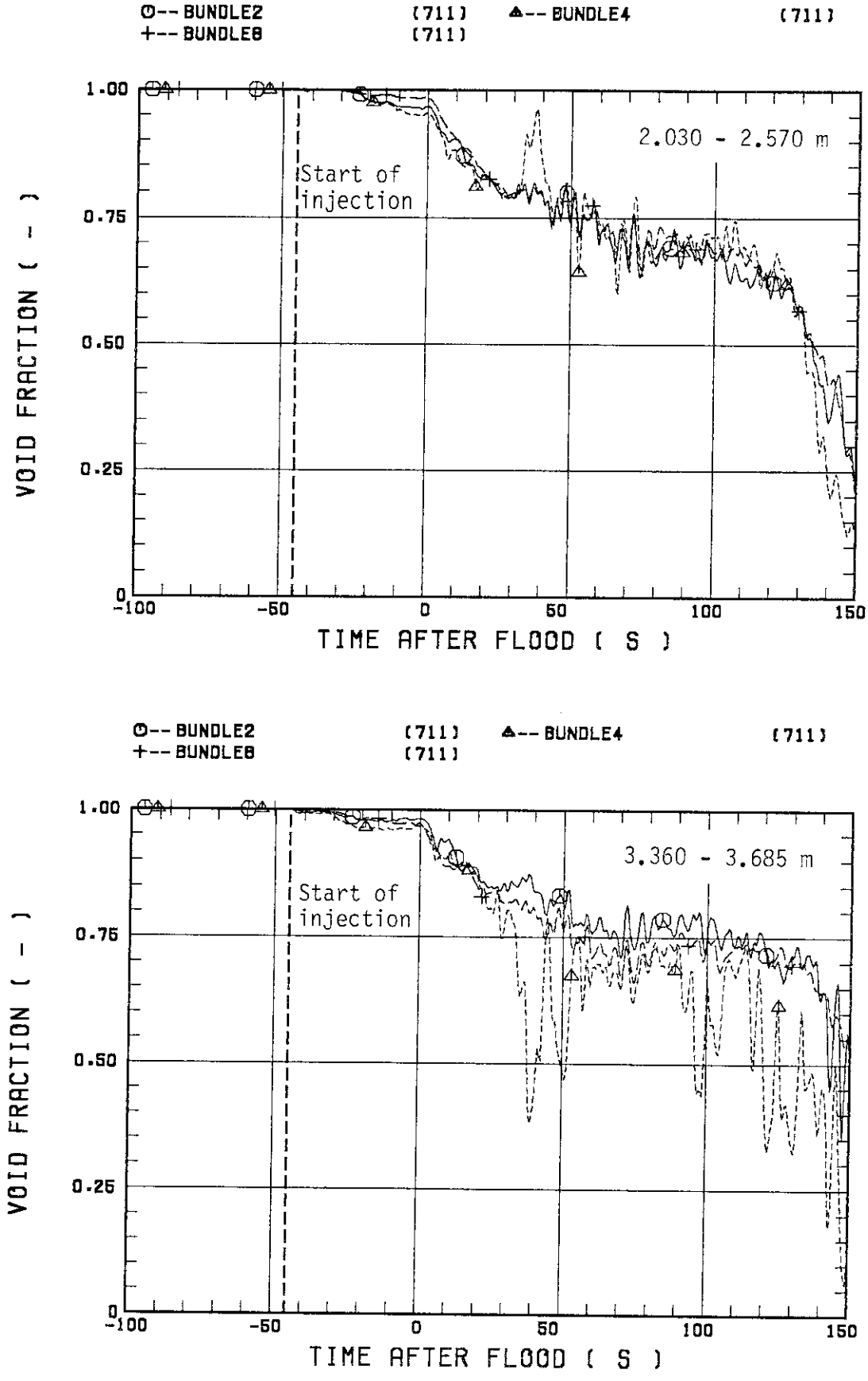

Fig. 3.12(a) Apparent core void fractions converted from differential pressures for Test S3-7

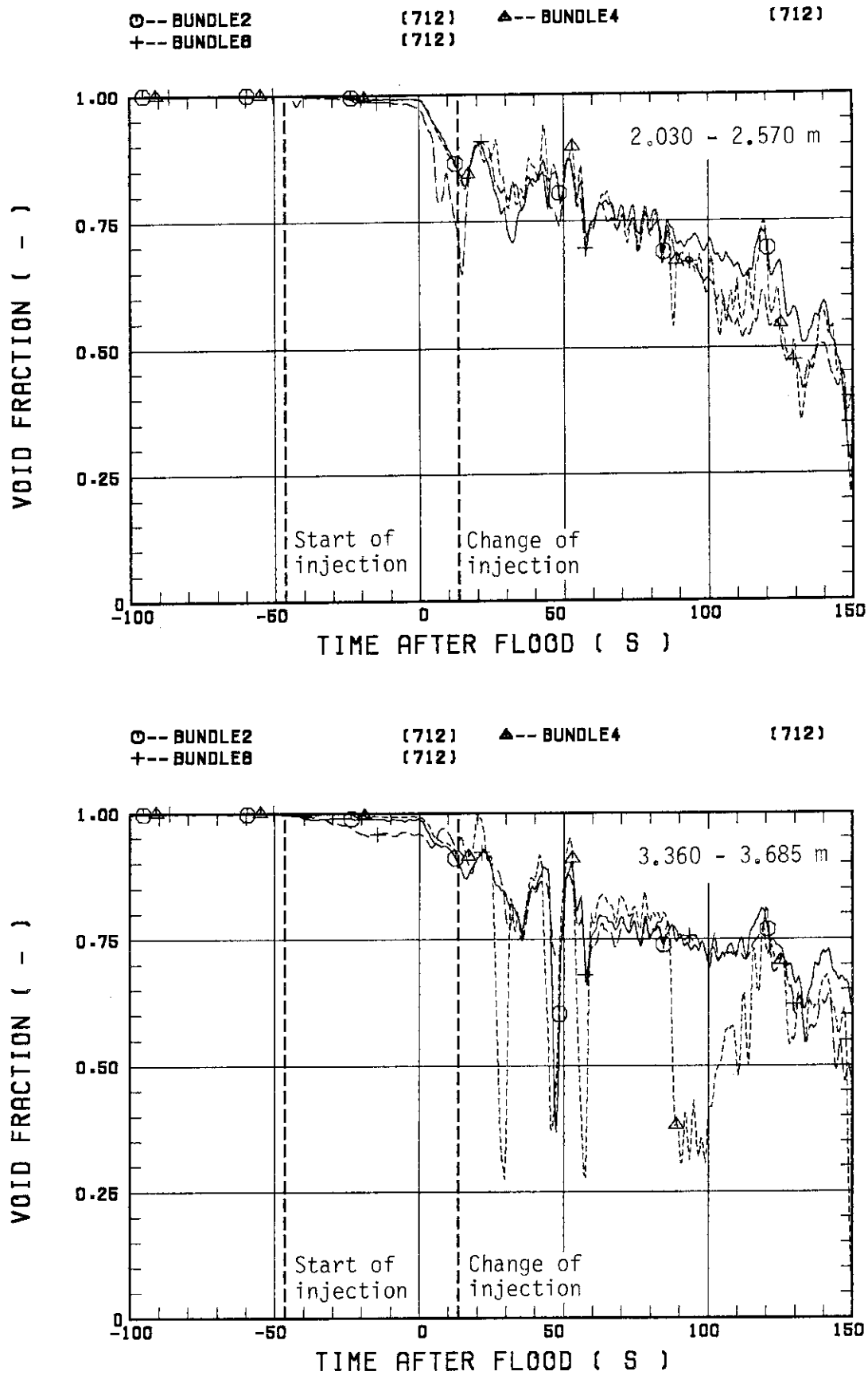

Fig. 3.12(b) Apparent core void fractions converted from differential pressures for Test S3-8

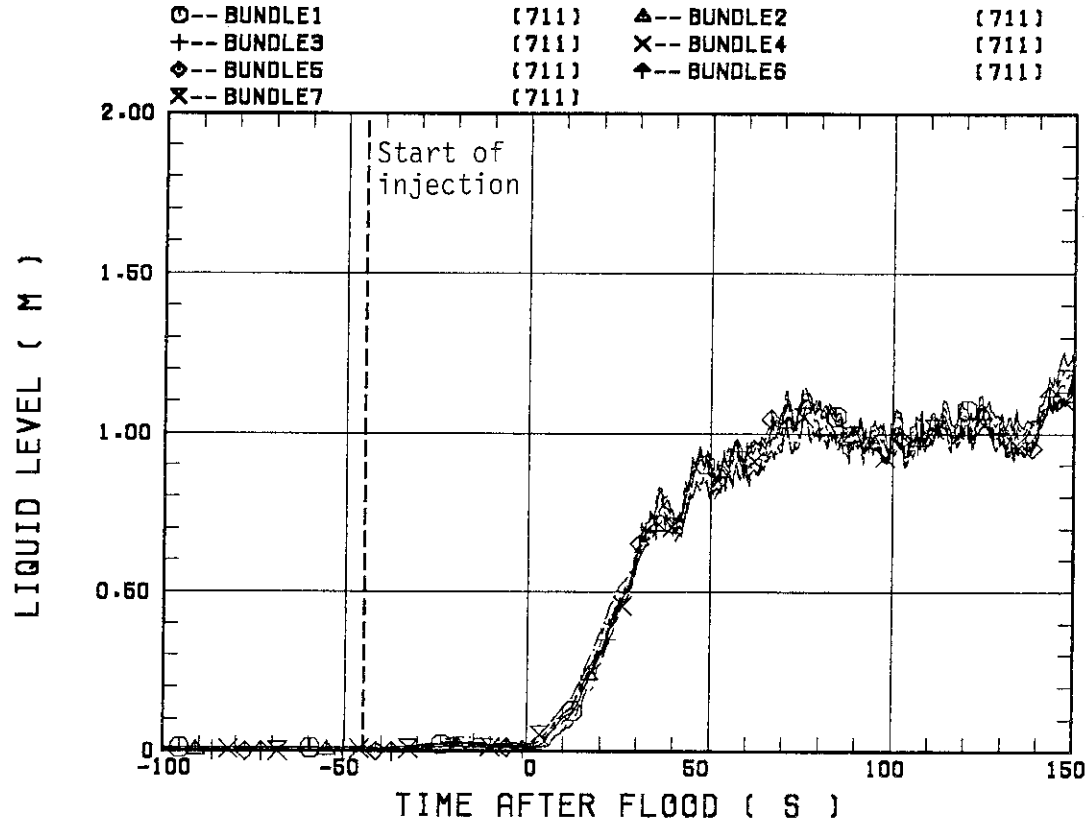

Fig. 3.13(a) Upper plenum water levels converted from differential pressures for Test S3-7

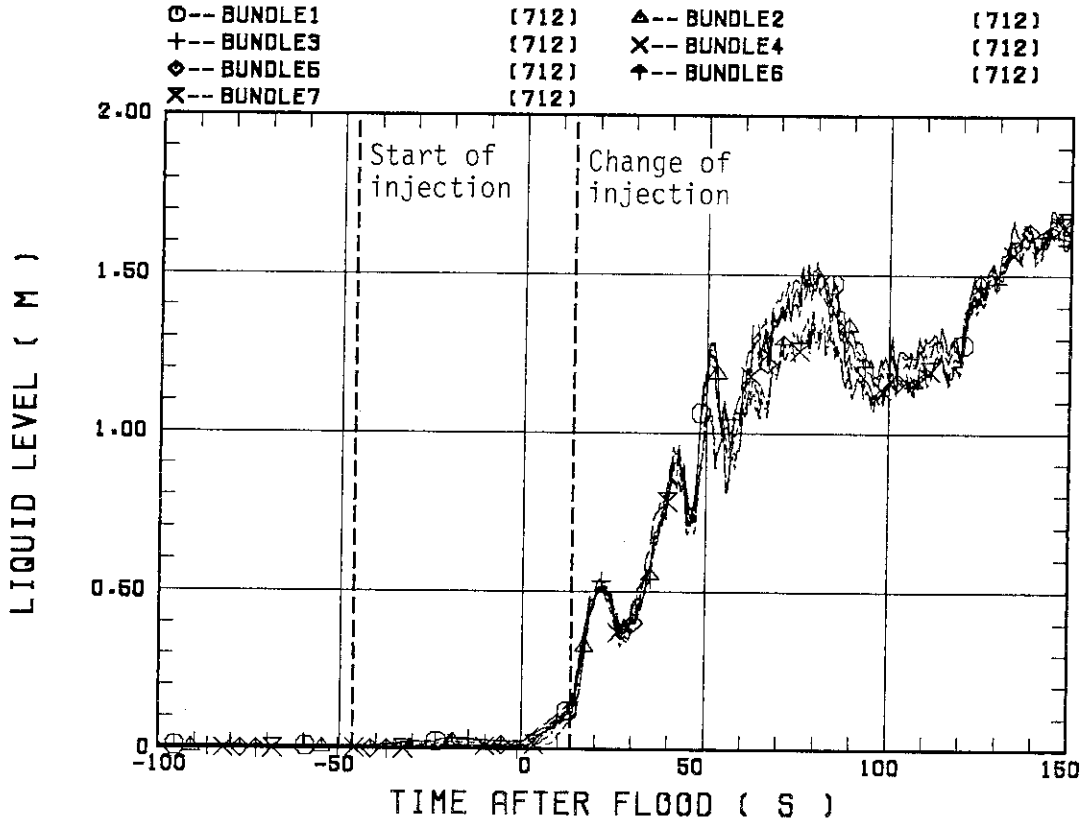

Fig. 3.13(b) Upper plenum water levels converted from differential pressures for Test S3-8

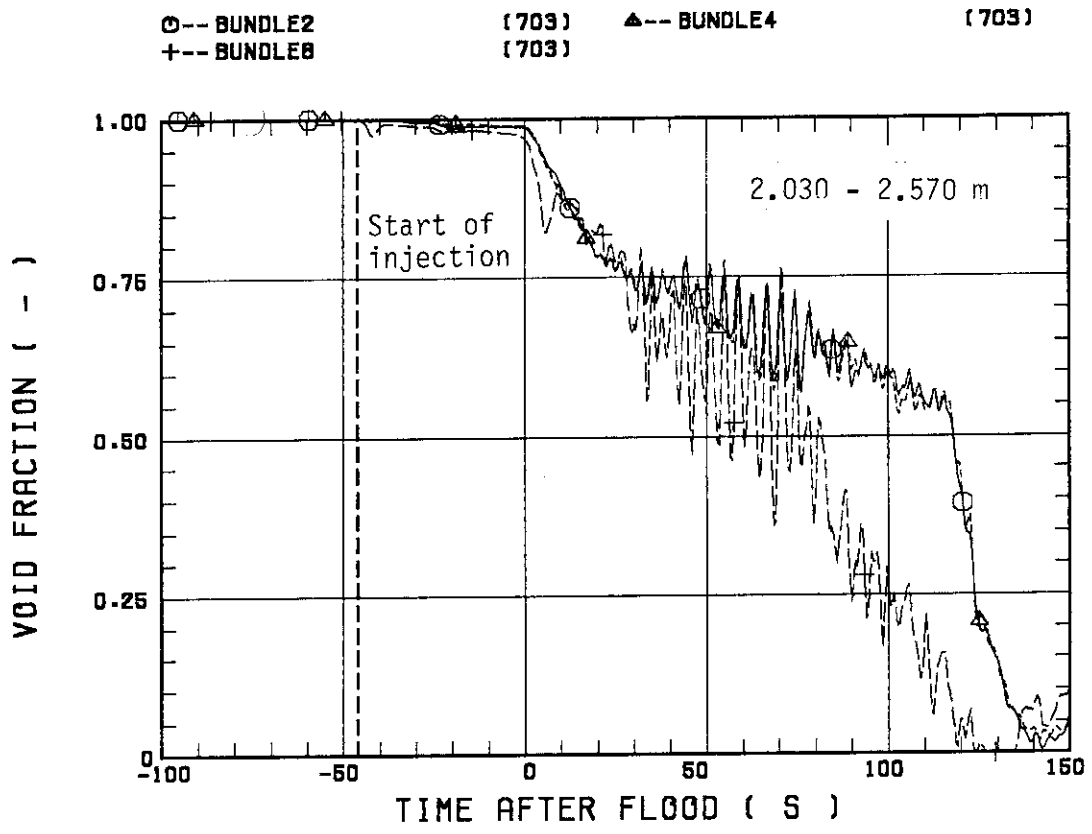

Fig. 3.14(a) Apparent core void fractions converted from differential pressures for Test S3-SH1

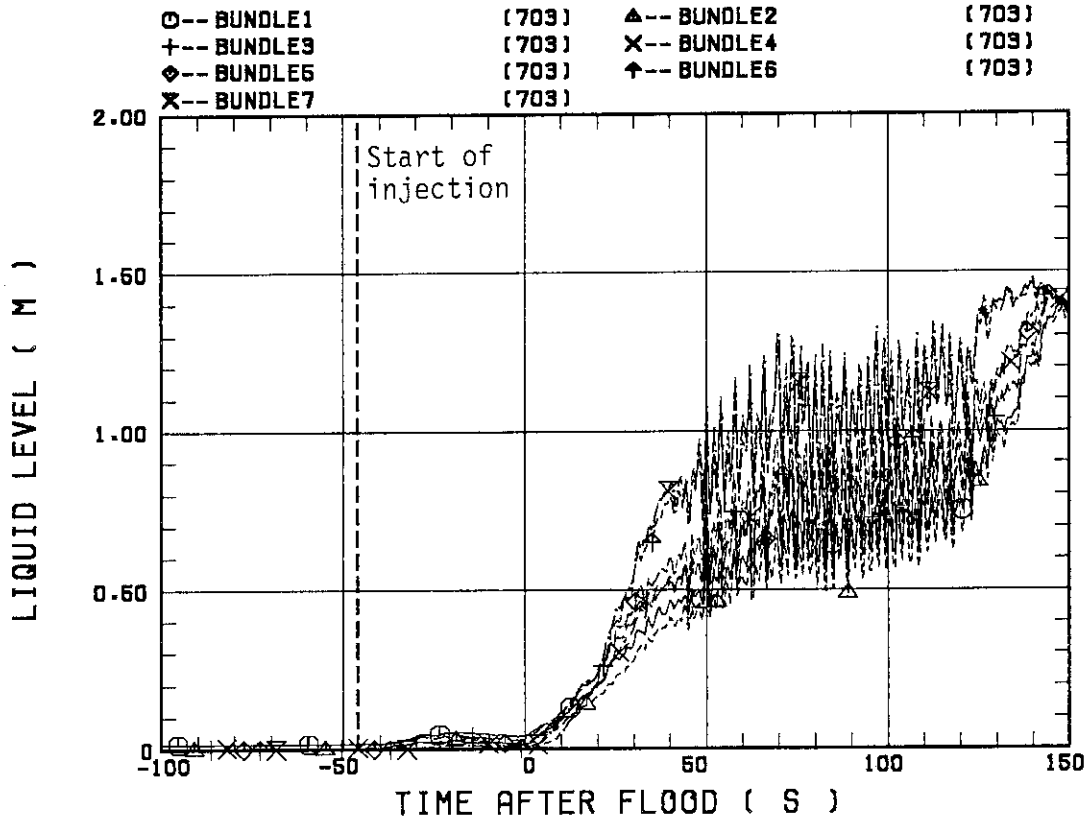

Fig. 3.14(b) Upper plenum water levels converted from differential pressures for Test S3-SH1

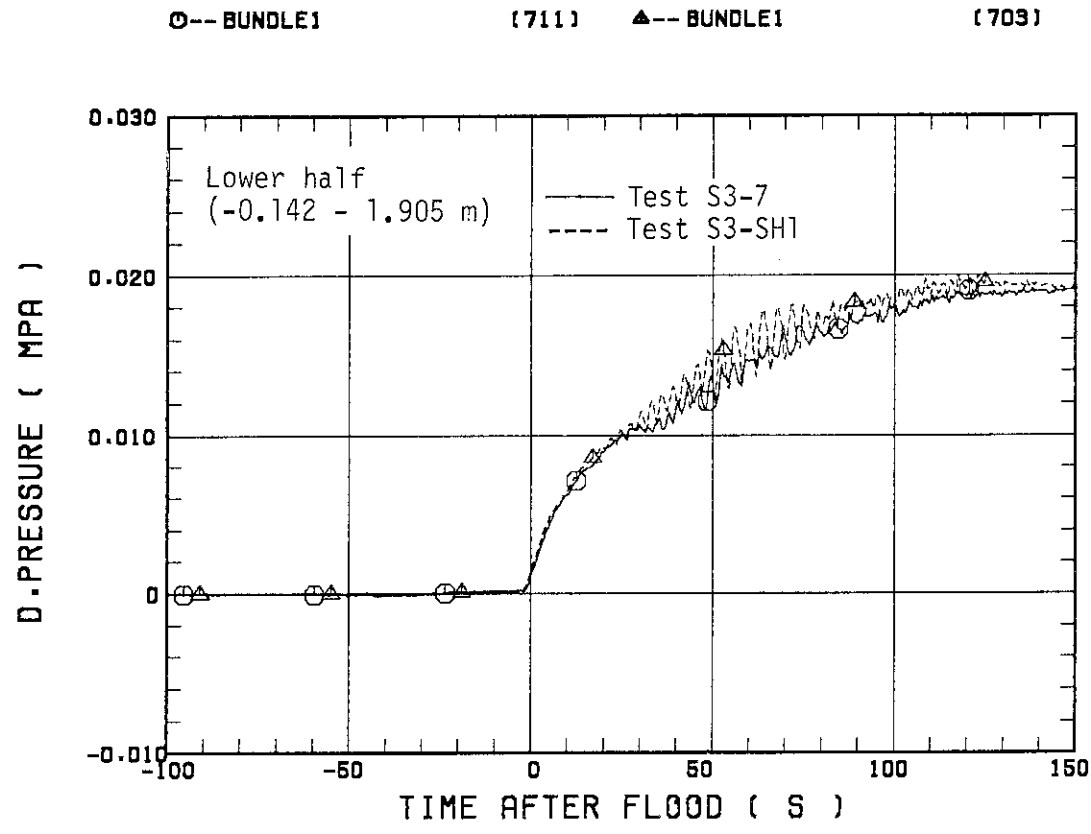

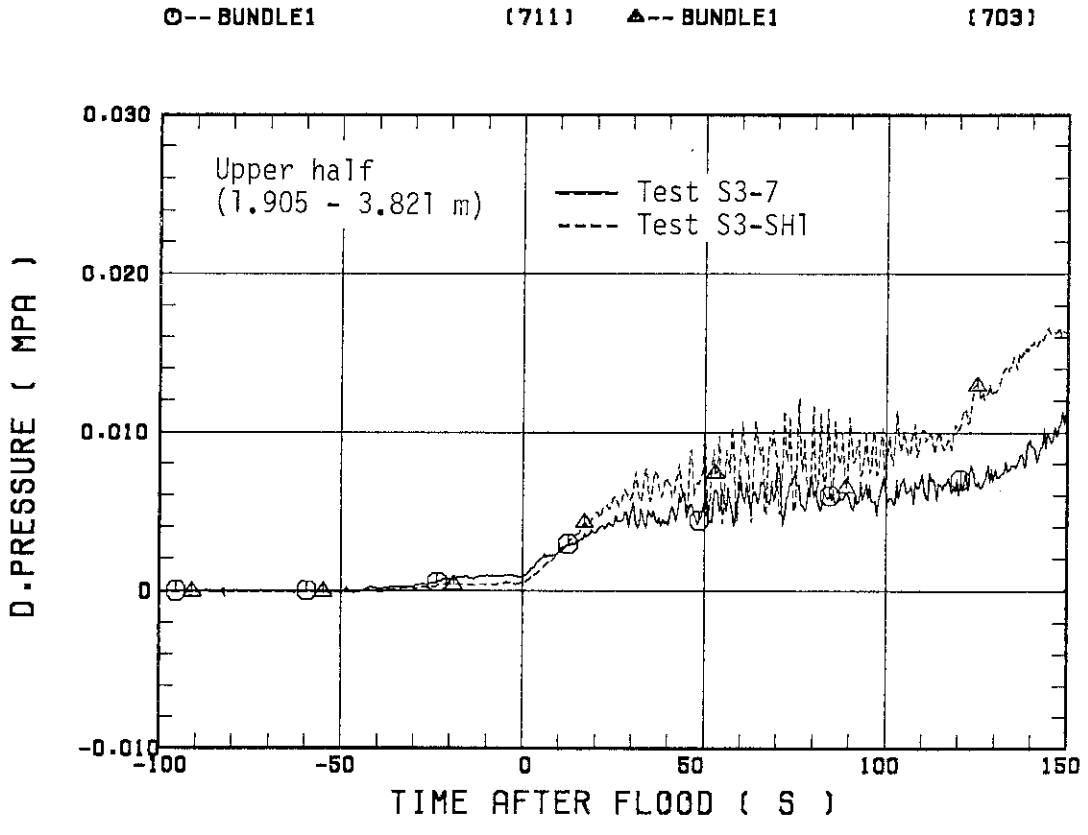

Fig. 3.15(a) Comparison of core differential pressures between Tests S3-7 and S3-SH1

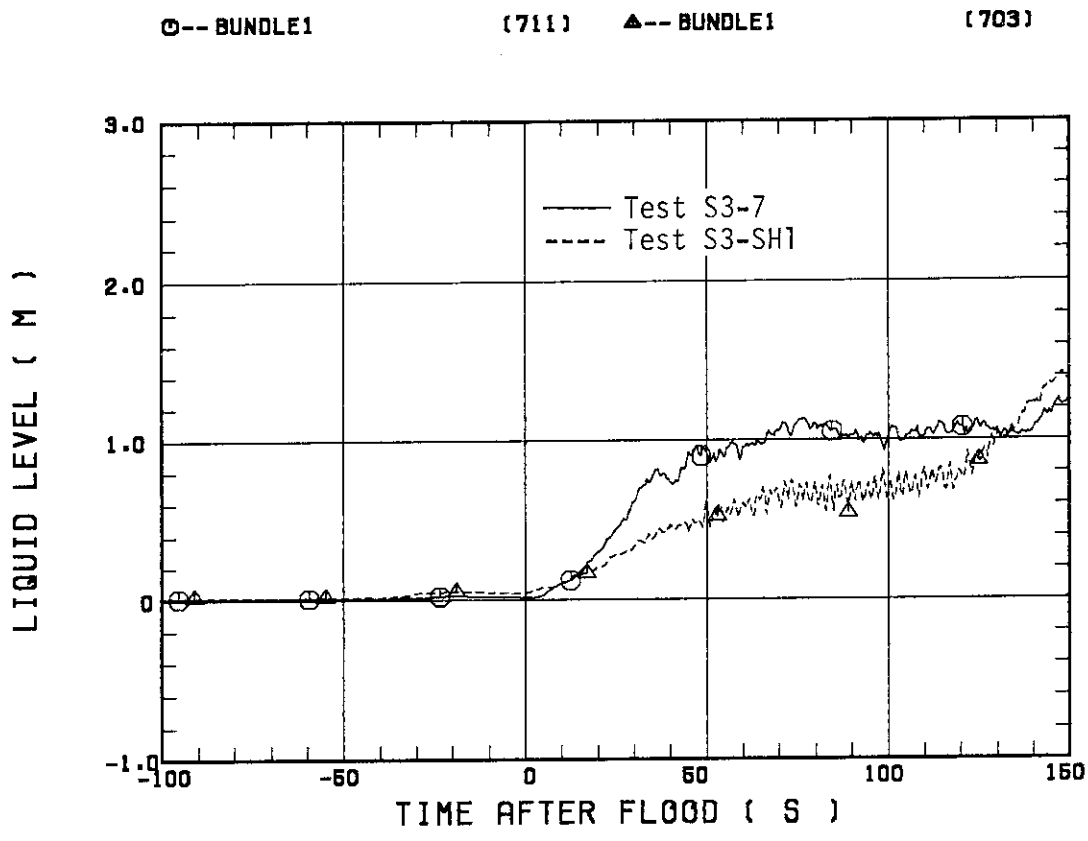

Fig. 3.15(b) Comparison of upper plenum water levels between Tests S3-7 and S3-SH1

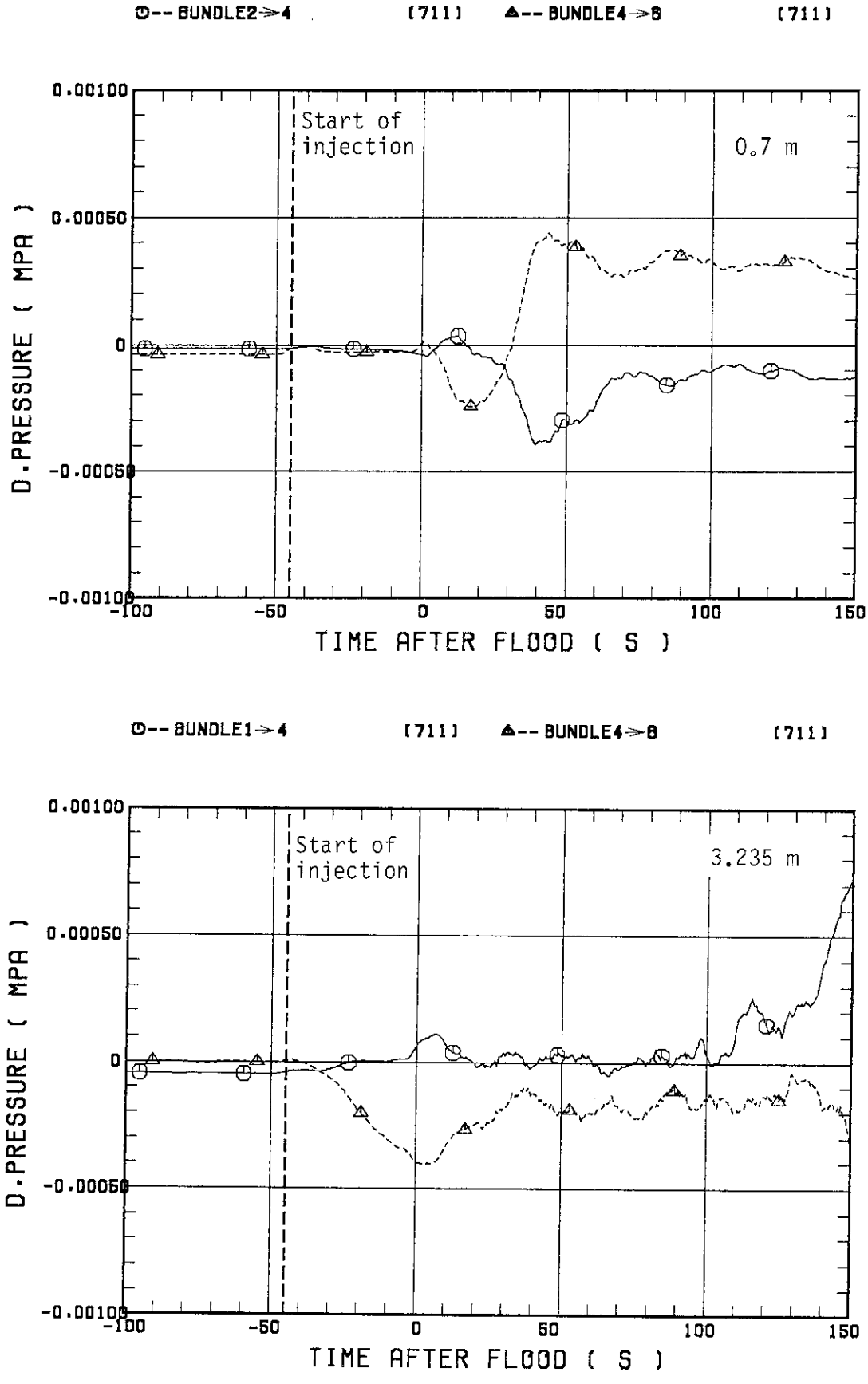

Fig. 3.16 Core horizontal differential pressures for Test S3-7

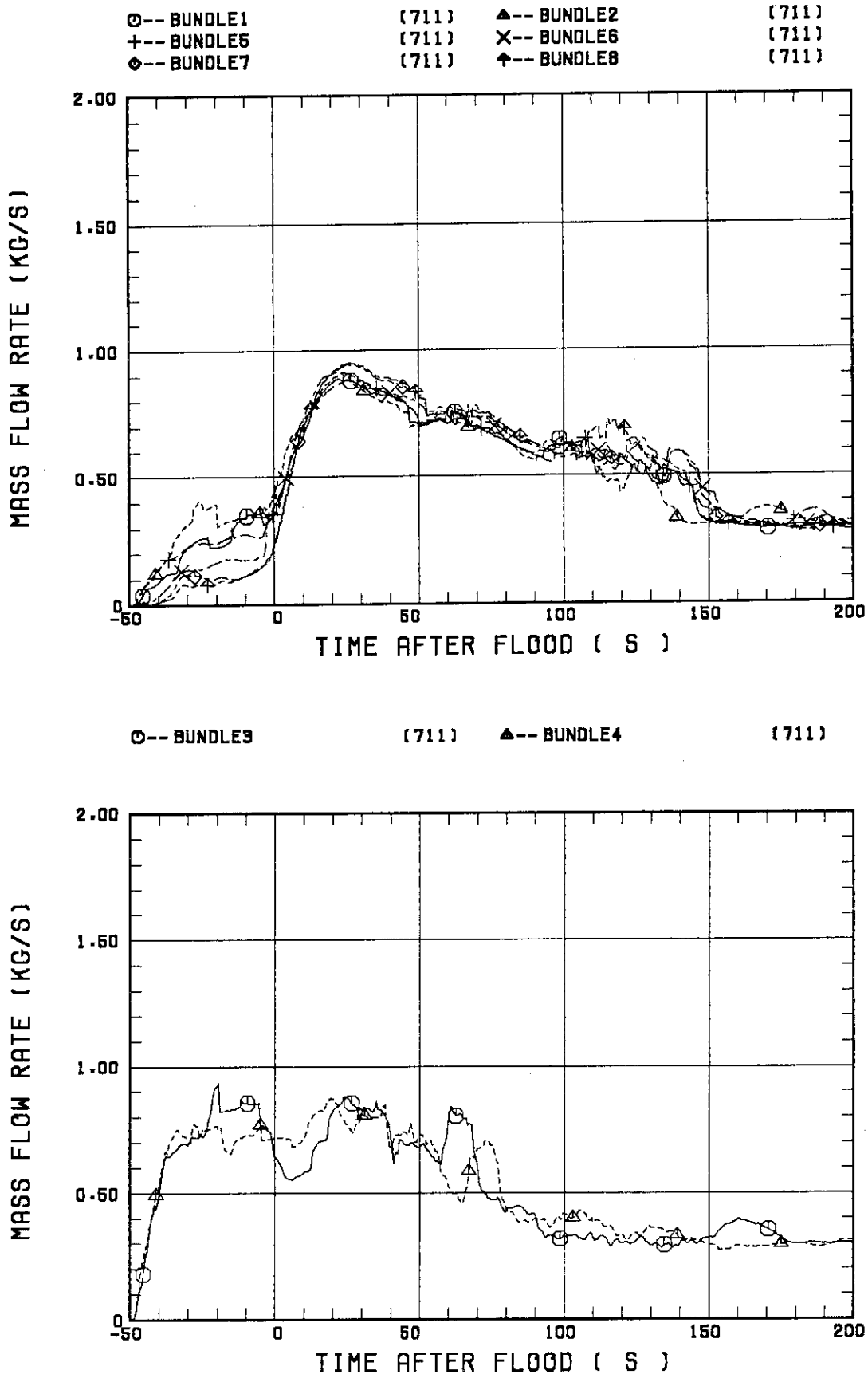

Fig. 3.17(a) Estimated maximum steam generation rate in each bundle for Test S3-7

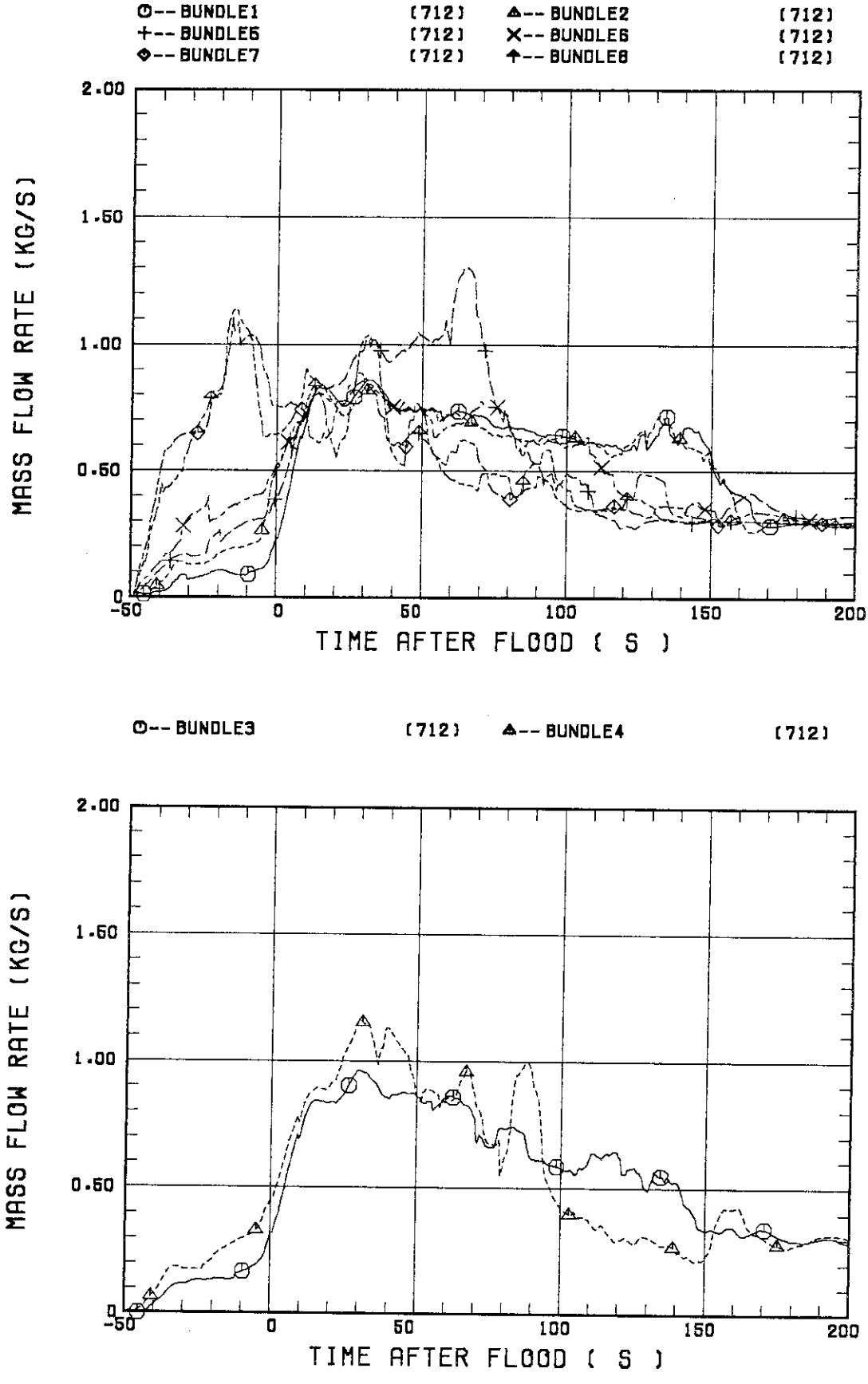

Fig. 3.17(b) Estimated maximum steam generation rate in each bundle for Test S3-8

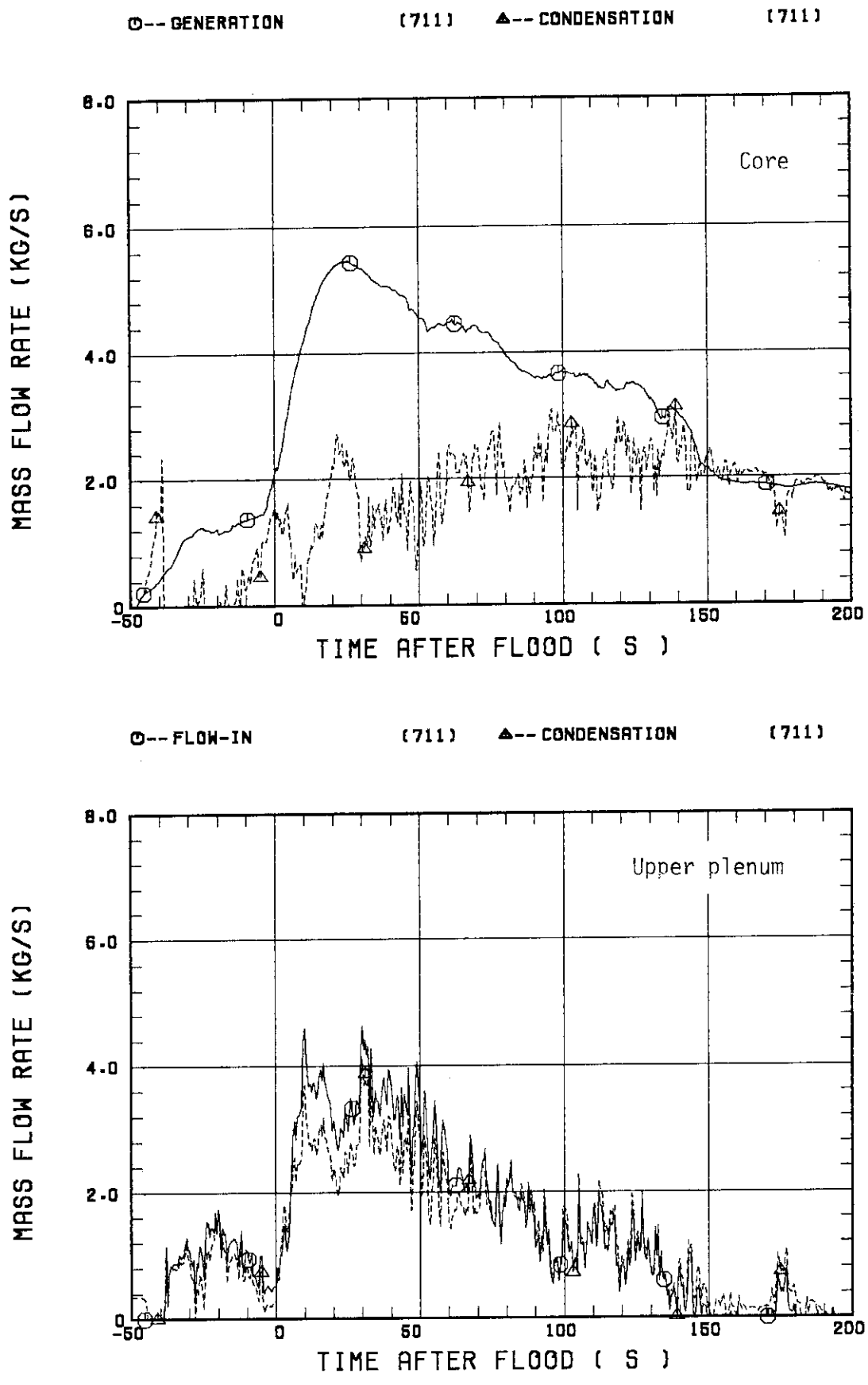

Fig. 3.18(a) Steam condensation rate in core (non-break-through region) and upper plenum for S3-7

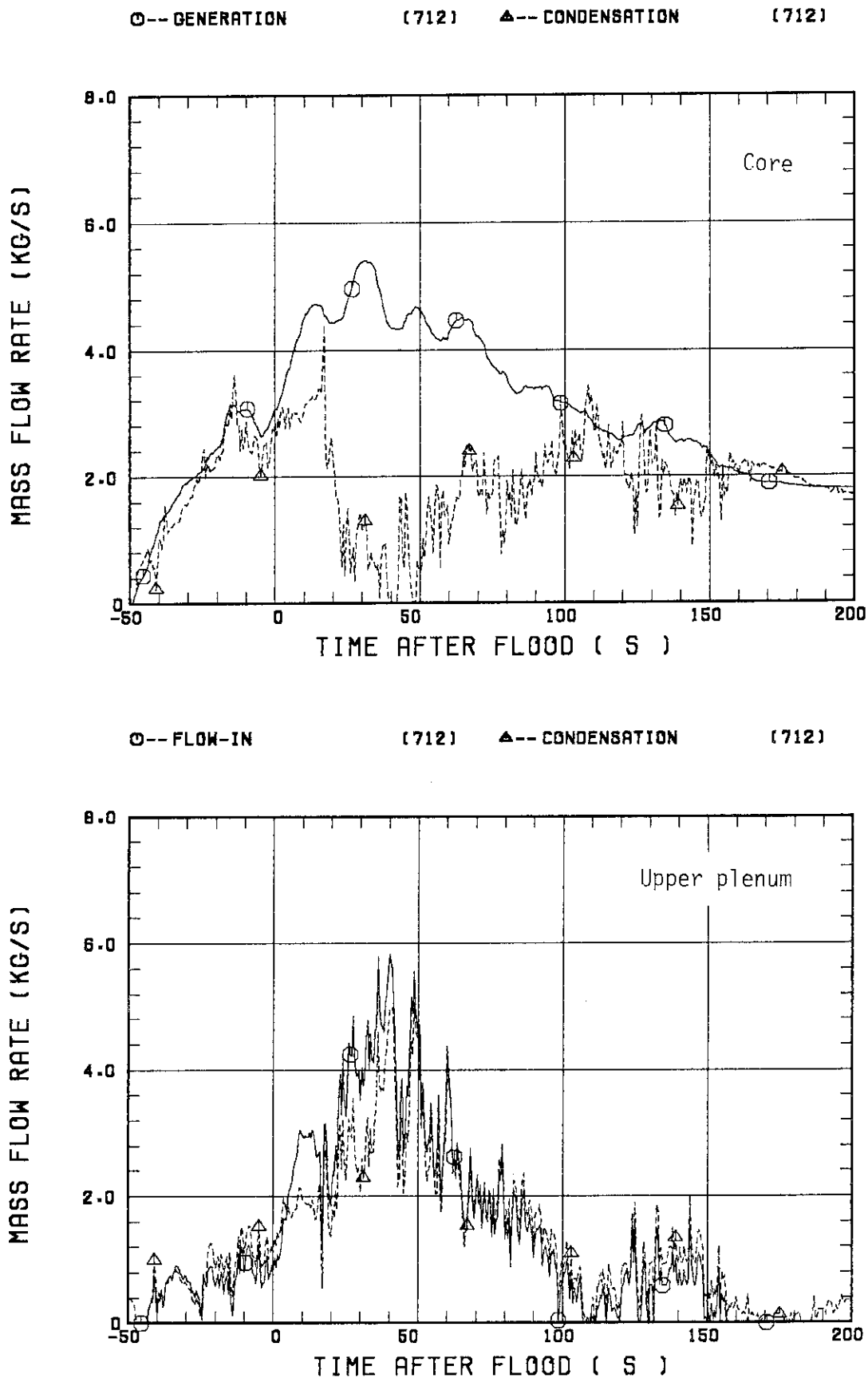

Fig. 3.18(b) Steam condensation rate in core (non-break-through region) and upper plenum for S3-8

4. Conclusions

Analyzing the data of SCTF Tests S3-7 and S3-8 together with those of Test S3-SH1, the following conclusions are obtained on the effects of the water temperature distribution at tie plate area on the break-through and the core cooling behavior during the reflood phase of a GPWR:

(1) The break-through occurs at the location where the water temperature is subcooled at the tie plate area.

(2) When the water temperature distribution is changed, the break-through location also changes following the change. In this case, it was observed to take a certain time to establish the new stable or continuous break-through.

(3) When the stable break-through occurs, the core cooling behavior is distinguished clearly between the break-through and the non-break-through region, and the core cooling in the break-through region is significantly good.

(4) Even when the break-through locations are different, the core cooling in each non-break-through region is almost the same being regardless of the difference in the break-through location, and so is in the break-through region.

(5) When the break-through location is changed during reflooding and when it take a certain time to establish a new stable break-through, the core cooling in the non-break-through region becomes worse. This time lag is considered to depend on the flow rate and the temperature of the supplied water above the tie plate.

Acknowledgments

The authors would like to express their appreciation to Messrs. A. Kamoshida, T. Oyama, Y. Niitsuma, K. Nakajima, T. Chiba, K. Komori, H. Sonobe and A. Owada for their contribution to the test conduction.

This work was performed under a contract with the Atomic Energy Bureau of Science and Technology Agency of Japan.

References

1. Hirano, K. and Murao, Y.: "Large Scale Reflood Test", Nihon-Genshiryoku-Gakkai Shi (J. At. Energy Sco. Jpn.) [in Japanese], 22[10], 681(1980)
2. Murao, Y. *et al.*: "Analysis report on CCTF Core-I reflood tests", to be published as a JAERI-M report
3. Adachi, H. *et al.*: "Design of Slab Core Test Facility (SCTF) in Large Scale Reflood Test Program, Part I: Core-I", JAERI-M 83-080 (1983)
4. Sobajima, M. *et al.*: "Design of Slab Core Test Facility (SCTF) in Large Scale Reflood Test Program, Part II: Core-II", to be published as a JAERI-M report
5. Adachi, H. *et al.*: "Design of Slab Core Test Facility (SCTF) in Large Scale Reflood Test Program, Part III: Core-III", to be published as a JAERI-M report
6. Iwamura, T. *et al.*: "Evaluation Report on SCTF Core-III Test S3-SH1 (Effect of Hot Leg Injection on Core Thermal-hydraulics for PWRs with a Combined Injection Type ECCS)", JAERI-M 88-125 (1988)

Acknowledgments

The authors would like to express their appreciation to Messrs. A. Kamoshida, T. Oyama, Y. Niitsuma, K. Nakajima, T. Chiba, K. Komori, H. Sonobe and A. Owada for their contribution to the test conduction.

This work was performed under a contract with the Atomic Energy Bureau of Science and Technology Agency of Japan.

References

1. Hirano, K. and Murao, Y.: "Large Scale Reflood Test", Nihon-Genshiryoku-Gakkai Shi (J. At. Energy Sco. Jpn.) [in Japanese], 22[10], 681(1980)
2. Murao, Y. *et al.*: "Analysis report on CCTF Core-I reflood tests", to be published as a JAERI-M report
3. Adachi, H. *et al.*: "Design of Slab Core Test Facility (SCTF) in Large Scale Reflood Test Program, Part I: Core-I", JAERI-M 83-080 (1983)
4. Sobajima, M. *et al.*: "Design of Slab Core Test Facility (SCTF) in Large Scale Reflood Test Program, Part II: Core-II", to be published as a JAERI-M report
5. Adachi, H. *et al.*: "Design of Slab Core Test Facility (SCTF) in Large Scale Reflood Test Program, Part III: Core-III", to be published as a JAERI-M report
6. Iwamura, T. *et al.*: "Evaluation Report on SCTF Core-III Test S3-SH1 (Effect of Hot Leg Injection on Core Thermal-hydraulics for PWRs with a Combined Injection Type ECCS)", JAERI-M 88-125 (1988)

Appendix A

Description of SCTF Core－III

A.1 Test Facility

The overall schematic diagram of SCTF is shown in Fig. A-1. The principal dimensions of the facility is shown in Table A-1, and the comparison of dimensions between SCTF and the reference PWR is shown in Fig. A-2.

A.1.1 Pressure Vessel

The pressure vessel is of slab geometry as shown in Fig. A-3. The height of the components in the pressure vessel is almost the same as the reference reactor's, and the flow area and the fluid volume of each component are scaled down based on the nominal core flow area scaling, 1/21.

The core consists of 8 bundles arranged in a row and each bundle includes heater rods and non-heated rods with 16×16 array. The core is enveloped by the honeycomb thermal insulator which is attached on the back surface of core wall plate.

The downcomer is located at one end of the pressure vessel which corresponds to the periphery of the actual reactor pressure vessel. The core baffle region located between the core and the downcomer is isolated for Core-III to minimize uncertainty in actual core flow. The cross sections of the pressure vessel at the upper head, upper plenum, core and lower plenum are shown in Fig. A-4.

A.1.2 Interface between Core and Upper Plenum

The interface between the core and the upper plenum consists of upper core support plate (UCSP), end box and various structures in the end box such as control rod spider which is paired with the control rod guid assembly (CRGA) and its support column bottom and special baffle plate spider which is paired with the hold-down bridge. These structures are exactly the same as those for a German PWR except some minor modifications.

Figure A-5 shows arrangement of the UCSP, the end box and the top grid spacer. The configuration of the end box is shown in Fig. A-6.

Detail of the end boxes with drag transducer device and other internals is shown in Fig. A-7. The UCSP shown in Fig. A-8 has two kinds of holes, i.e., the square holes correspond to the end boxes with control rod spider and the circular holes correspond to the end boxes with special baffle plate spider.

A.1.3 Upper Plenum and Upper Head

The vertical and horizontal cross sections of the upper plenum are shown in Figs. A-9 and A-4, respectively. In the SCTF Core-III, the slab cut of the upper plenum of a German (KWU) PWR is simulated. The splitted and staggered arrangement of the CRGA support columns was chosen to make good simulation of horizontal flow in the upper plenum.

As shown in Fig. A-10, there are three kinds of CRGA support column. Support column-1 is installed above Bundles 3 and 5 and connected to the CRGA support column bottom with the transition cone. Cross section of the CRGA support calumn changes from a circle to a half circle in this transition cone. Support column 2 is installed above Bundles 6 and 7 and the bottom is closed with the half conical bottom seal plate with many flow holes. Support column 3 is essentially the same as support column 2 but the edge of one side is cut off in order to install above Bundle 1. Each CRGA support column has ten or eleven baffle plates with flow holes. Top flow paths to the upper head bottom and to the upper plenum top are also provided.

Figure A-11 shows vertical cross section of the bottom part of the upper plenum and the interface between the core and the upper plenum. There are eight side flow injection nozzles and eight side flow extraction nozzles just at the opposite side of the upper plenum bottom, corresponding to each bundle.

The upper plenum is separated from the upper head by an upper support plate. Four top injection nozzles penetrate the upper head and open the top of upper plenum as shown in Fig. A-12. Outlet part of the top injection nozzle has a rectangular cross section and double mesh screen with 45 degree cross angle is attached at the mouth.

A.1.4 Simulated Core

The simulated core for the SCTF Core-III consists of 8 heater rod bundles arranged in a row. Each bundle has 236 electrically heated rods and 20 non-heated rods. The arrangement of rods in a bundle is shown in Fig. A-13. The dimensions of the heater rods are based on 15×15 fuel rods bundle for a PWR and the heated length and the outer diameter of each heater rod are 3.613 m and 10.7 mm, respectively. A heater rod consists of a nichrome heater element, boron nitride (BN) or magnesium oxide (MgO) depending on elevation in the heated zone and Nichrofer 7216 (equivalent to Inconel 600) sheath. The sheath thickness is about 1.0 mm and is thicker than the actual fuel cladding because of the requirements for thermocouple installation. The heater element is a helical coil and has a 17 step chopped cosine axial power profile as shown in Fig. A-14. The peaking factor is 1.4.

Non-heated rods are either pipes or solid rods of stainless steel with 13.8 mm O.D. The heater rods and non-heated rods are fixed at the top of the core allowing downward expansion. In Fig. A-15, relative elevation of rods and spacers is shown.

For better simulation of flow resistance in the lower plenum, the simulated fuel rods end in the lower plenum and do not penetrate through the bottom plate of the lower plenum as shown in Fig. A-15.

A.1.5 Primary Loops

Primary loops consist of a hot leg equivalent to four hot legs in area, a steam/water separator for simulating single steam phase flow downstream of the steam generator and for measuring flow rate of carry over water, an intact cold leg equivalent to three intact loops, a broken cold leg on the pressure vessel side and a broken cold leg on the steam/water separator side. These two broken cold legs are connected to two containment tanks through break valves, respectively. The arrangement of the primary loops is shown in Fig. A-16. The flow area of each loop is scaled down based on the core flow area scaling, 1/21. It should be emphasized that the cross section of the hot leg is an elongated circle with an actual height to realize proper flow pattern in the hot leg. The steam/water separator has a steam generator inlet plenum simulator to correctly simulate the flow

characteristics of carryover water into the U-tubes. The cross section of the hot leg and the configuration of the steam genrator inlet plenum simulator are shown in Fig. A-17.

A pump simulator and a loop seal part are provided for the intact cold leg. The arangement of the intact cold leg is shown in Fig. A-18. The pump simulator consists of the casing and duct simulators and an orifice plate as shown in Fig. A-19. The loop resistance is adjusted with the orifice plates attached to the intact cold leg, the steam/water separator side and pressure vessel side broken cold legs and the pump simulator.

A.1.6 ECC Water Injection System

Three kinds of ECCSs are provided, i.e., the accumulator injection system (Acc), low pressure coolant injection system (LPCI) and combined injection system. Available injection locations for the former two are the intact and broken cold legs, the hot leg, the lower plenum and the downcomer. On the other hand, those for the last one are the top and bottom-side of the upper plenum and the intact and broken cold legs.

A.1.7 Containment Tanks and Auxiliary System

Two containment tanks are provided to SCTF. The containment tank-I is connected with the downcomer through the pressure vessel side broken cold leg and the containment tank-II is connected with the steam/water separator through the steam/water separator side broken cold leg. Especially in the containment tank-I, carryover water from the downcomer is measured by the differentiation of the liquid level. These containment tanks and auxiliary system such as a pressurizer for injecting water from the Acc tanks, etc. are shared with CCTF.

A.2 Instrumentation

The instrumentation in SCTF has been provided both by JAERI and USNRC. The JAERI-provided instrumentation includes the measurement of temperatures, pressures, differential pressures, liquid levels, flow velocities, and heating powers. USNRC has provided film probes, impedance probes, string probes, liquid level detectors (LLDs), fluid distribution grids (FDGs), turbine meters, drag disks, densitometers, spool pieces, drag bodies, break through detectors and video optical probes. Locations of the JAERI-provided instruments are shown in Figs. A-20 through A-43.

Table A-1 Principal Dimensions of the SCTF

1.	**Core Dimension**	
	(1) Quantity of Bundle	8 Bundles
	(2) Bundle Array	1 × 8
	(3) Bundle Pitch	230 mm
	(4) Rod Array in a Bundle	16 × 16
	(5) Rod Pitch in a Bundle	14.3 mm
	(6) Quantity of Heater Rod in a Bundle	236 rods
	(7) Quantity of Non-Heated Rod in a Bundle	20 rods
	(8) Total Quantity of Heater Rods	236×8=1,888 rods
	(9) Total Quantity of Non-Heated Rods	20×8=160 rods
	(10) Effective Heated Length of Heater Rod	3613 mm
	(11) Diameter of Heater Rod	10.7 mm
	(12) Diameter of Non-Heated Rod	13.8 mm
2.	**Flow Area & Fluid Volume**	
	(1) Core Flow Area	0.25 m^2
	(2) Core Fluid Volume	0.903 m^3
	(3) Baffle Region Flow Area (isolated)	(0.096) m^2
	(4) Baffle Region Fluid Volume (nominal)	0.355 m^3
	(5) Cross-Sectional Area of Core Additional Fluid Volumes Including Gap between Core Barrel and Pressure Vessel Wall and Various Penetration Holes	0.07 m^2 0.10 m^2
	(6) Downcomer Flow Area	0.158 m^2
	(7) Upper Annulus Flow Area	0.158 m^2
	(8) Upper Plenum Horizontal Flow Area (max.)	0.541 m^2
	(9) Upper Plenum Vertical Flow Area	0.525 m^2
	(10) Upper Plenum Fluid Volume	1.156 m^3
	(11) Upper Head Fluid Volume	0.86 m^3
	(12) Lower Plenum Fluid Volume (excluding below downcomer)	1.305 m^3
	(13) Steam Generator Inlet Plenum Simulator Flow Area	0.626 m^2
	(14) Steam Generator Inlet Plenum Simulator Fluid Volume	0.931 m^3
	(15) Steam Water Separator Fluid Volume	5.3 m^3
	(16) Flow Area at the Top Plate of Steam Generator Inlet Plenum Simulator	0.195 m^2
	(17) Hot Leg Flow Area	0.0826 m^2

Table A-1 (continue)

(18)	Intact Cold Leg Flow Area (Diameter = 297.9 mm) Inverted U-Tube with 0.0314 m^2 Cross-Sectional Area (Diameter = 200 mm) and 10 m Height from the Top of Steam Generator Inlet Plenum Simulator Can Be Added As an Option.	0.0697 m^2
(19)	Broken Cold Leg Flow Area (Diameter = 151.0 mm)	0.0197 m^2
(20)	Containment Tank-I Fluid Volume	30 m^3
(21)	Containment Tank-II Fluid Volume	50 m^3
(22)	Flow Area of Exhausted Steam Line from Containment Tank-II to the Atmosphere	see Fig. 3-63

3. Elevation & Height

(1)	Top Surface of Upper Core Support Plate (UCSP)	0 mm
(2)	Bottom Surface of UCSP	- 40 mm
(3)	Top of the Effective Heated Length of Heater Rod	- 444 mm
(4)	Bottom of the Effective Heated Length of Heater Rod	-4,057 mm
(5)	Bottom of the Skirt in the Lower Plenum	-5,270 mm
(6)	Bottom of Intact Cold Leg	+ 724 mm
(7)	Bottom of Hot Leg	+1,050 mm
(8)	Top of Upper Plenum	+2,200 mm
(9)	Bottom of Steam Generator Inlet Plenum Simulator	+1,933 mm
(10)	Centerline of Loop Seal Bottom	-2,281 mm
(11)	Bottom Surface of End Box	- 263 mm
(12)	Top of Upper Annulus of Downcomer	+2,234 mm
(13)	Height of Steam Generator Inlet Plenum Simulator	1,595 mm
(14)	Height of Loop Seal	3,140 mm
(15)	Inner Height of Hot Leg Pipe	737 mm
(16)	Bottom of Lower Plenum	-5,772 mm
(17)	Top of Upper Head	+2,887 mm

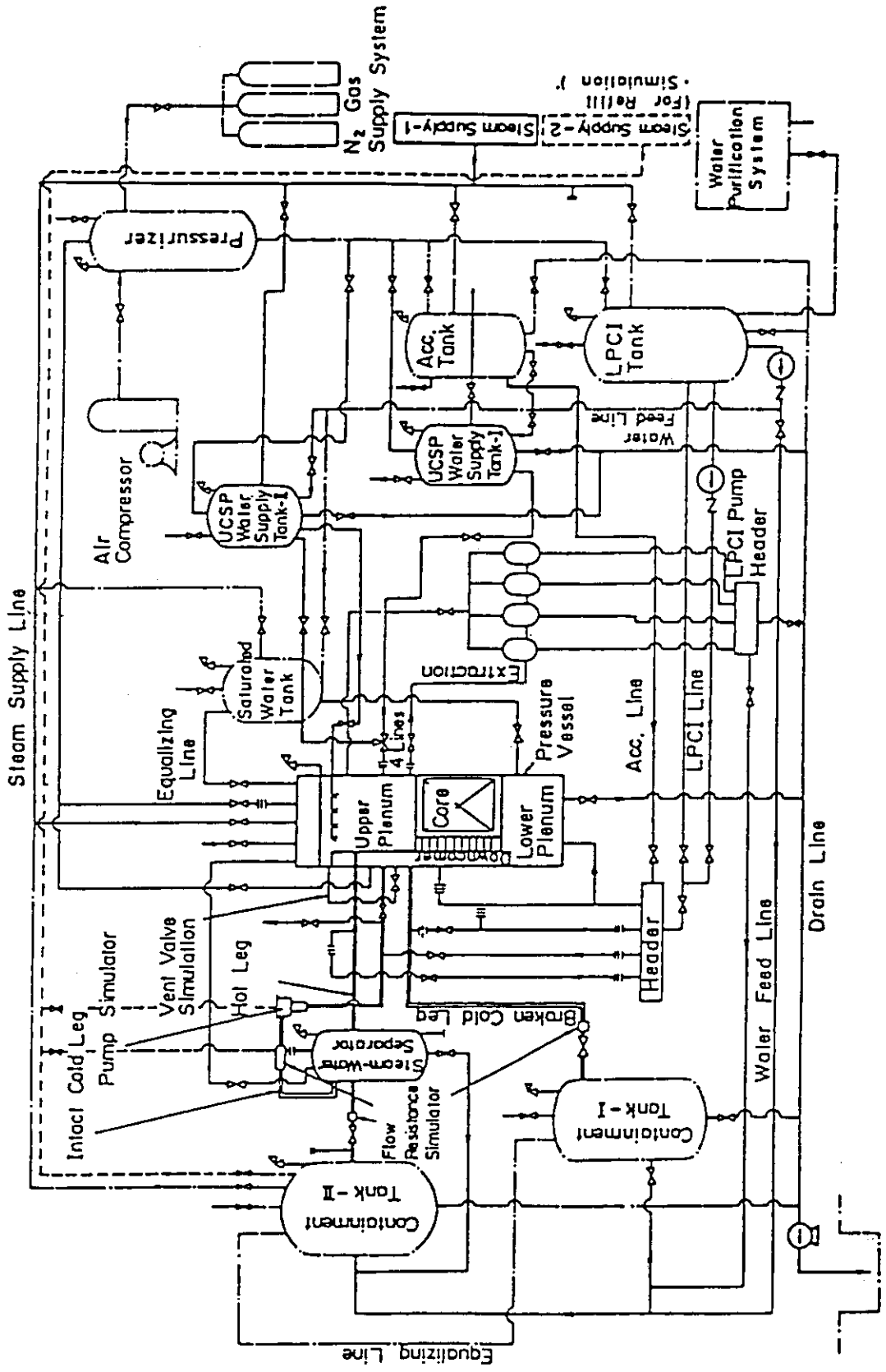

Fig. A-1 Schematic Diagram of Slab Core Test Facility

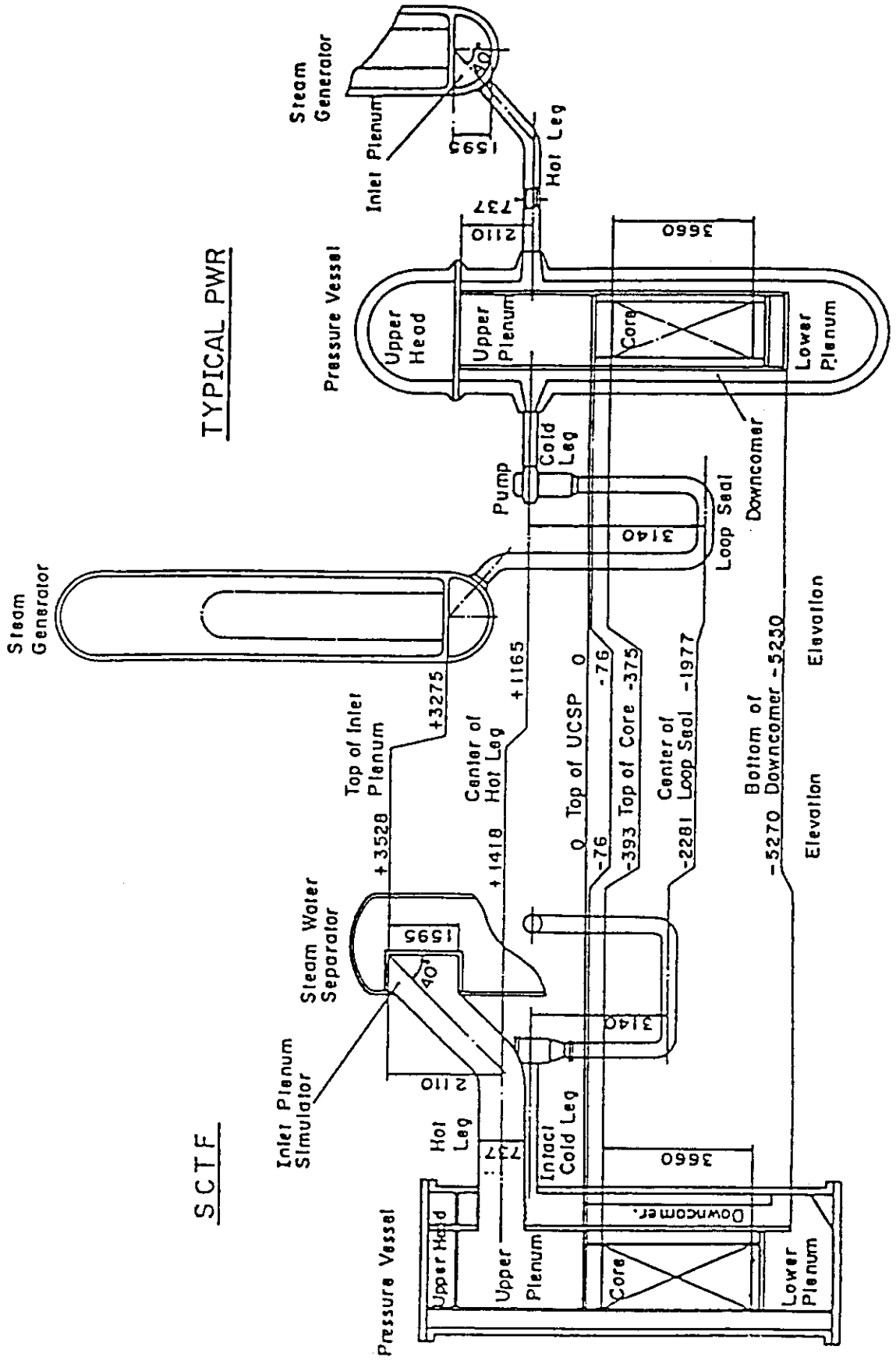

Fig. A-2 Comparison of Dimensions between SCTF and a Reference PWR

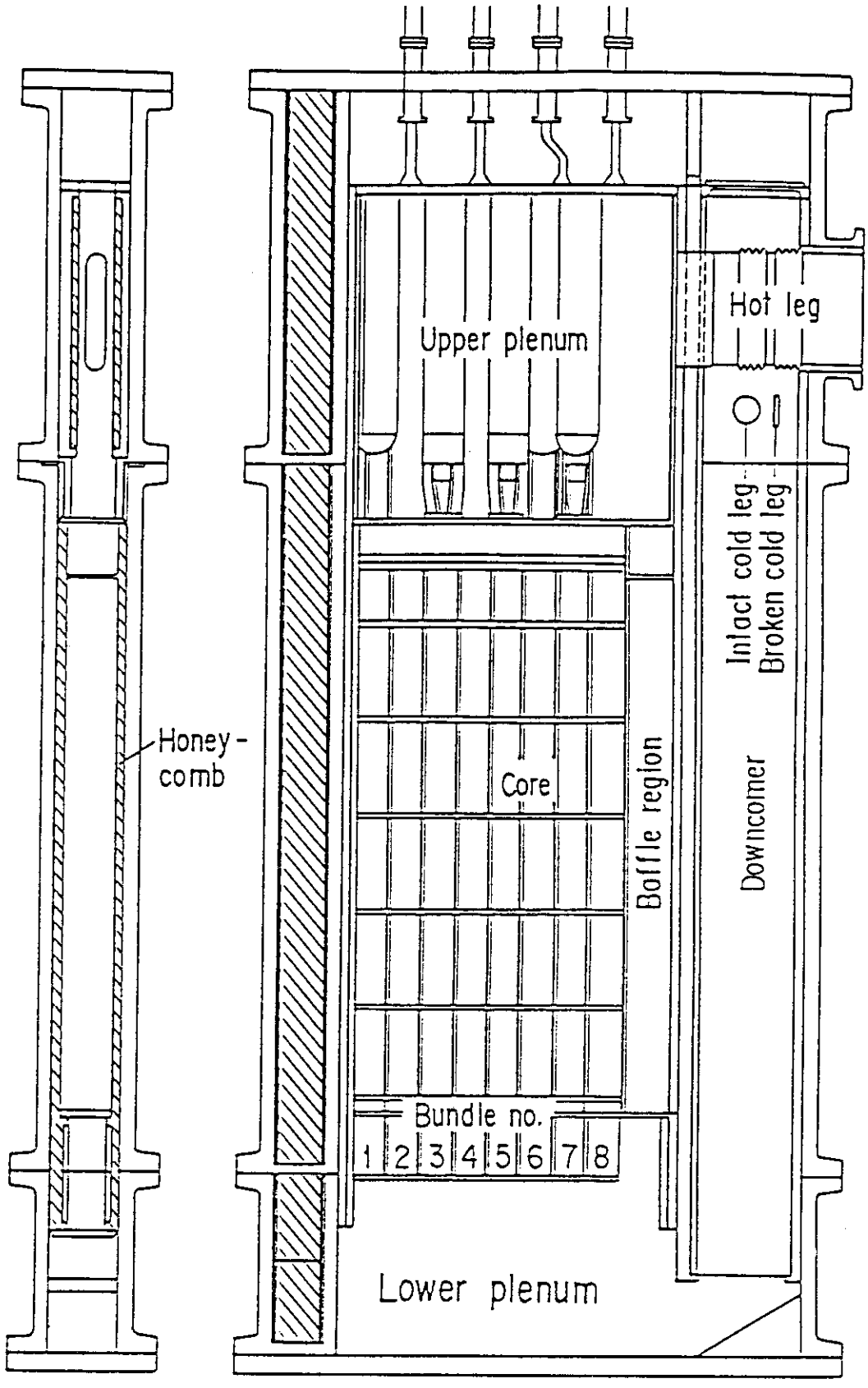

Fig. A-3 Vertical Cross Sections of Pressure Vessel

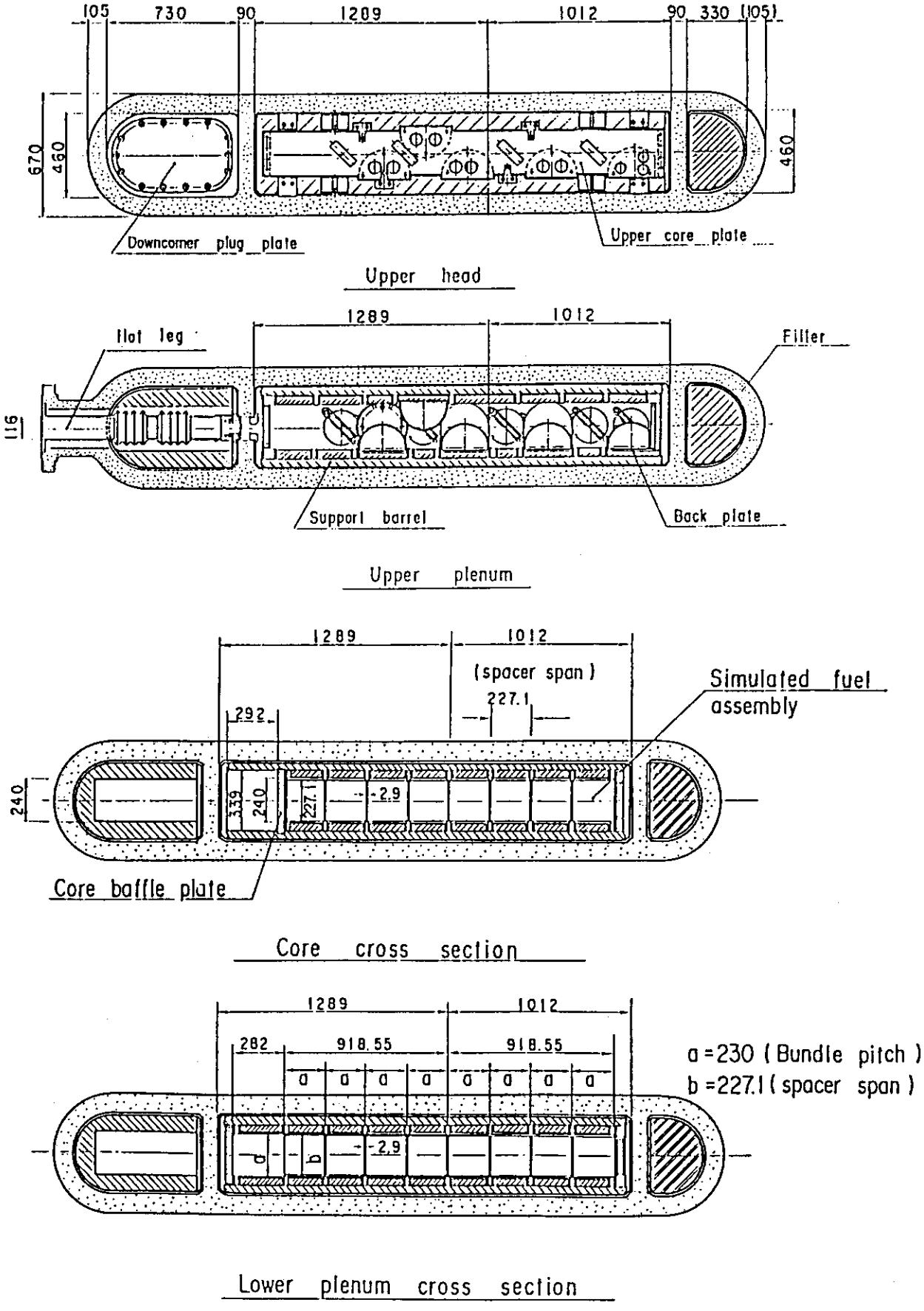

Fig. A-4 Horizontal Cross Sections of Pressure Vessel

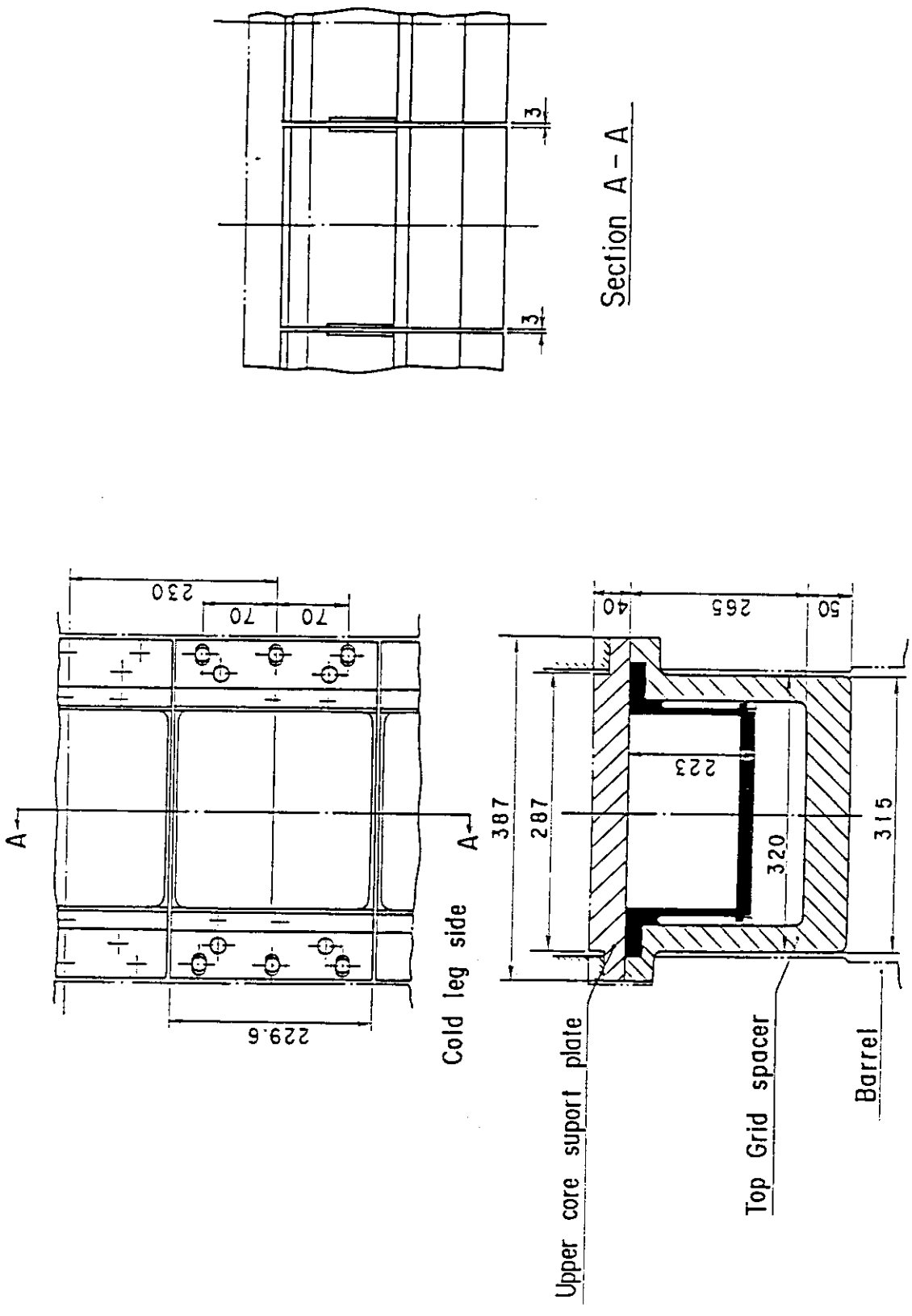

Fig. A-5 Arrangement and Principal Dimension of End Boxes and Top Grid Spacers

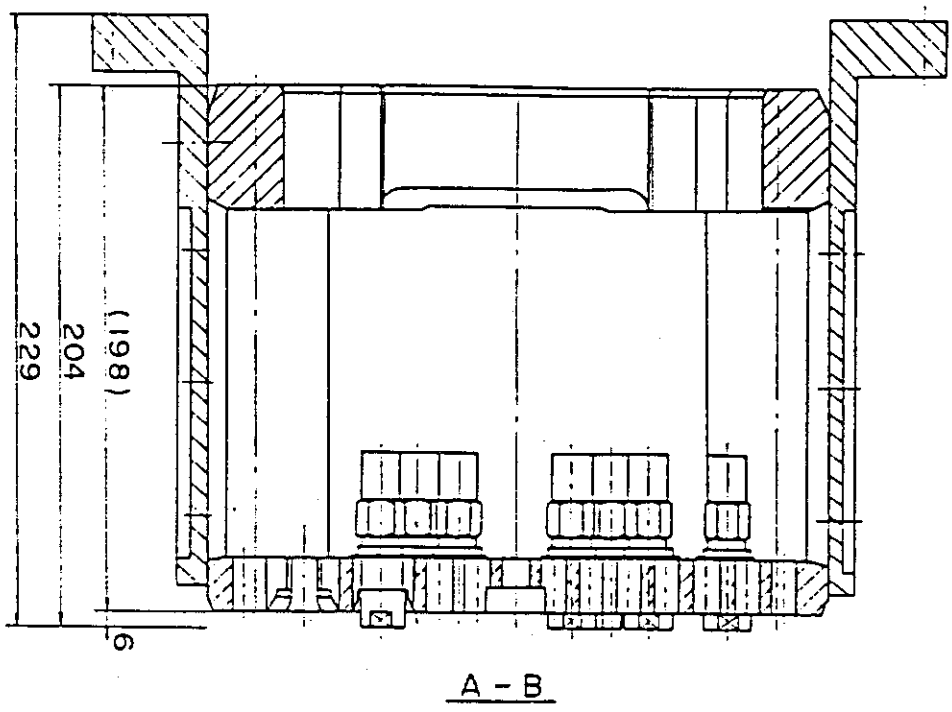

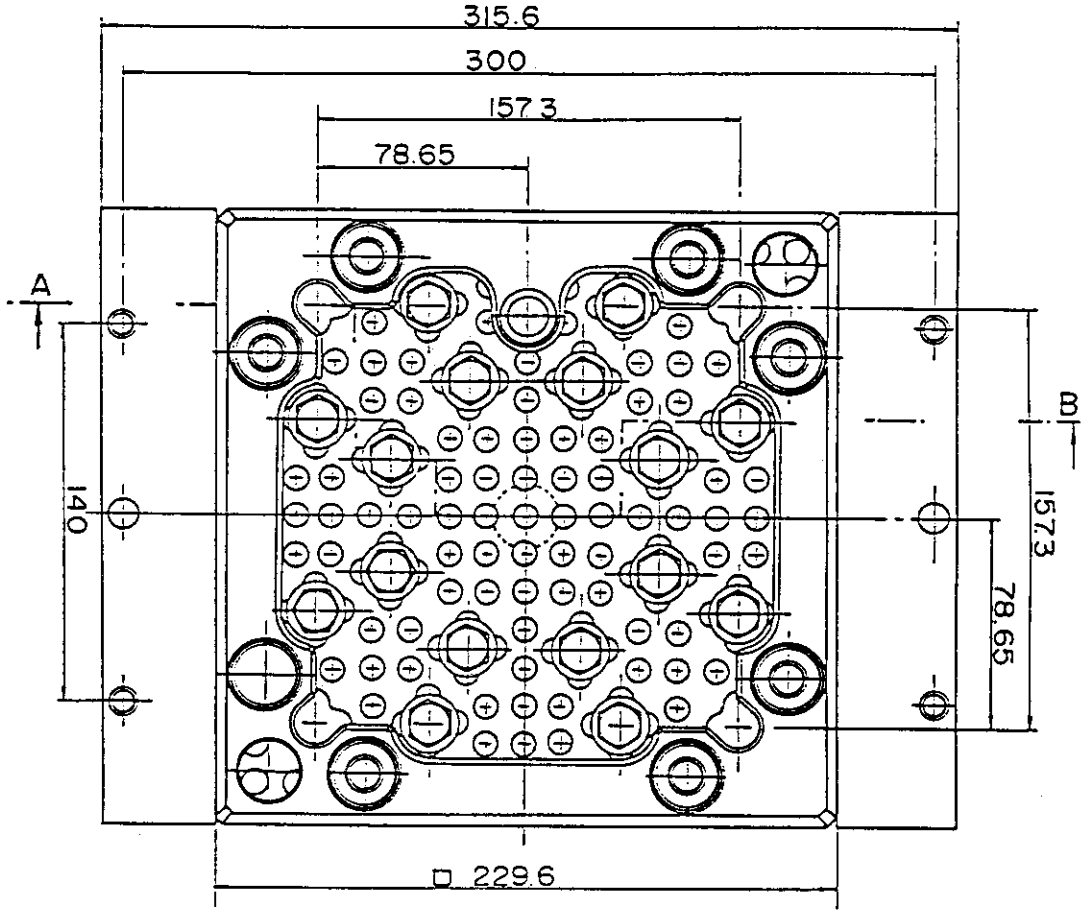

Fig. A-6 Configuration and Dimension of End Boxes

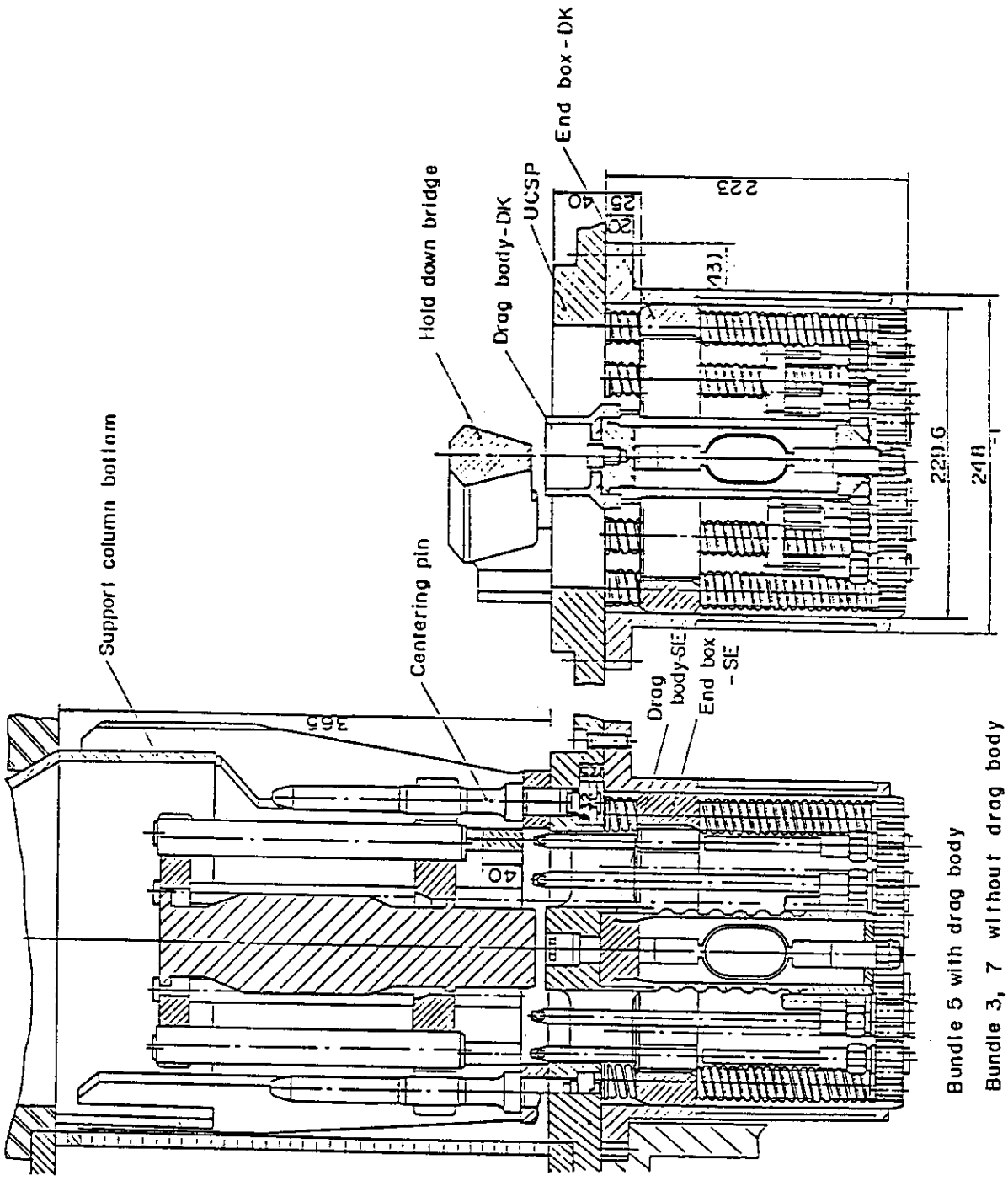

Fig. A-7 Detail of End Boxes with Drag Bodies

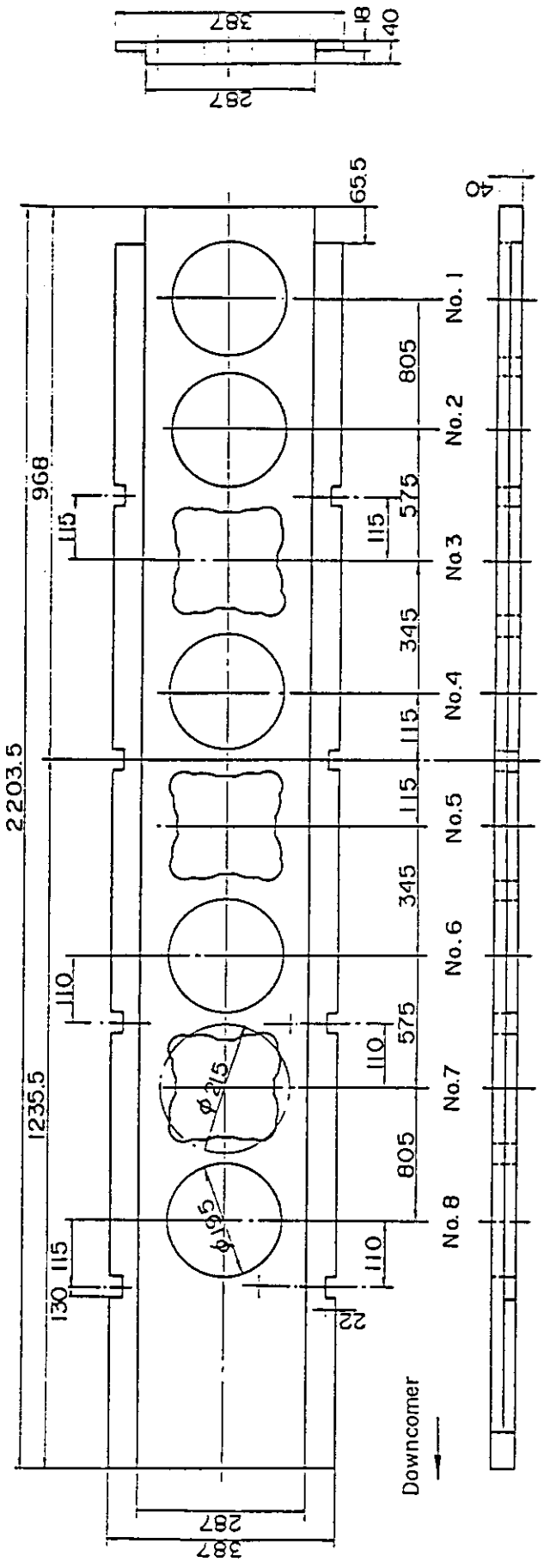

Fig. A-8 Dimension of Upper Core Support Plate

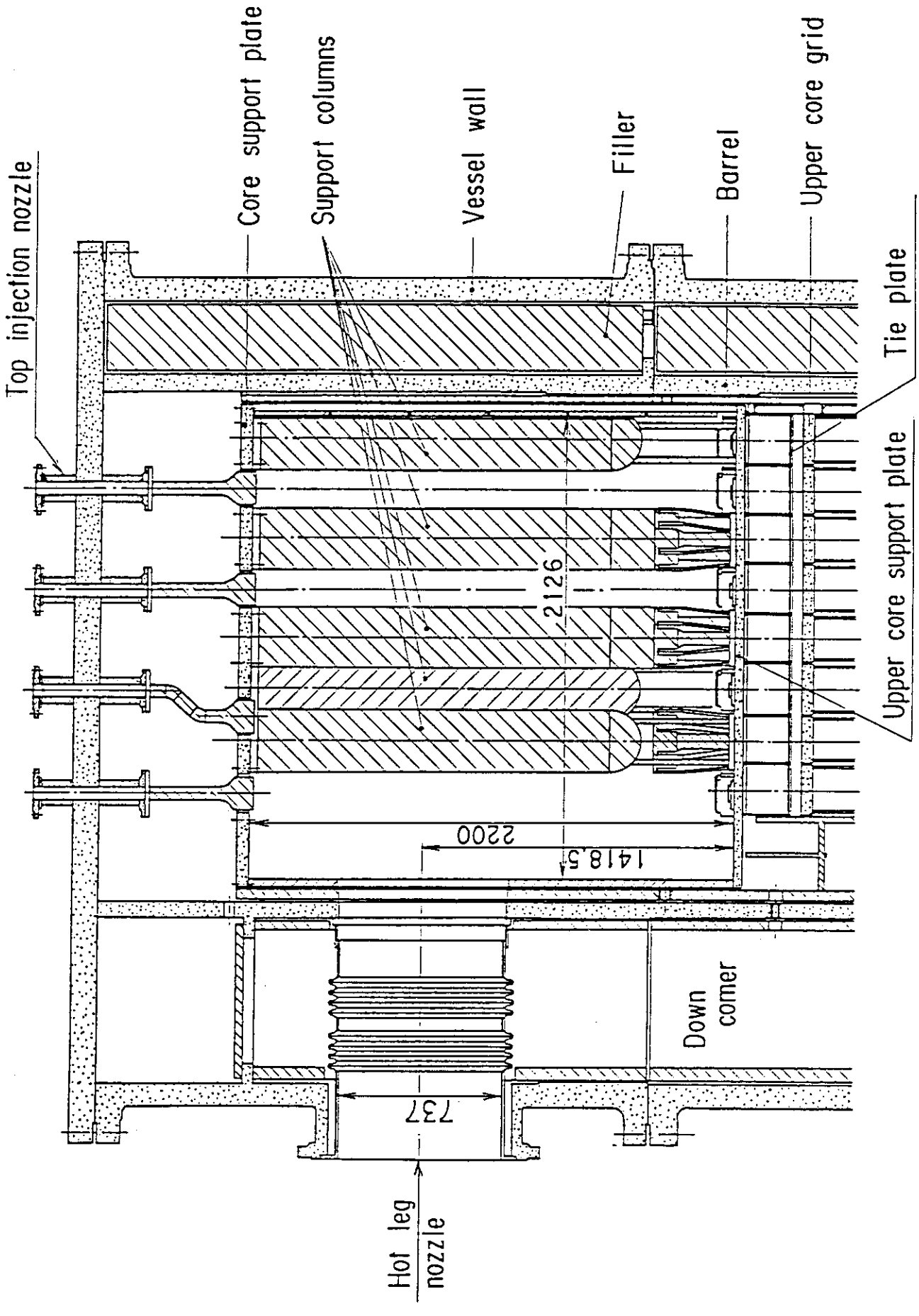

Fig. A-9 Vertical Cross Section of Upper Plenum Internals

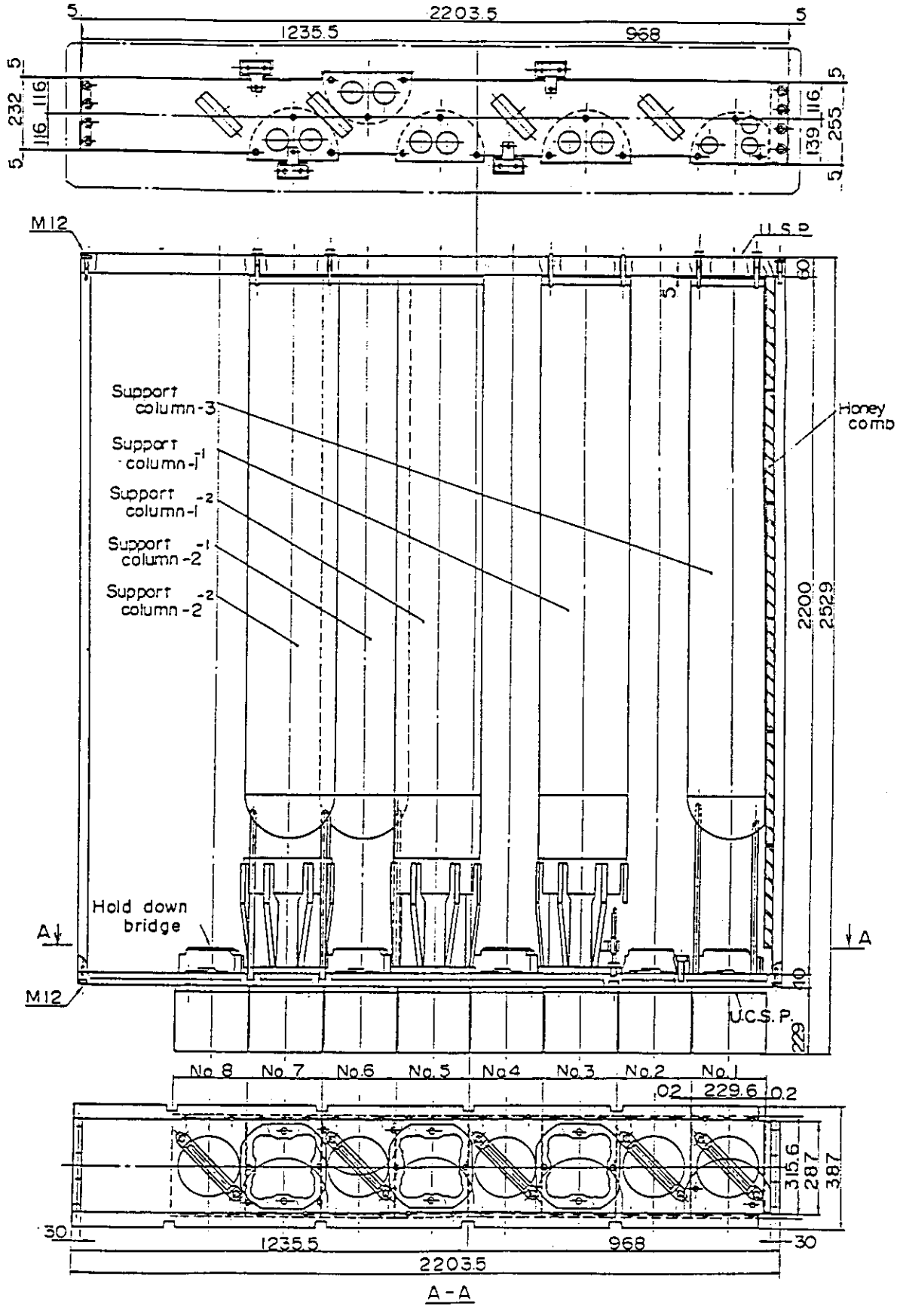

Fig. A-10 Three Kinds of CRGA Support Column

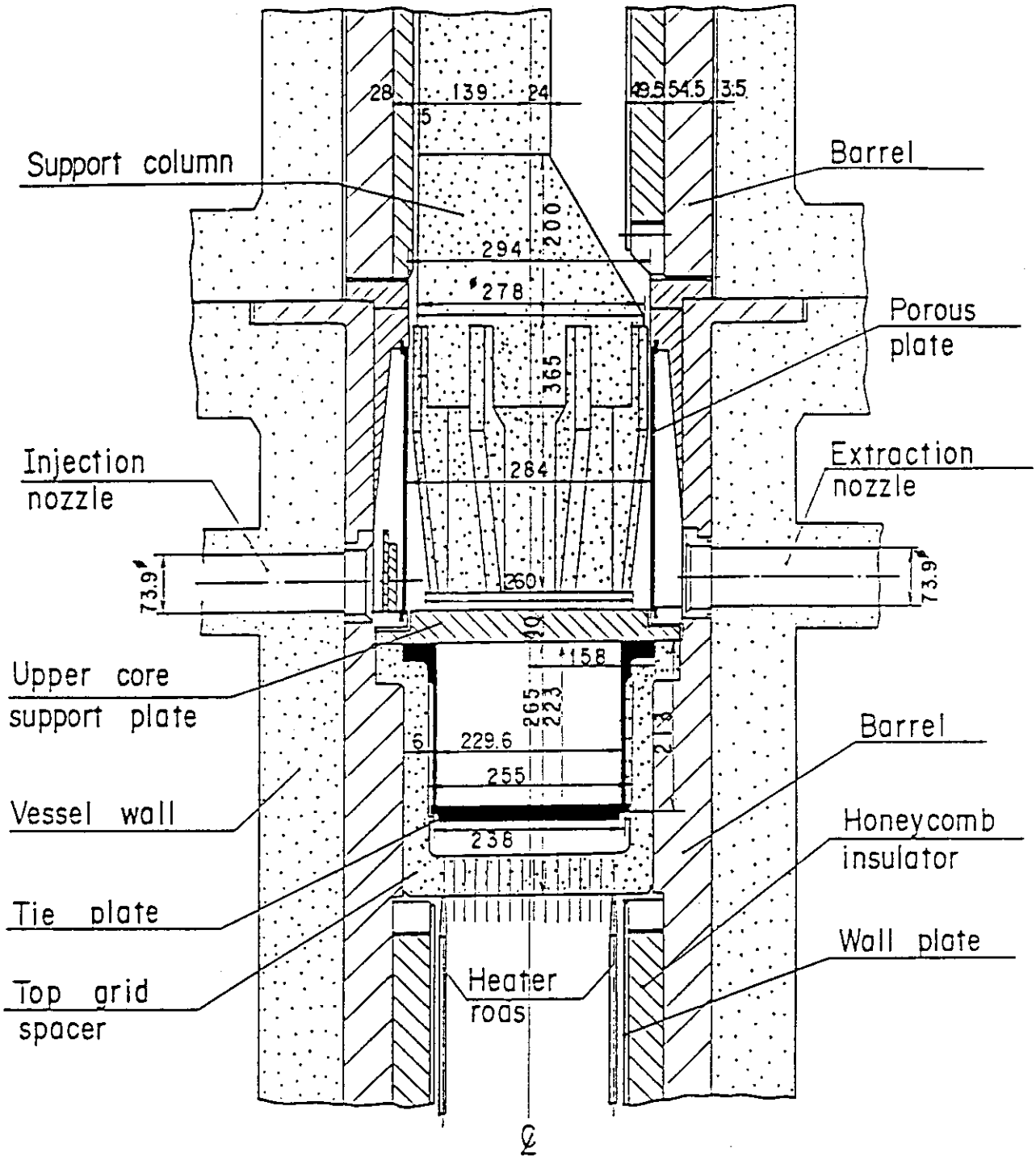

Fig. A-11 Vertical Cross Section of Interface between Core and Upper Plenum

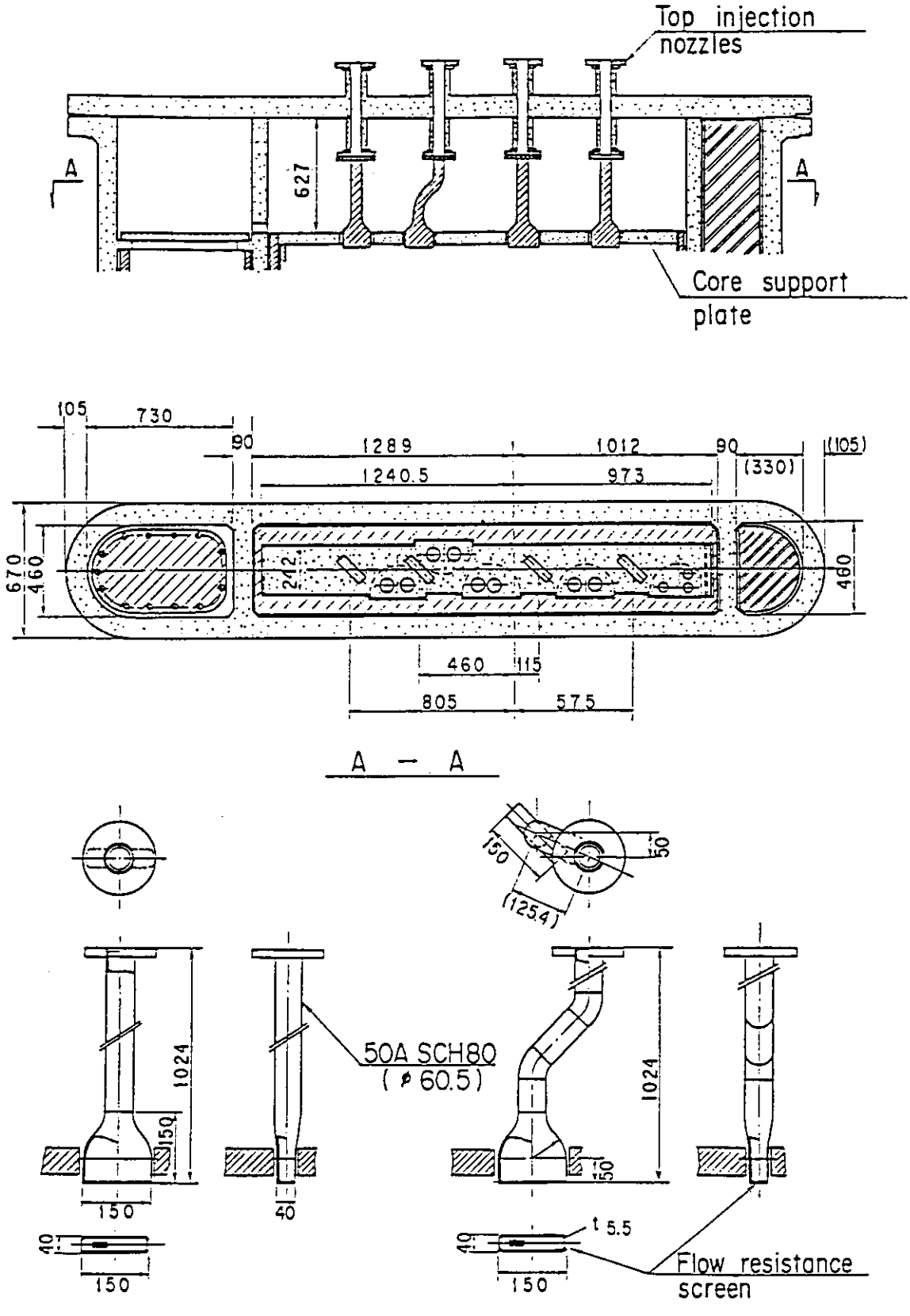

Fig. A-12 Schematic of Upper Head

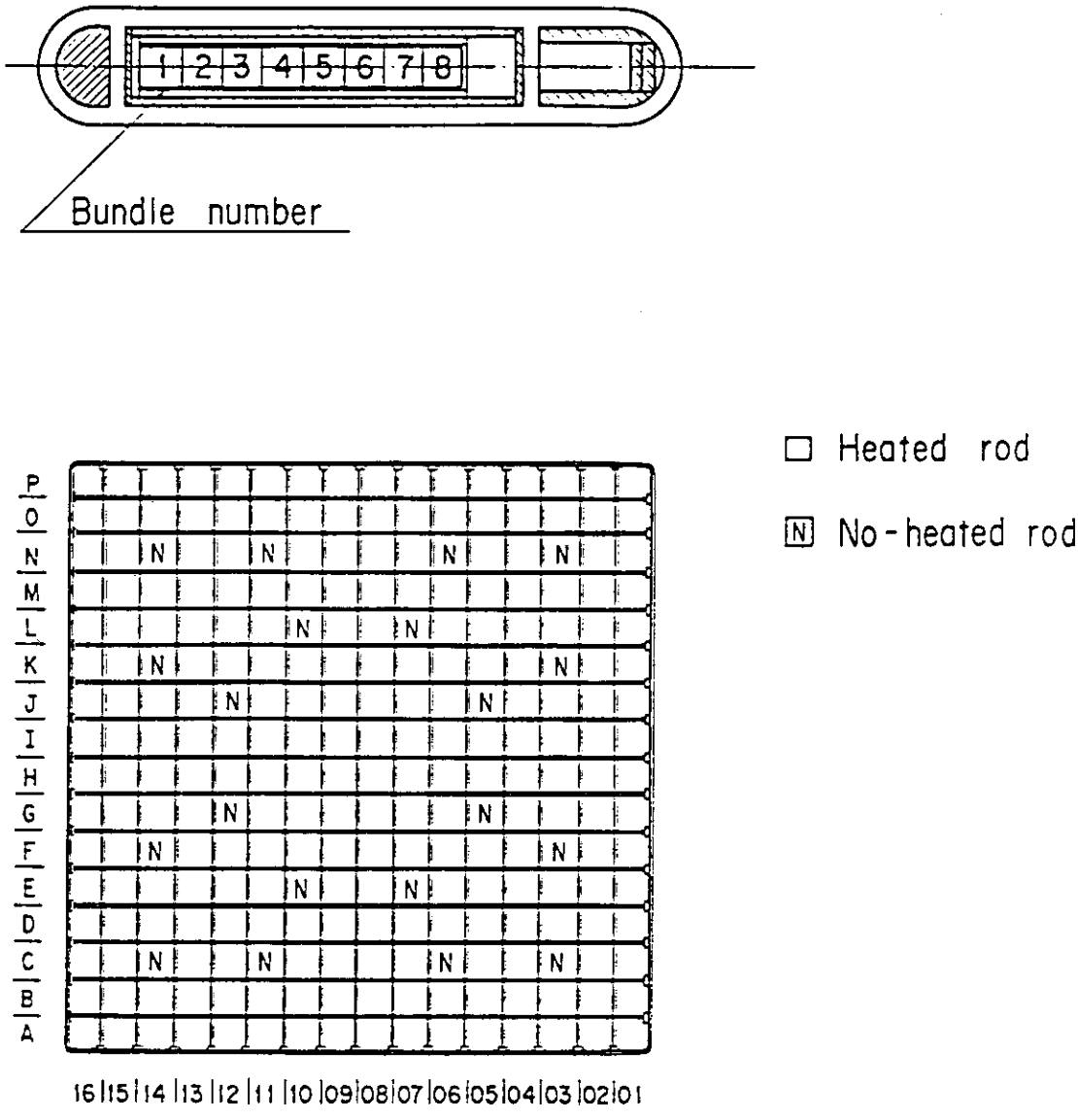

Fig. A-13 Arrangement of Heater Rod Bundles

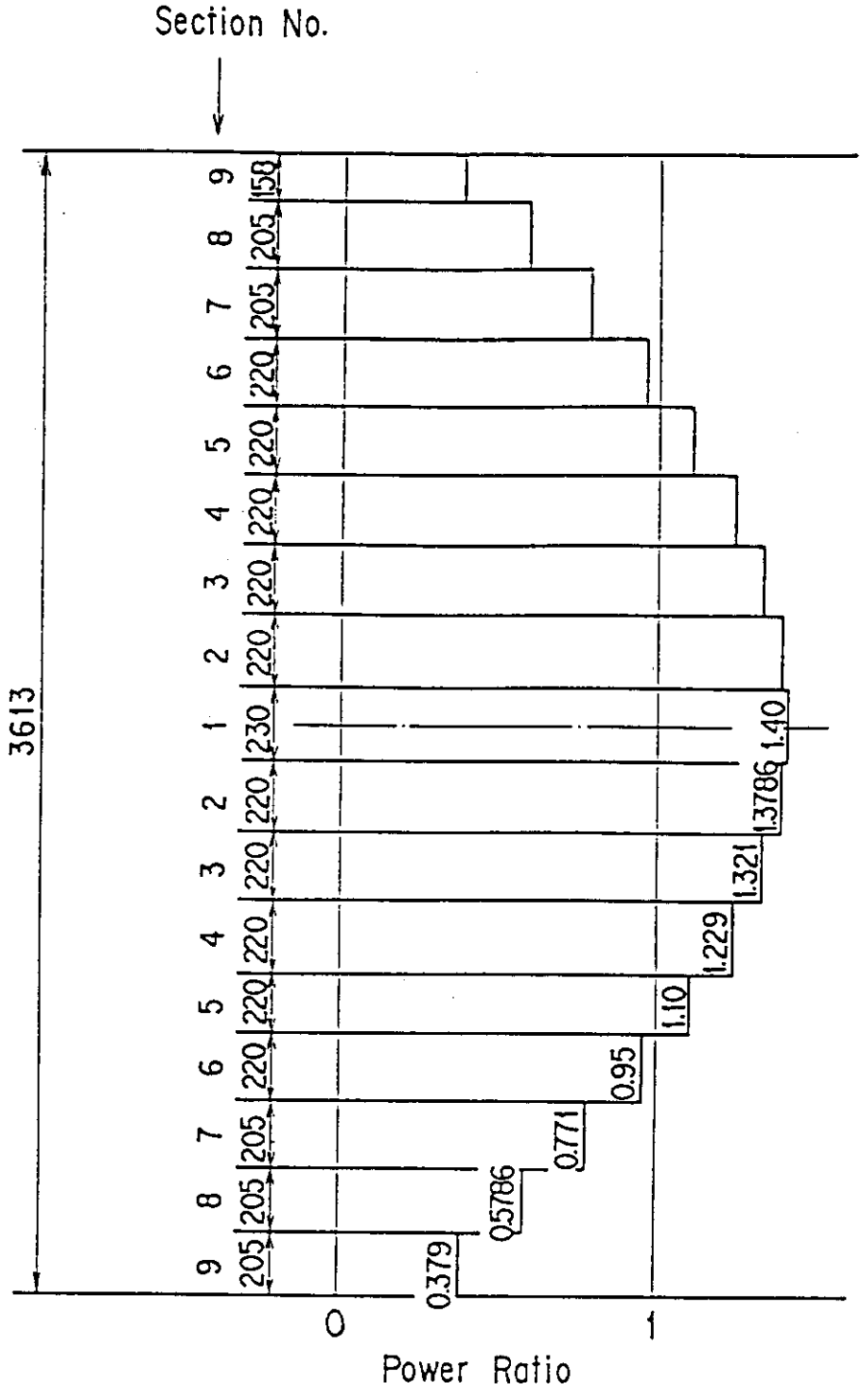

Fig. A-14 Axial Power Distribution of Heater Rods

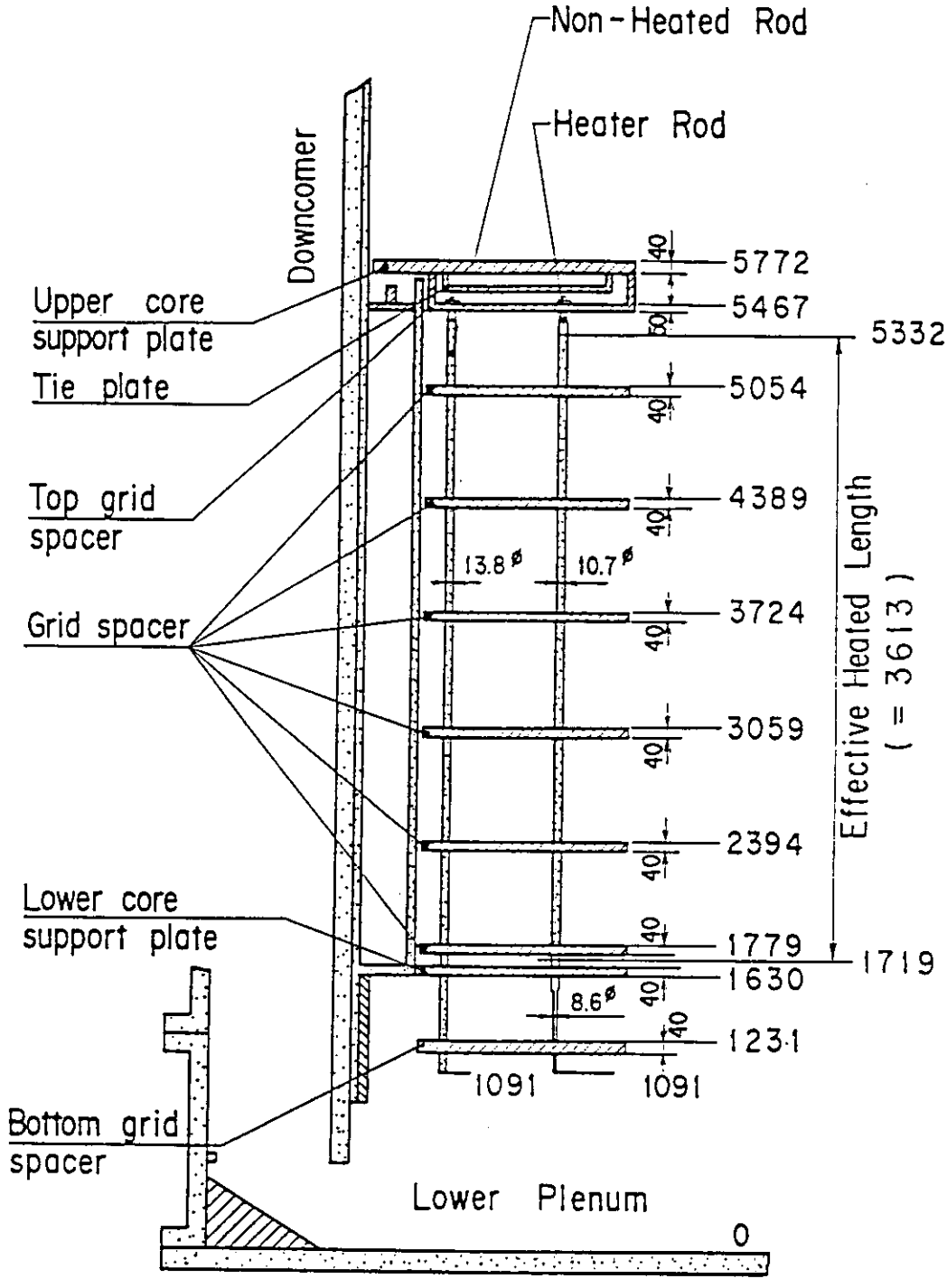

Fig. A-15 Relative Elevation and Dimension of Core

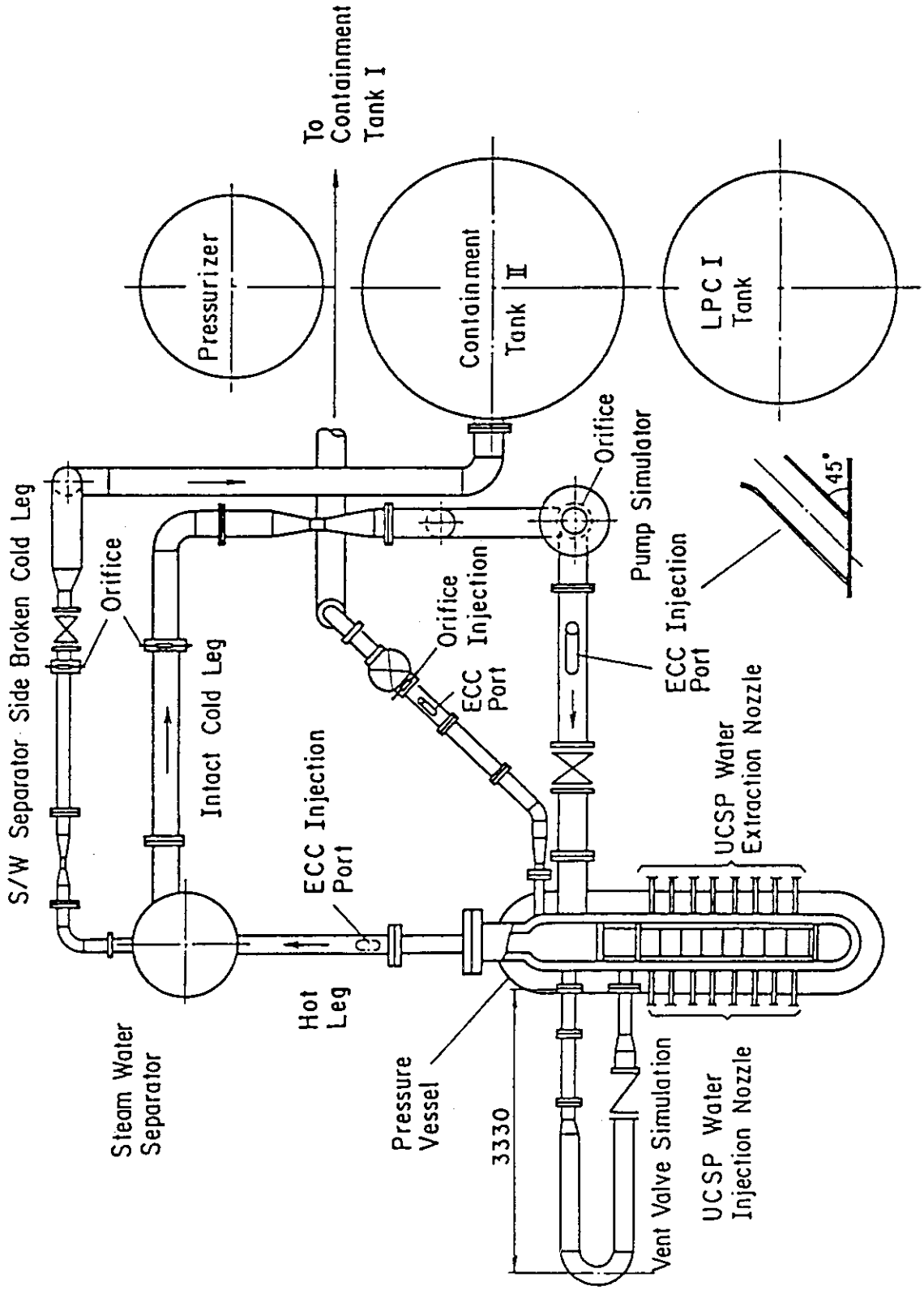

Fig. A-16 Overview of the Arrangements of SCTF

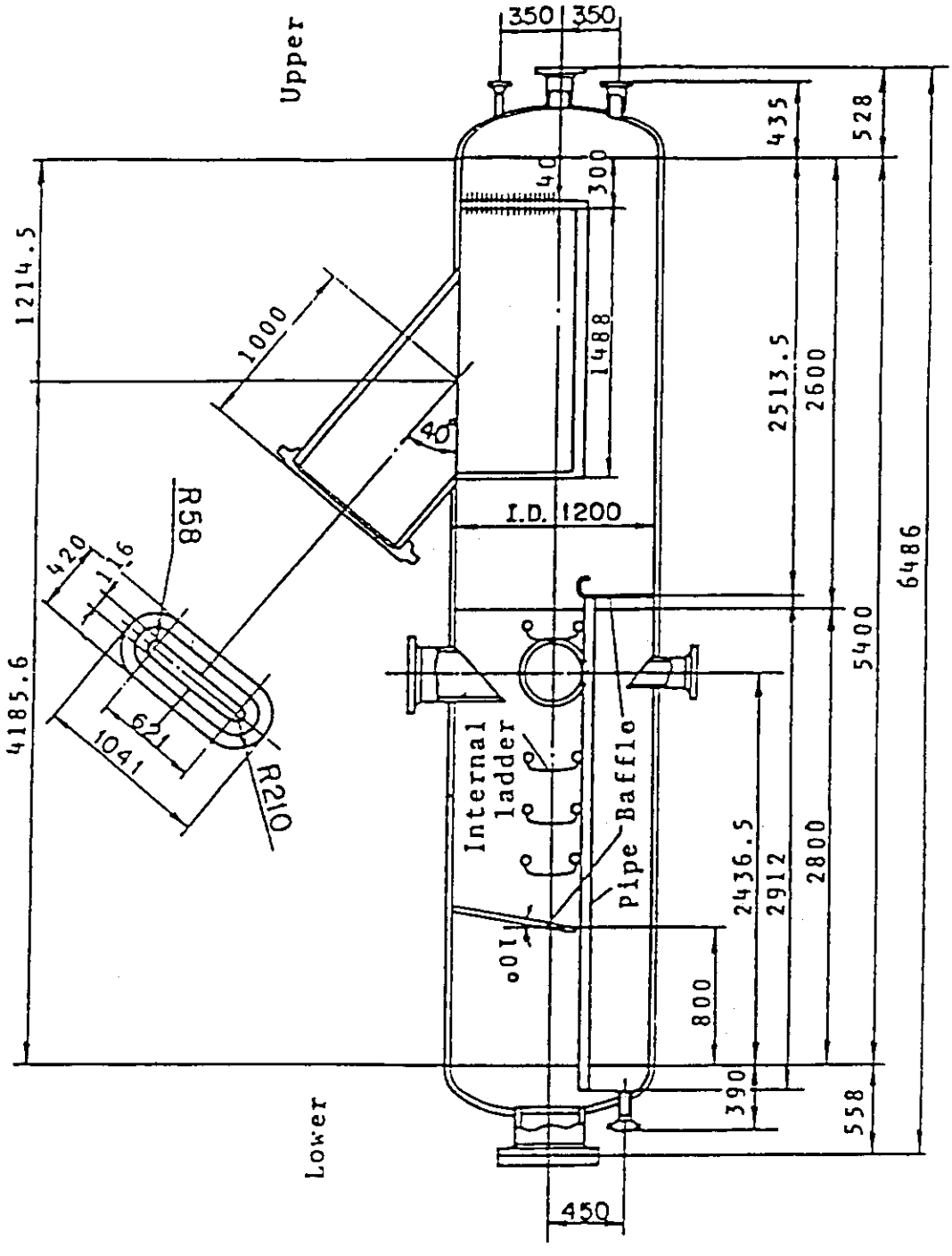

Fig. A-17 Steam/Water Separator

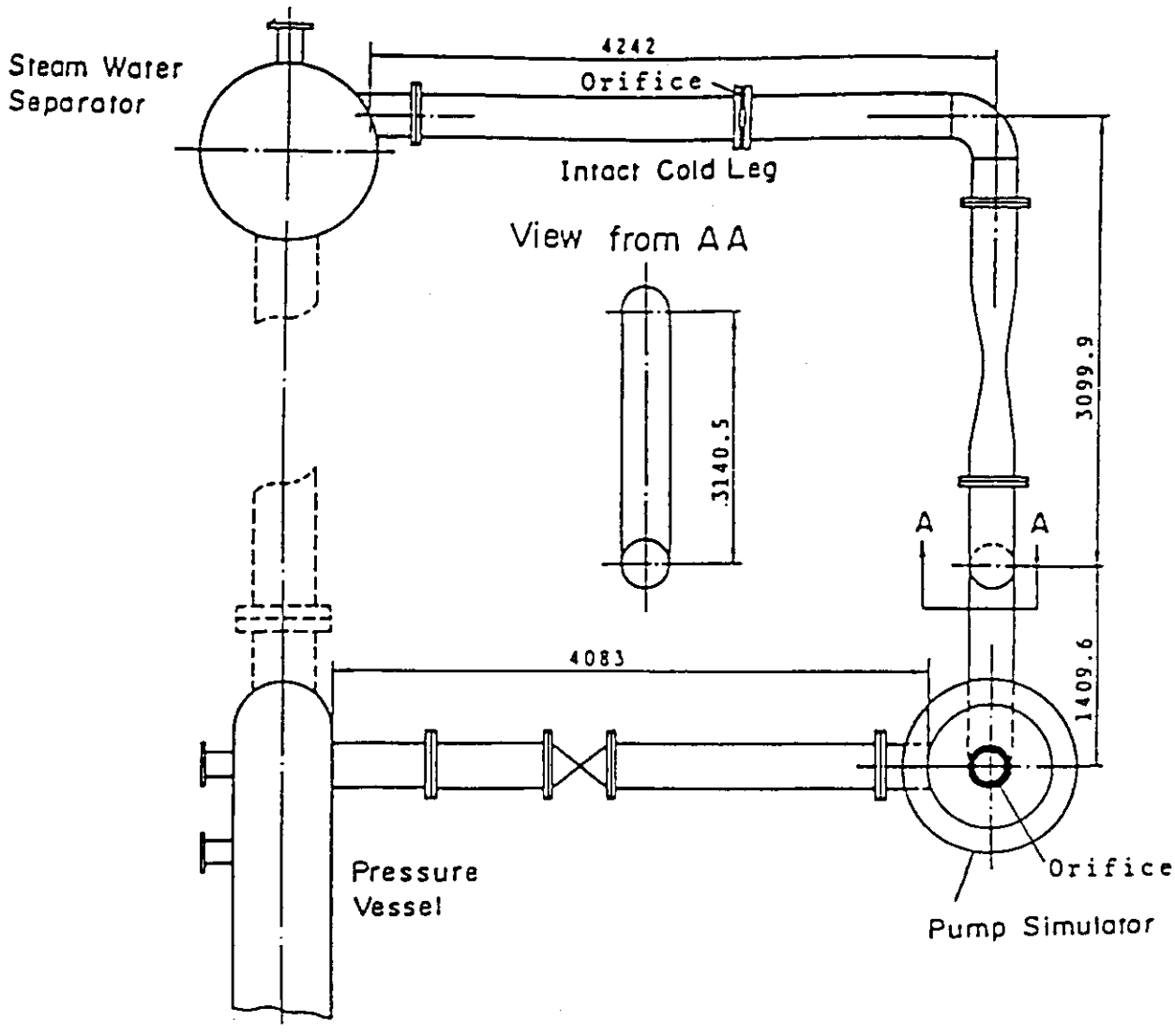

Fig. A-18 Arrangement of Intact Cold Leg

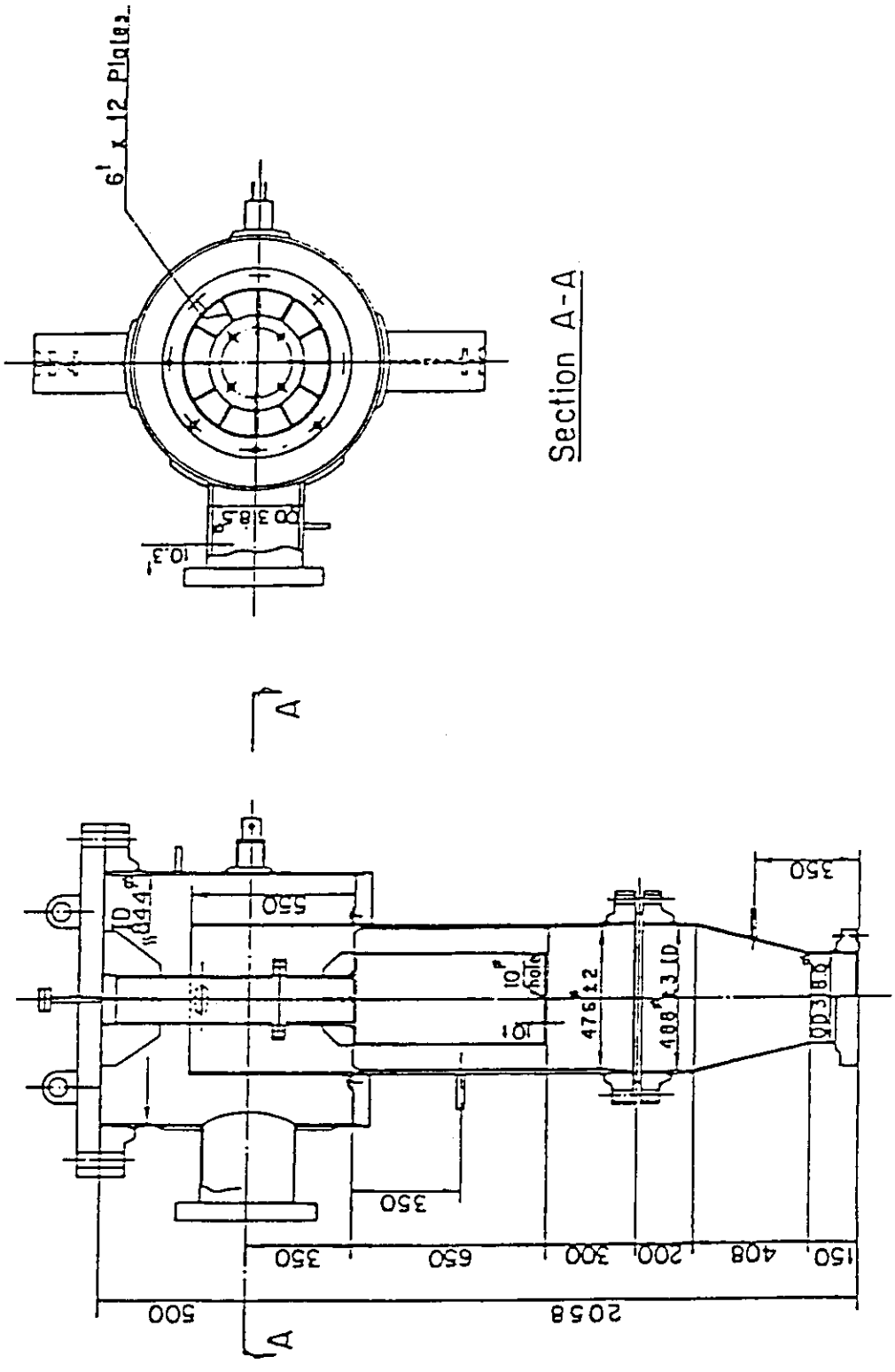

Fig. A-19 Configuration and Dimension of Pump Simulator

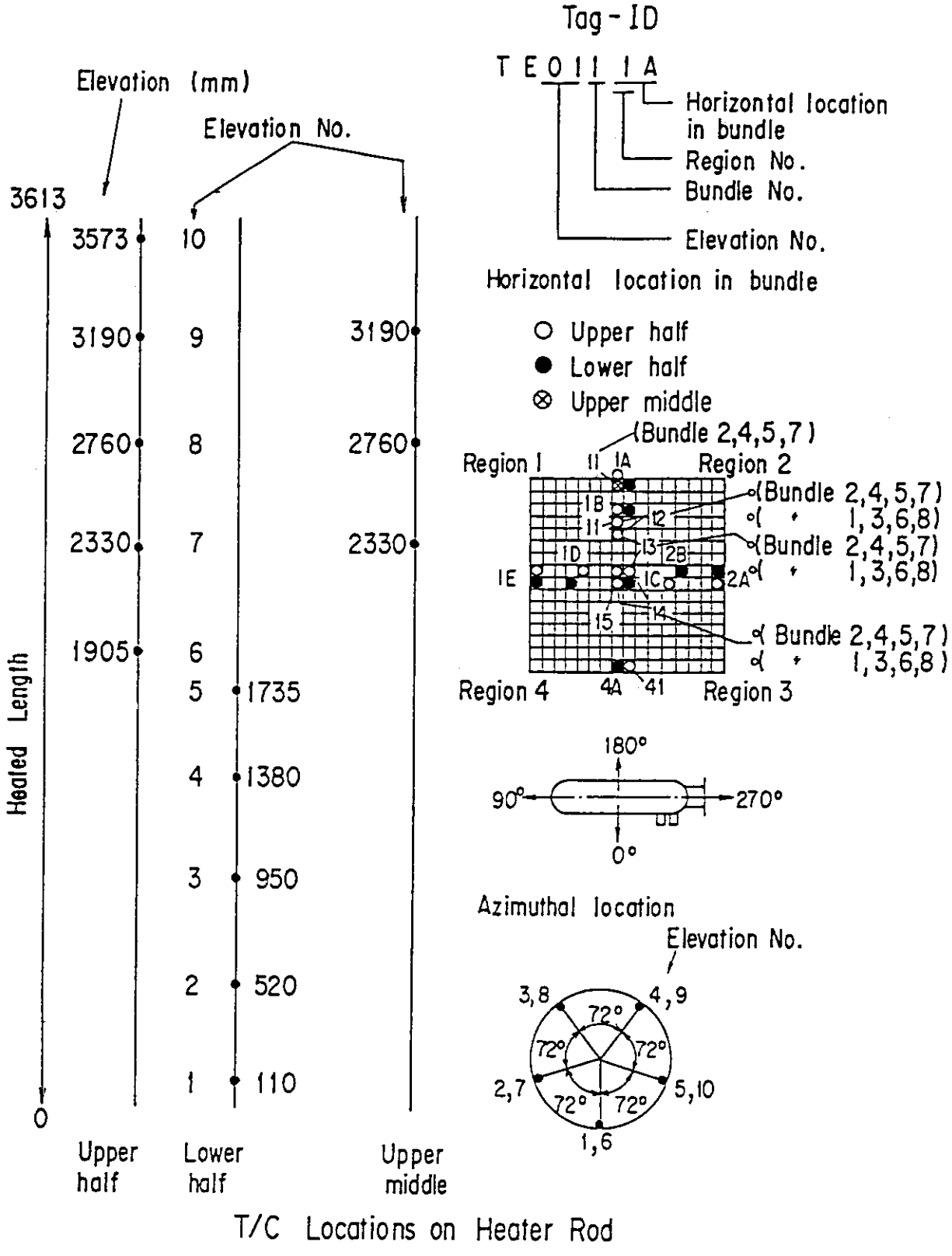

T/C Locations on Heater Rod

Fig. A-20 Thermocouple Locations of Heater Rod Surface Temperature Measurements

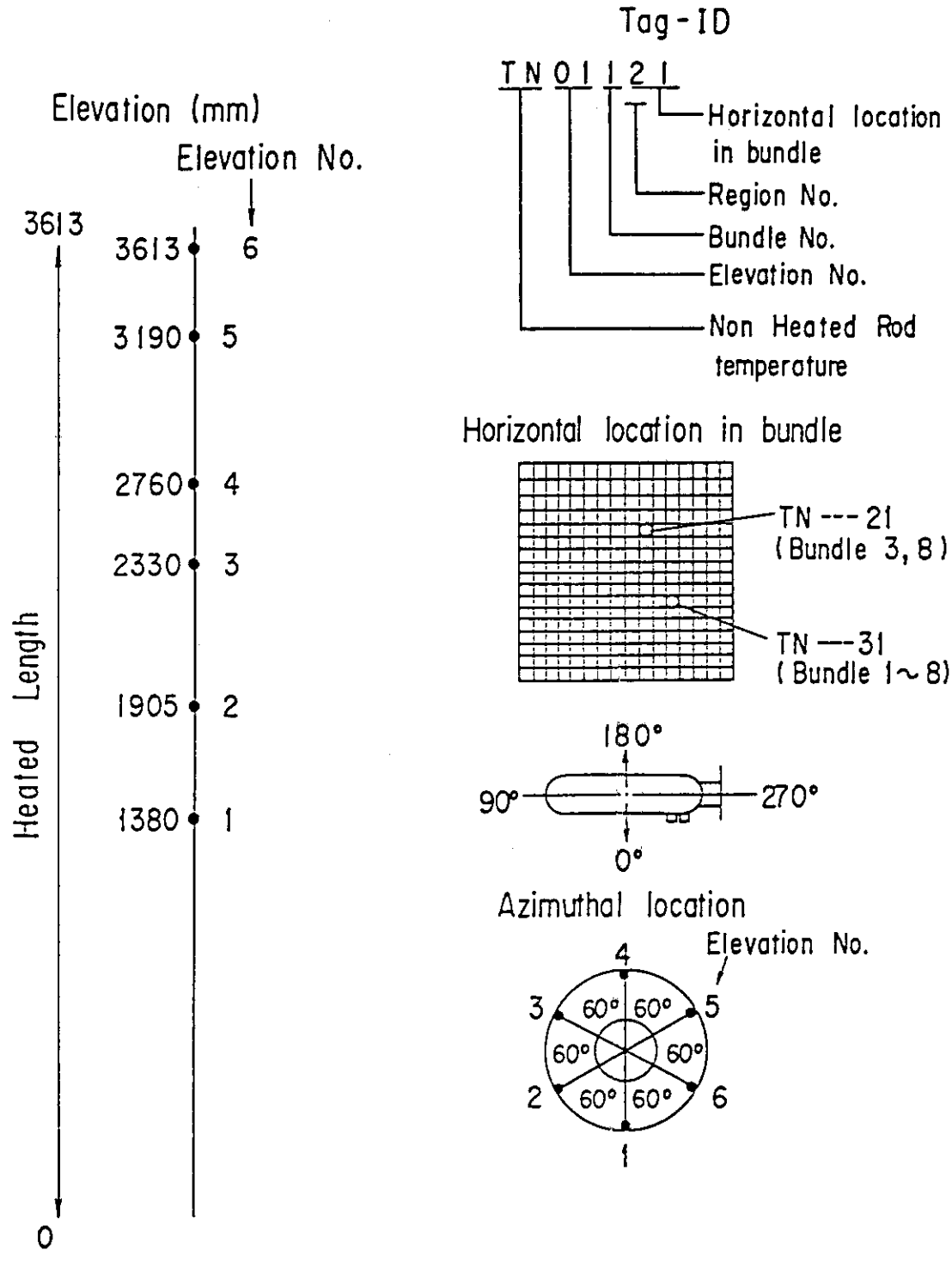

Fig. A-21 Thermocouple Locations of Non-Heated Rod Surface temperature Measurements

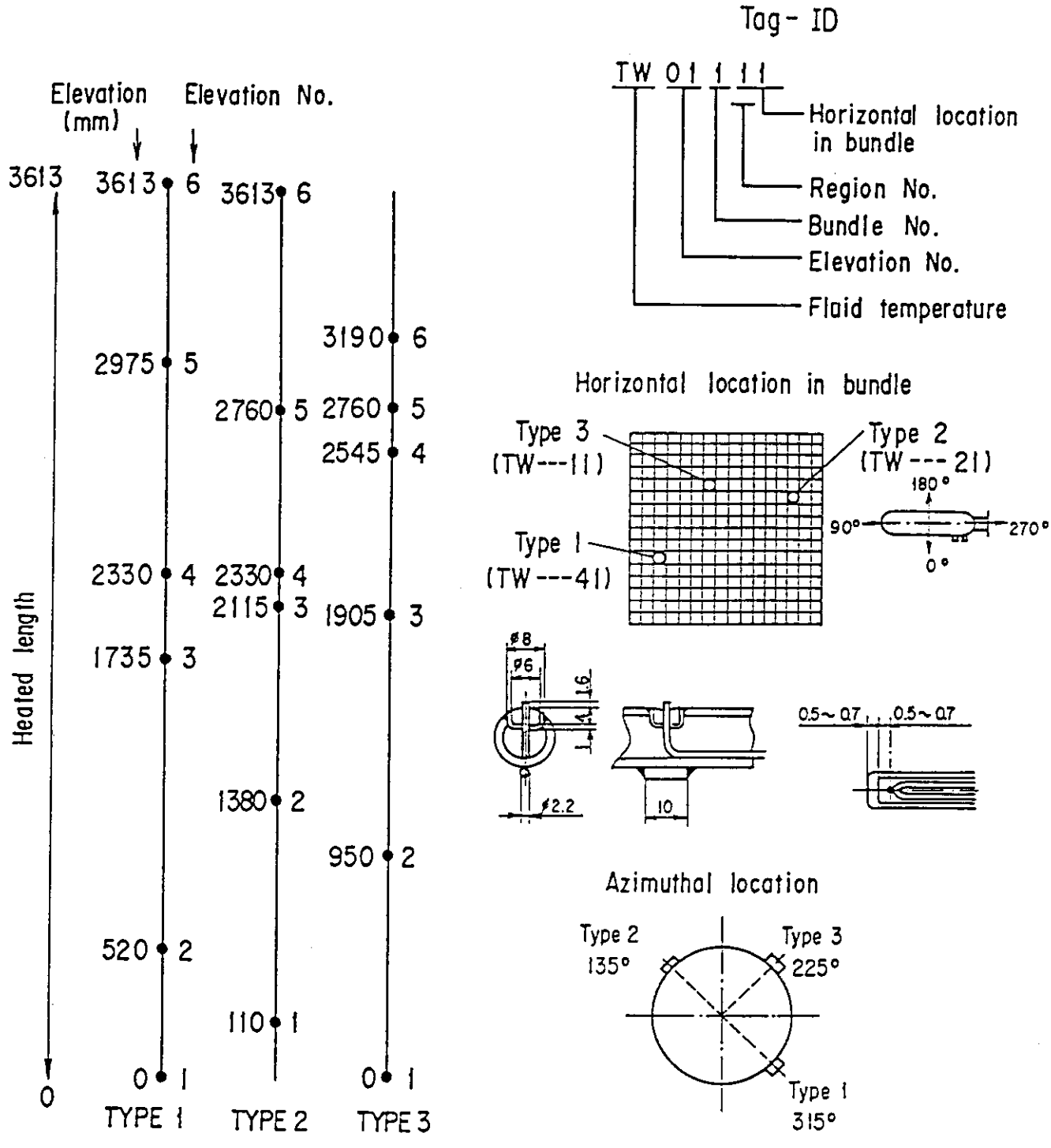

Fig. A-22 Thermocouple Locations of Fluid Temperature Measurements in Core

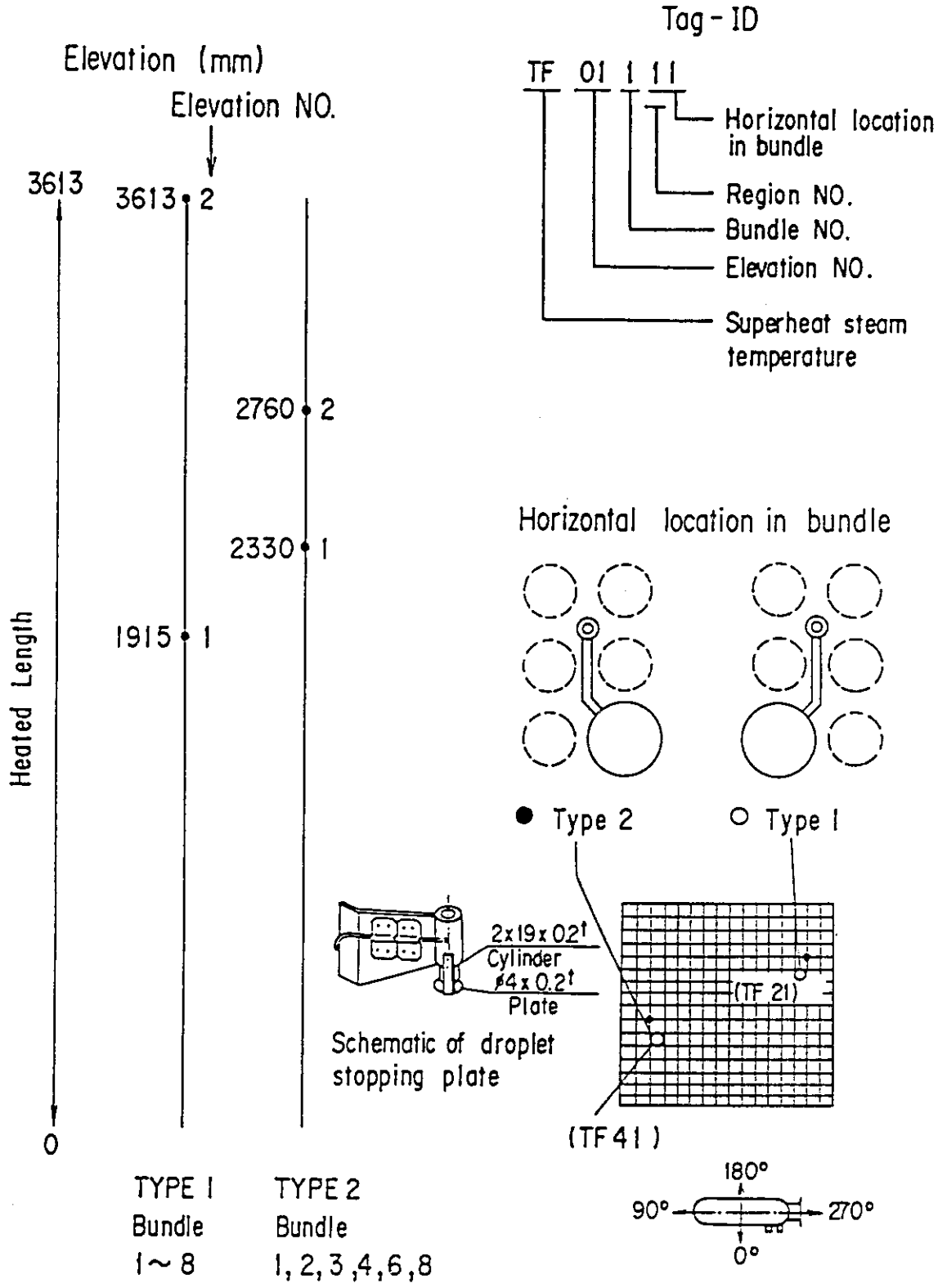

Fig. A-23 Thermocouple Locations of Steam Temperature Measurements in Core

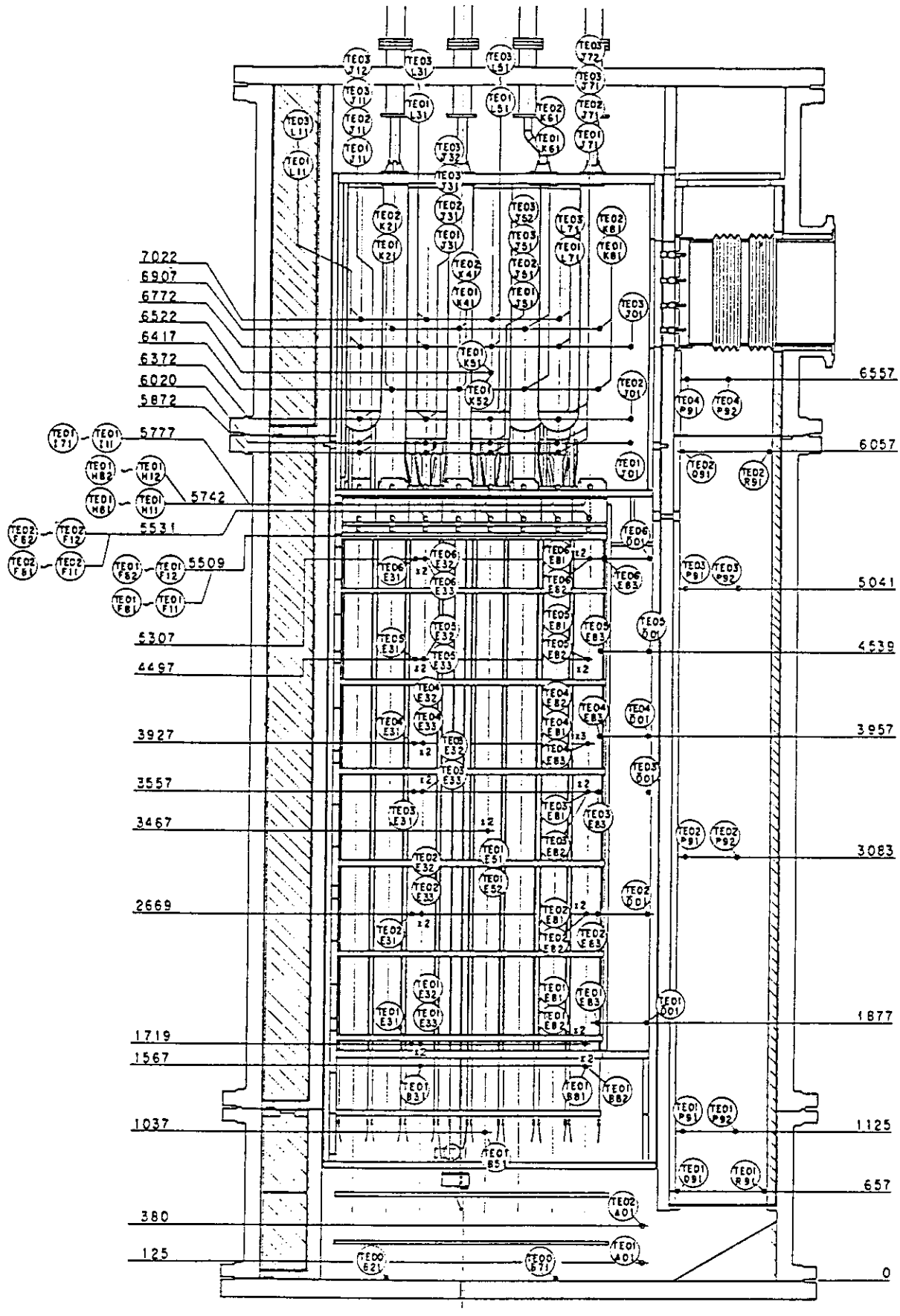

Fig. A-24 Thermocouple Locations of Temperature Measurements in Pressure Vessel except Core Region (Vertical View)

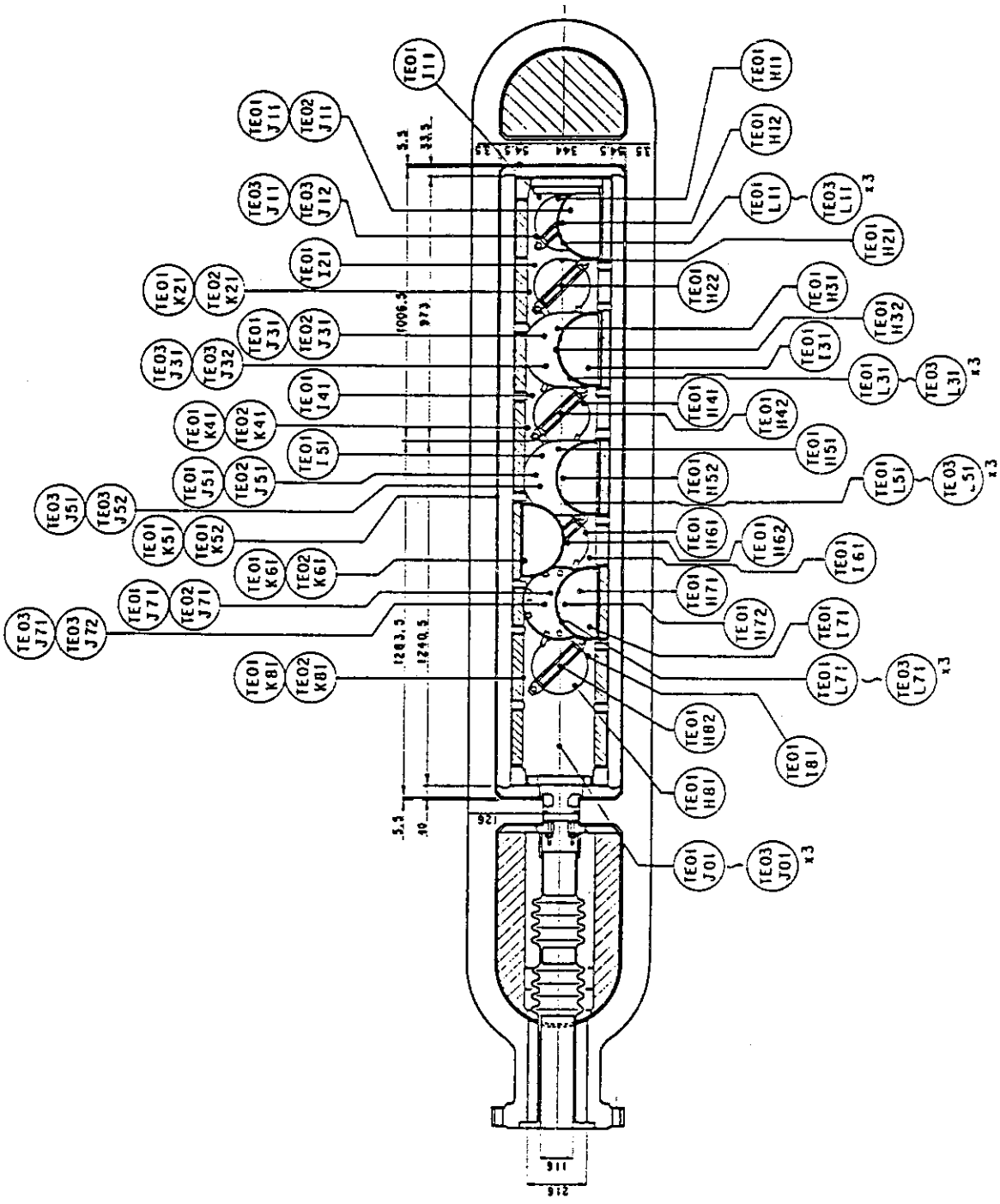

Fig. A-25 Thermocouple Locations of Temperature Measurements in Upper Plenum (Horizontal View)

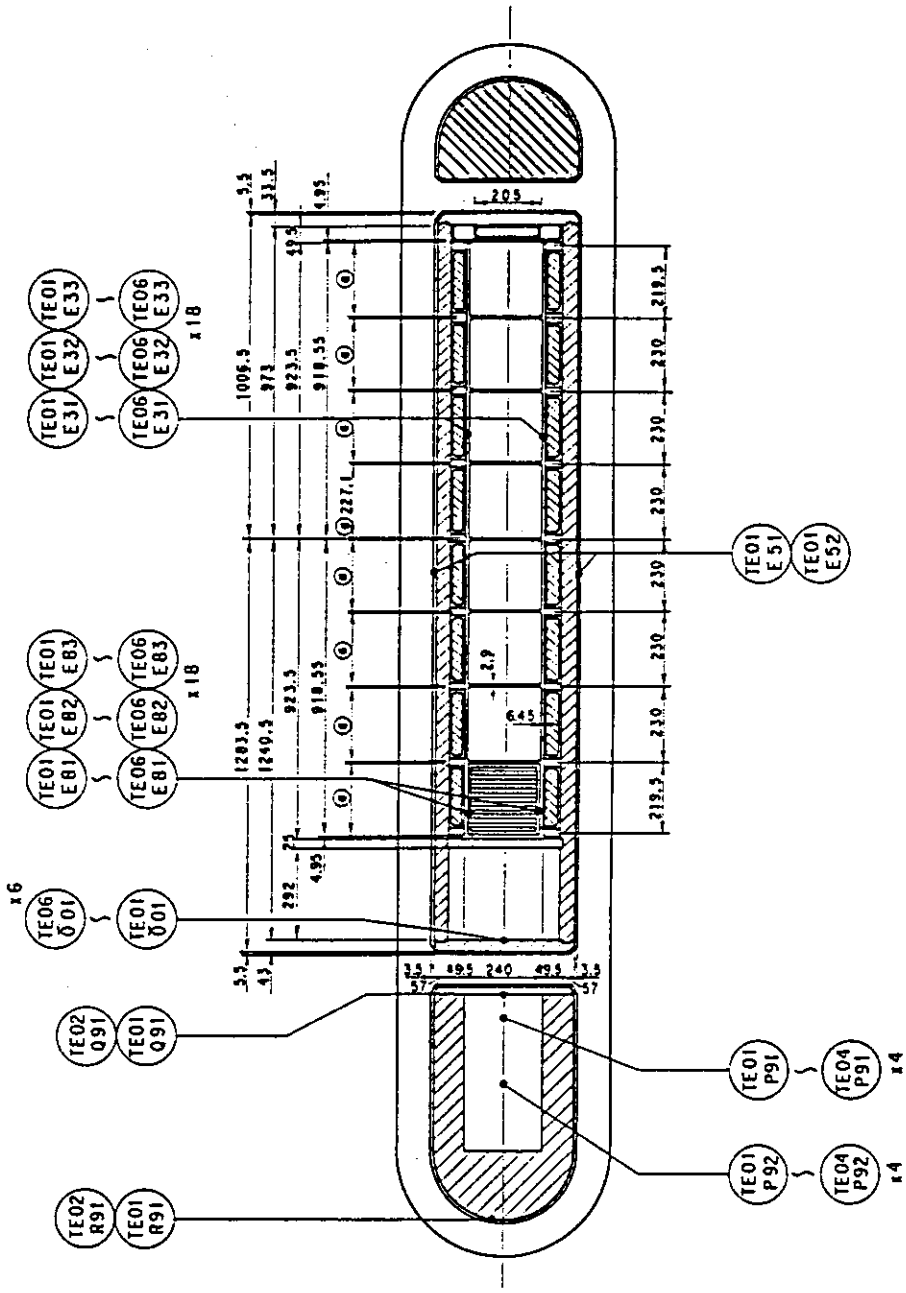

Fig. A-26 Thermocouple Locations of Temperature Measurements in Pressure Vessel except Upper Plenum (Horizontal View)

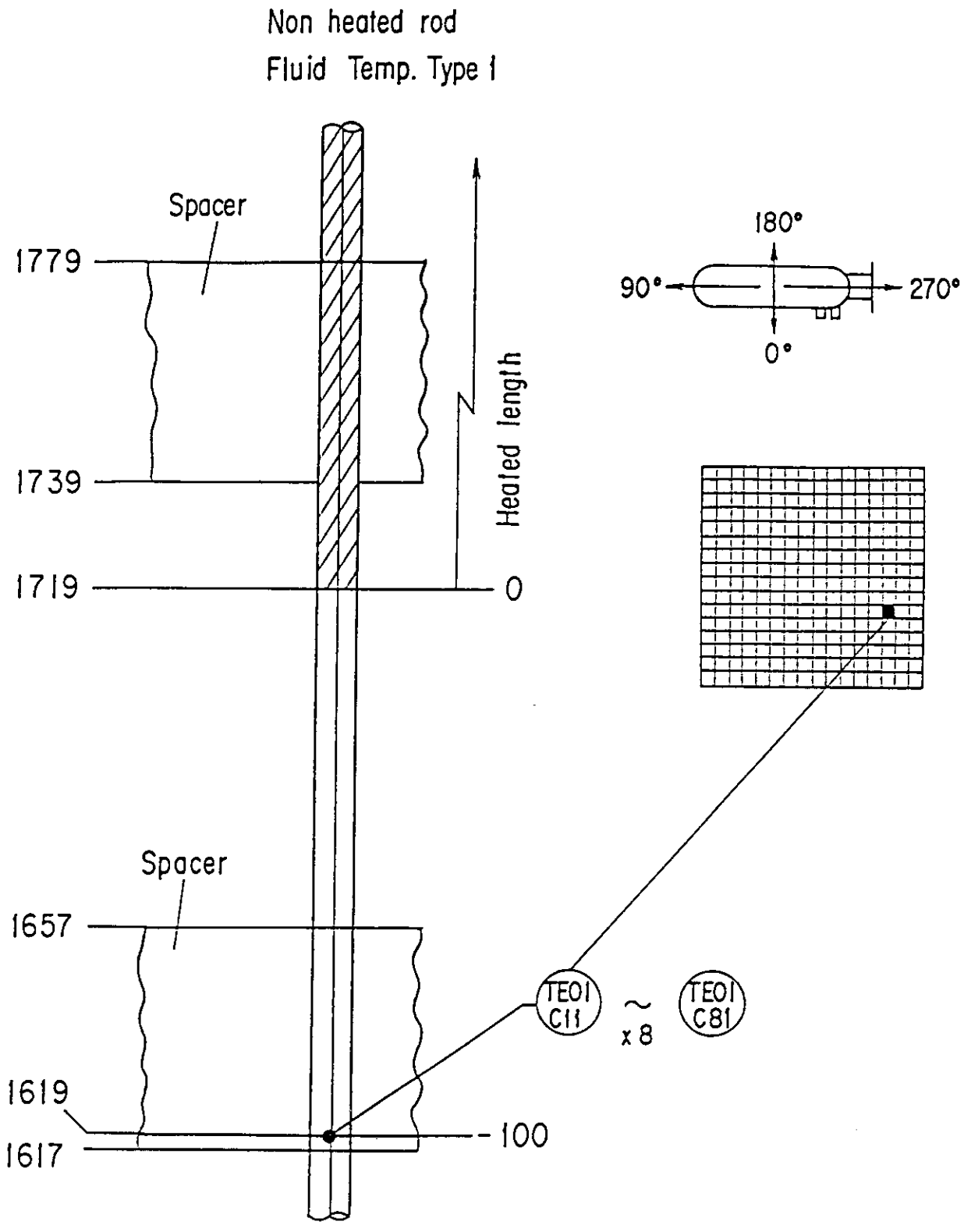

Fig. A-27 Thermocouple Locations of Fluid Temperature Measurements at Core Inlet

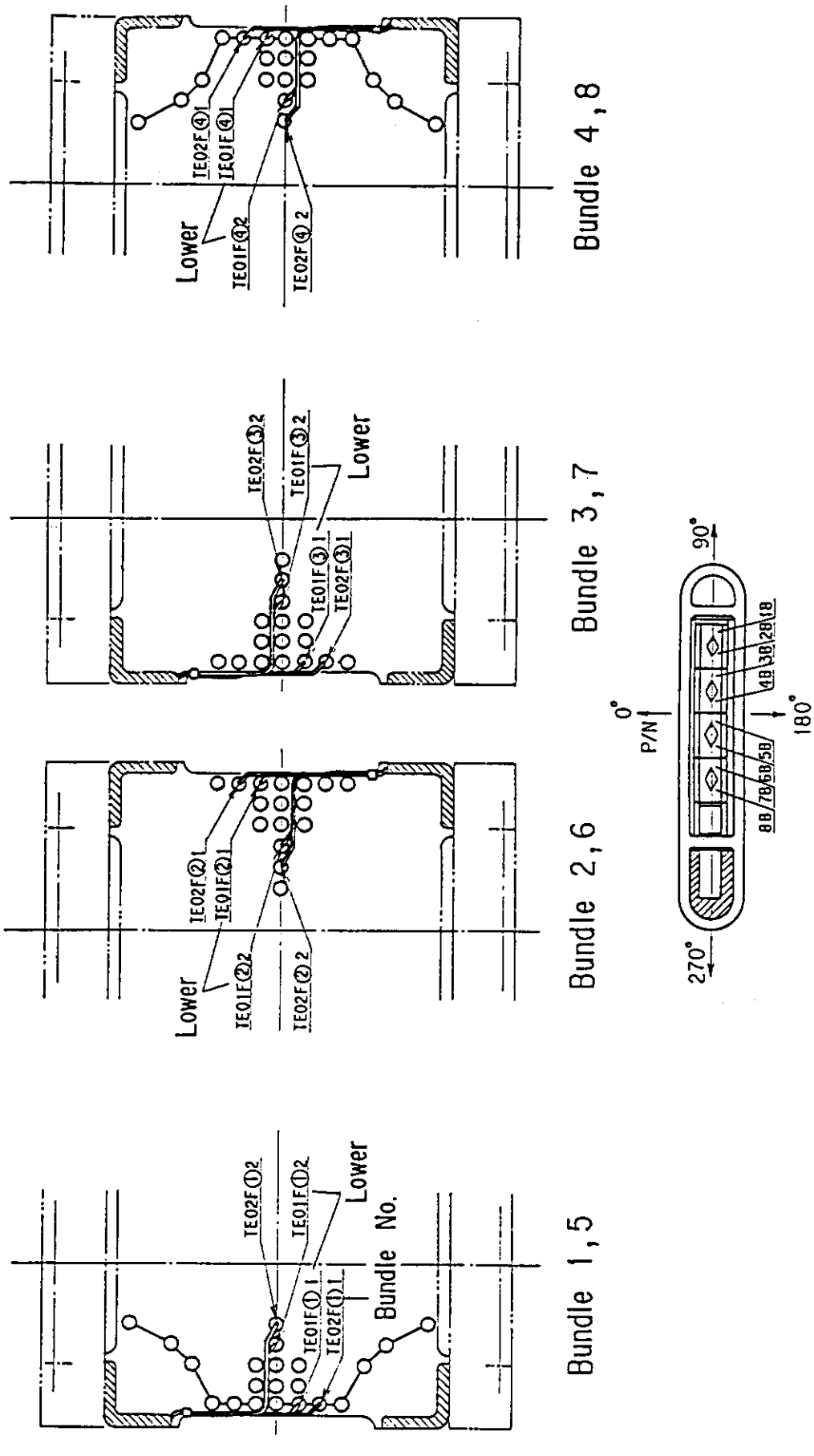

Fig. A-28 Thermocouple Locations of Fluid Temperature Measurements just above and below End Box Tie Plates

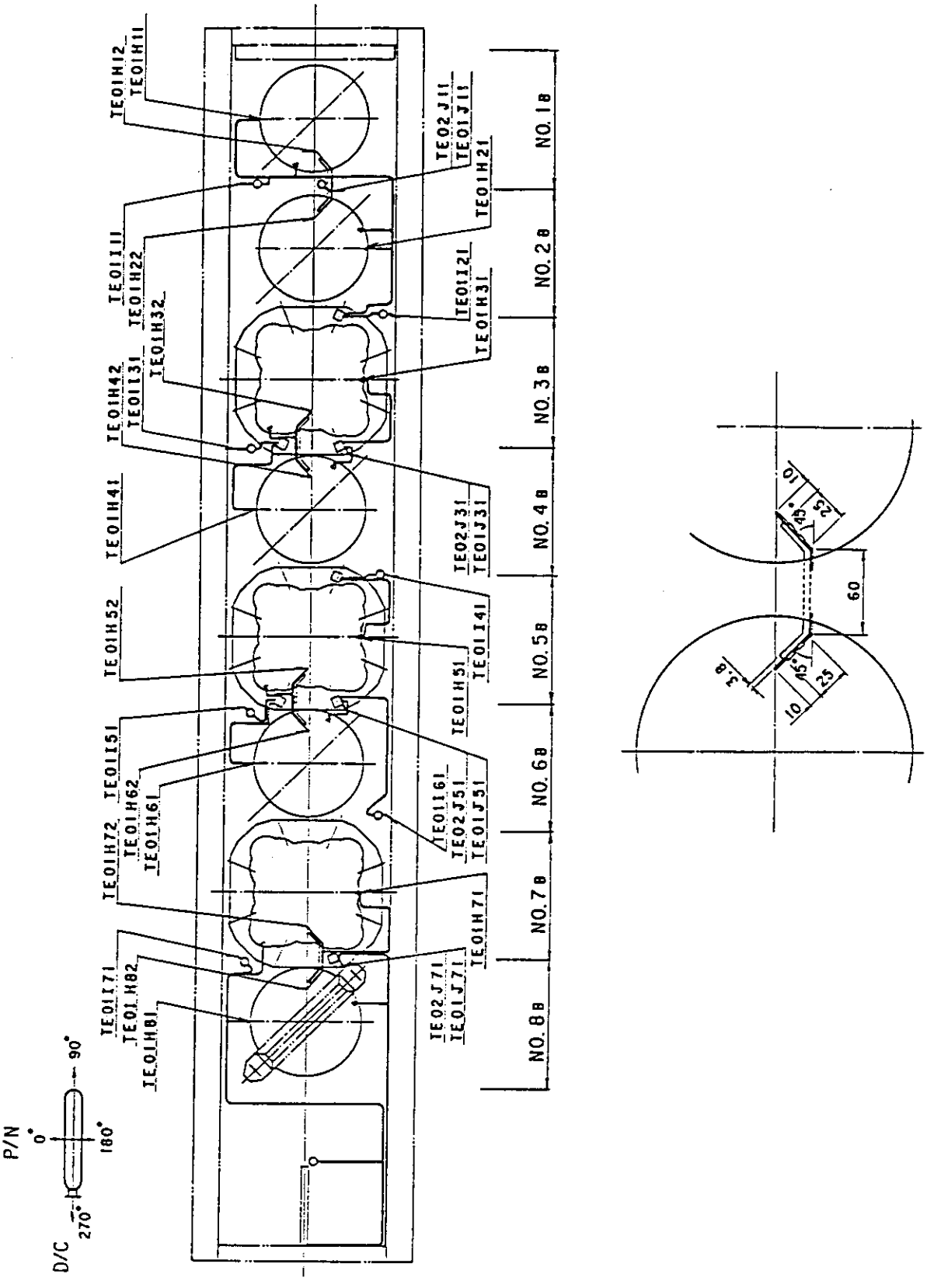

Fig. A-29 Thermocouple Locations of Fluid Temperature Measurements on UCSP and at Inside and Periphery of UCSP Holes

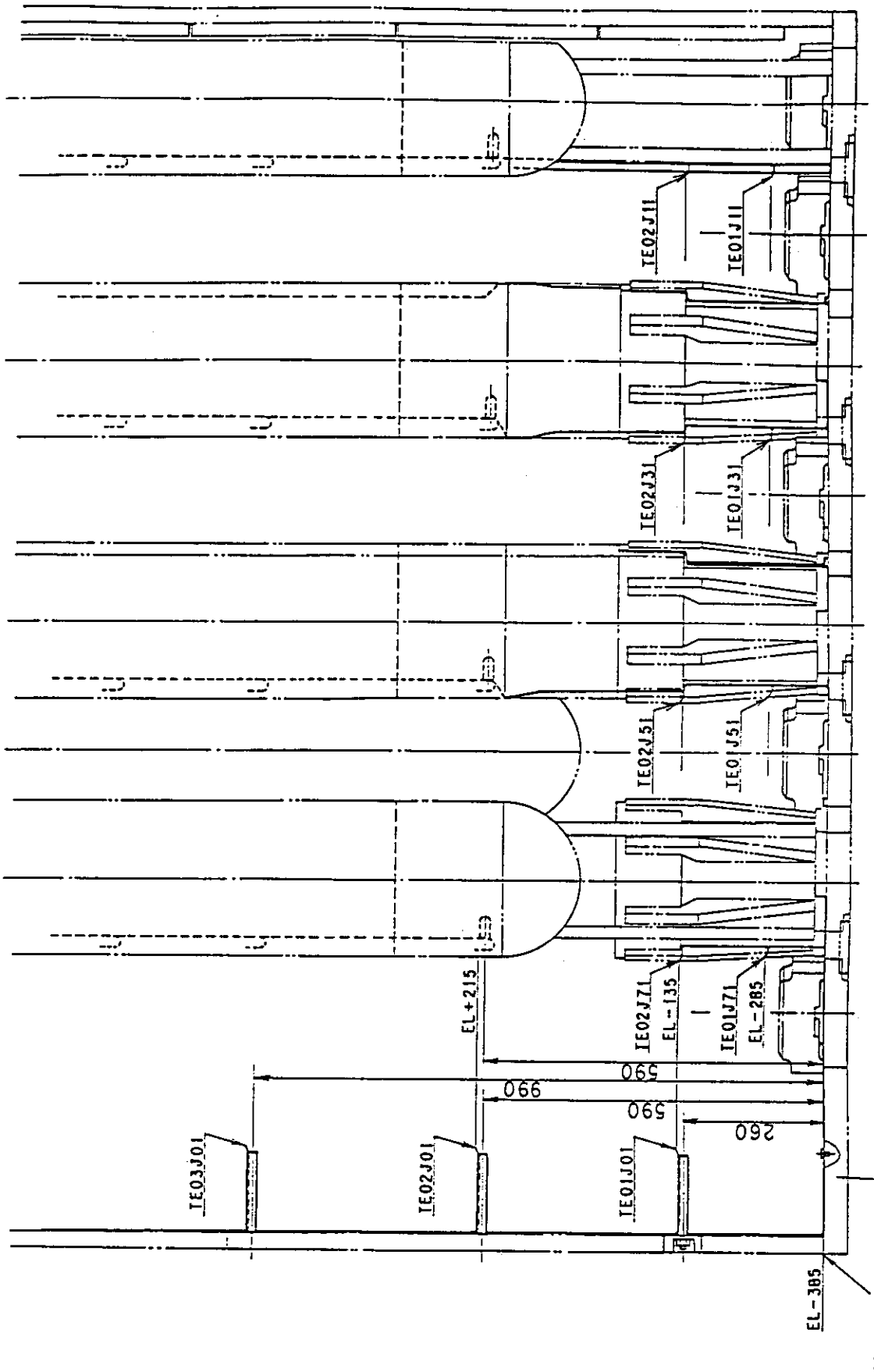

Fig. A-30 Thermocouple Locations of Fluid Temperature Measurements on and above UCSP

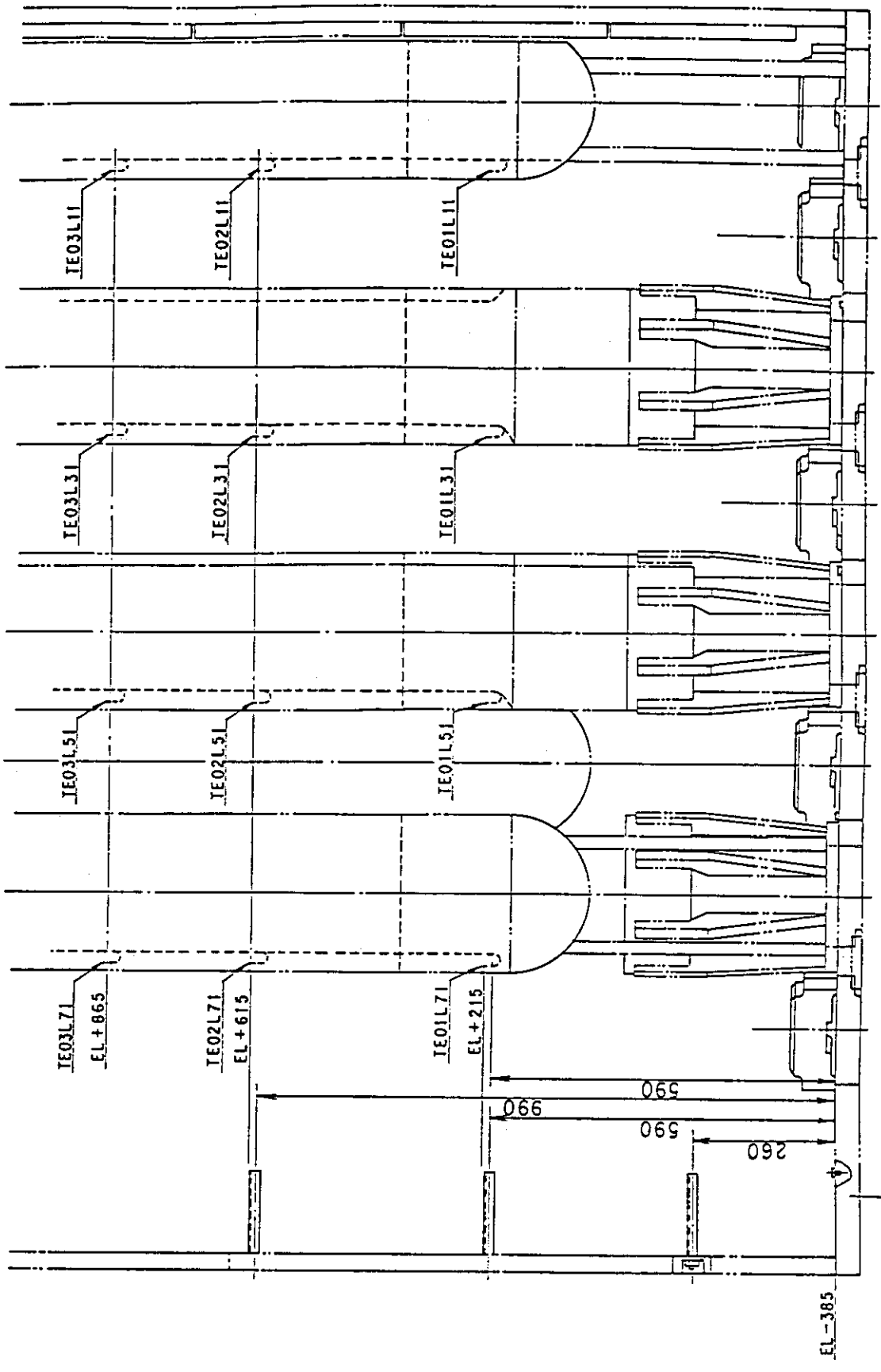

Fig. A-31 Thermocouple Locations of Surface Temperature Measurements of Upper Plenum Structures

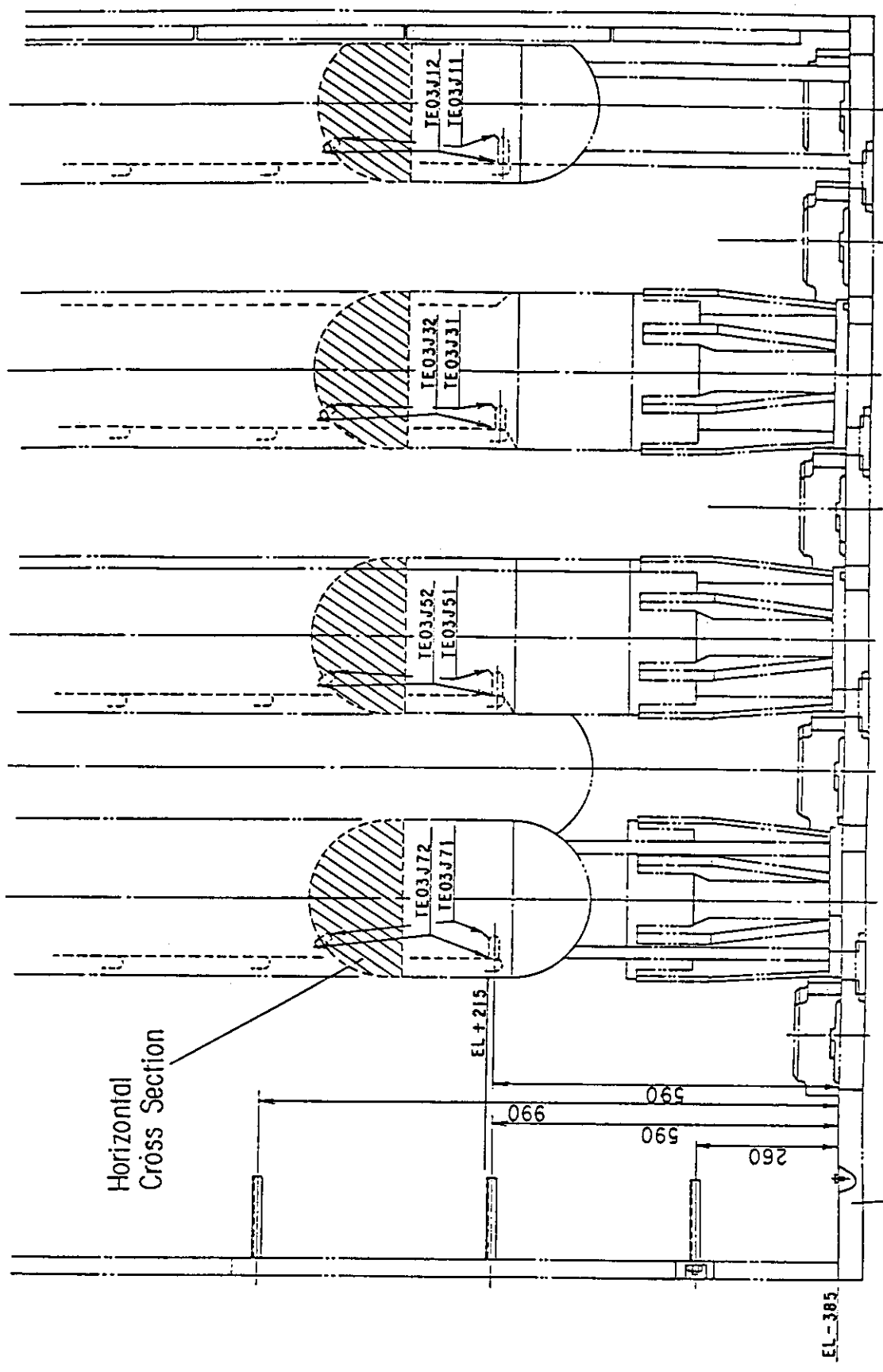

Fig. A-32 Thermocouple Locations of Steam Temperature Measurements above UCSP Holes

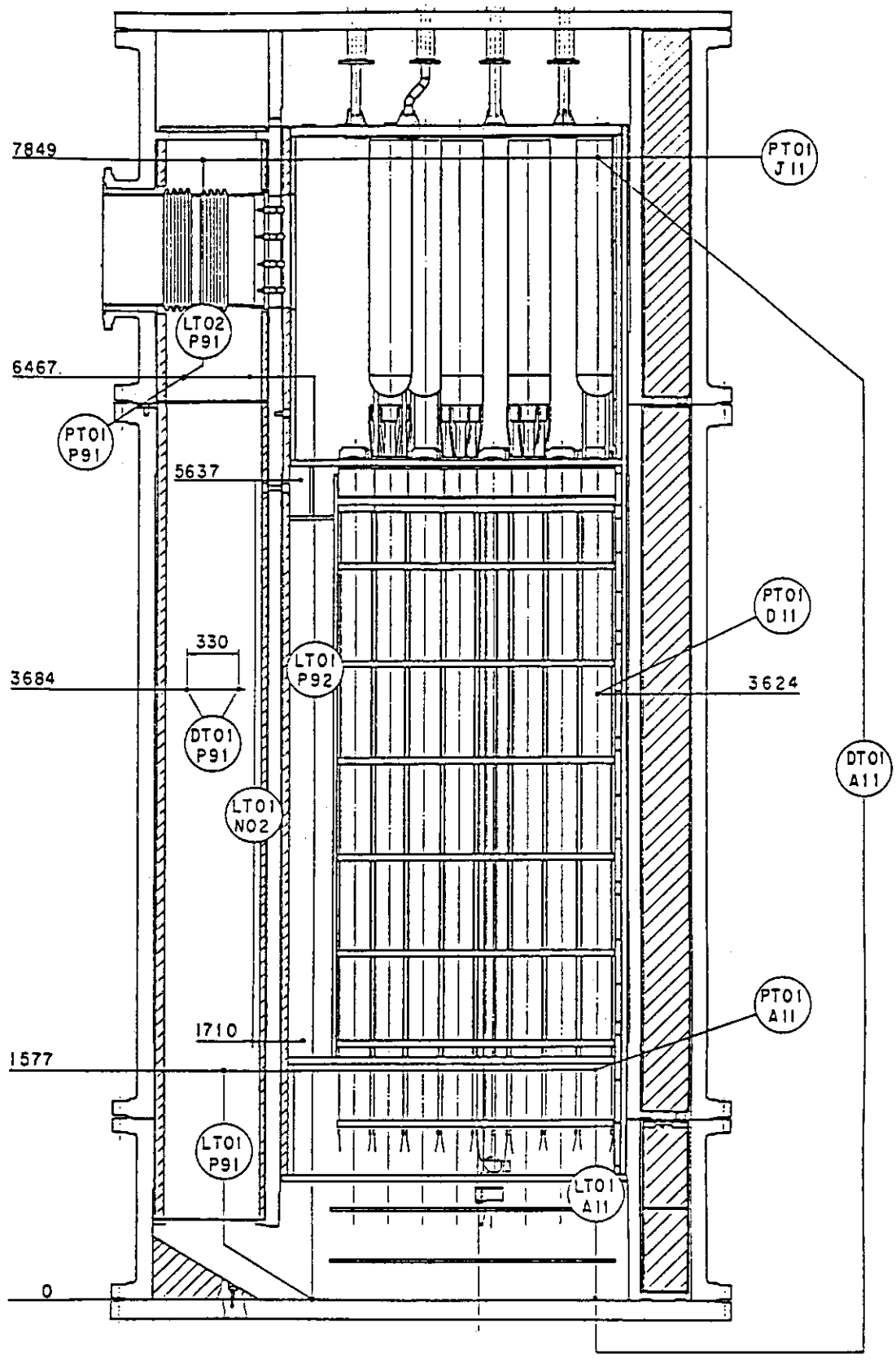

Fig. A-33 Locations of Pressure Measurements in Pressure Vessel, Differential Pressure Measurements between Upper and Lower Plenums and Liquid Level Measurements in Downcomer and Lower Plenum

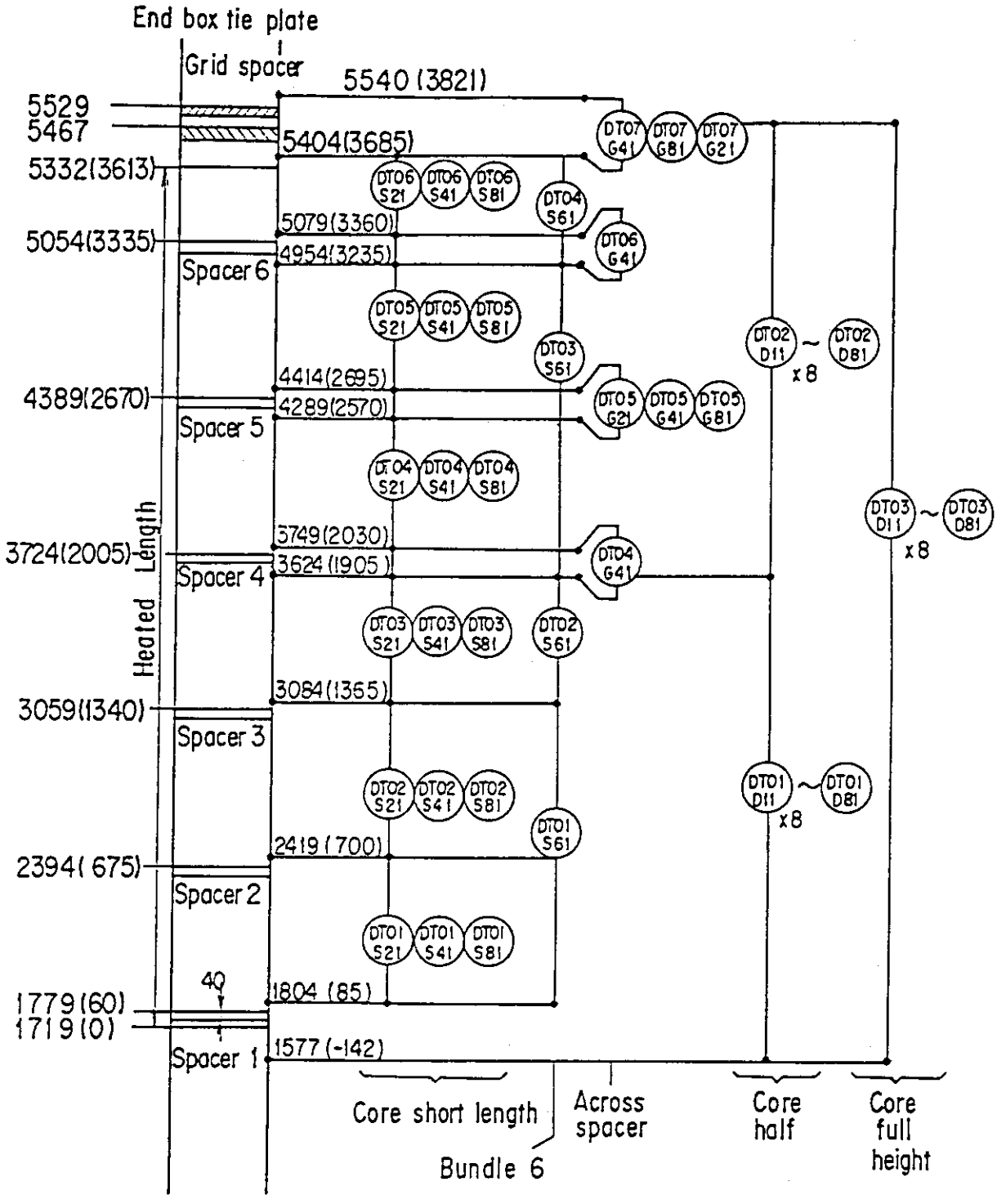

Fig. A-34 Locations of Vertical Differential Pressure Measurements in Core

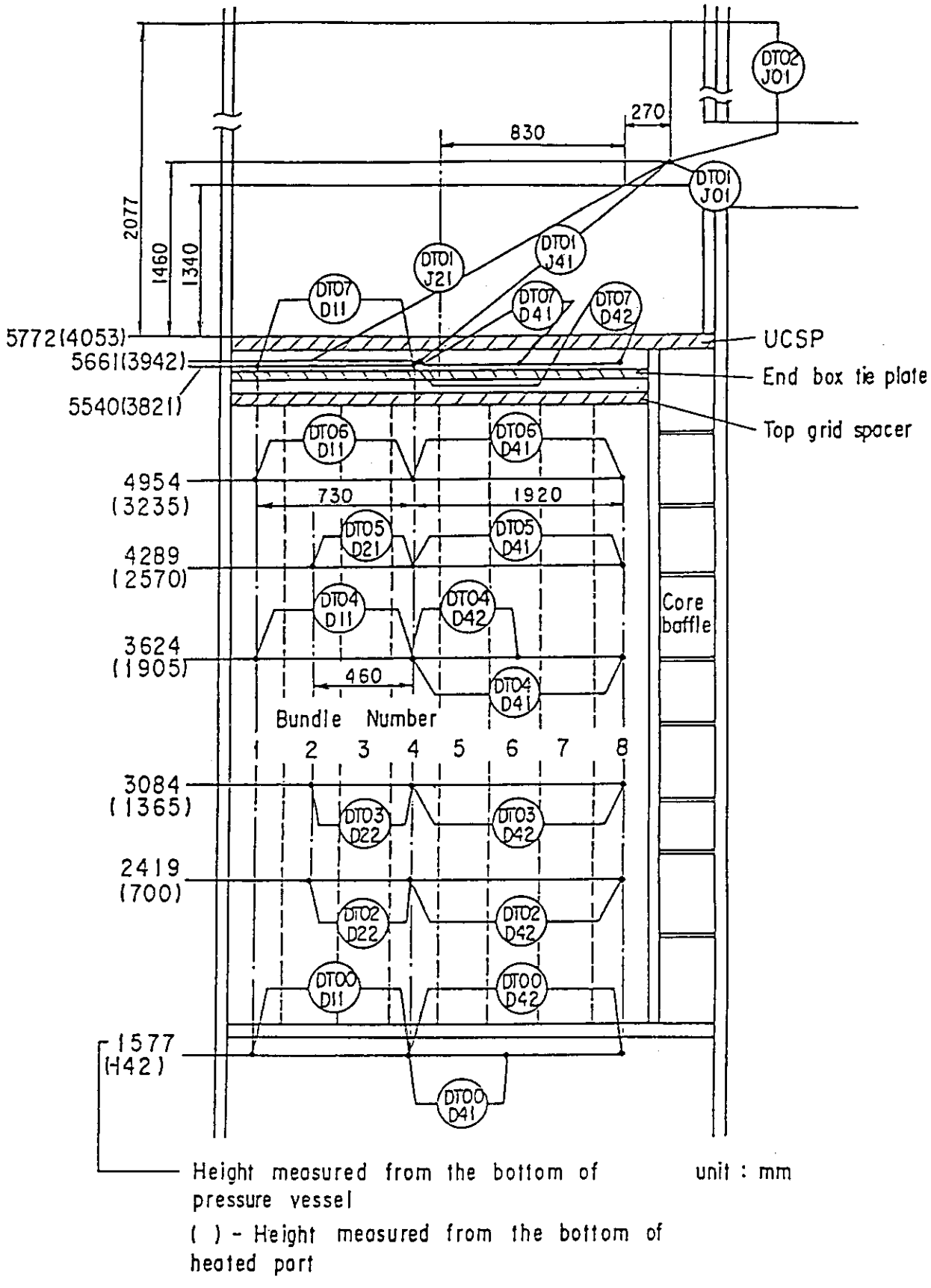

Fig. A-35 Locations of Horizontal Differential Pressure Measurements in Core and Differential Pressure Measurements between End Boxes and Inlet of Hot Leg

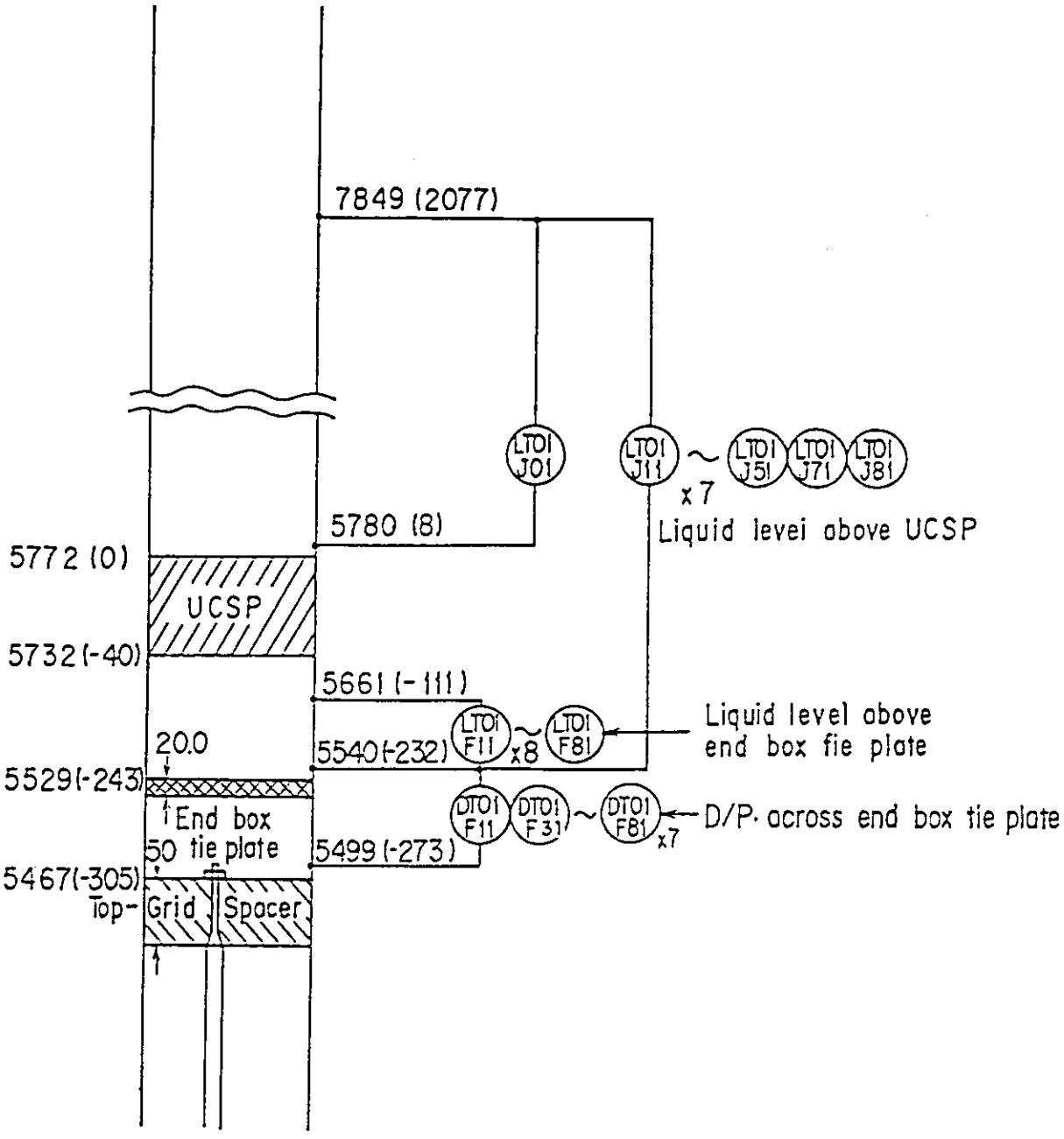

Fig. A-35 Locations of Differential Pressure Measurements across End Box Tie Plate

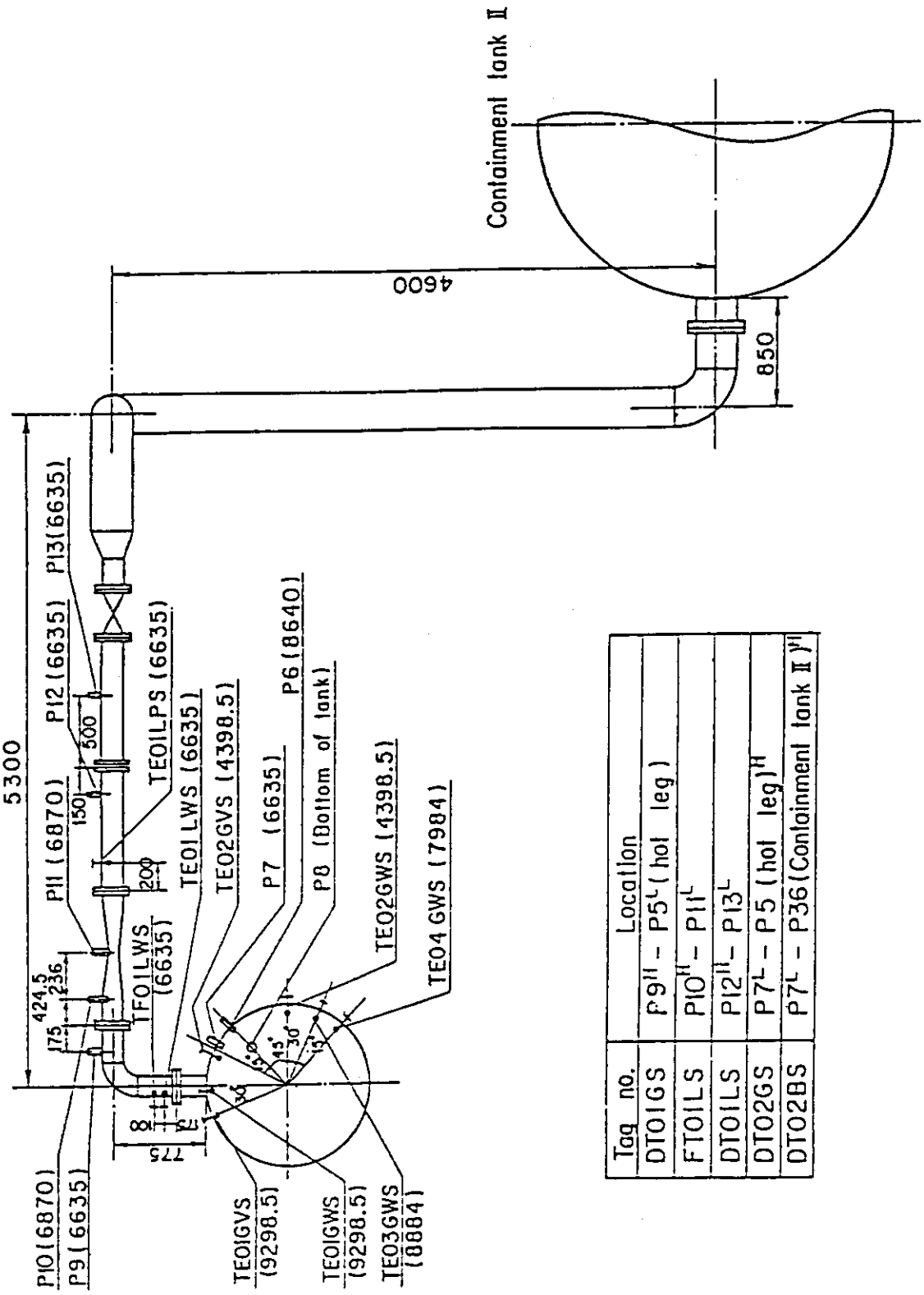

Tag no.	Location
DT01GS	$P9^{H}$ – $P5^{L}$ (hot leg)
FT01LS	$P10^{H}$ – $P11^{L}$
DT01LS	$P12^{H}$ – $P13^{L}$
DT02GS	$P7^{L}$ – P5 (hot leg)^{H}
DT02BS	$P7^{L}$ – P36(Containment tank II)^{H}

Fig. A-37 Locations of Broken Cold Leg Instruments
(Steam-Water Separator Side)

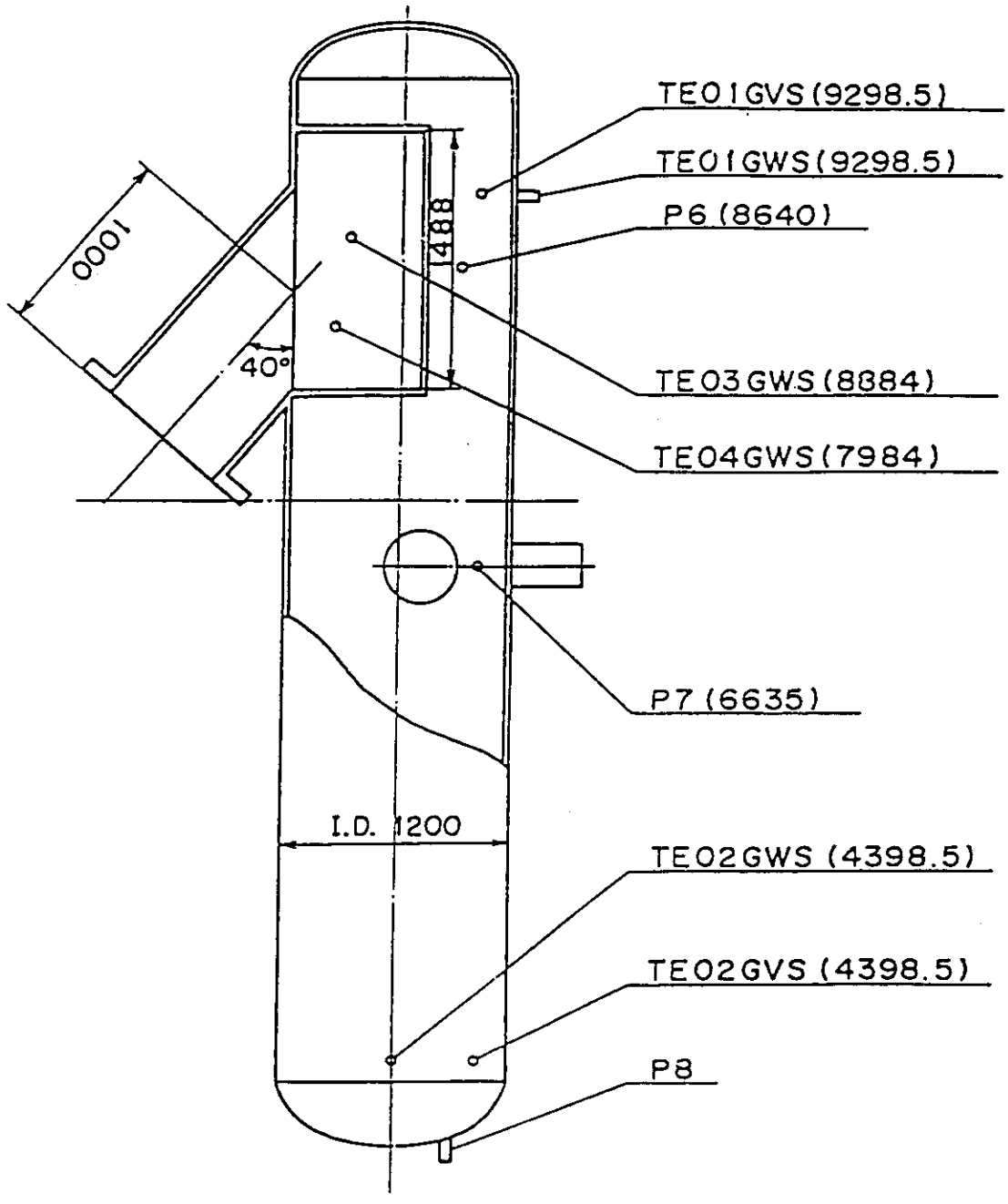

Fig. A-38 Locations of Steam-Water Separator Instruments

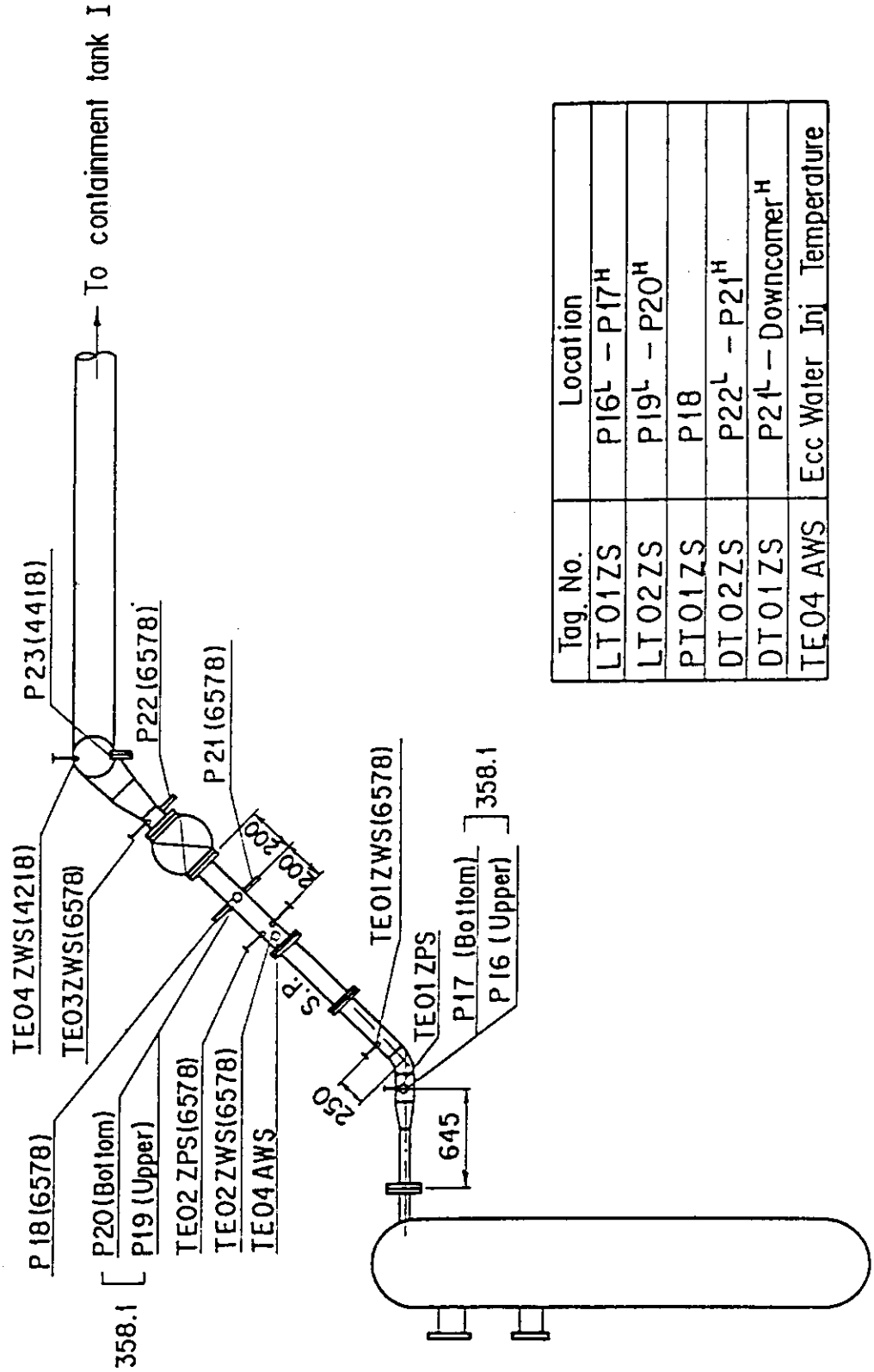

Tag. No.	Location
LT01ZS	$P16^{L} - P17^{H}$
LT02ZS	$P19^{L} - P20^{H}$
PT01ZS	P18
DT02ZS	$P22^{L} - P21^{H}$
DT01ZS	$P21^{L}$ — Downcomer^{H}
TE04AWS	Ecc Water Inj Temperature

Fig. A-39 Locations of Broken Cold Leg Instruments (Pressure Vessel Side)

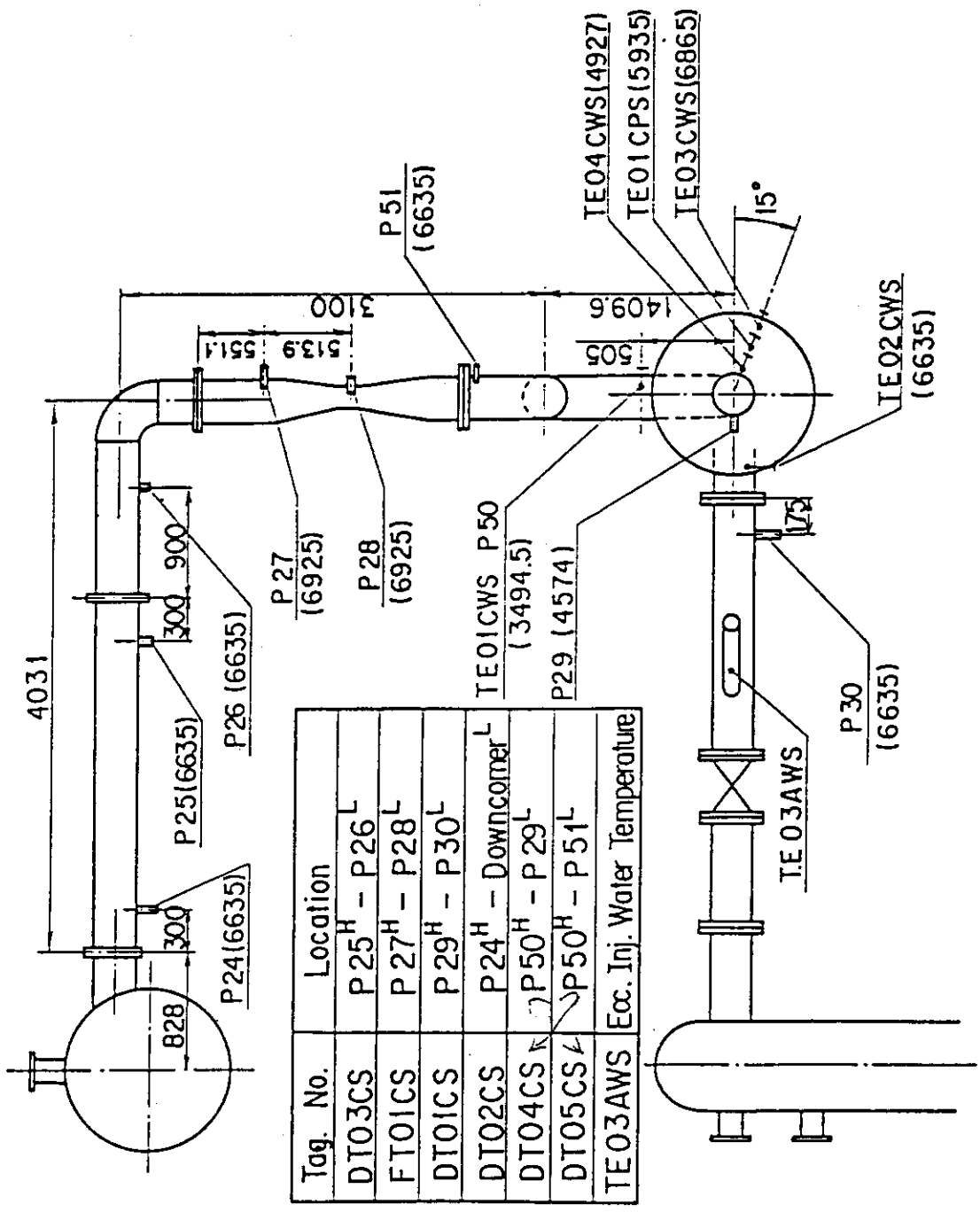

Fig. A-40 Locations of Intact Cold Leg Instruments

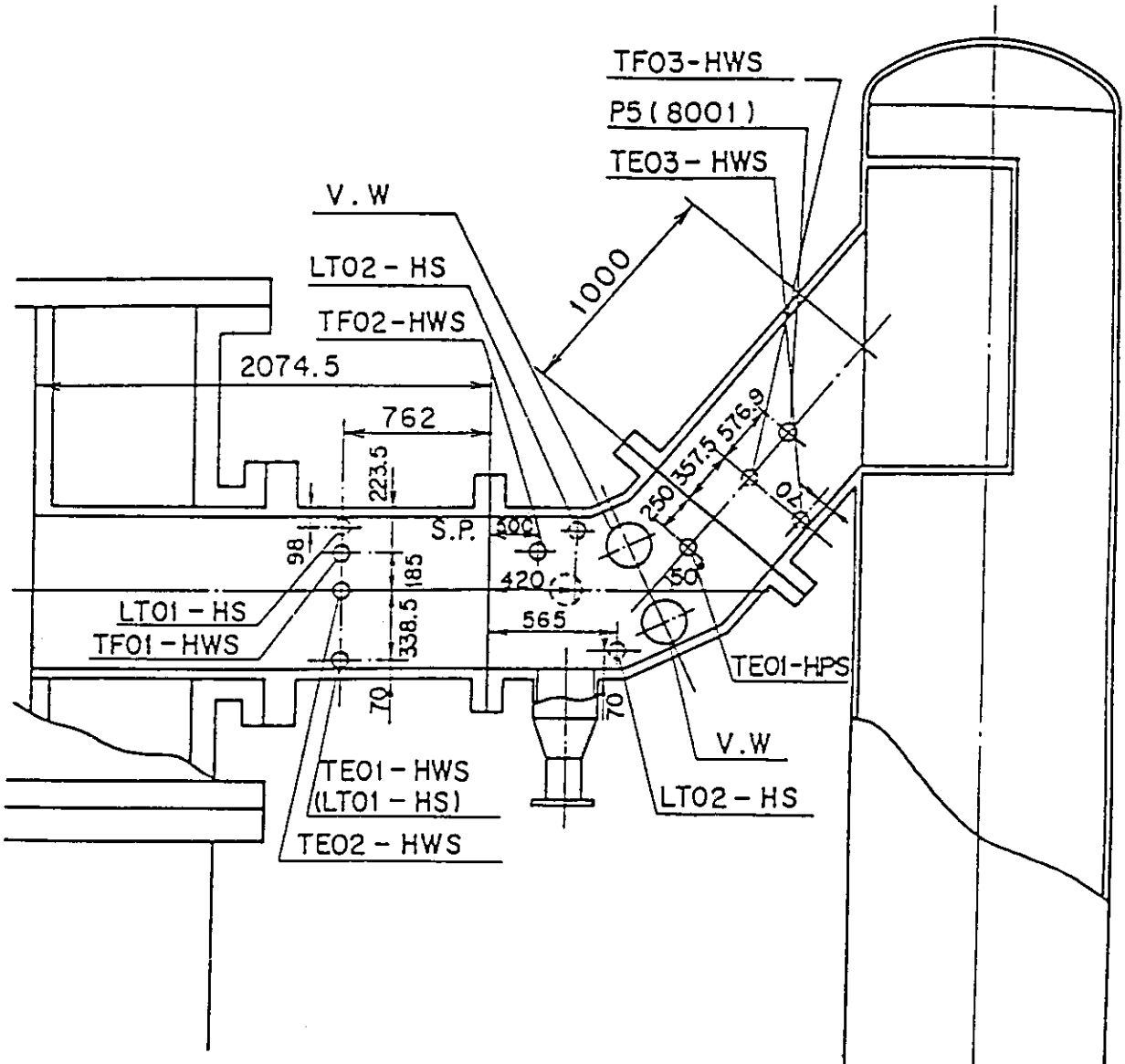

Tag no.	Location
DT01HS	$P5^{L}$ – Inlet of hot leg^{H}
DT01GS	$P5^{L}$ – Broken cold leg (S-W separator side)^{H}
DT02GS	$P5^{H}$ – S-W separator tank^{L}

Fig. A-41 Locations of Hot Leg Instruments

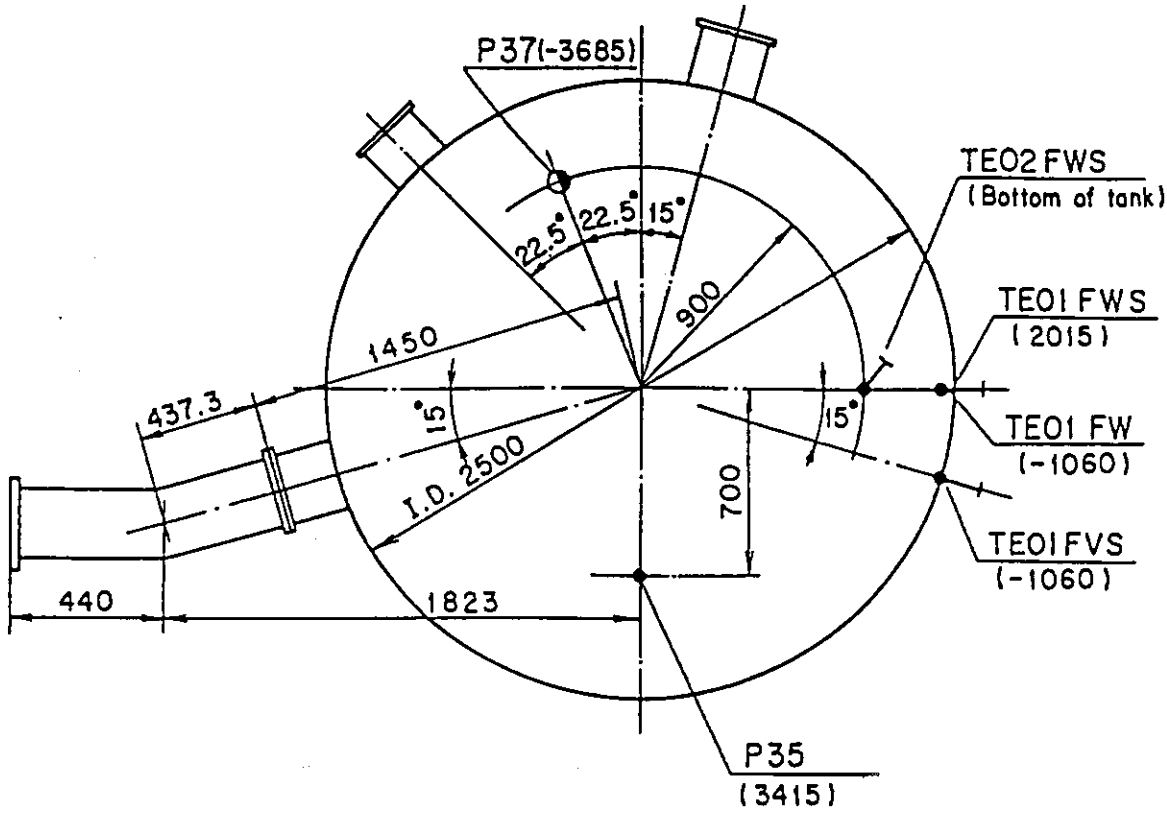

Tag. no.	Location
LT01 FS	$P35^{L}$ – $P37^{H}$
DT01 FS	$P35^{H}$ – $Downcomer^{L}$
DT01 E	$P35^{L}$ – P36(C.T. II)^{H}
PT01 F	P35

Fig. A-42 Locations of Containment Tank-I Instruments

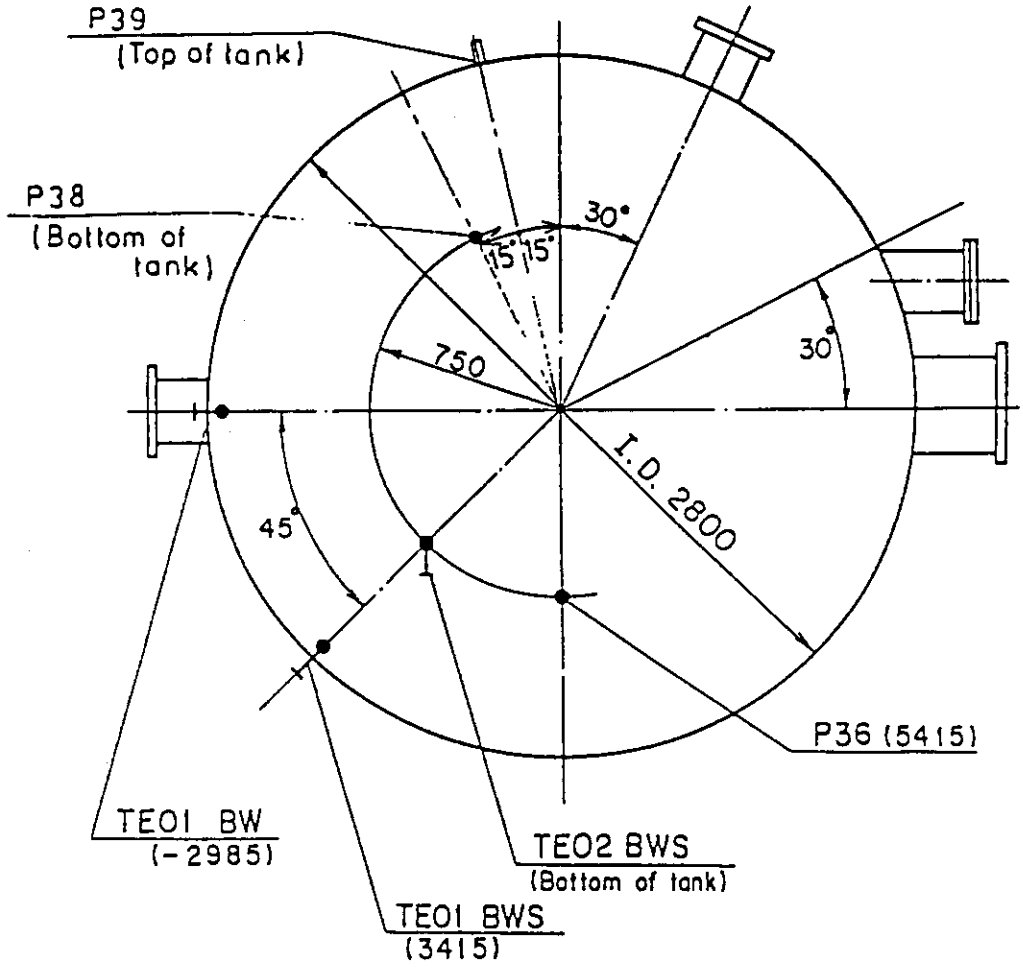

Tag no.	Location
DT01 BS	$P36^{H}$－ Upper plenum^{L}
DT02 BS	$P36^{H}$－ S-W Separator^{L}
DT01 E	$P36^{H}$－ P35 (C.T.I)^{L}
PT01 B	P36
LT01 1B	$P38^{H}$－ $P39^{L}$

Fig. A-43 Locations of Containment Tank-II Instruments

Appendix B

Selected Data from Test S3－7

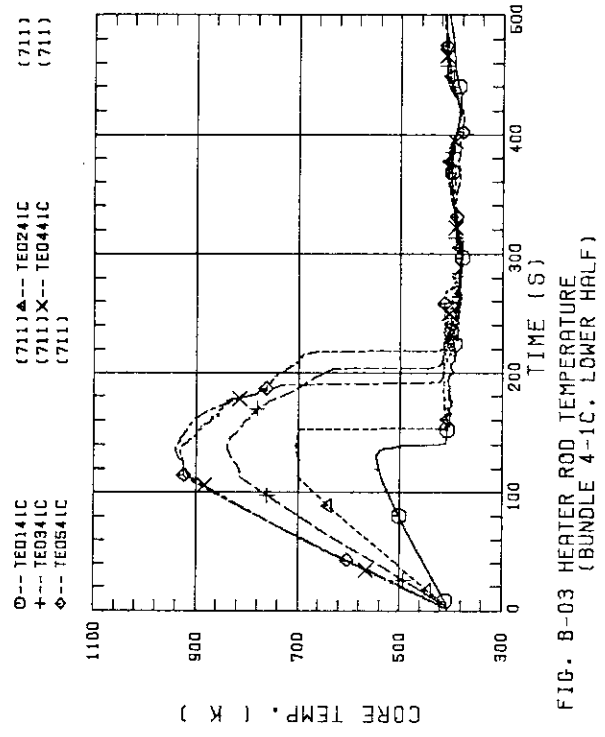

FIG. B-03 HEATER ROD TEMPERATURE
(BUNDLE 4-1C, LOWER HALF)

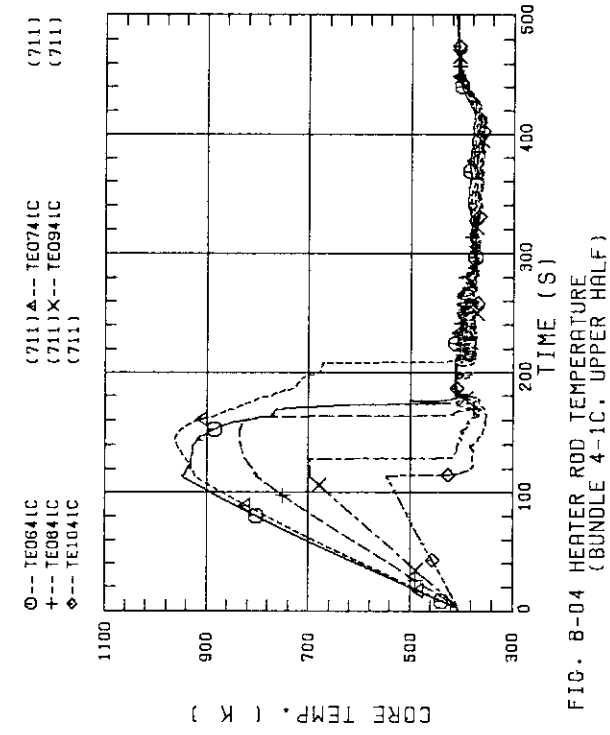

FIG. B-04 HEATER ROD TEMPERATURE
(BUNDLE 4-1C, UPPER HALF)

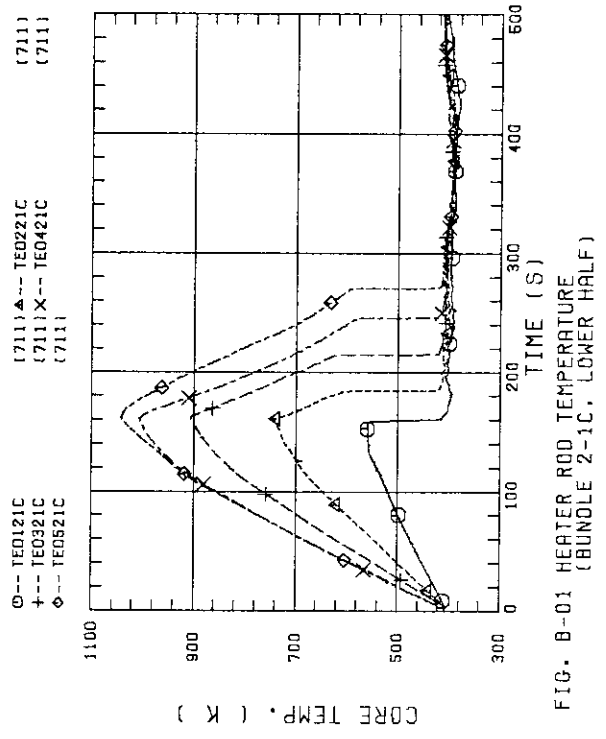

FIG. B-01 HEATER ROD TEMPERATURE
(BUNDLE 2-1C, LOWER HALF)

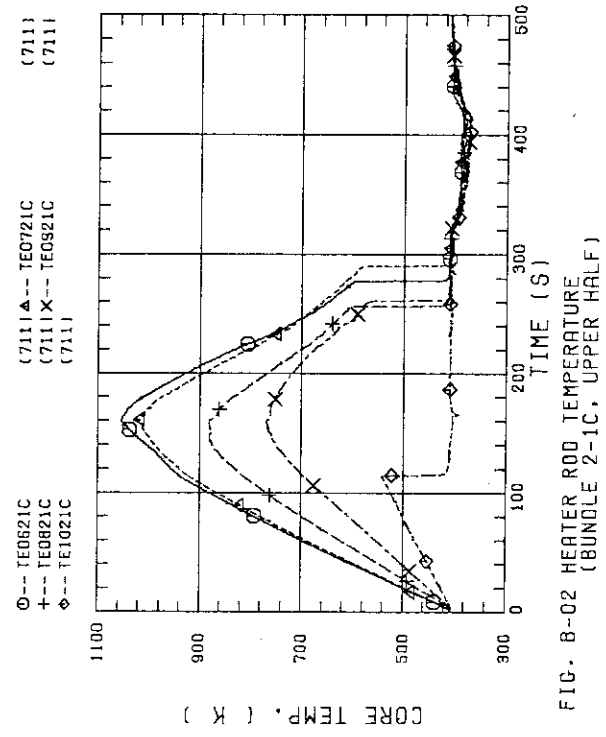

FIG. B-02 HEATER ROD TEMPERATURE
(BUNDLE 2-1C, UPPER HALF)

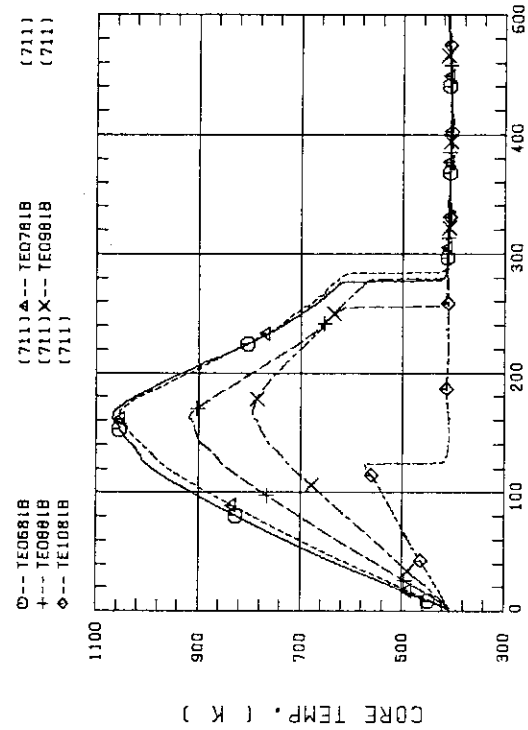

FIG. B-07 HEATER ROD TEMPERATURE
(BUNDLE 8-1B, UPPER HALF)

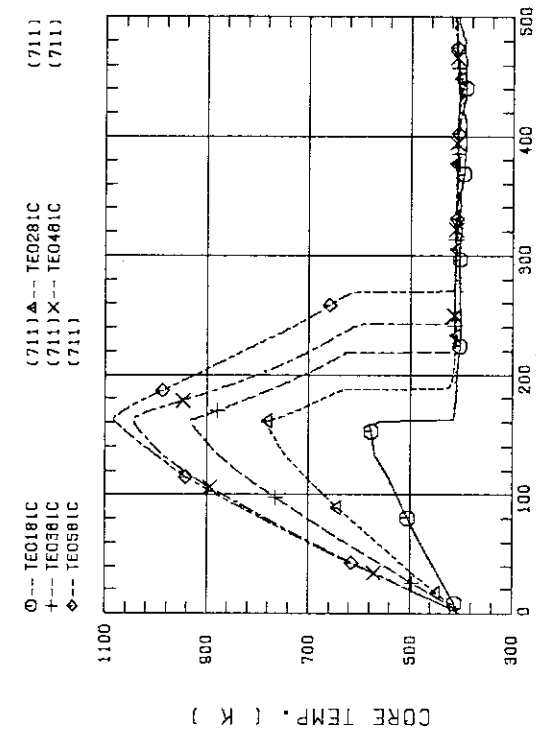

FIG. B-08 HEATER ROD TEMPERATURE
(BUNDLE 8-1C, LOWER HALF)

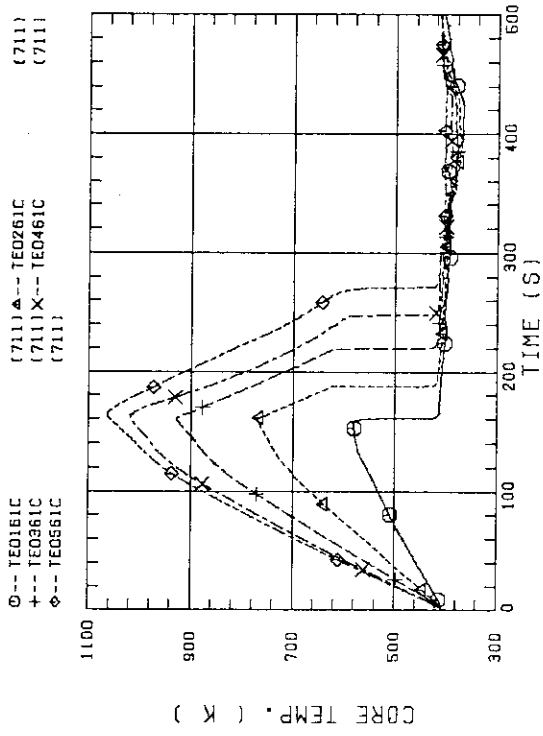

FIG. B-05 HEATER ROD TEMPERATURE
(BUNDLE 6-1C, LOWER HALF)

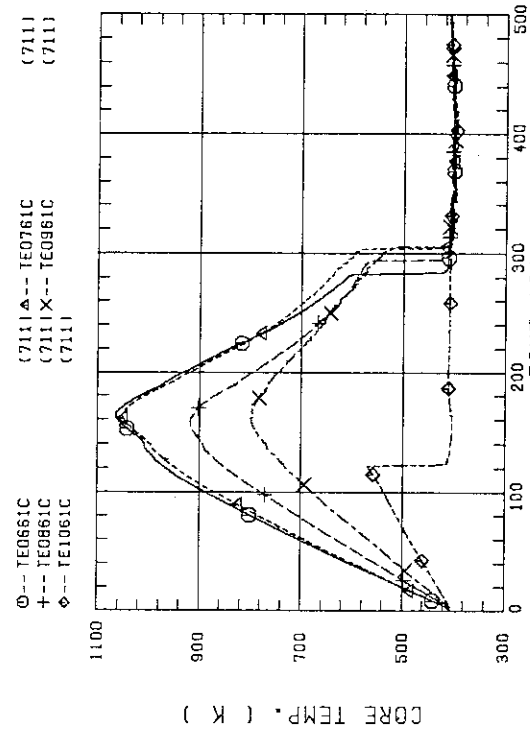

FIG. B-06 HEATER ROD TEMPERATURE
(BUNDLE 6-1C, UPPER HALF)

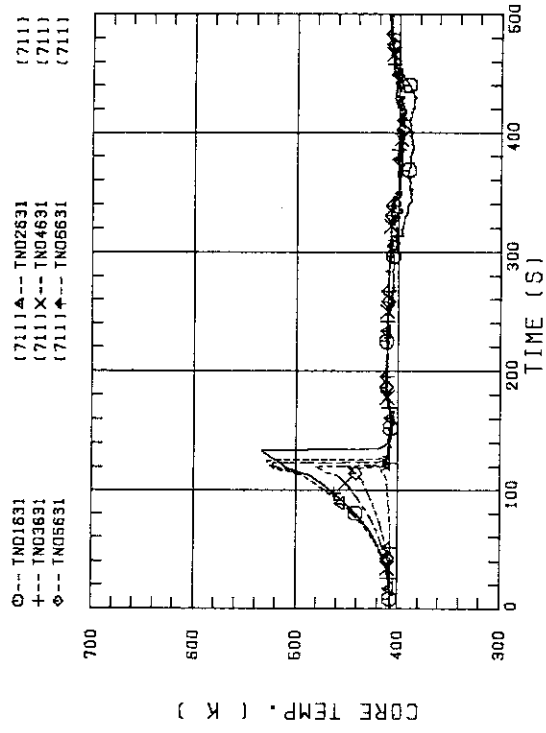

FIG. B-11 NON-HEATED ROD TEMPERATURE (BUNDLE 6-31)

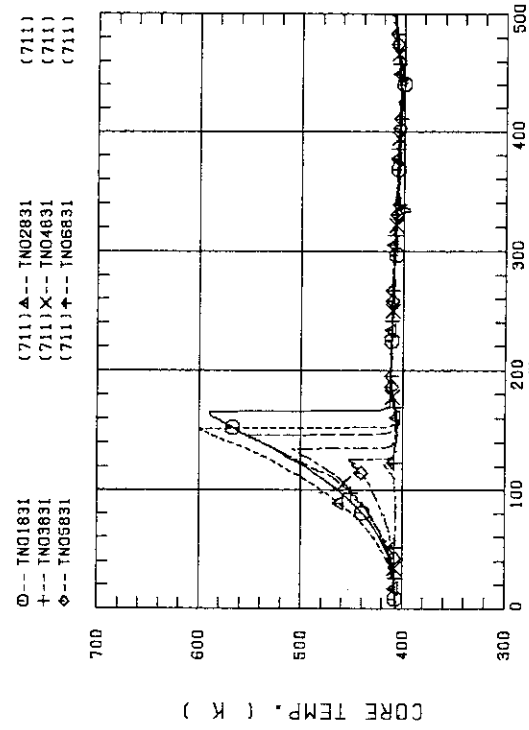

FIG. B-12 NON-HEATED ROD TEMPERATURE (BUNDLE 6-31)

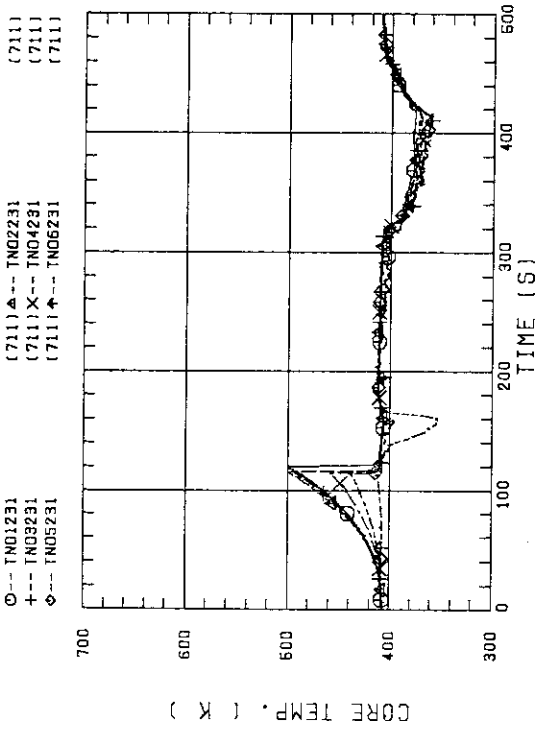

FIG. B-09 NON-HEATED ROD TEMPERATURE (BUNDLE 2-31)

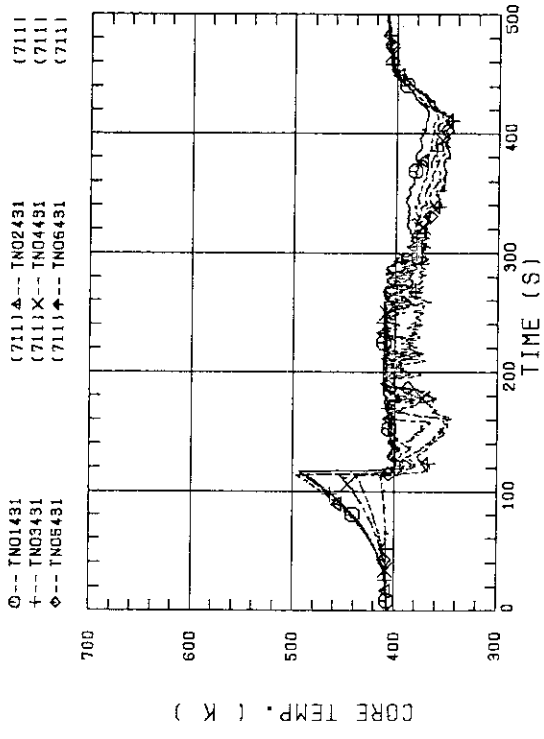

FIG. B-10 NON-HEATED ROD TEMPERATURE (BUNDLE 4-31)

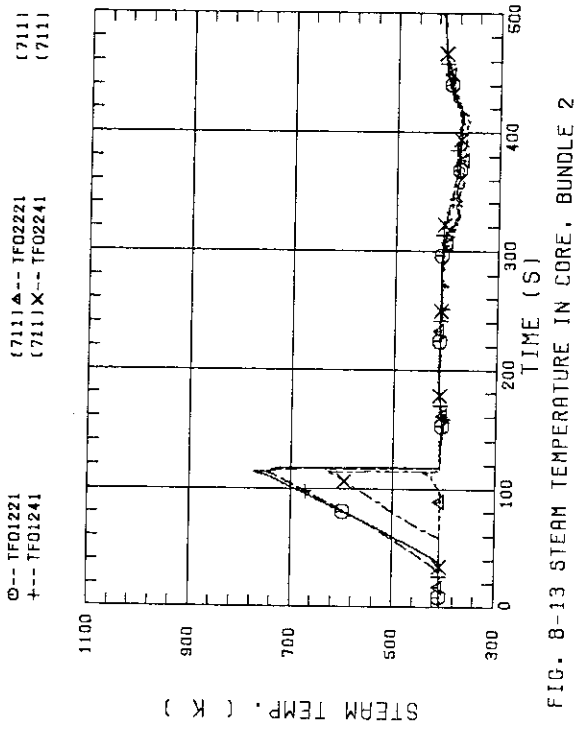

FIG. B-13 STEAM TEMPERATURE IN CORE, BUNDLE 2

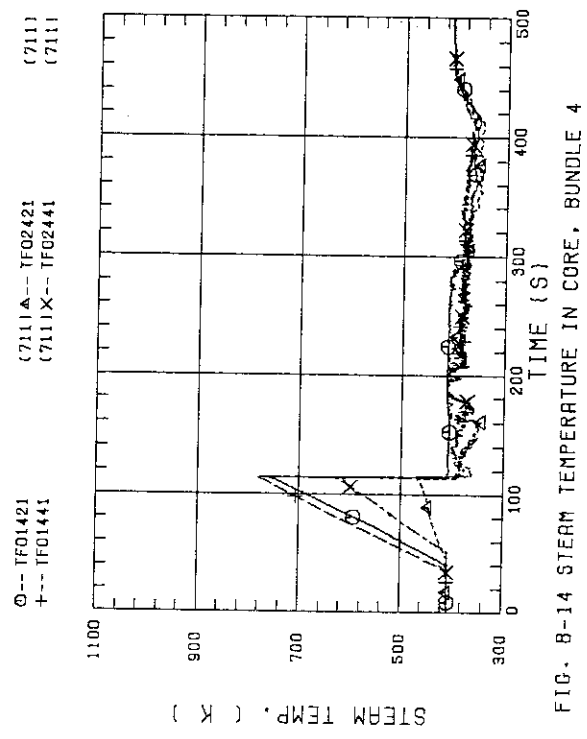

FIG. B-14 STEAM TEMPERATURE IN CORE, BUNDLE 4

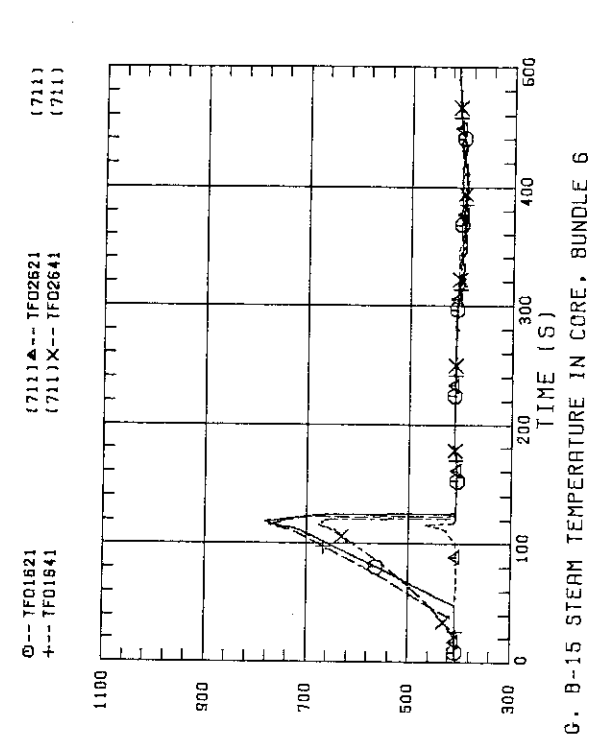

FIG. B-15 STEAM TEMPERATURE IN CORE, BUNDLE 6

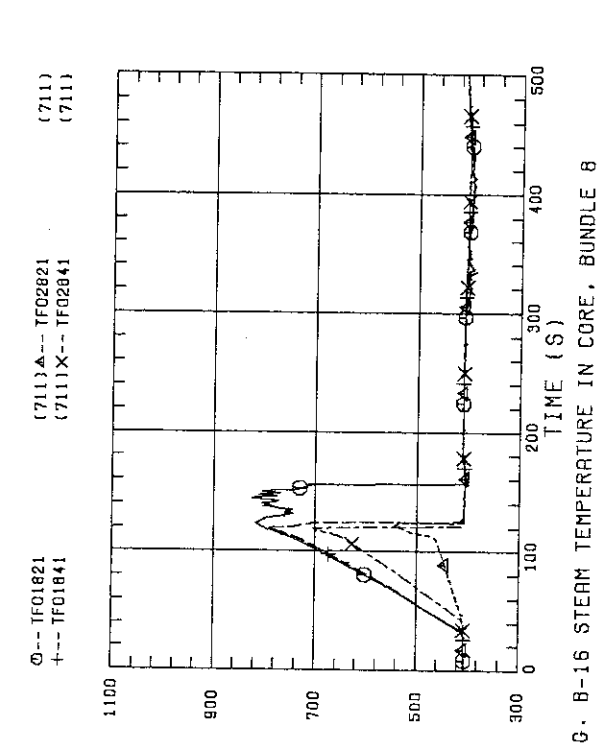

FIG. B-16 STEAM TEMPERATURE IN CORE, BUNDLE 8

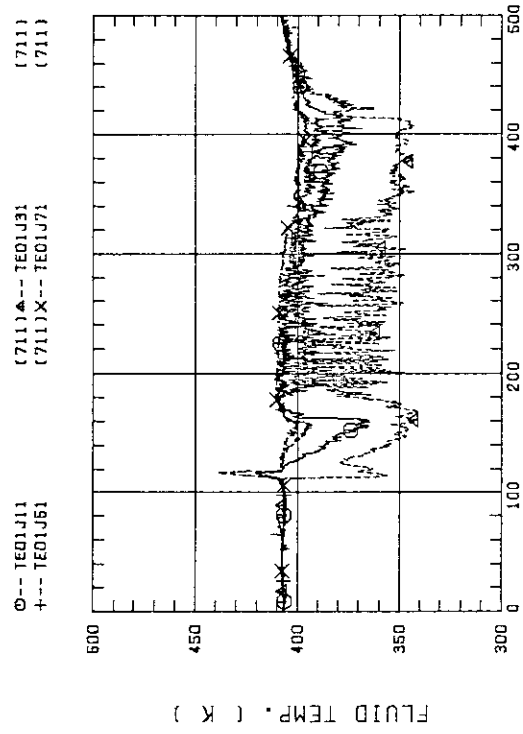

FIG. B-19 FLUID TEMPERATURE ABOVE UCSP
(BUNDLE 1.3.5.7 100MM ABOVE UCSP)

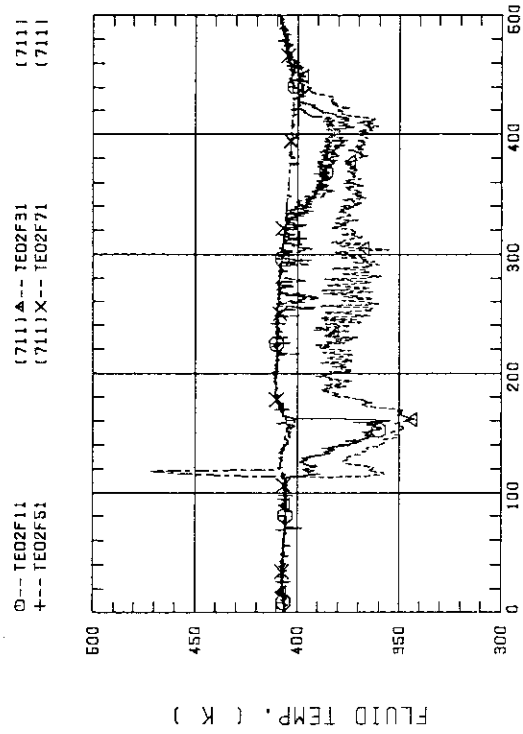

FIG. B-17 FLUID TEMPERATURE JUST ABOVE END BOX TIE PLATE
(BUNDLE 1.3.5.7 OPPOSITE SIDE OF COLD LEG, OUTER)

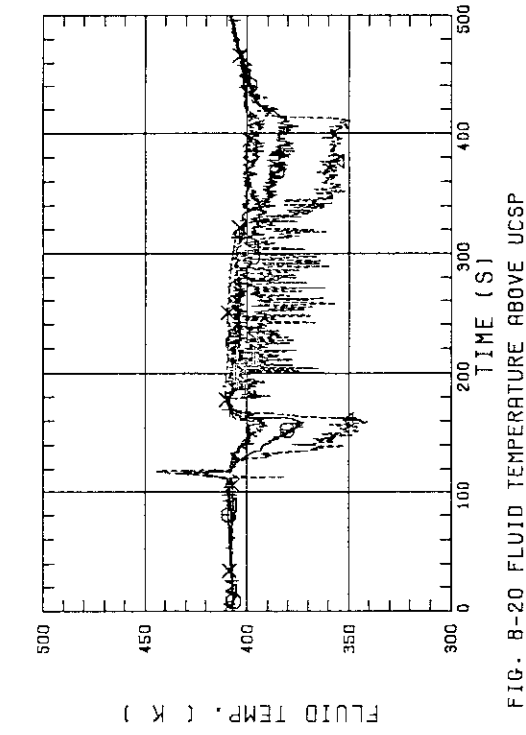

FIG. B-20 FLUID TEMPERATURE ABOVE UCSP
(BUNDLE 1.3.5.7 250MM ABOVE UCSP)

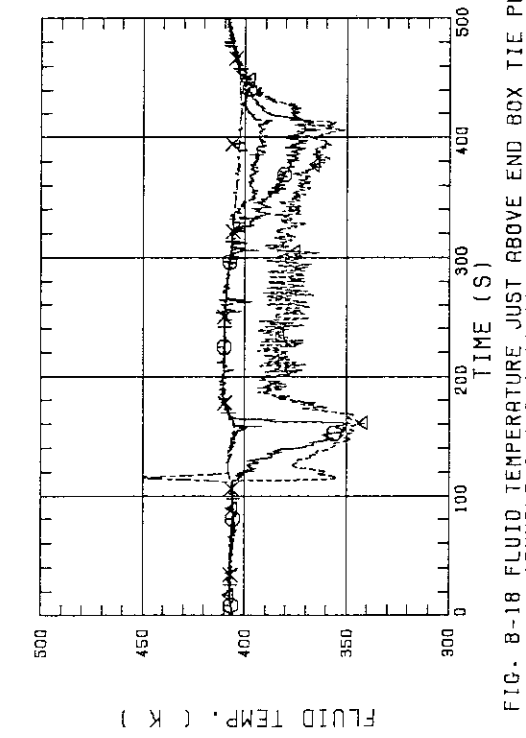

FIG. B-18 FLUID TEMPERATURE JUST ABOVE END BOX TIE PLATE
(BUNDLE 2.4.6.8 OPPOSITE SIDE OF COLD LEG, OUTER)

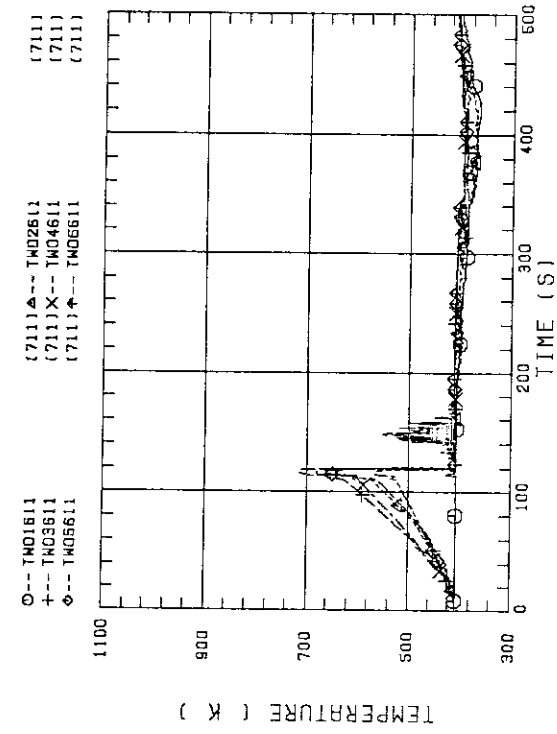

FIG. B-23 TEMPERATURE FOR SPUTTERING DETECTION
BUNDLE 6 , REGION 1 , TYPE 3

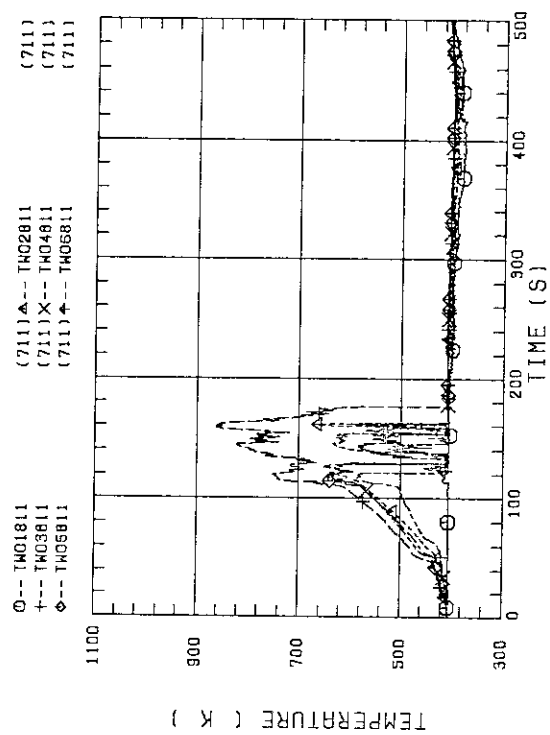

FIG. B-24 TEMPERATURE FOR SPUTTERING DETECTION
BUNDLE 8 , REGION 1 , TYPE 3

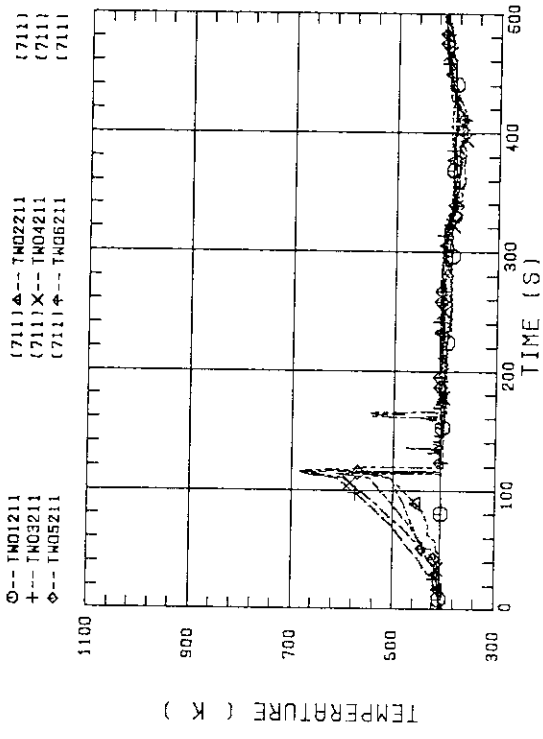

FIG. B-21 TEMPERATURE FOR SPUTTERING DETECTION
BUNDLE 2 , REGION 1 , TYPE 3

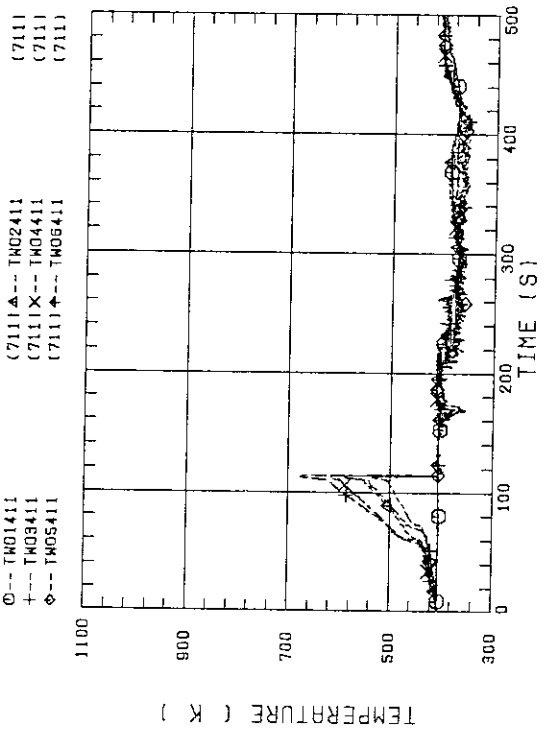

FIG. B-22 TEMPERATURE FOR SPUTTERING DETECTION
BUNDLE 4 , REGION 1 , TYPE 3

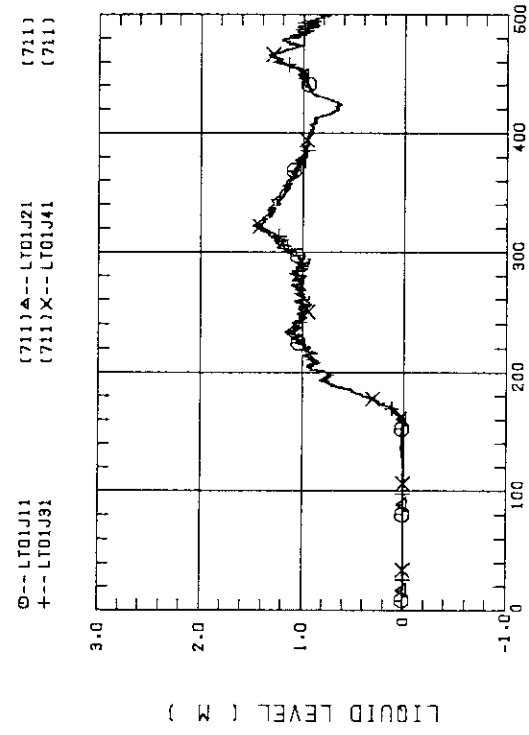

FIG. B-27 LIQUID LEVEL ABOVE UCSP
(BUNDLE 1,2,3,4)

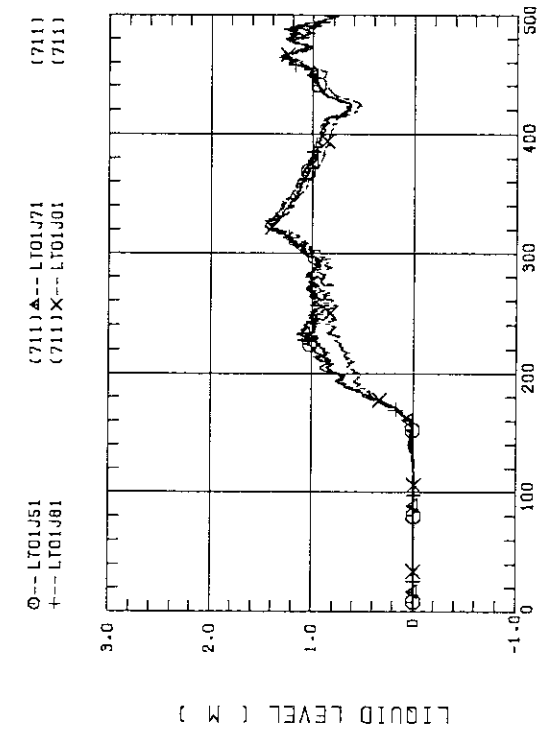

FIG. B-28 LIQUID LEVEL ABOVE UCSP
(BUNDLE 5,6,7,8 AND CORE BUFFLE)

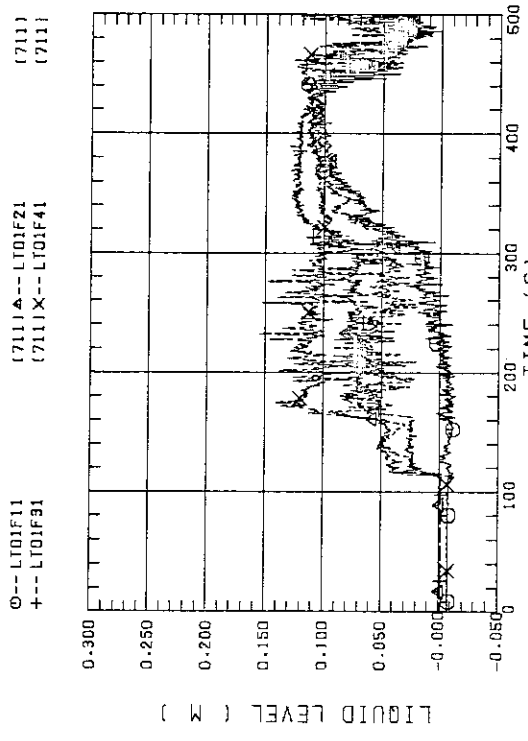

FIG. B-25 LIQUID LEVEL ABOVE END BOX TIE PLATE
(BUNDLE 1,2,3,4)

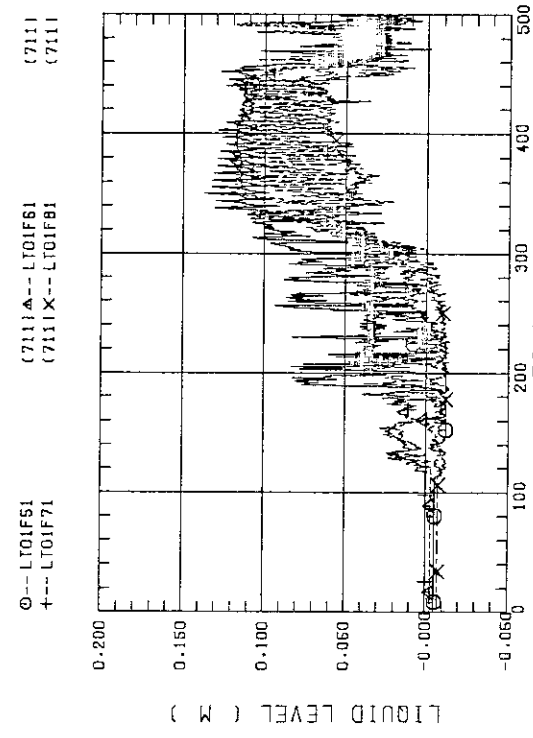

FIG. B-26 LIQUID LEVEL ABOVE END BOX TIE PLATE
(BUNDLE 5,6,7,8)

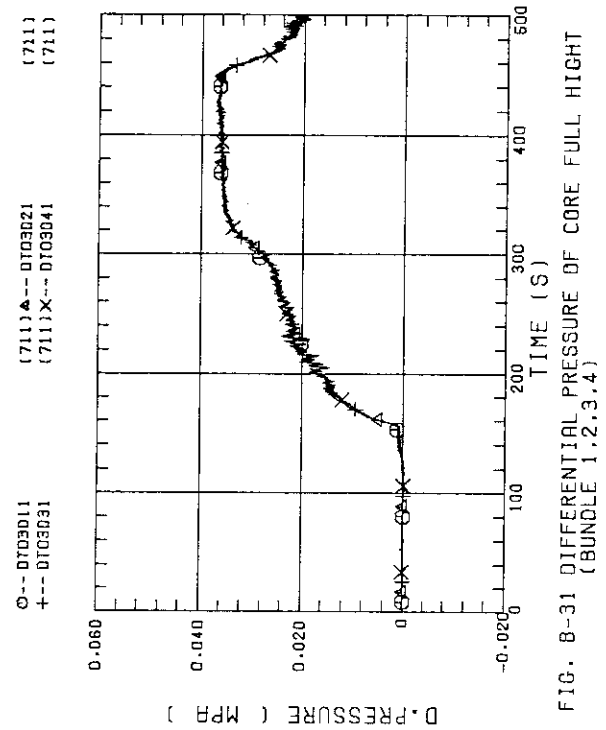

FIG. B-31 DIFFERENTIAL PRESSURE OF CORE FULL HIGHT (BUNDLE 1,2,3,4)

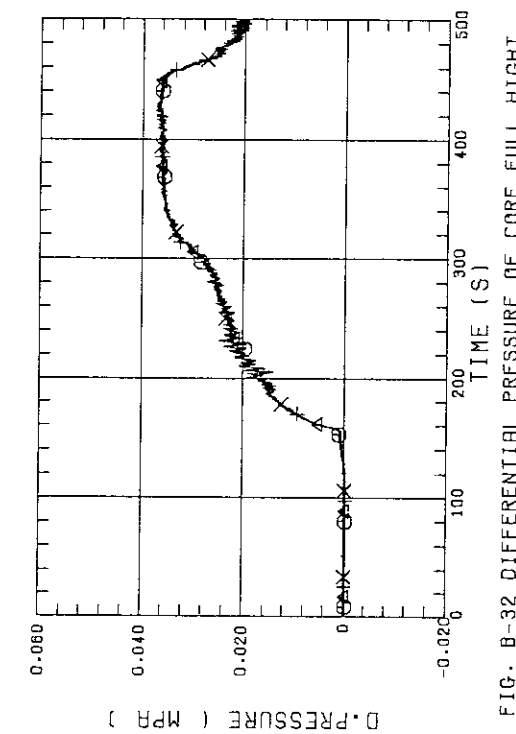

FIG. B-32 DIFFERENTIAL PRESSURE OF CORE FULL HIGHT (BUNDLE 5,6,7,8)

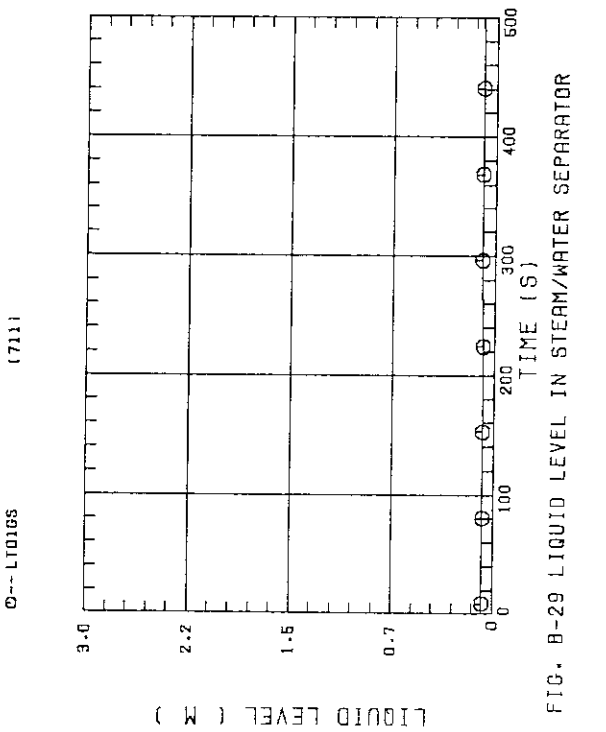

FIG. B-29 LIQUID LEVEL IN STEAM/WATER SEPARATOR

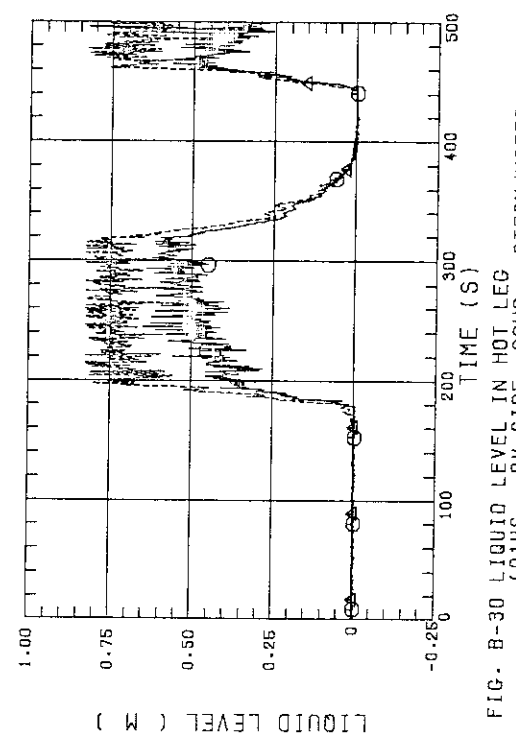

FIG. B-30 LIQUID LEVEL IN HOT LEG (01HS - PV SIDE, 02HS - STEAM/WATER SEPARATOR SIDE)

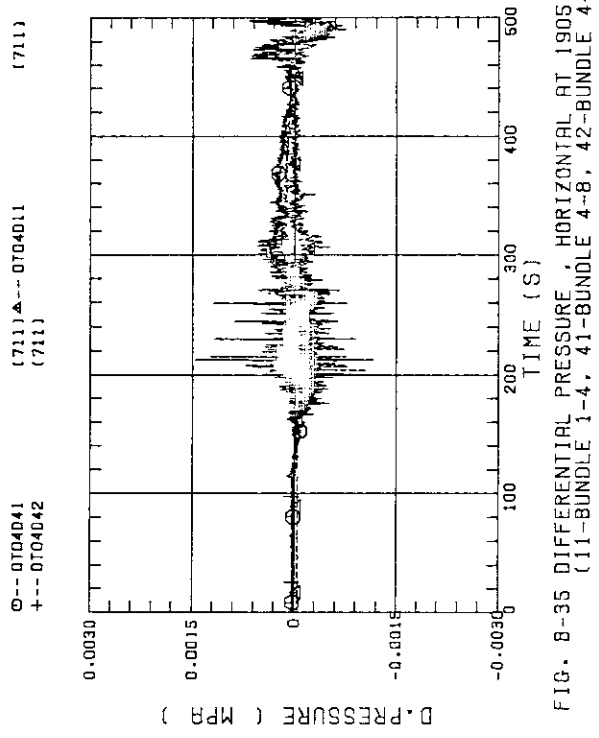

FIG. B-35 DIFFERENTIAL PRESSURE , HORIZONTAL AT 1905 MM
(11-BUNDLE 1-4, 41-BUNDLE 4-8, 42-BUNDLE 4-6)

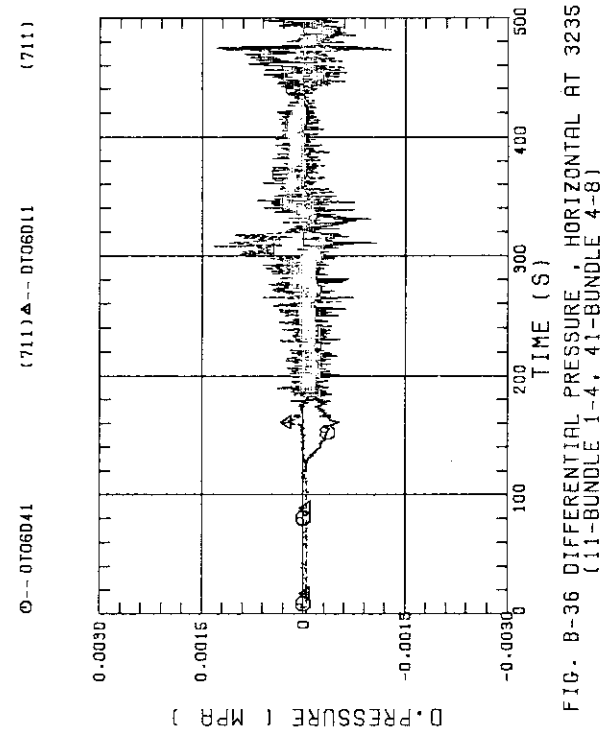

FIG. B-36 DIFFERENTIAL PRESSURE , HORIZONTAL AT 3235 MM
(11-BUNDLE 1-4, 41-BUNDLE 4-8)

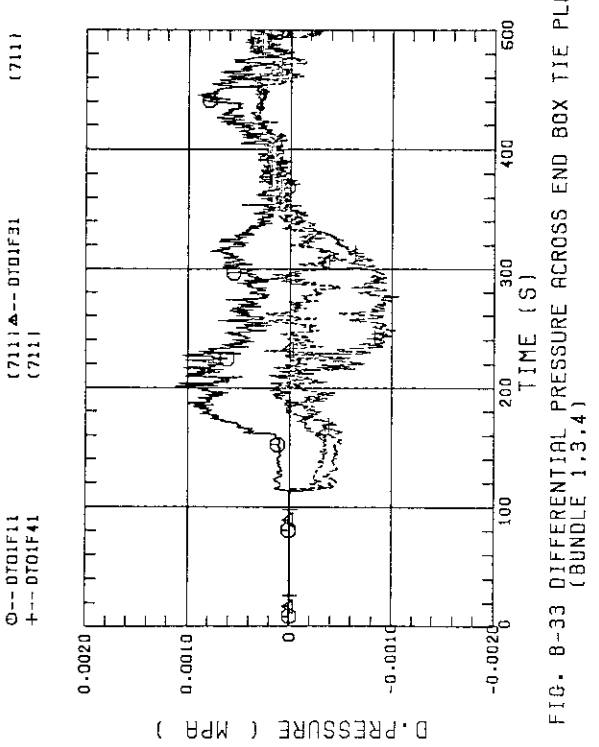

FIG. B-33 DIFFERENTIAL PRESSURE ACROSS END BOX TIE PLATE
(BUNDLE 1,3,4)

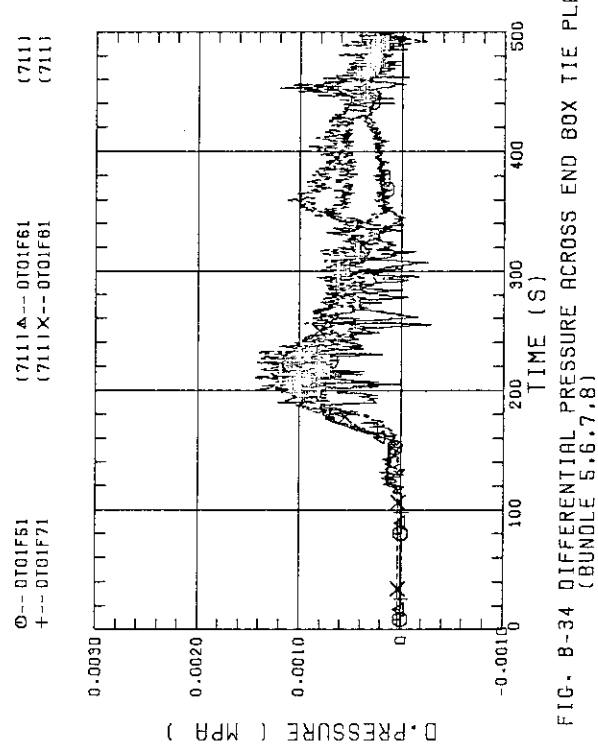

FIG. B-34 DIFFERENTIAL PRESSURE ACROSS END BOX TIE PLATE
(BUNDLE 5,6,7,8)

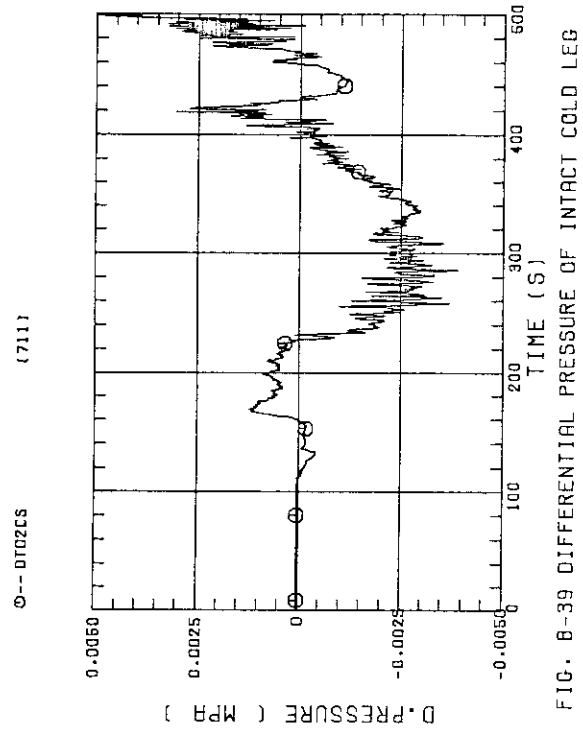

FIG. B-39 DIFFERENTIAL PRESSURE OF INTACT COLD LEG

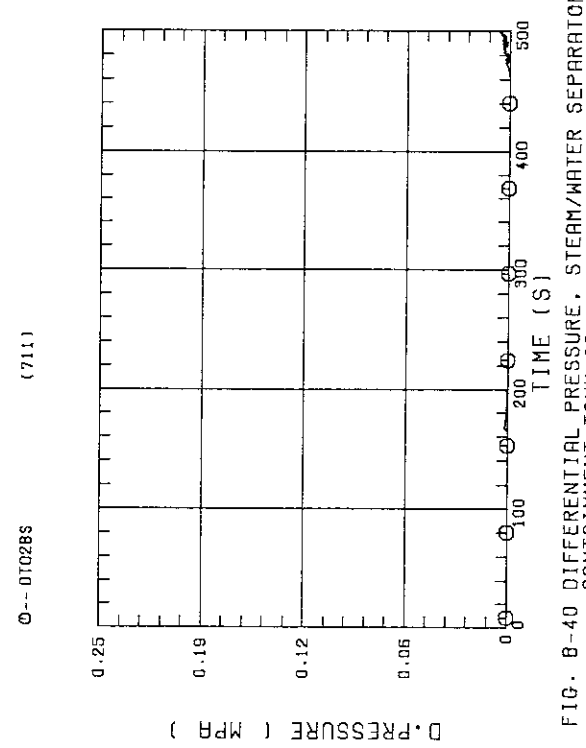

FIG. B-40 DIFFERENTIAL PRESSURE, STEAM/WATER SEPARATOR - CONTAINMENT TANK-II

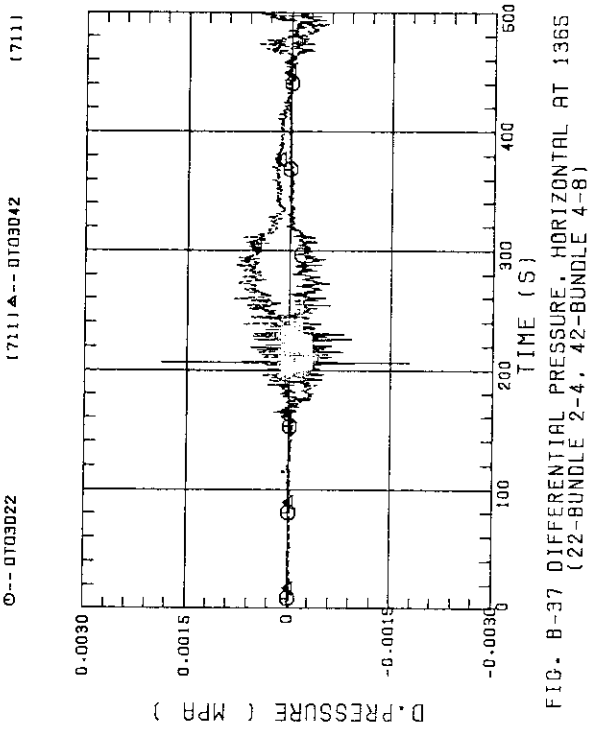

FIG. B-37 DIFFERENTIAL PRESSURE, HORIZONTAL AT 1365 MM (22-BUNDLE 2-4, 42-BUNDLE 4-8)

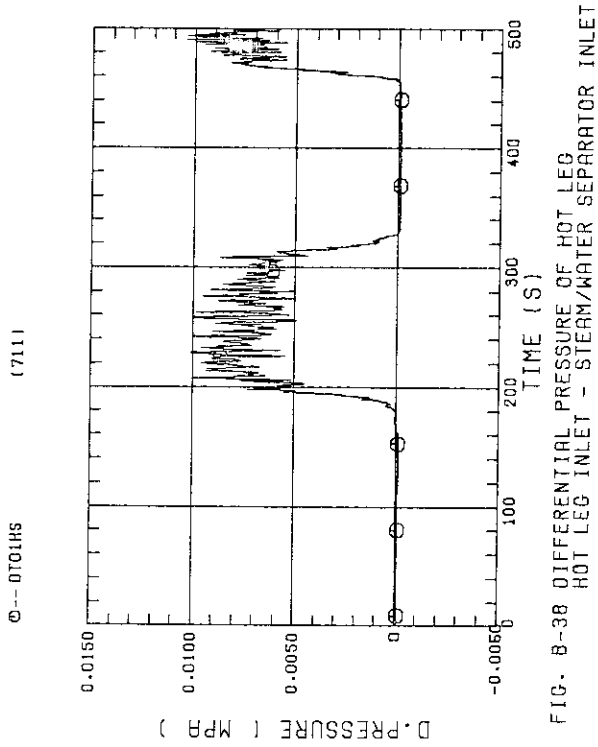

FIG. B-38 DIFFERENTIAL PRESSURE OF HOT LEG HOT LEG INLET - STEAM/WATER SEPARATOR INLET

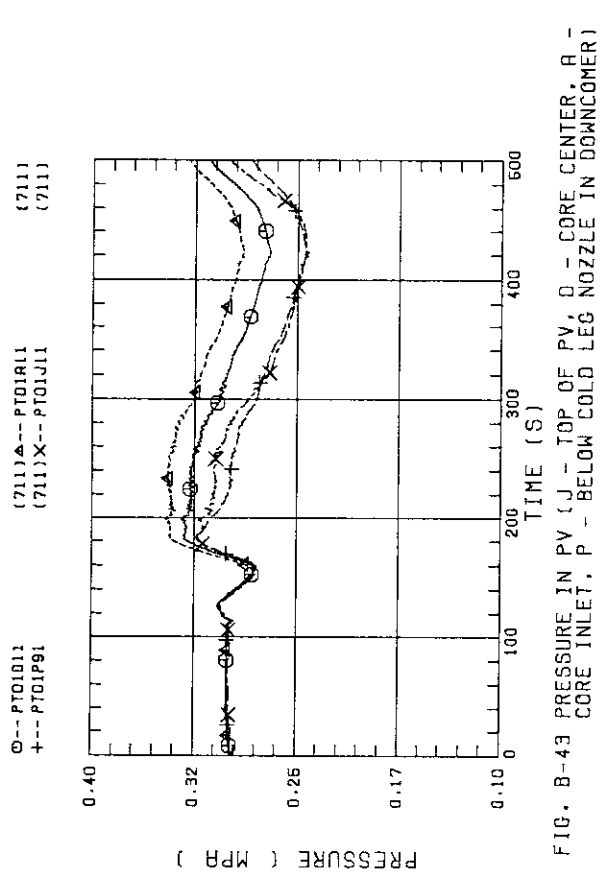

FIG. B-43 PRESSURE IN PV (J - TOP OF PV, Q - CORE CENTER, A - CORE INLET, P - BELOW COLD LEG NOZZLE IN DOWNCOMER)

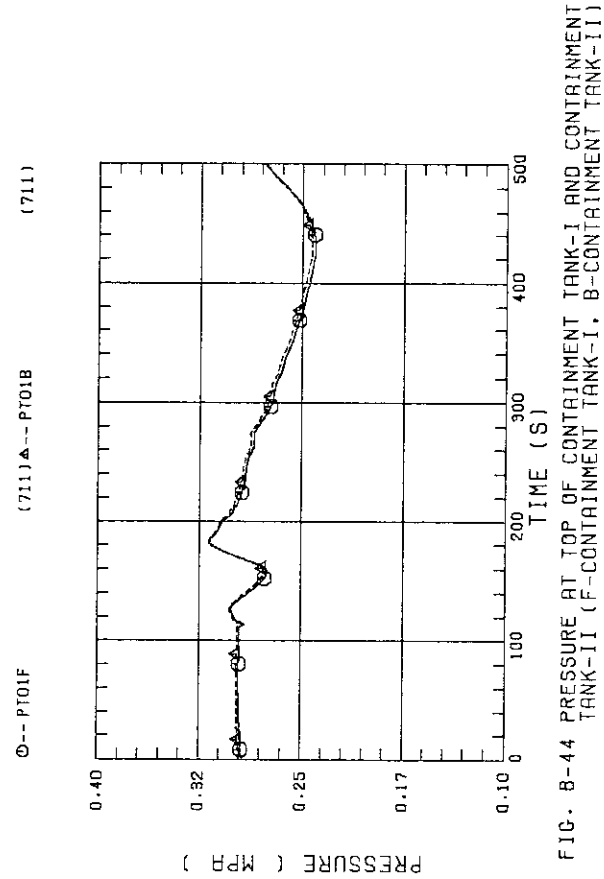

FIG. B-44 PRESSURE AT TOP OF CONTAINMENT TANK-I AND CONTAINMENT TANK-II (F-CONTAINMENT TANK-I, B-CONTAINMENT TANK-II)

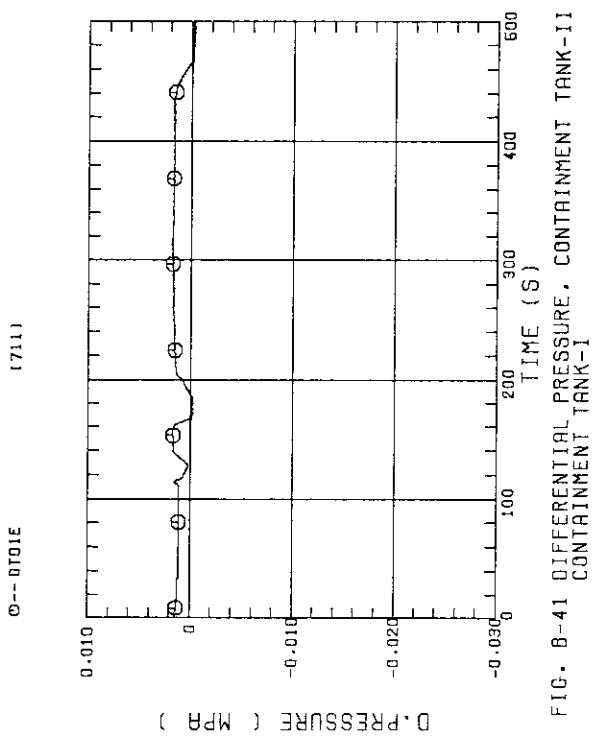

FIG. B-41 DIFFERENTIAL PRESSURE, CONTAINMENT TANK-II - CONTAINMENT TANK-I

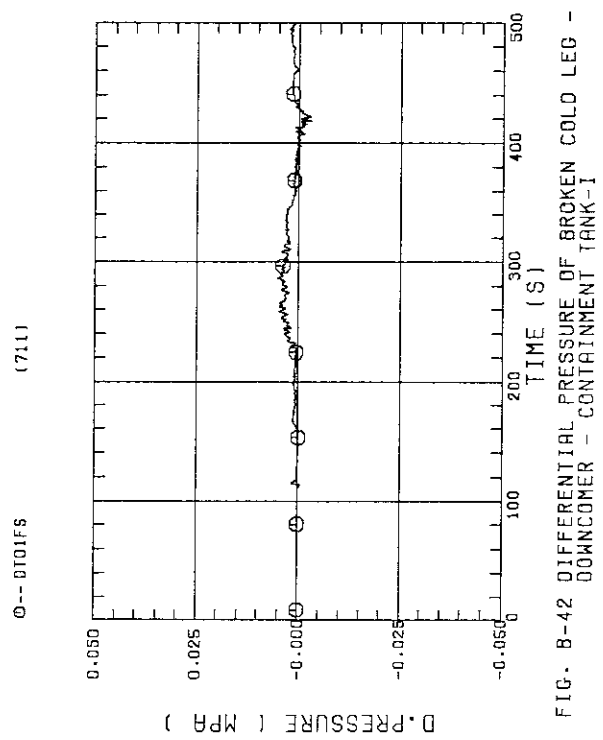

FIG. B-42 DIFFERENTIAL PRESSURE OF BROKEN COLD LEG - PV SIDE, DOWNCOMER - CONTAINMENT TANK-I

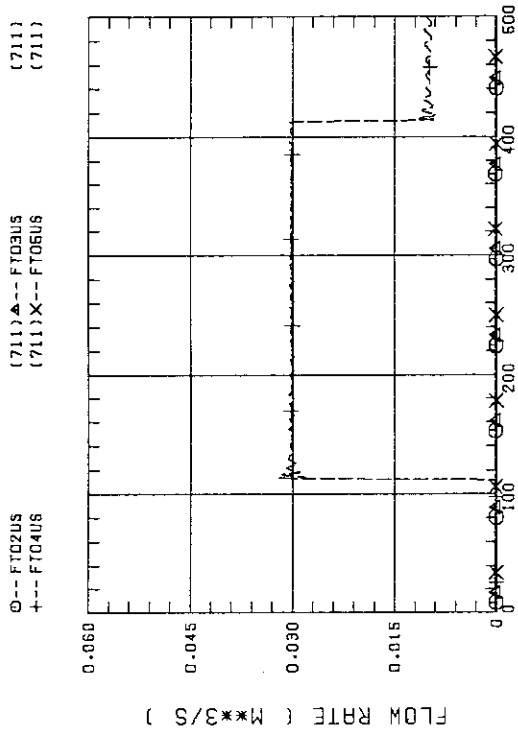

FIG. B-47 FLOW RATE OF UCSP INJECTION
LINE-1(BUNDLE7,8),LINE-2(5,6),LINE-3(3,4),
LINE-4(1,2)

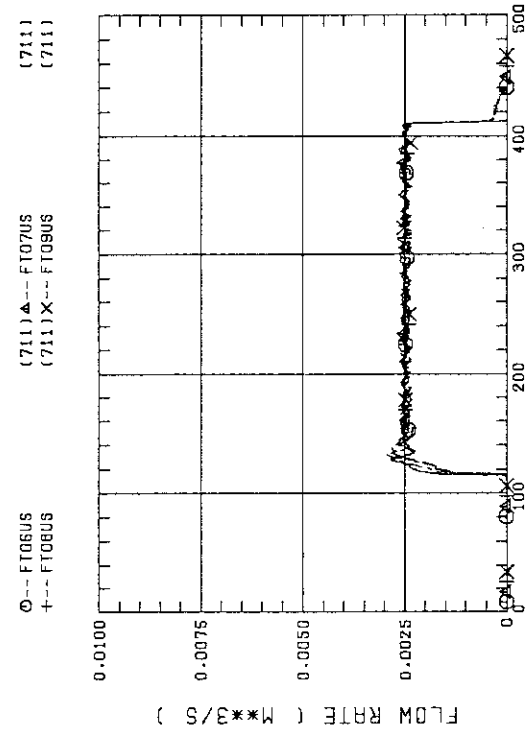

FIG. B-48 FLOW RATE OF UPPER HEAD INJECTION
LINE-4(BUNDLE1,2),LINE-3(3,4),LINE-2(5,6),
LINE-1(7,8)

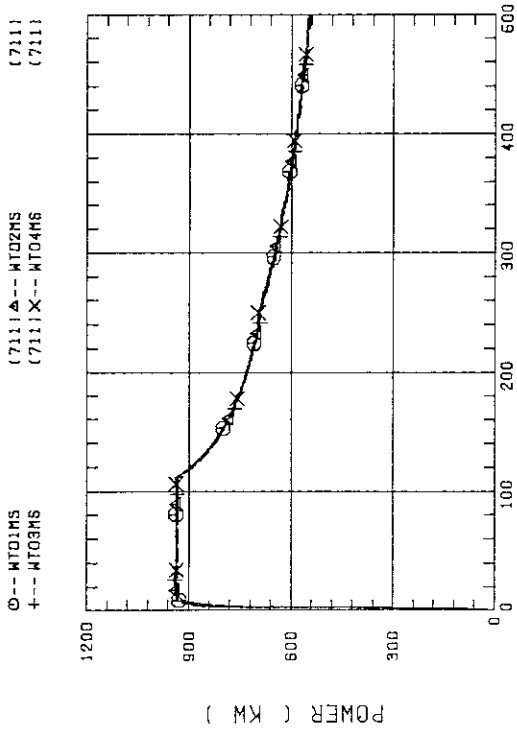

FIG. B-45 BUNDLE POWER
(BUNDLE 1.2.3.4)

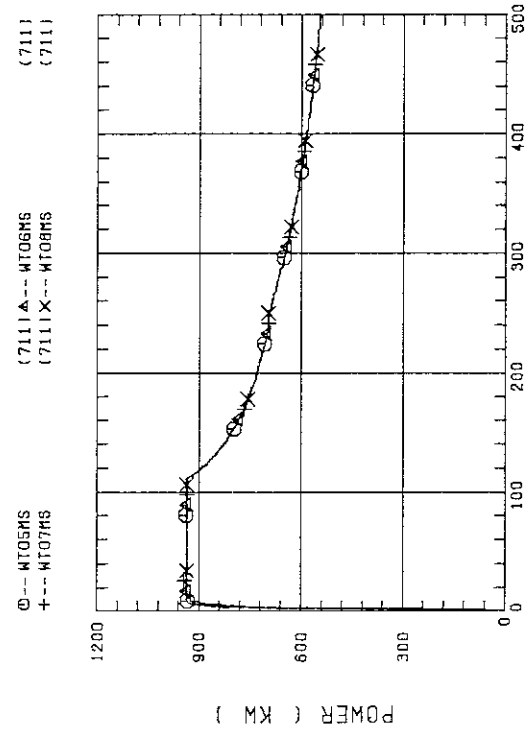

FIG. B-46 BUNDLE POWER
(BUNDLE 5.6.7.8)

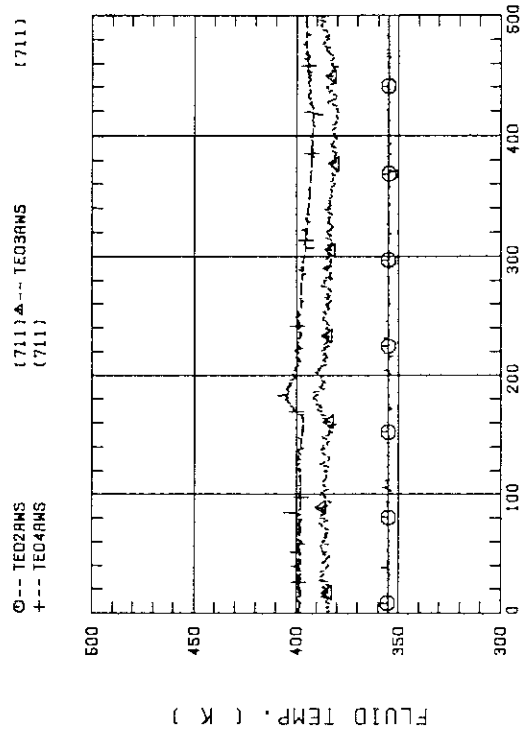

FIG. B-51 FLUID TEMPERATURE IN ECC INJECTION PORT
HOT LEG, IC LEG, BC LEG

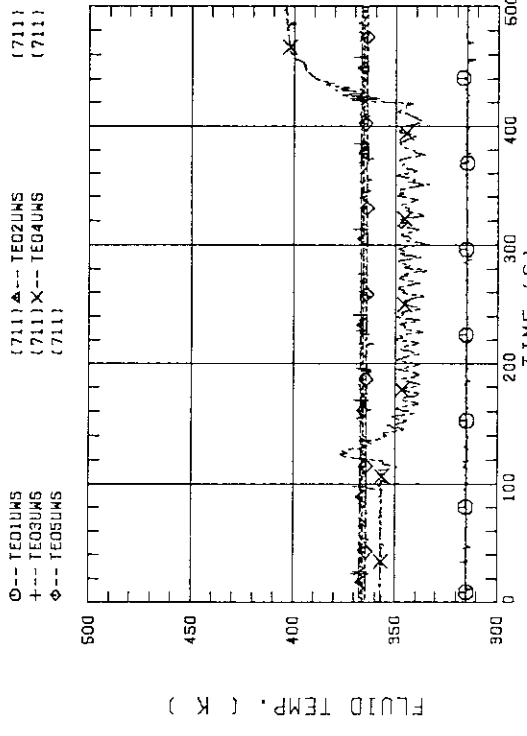

FIG. B-49 FLUID TEMPERATURE IN UCSP INJECTION LINE,
02(BUNDLE7,8),03(5,6),04(3,4),05(1,2),01(LOWER PLENUM)

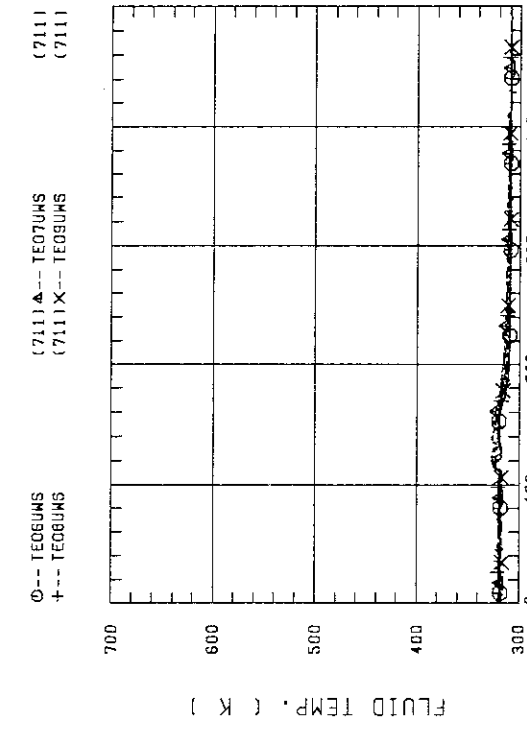

FIG. B-50 FLUID TEMPERATURE IN UCSP INJECTION LINE,
LINE-4(BUNDLE1,2),LINE-3(3,4),LINE-2(5,6),LINE-1(7,8)

Appendix C

Selected Data from Test S3－8

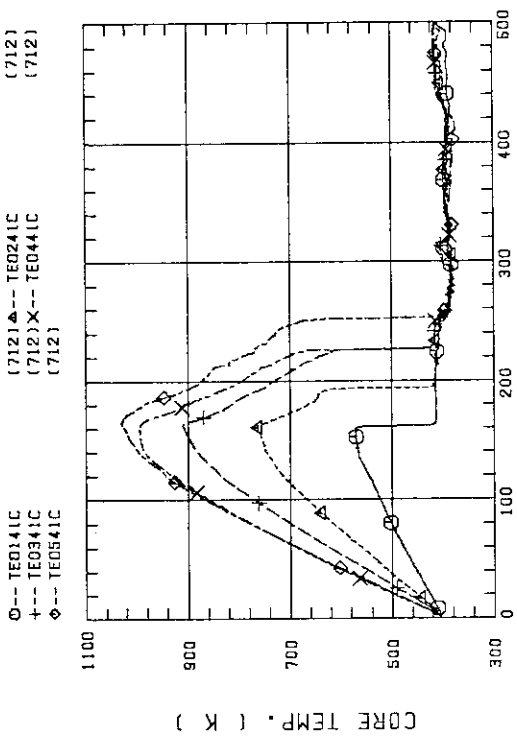

FIG. C-03 HEATER ROD TEMPERATURE (BUNDLE 4-1C, LOWER HALF)

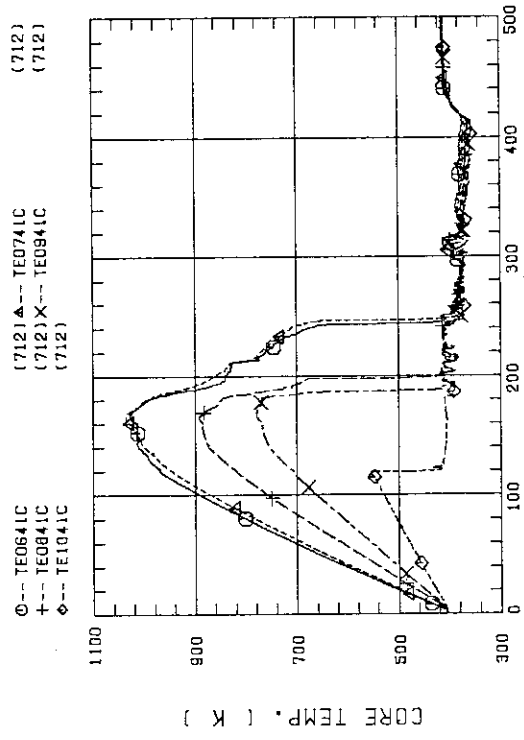

FIG. C-04 HEATER ROD TEMPERATURE (BUNDLE 4-1C, UPPER HALF)

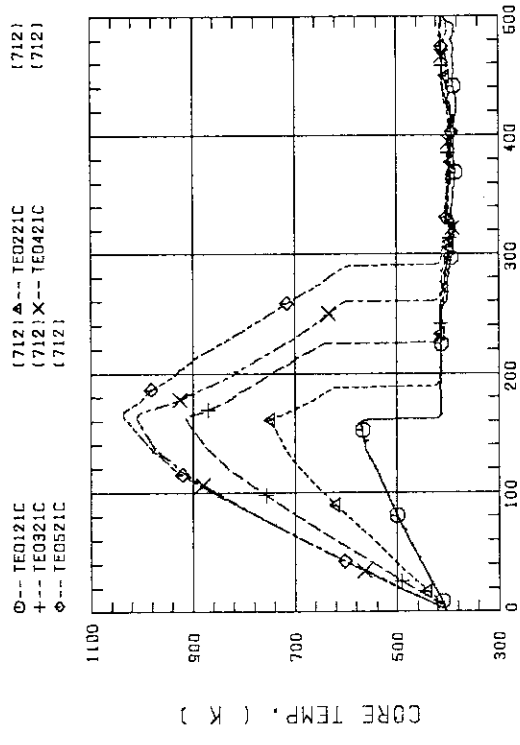

FIG. C-01 HEATER ROD TEMPERATURE (BUNDLE 2-1C, LOWER HALF)

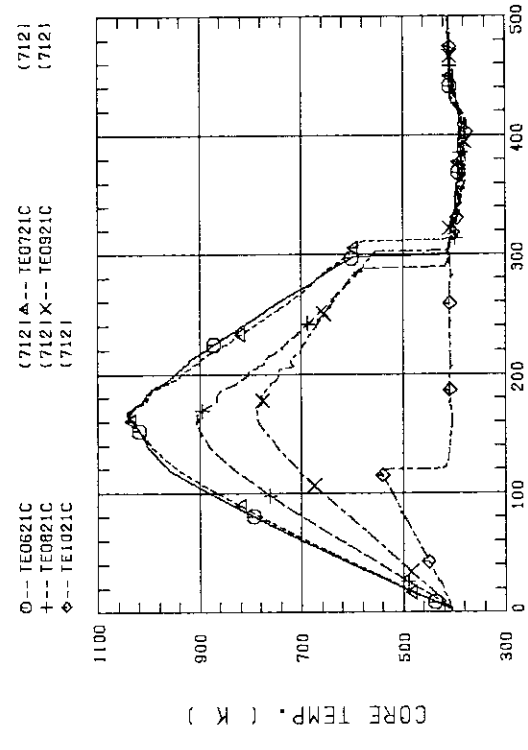

FIG. C-02 HEATER ROD TEMPERATURE (BUNDLE 2-1C, UPPER HALF)

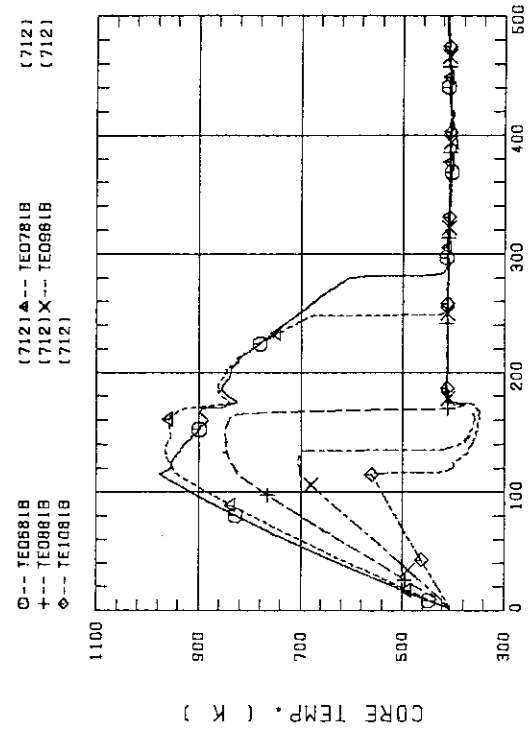

FIG. C-07 HEATER ROD TEMPERATURE (BUNDLE 8-1B, UPPER HALF)

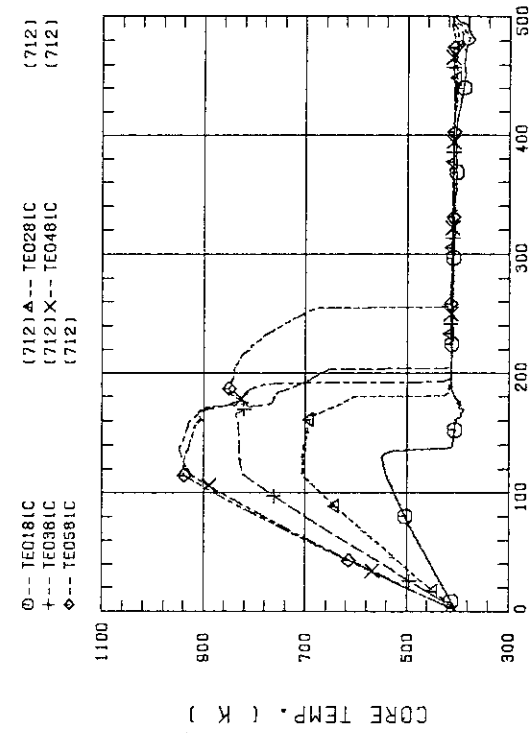

FIG. C-08 HEATER ROD TEMPERATURE (BUNDLE 8-1C, LOWER HALF)

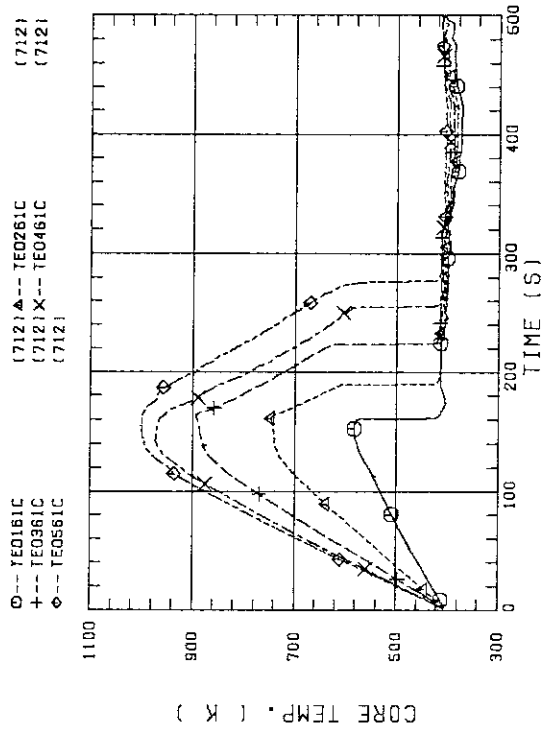

FIG. C-05 HEATER ROD TEMPERATURE (BUNDLE 6-1C, LOWER HALF)

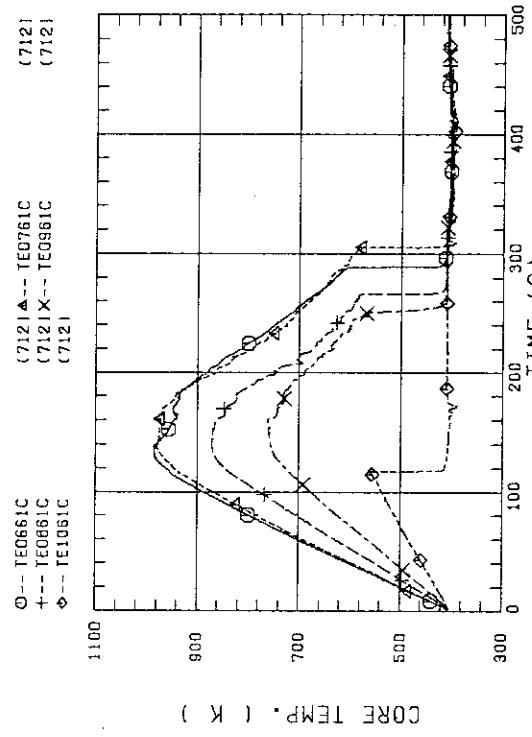

FIG. C-06 HEATER ROD TEMPERATURE (BUNDLE 6-1C, UPPER HALF)

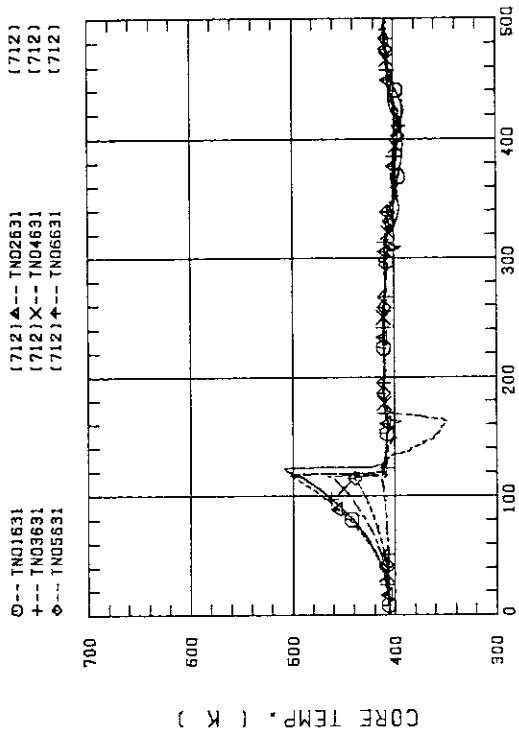

FIG. C-11 NON-HEATED ROD TEMPERATURE (BUNDLE 6-31)

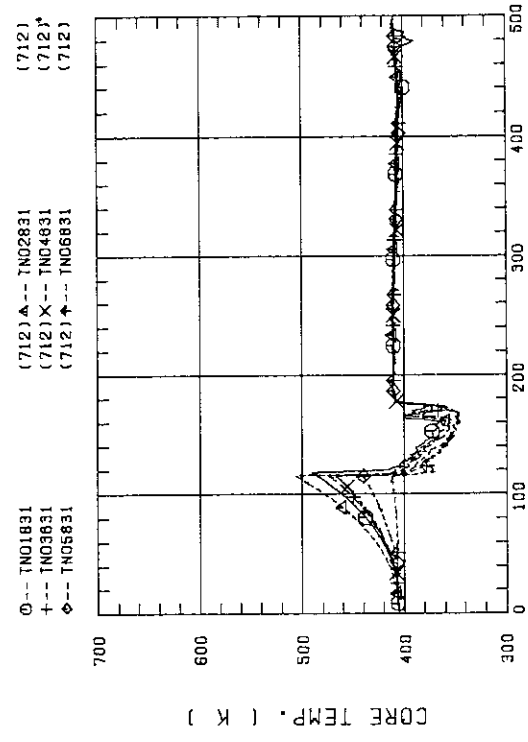

FIG. C-12 NON-HEATED ROD TEMPERATURE (BUNDLE 6-31)

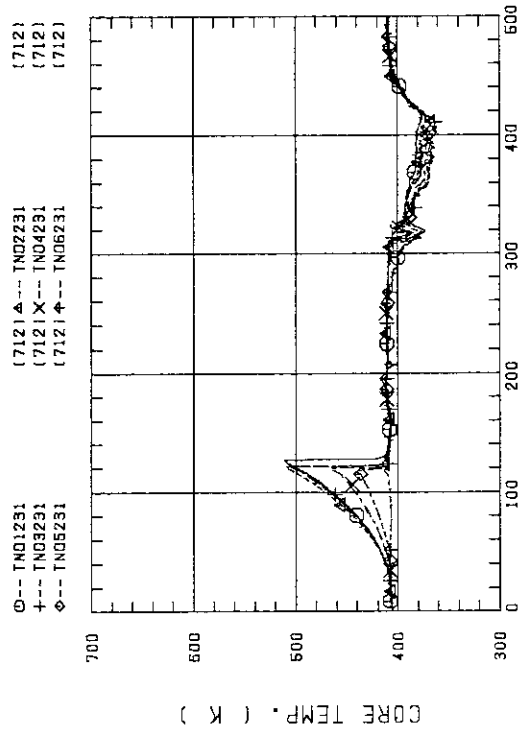

FIG. C-09 NON-HEATED ROD TEMPERATURE (BUNDLE 2-31)

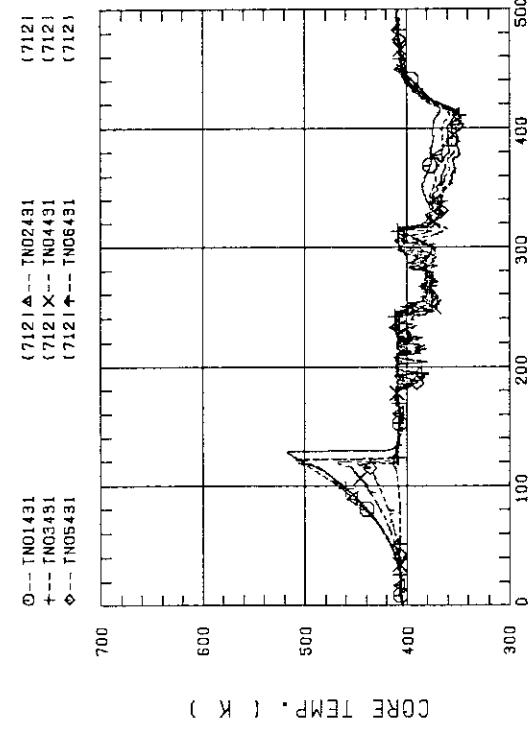

FIG. C-10 NON-HEATED ROD TEMPERATURE (BUNDLE 4-31)

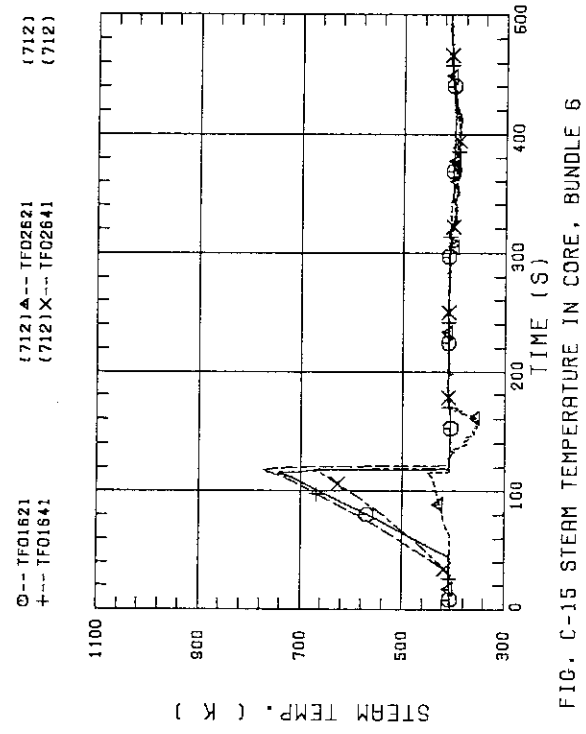

FIG. C-15 STEAM TEMPERATURE IN CORE, BUNDLE 6

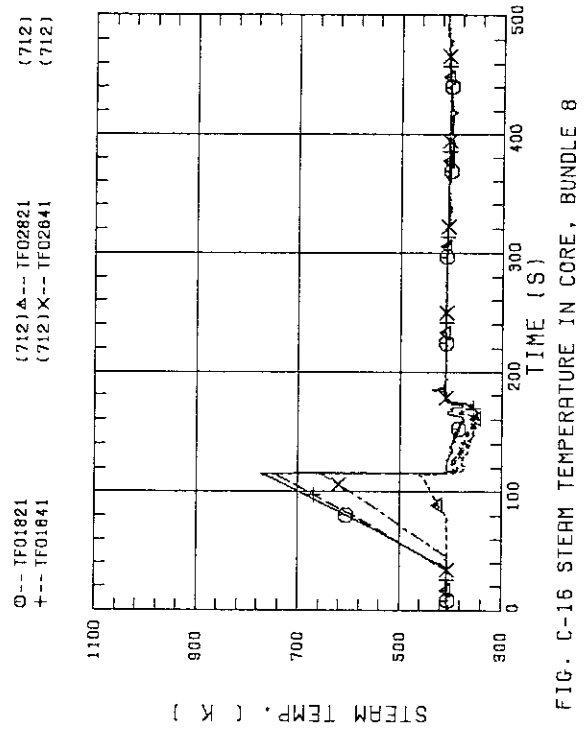

FIG. C-16 STEAM TEMPERATURE IN CORE, BUNDLE 8

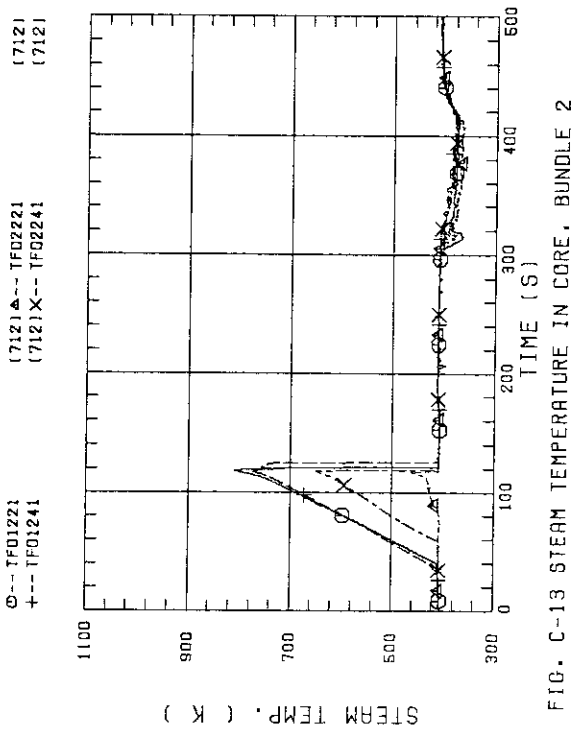

FIG. C-13 STEAM TEMPERATURE IN CORE, BUNDLE 2

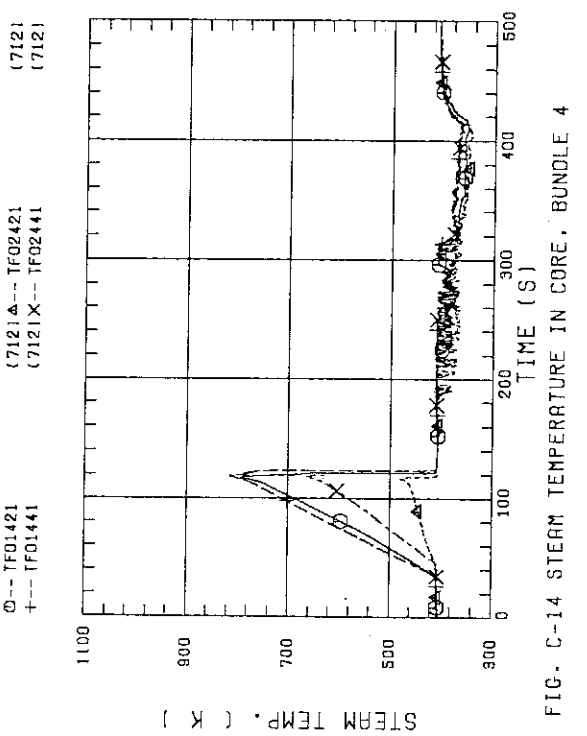

FIG. C-14 STEAM TEMPERATURE IN CORE, BUNDLE 4

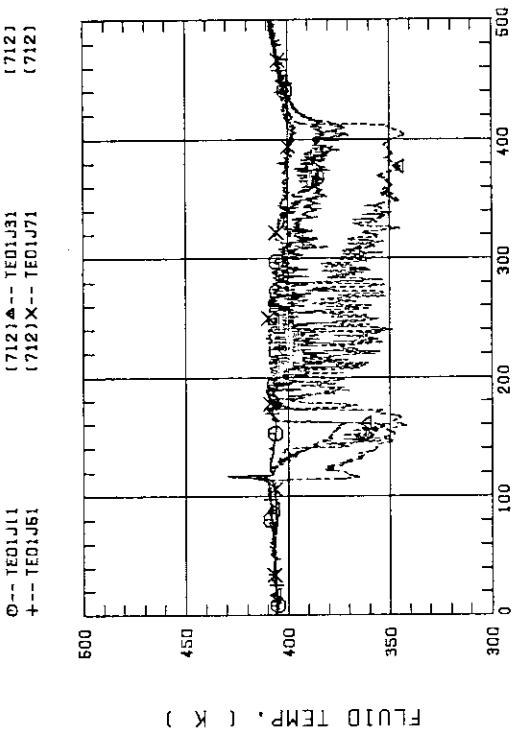

FIG. C-19 FLUID TEMPERATURE ABOVE UCSP
(BUNDLE 1.3.5.7 100MM ABOVE UCSP)

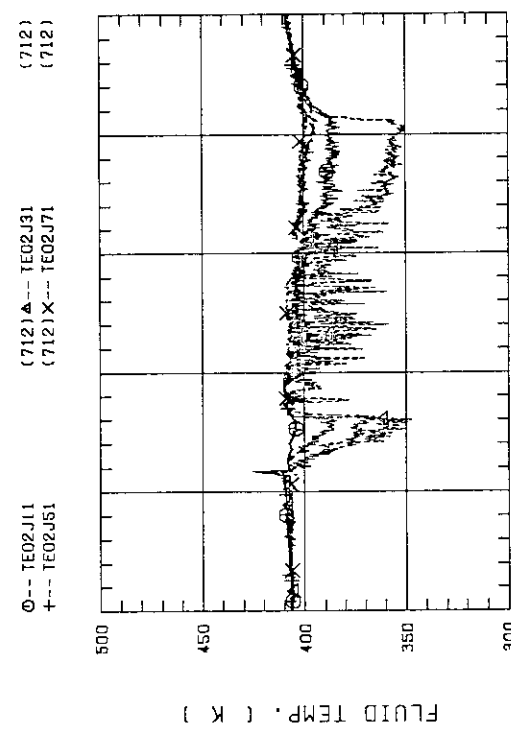

FIG. C-20 FLUID TEMPERATURE ABOVE UCSP
(BUNDLE 1.3.5.7 250MM ABOVE UCSP)

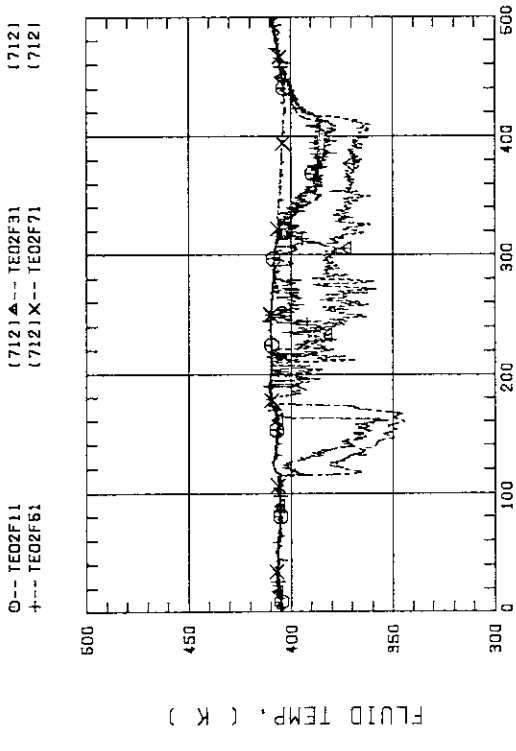

FIG. C-17 FLUID TEMPERATURE JUST ABOVE END BOX TIE PLATE
(BUNDLE 1.3.5.7 OPPOSITE SIDE OF COLD LEG, OUTER)

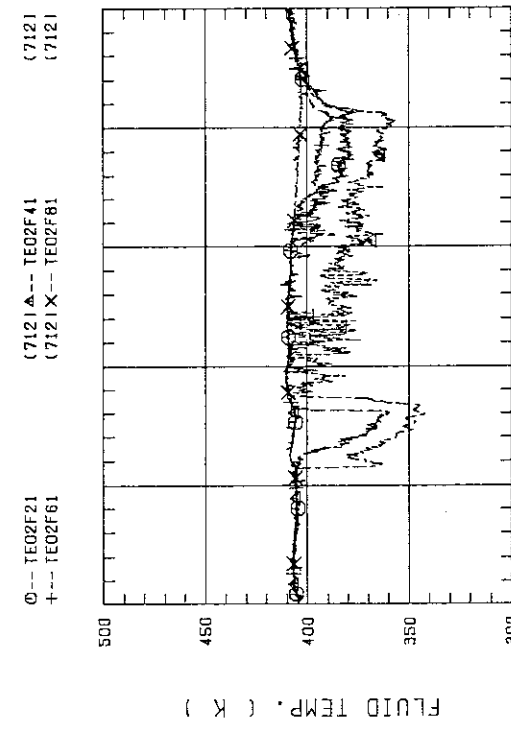

FIG. C-18 FLUID TEMPERATURE JUST ABOVE END BOX TIE PLATE
(BUNDLE 2.4.6.8 OPPOSITE SIDE OF COLD LEG, OUTER)

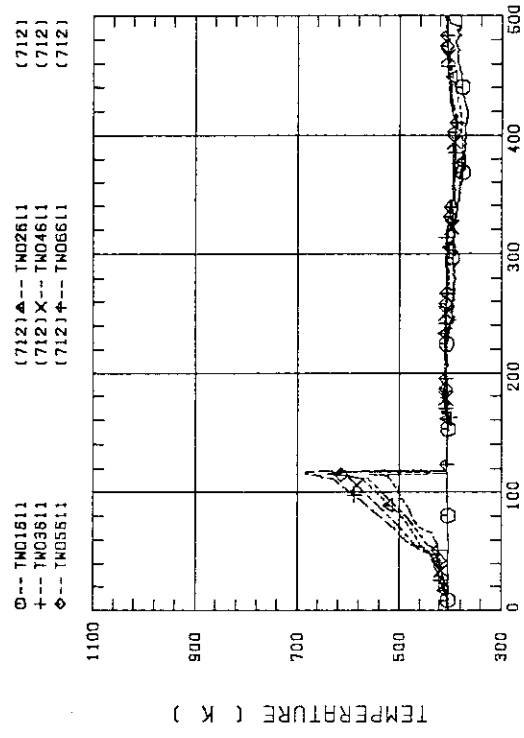

FIG. C-21 TEMPERATURE FOR SPUTTERING DETECTION
BUNDLE 2 , REGION 1 , TYPE 3

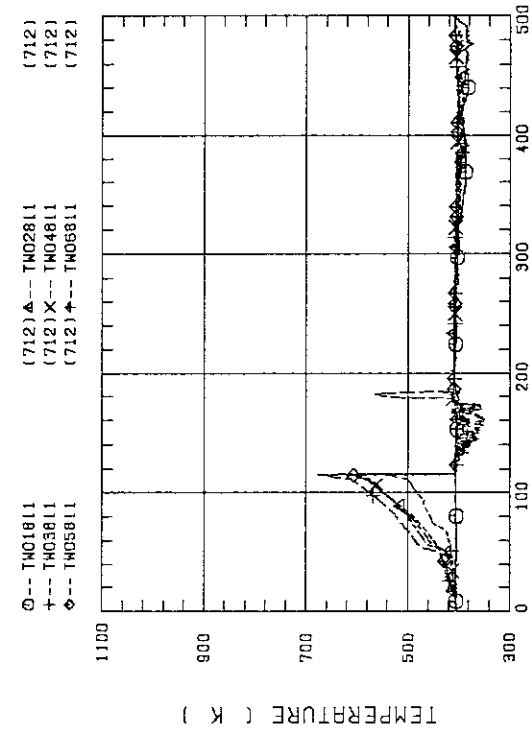

FIG. C-23 TEMPERATURE FOR SPUTTERING DETECTION
BUNDLE 6 , REGION 1 , TYPE 3

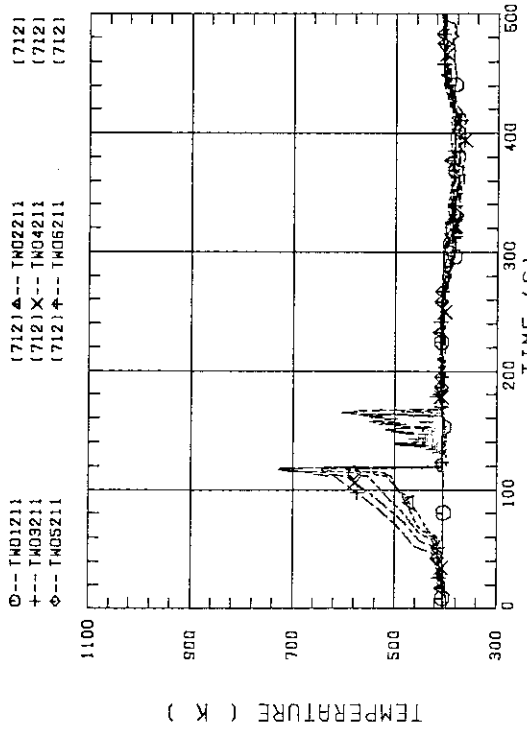

FIG. C-22 TEMPERATURE FOR SPUTTERING DETECTION
BUNDLE 4 , REGION 1 , TYPE 3

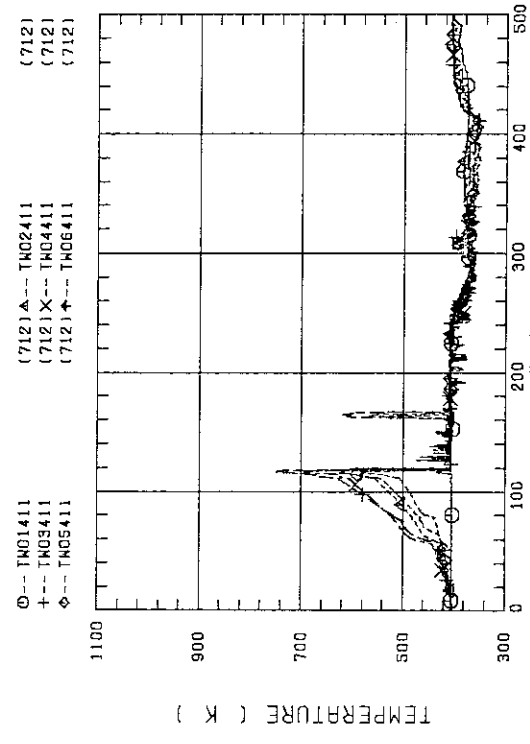

FIG. C-24 TEMPERATURE FOR SPUTTERING DETECTION
BUNDLE 8 , REGION 1 , TYPE 3

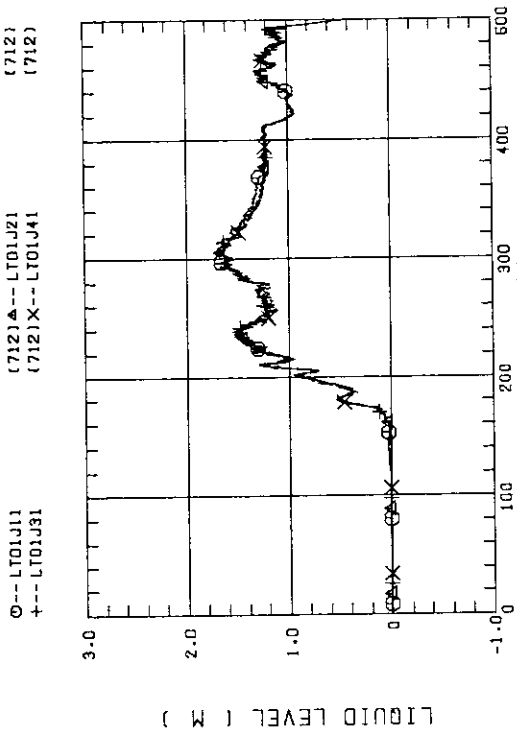

FIG. C-27 LIQUID LEVEL ABOVE UCSP (BUNDLE 1,2,3,4)

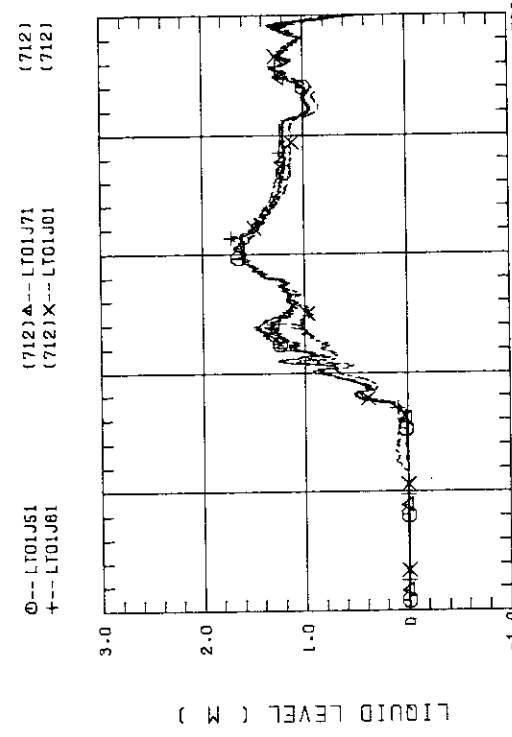

FIG. C-28 LIQUID LEVEL ABOVE UCSP (BUNDLE 5,6,7,8 AND CORE BUFFLE)

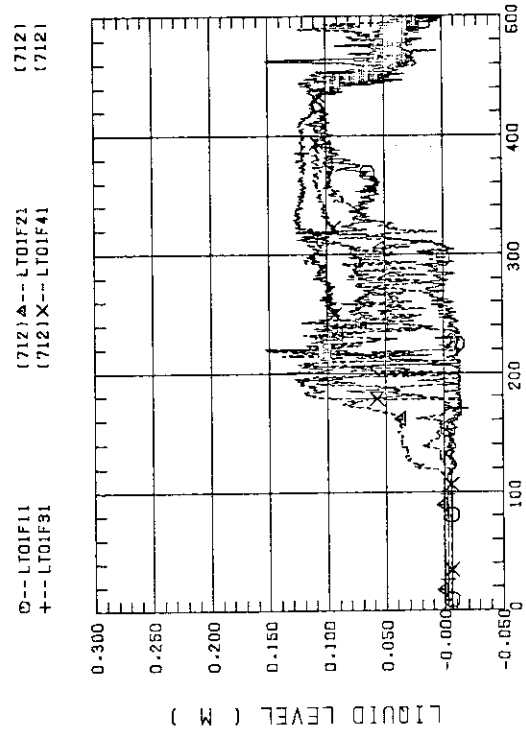

FIG. C-25 LIQUID LEVEL ABOVE END BOX TIE PLATE (BUNDLE 1,2,3,4)

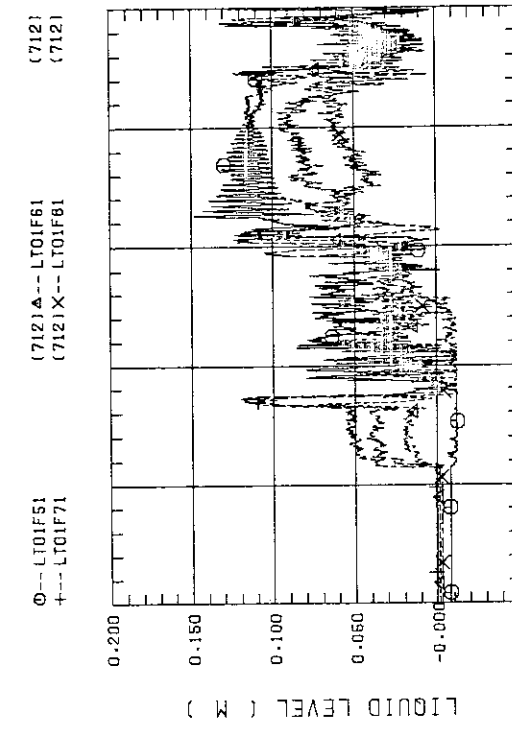

FIG. C-26 LIQUID LEVEL ABOVE END BOX TIE PLATE (BUNDLE 5,6,7,8)

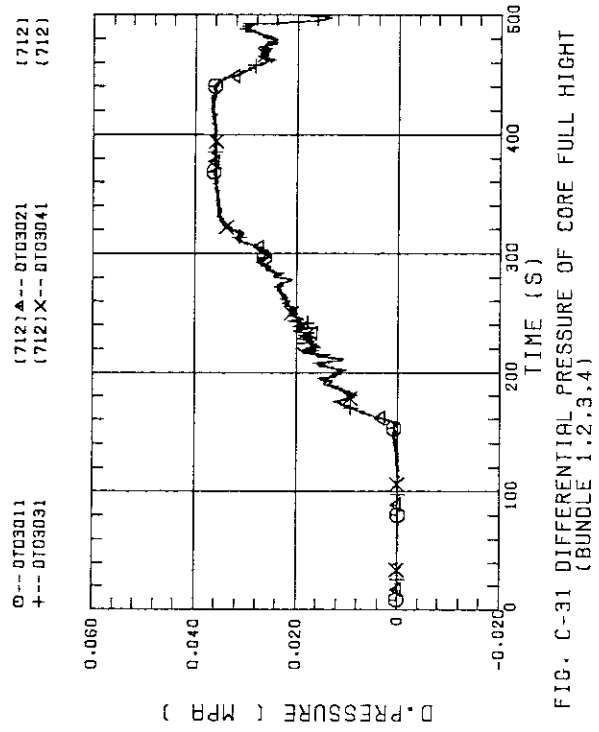

FIG. C-31 DIFFERENTIAL PRESSURE OF CORE FULL HIGHT (BUNDLE 1,2,3,4)

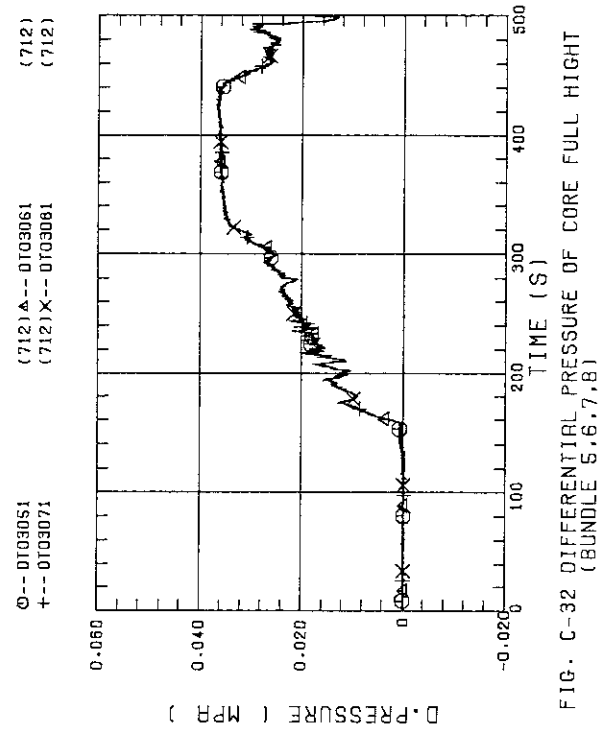

FIG. C-32 DIFFERENTIAL PRESSURE OF CORE FULL HIGHT (BUNDLE 5,6,7,8)

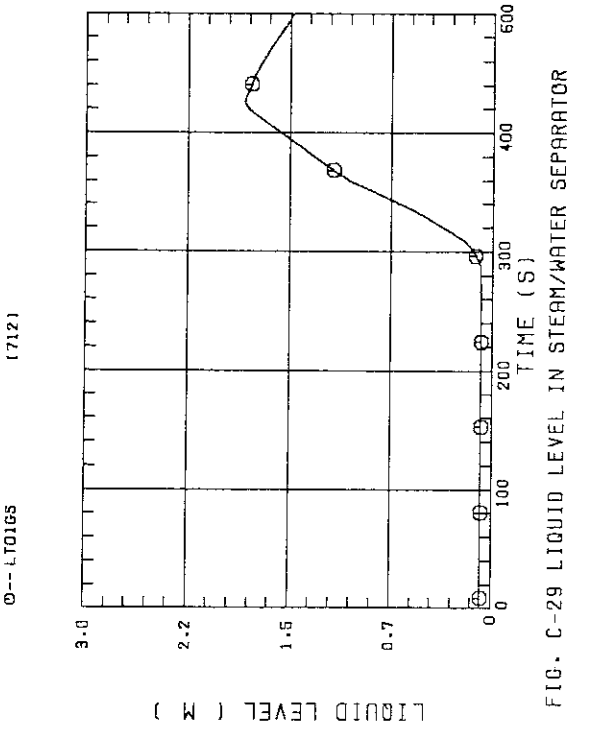

FIG. C-29 LIQUID LEVEL IN STEAM/WATER SEPARATOR

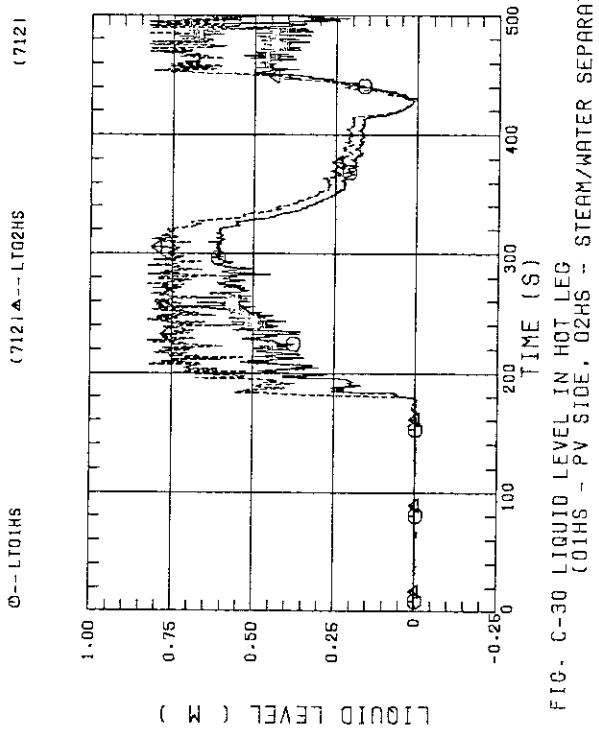

FIG. C-30 LIQUID LEVEL IN HOT LEG (O1HS - PV SIDE, O2HS - STEAM/WATER SEPARATOR SIDE)

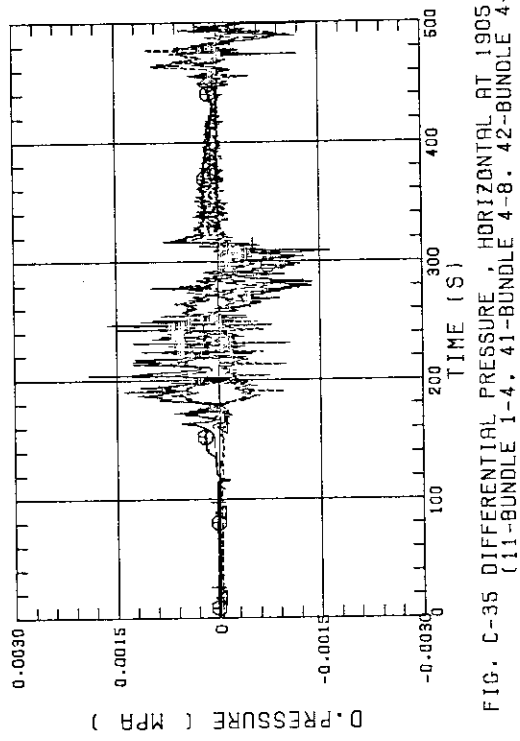

FIG. C-35 DIFFERENTIAL PRESSURE , HORIZONTAL AT 1905 MM
(11-BUNDLE 1-4, 41-BUNDLE 4-8, 42-BUNDLE 4-6)

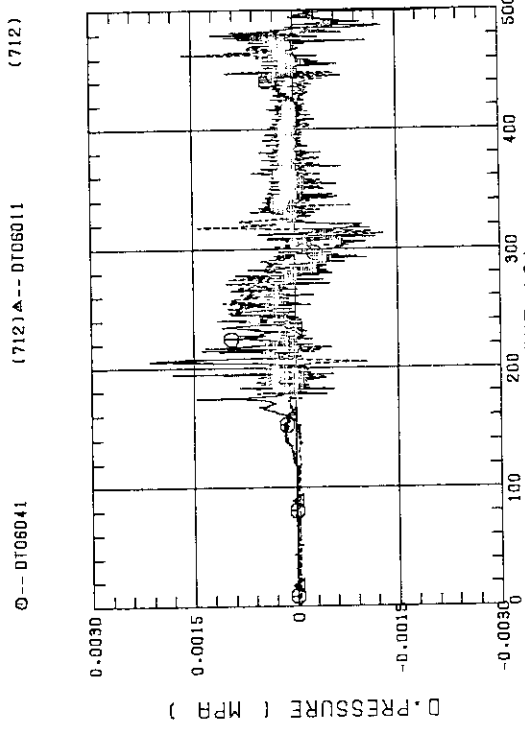

FIG. C-36 DIFFERENTIAL PRESSURE , HORIZONTAL AT 3235 MM
(11-BUNDLE 1-4, 41-BUNDLE 4-6)

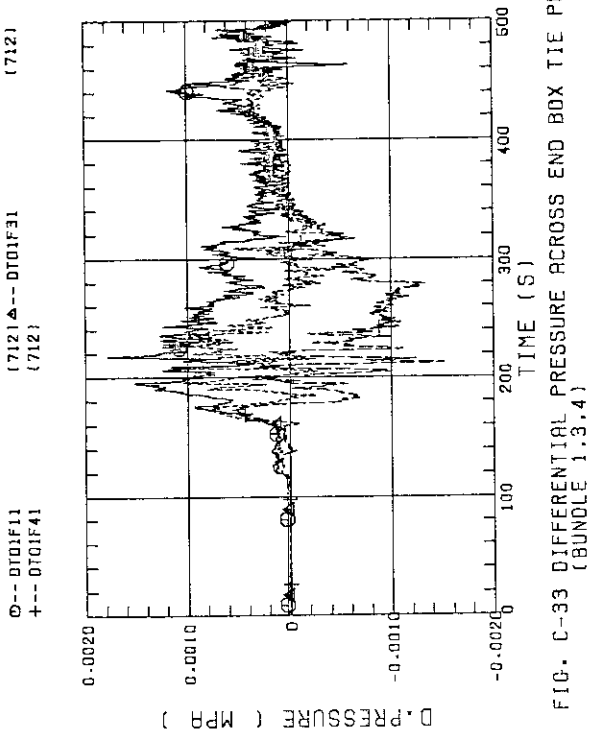

FIG. C-33 DIFFERENTIAL PRESSURE ACROSS END BOX TIE PLATE
(BUNDLE 1.3.4)

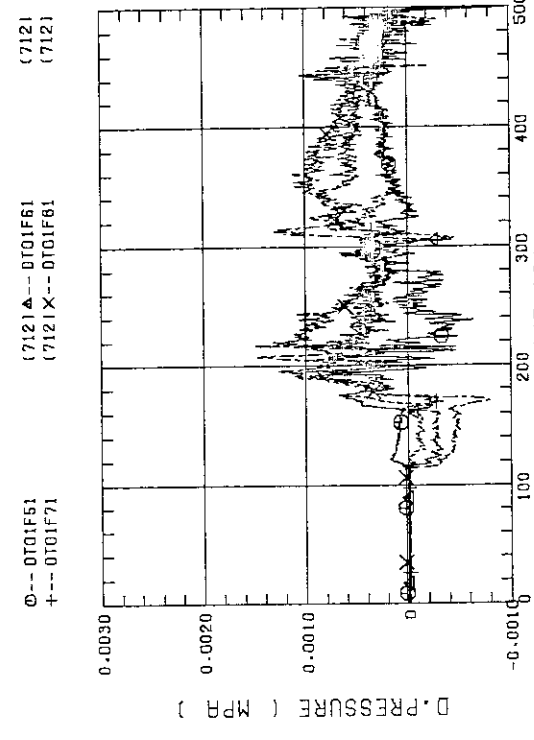

FIG. C-34 DIFFERENTIAL PRESSURE ACROSS END BOX TIE PLATE
(BUNDLE 5.6.7.8)

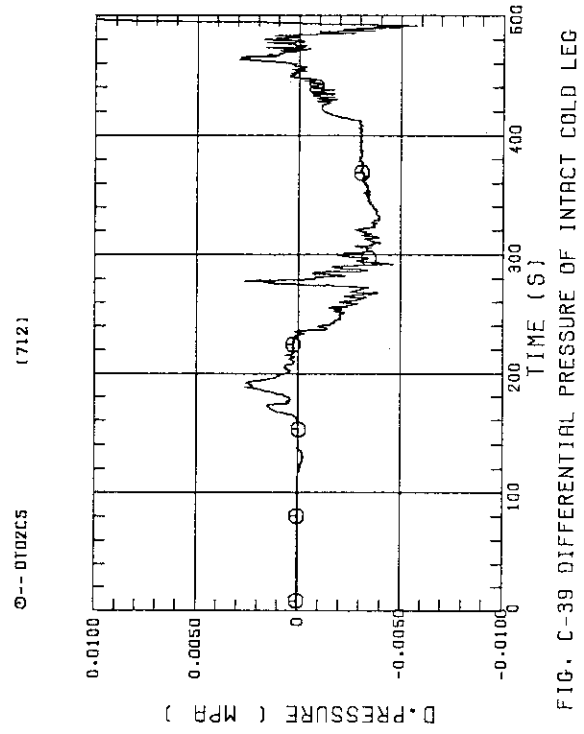

FIG. C-39 DIFFERENTIAL PRESSURE OF INTACT COLD LEG

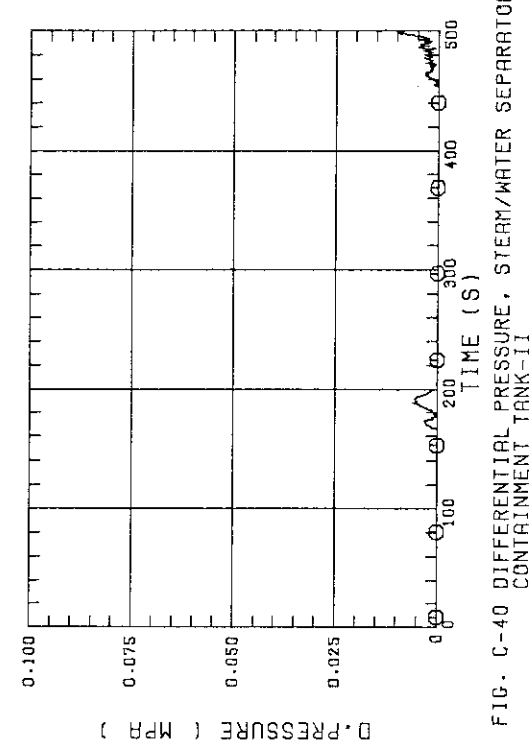

FIG. C-40 DIFFERENTIAL PRESSURE, STEAM/WATER SEPARATOR - CONTAINMENT TANK-II

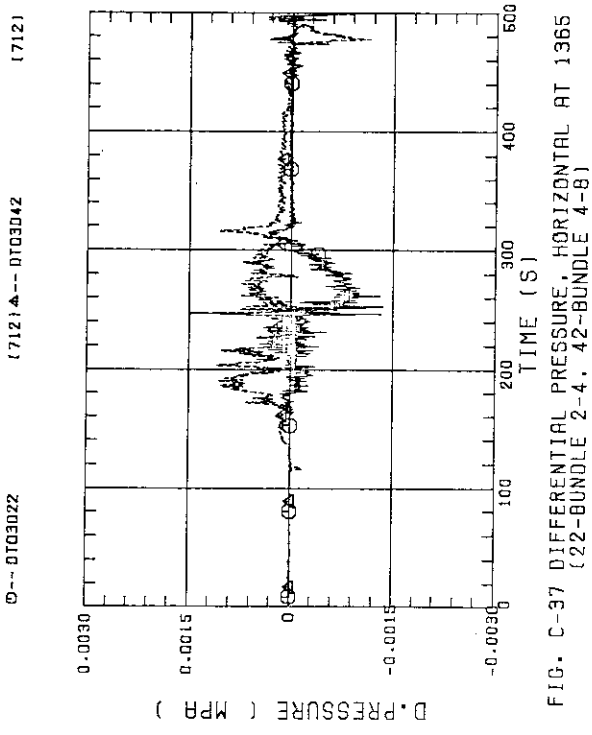

FIG. C-37 DIFFERENTIAL PRESSURE, HORIZONTAL AT 1365 MM (22-BUNDLE 2-4, 42-BUNDLE 4-8)

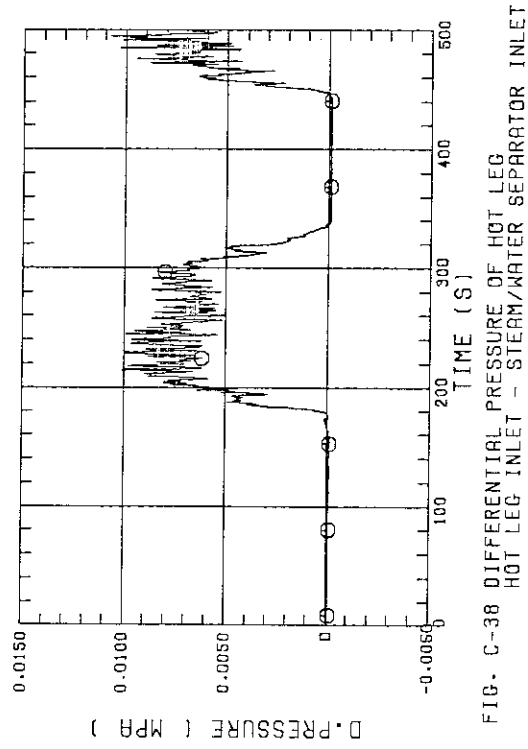

FIG. C-38 DIFFERENTIAL PRESSURE OF HOT LEG HOT LEG INLET - STEAM/WATER SEPARATOR INLET

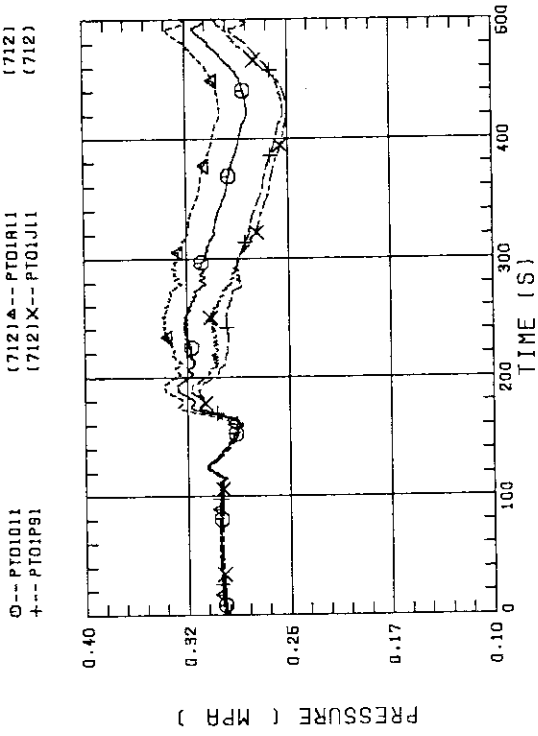

FIG. C-43 PRESSURE IN PV (J - TOP OF PV, D - CORE CENTER, A - CORE INLET, P - BELOW COLD LEG NOZZLE IN DOWNCOMER)

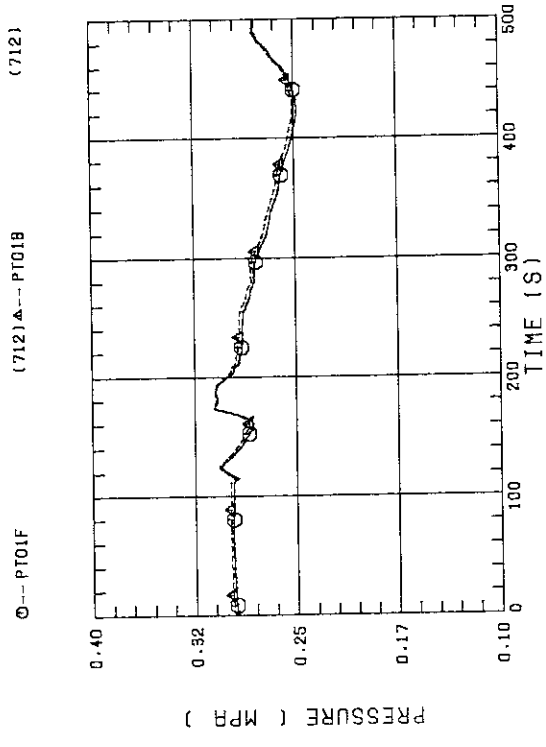

FIG. C-44 PRESSURE AT TOP OF CONTAINMENT TANK-I AND CONTAINMENT TANK-II (F-CONTAINMENT TANK-I, C-CONTAINMENT TANK-II)

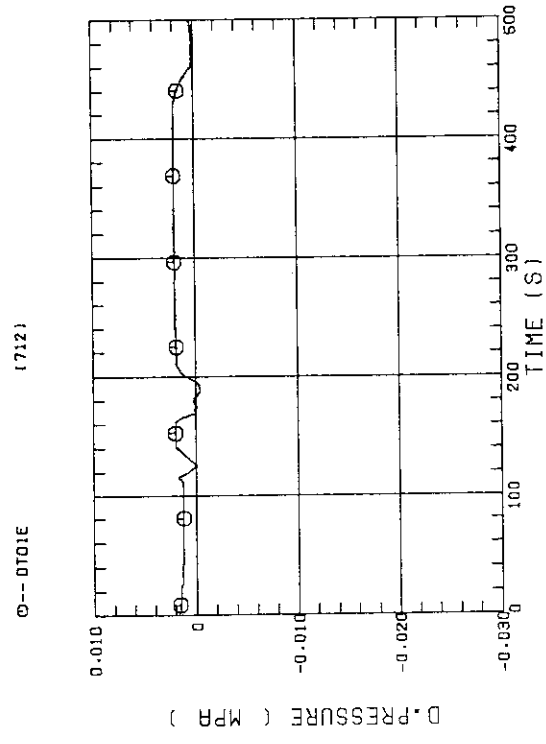

FIG. C-41 DIFFERENTIAL PRESSURE, CONTAINMENT TANK-II - CONTAINMENT TANK-I

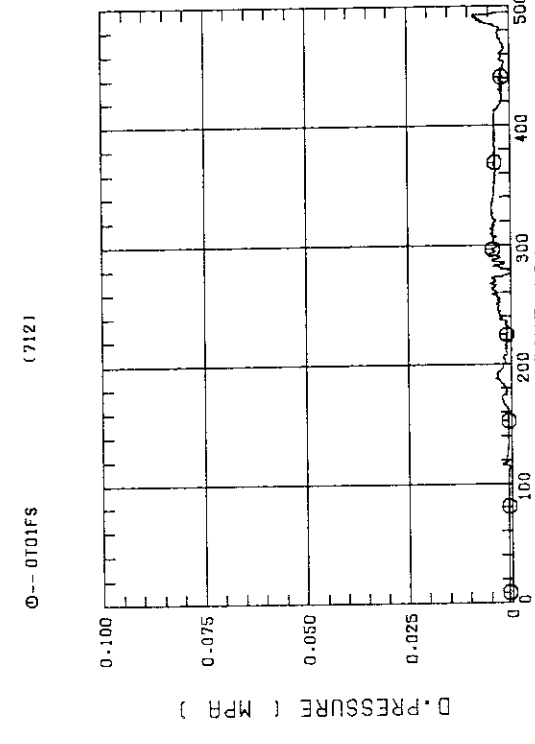

FIG. C-42 DIFFERENTIAL PRESSURE OF BROKEN COLD LEG - PV SIDE, DOWNCOMER - CONTAINMENT TANK-I

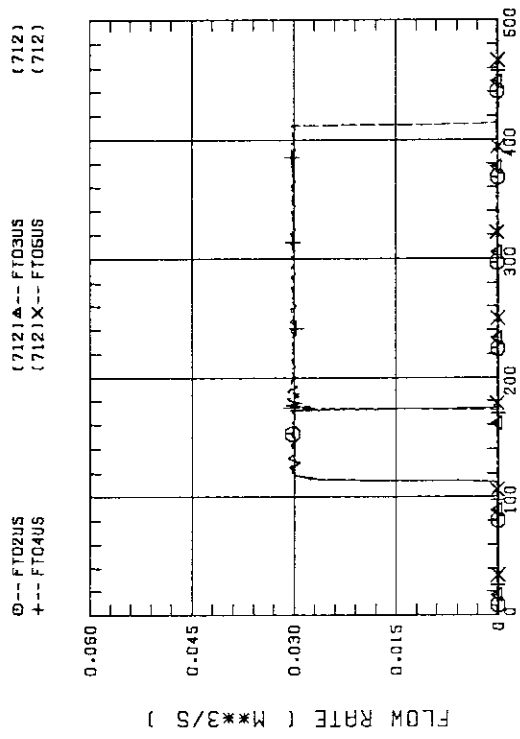

FIG. C-47 FLOW RATE OF UCSP INJECTION
LINE-1(BUNDLE7,8),LINE-2(5,6),LINE-3(3,4),
LINE-4(1,2)

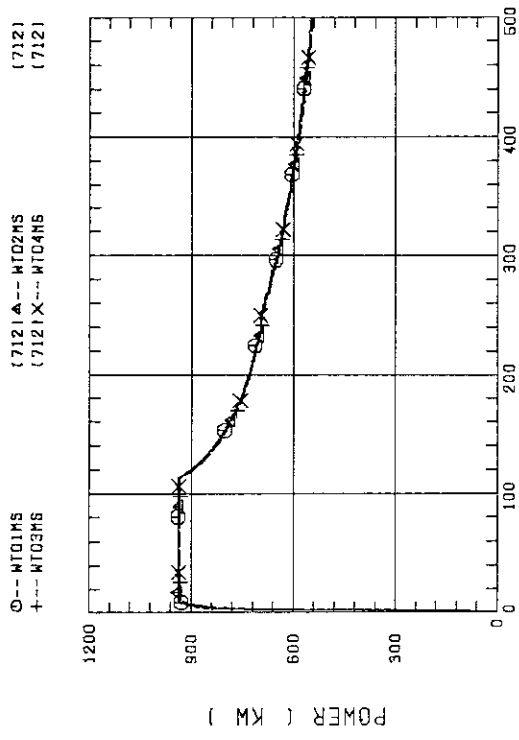

FIG. C-45 BUNDLE POWER
(BUNDLE 1.2.3.4)

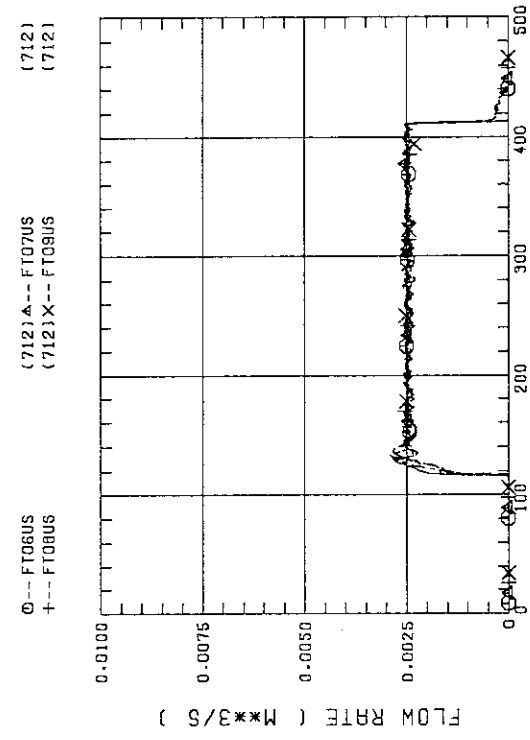

FIG. C-48 FLOW RATE OF UPPER HEAD INJECTION
LINE-4(BUNDLE1,2),LINE-3(3,4),LINE-2(5,6),
LINE-1(7,8)

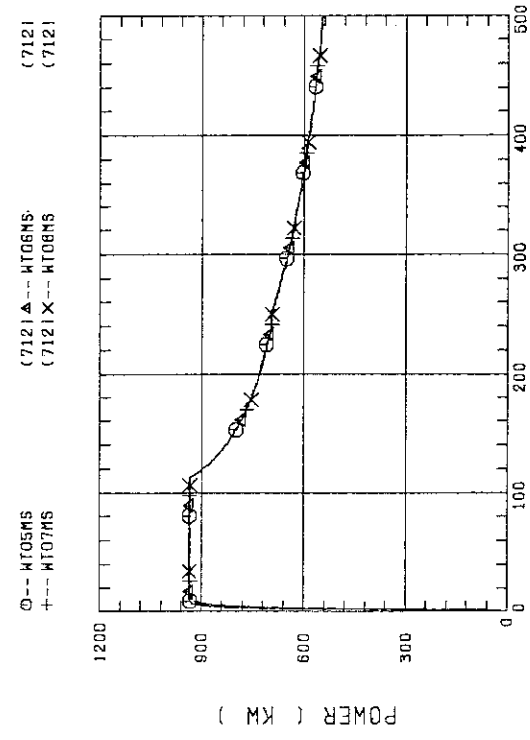

FIG. C-46 BUNDLE POWER
(BUNDLE 5.6.7.8)

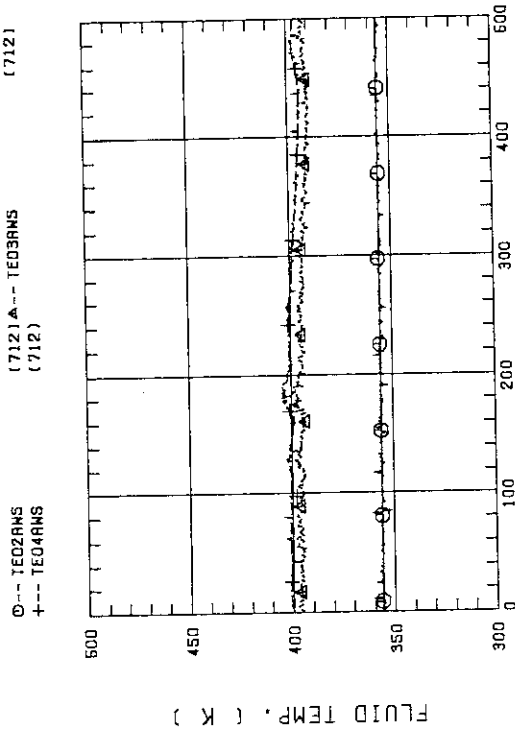

FIG. C-51 FLUID TEMPERATURE IN ECC INJECTION PORT HOT LEG, IC LEG, BC LEG

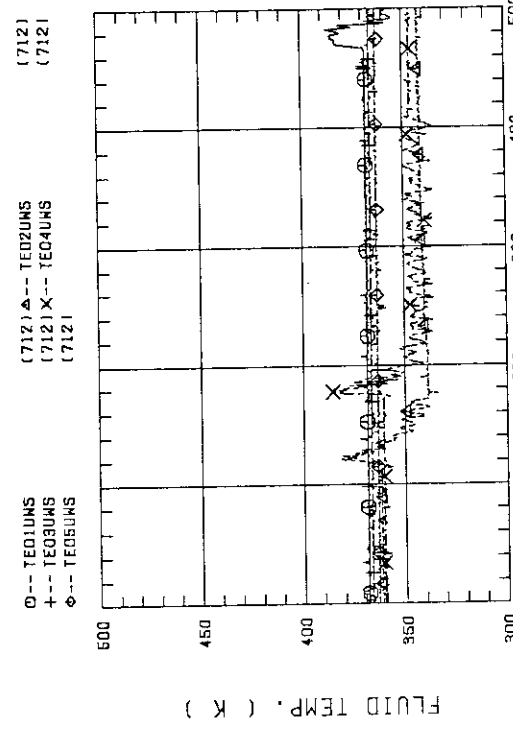

FIG. C-49 FLUID TEMPERATURE IN UCSP INJECTION LINE, 02(BUNDLE(7,8),03(5,6),04(3,4),05(1,2),01(LOWER PLENUM)

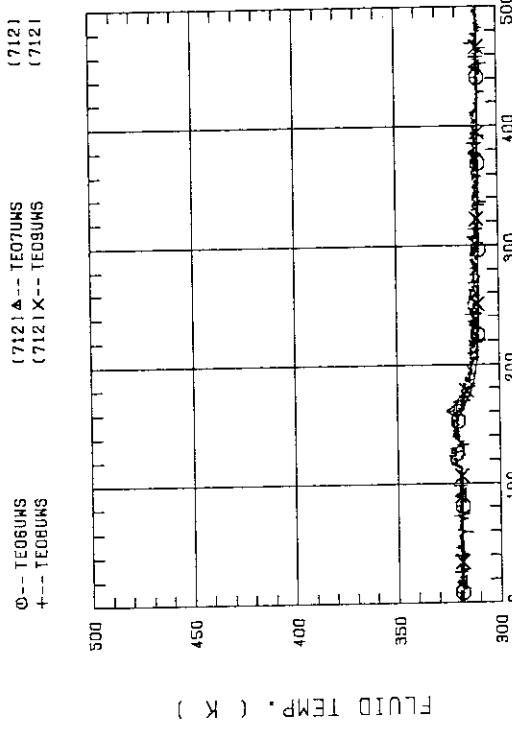

FIG. C-50 FLUID TEMPERATURE IN UCSP INJECTION LINE, LINE-4(BUNDLE(1,2),LINE-3(3,4),LINE-2(5,6),LINE-1(7,8)